SAND2013-1539P

Generic Disposal System Model: Architecture, Implementation, and Demonstration

Fuel Cycle Research & Development

Prepared for
U.S. Department of Energy
Used Fuel Disposition Campaign
P. Vaughn, G. Freeze, J. Lee, S. Chu,
K.D. Huff, W.M. Nutt, T. Hadgu,
R. Rogers, J. Prouty, E. Hardin,
B. Arnold, E. Kalinina, W.P. Gardner,
M. Bianchi, H.H. Liu, J. Birkholzer
Sandia National Laboratories
Argonne National Laboratory
Lawrence Berkeley National Laboratory
November 2012
FCRD-UFD-2012-000430

Sandia National Laboratories is a multi-program laboratory managed and operated by Sandia Corporation, a wholly owned subsidiary of Lockheed Martin Corporation, for the U.S. Department of Energy's National Nuclear Security Administration under contract DE-AC04-94AL85000.

FCT Quality Assurance Program Document

Appendix E
FCT Document Cover Sheet

Name/Title of Deliverable/Milestone	Generic Disposal System Model: Architecture, Implementation, and Demonstration
Work Package Title and Number	Generic Disposal System Level Modeling – SNL, FT-12SN080804
Work Package WBS Number	1.02.08.08
Milestone Number	M2FT- 12SN0808042
Responsible Work Package Manager	Geoff Freeze

(Name/Signature) (Date Submitted)

Quality Rigor Level for Deliverable/Milestone	☐ QRL-3	☒ QRL-2	☐ QRL-1 ☐ Nuclear Data	☐ N/A*

This deliverable was prepared in accordance with Sandia National Laboratories
(Participant/National Laboratory Name)

QA program which meets the requirements of
☒ DOE Order 414.1 ☐ NQA-1-2000 ☐ Other: _____

This Deliverable was subjected to:
☐ Technical Review ☒ Peer Review

Technical Review (TR)
Review Documentation Provided
☐ Signed TR Report, or
TR Report No.: _____
☐ Signed TR Concurrence Sheet (attached), or
☐ Signature of TR Reviewer(s) below

Peer Review (PR)
Review Documentation Provided
☐ Signed PR Report, or
PR Report No.: _____
☐ Signed PR Concurrence Sheet (attached), or
☒ Signature of PR Reviewers below

Name and Signature of Reviewers
Paul Mariner
Robert Rechard

(Name/Signature) (Date)

*Note: In some cases there may be a milestone where an item is being fabricated, maintenance is being performed on a facility, or a document is being issued through a formal document control process where it specifically calls out a formal review of the document. In these cases, documentation (e.g., inspection report, maintenance request, work planning package documentation, or the documented review of the issued document through the document control process) of the completion of the activity along with the Document Cover Sheet is sufficient to demonstrate achieving the milestone. QRL for such milestones may also be marked N/A in the work package provided the work package clearly specifies the requirement to use the Document Cover Sheet and provide supporting documentation.

SUMMARY

This report summarizes generic disposal system modeling (GDSM) activities performed in fiscal year (FY) 2012 for the evaluation of disposal system performance for a variety of options for the geologic disposal of used nuclear fuel (UNF) and high-level radioactive waste (HLW). The two key activities described are (1) the continuing development of a GDSM architecture capable of providing a single common structure for four generic disposal system (GDS) performance assessment (PA) models (representing the disposal options for UNF and HLW in salt, granite, clay, and deep boreholes), and (2) the refinement and application of simplified individual PA models for these four disposal options.

Progress on developing the common GDSM architecture occurred in several areas. A decision was made to pursue an advanced generic PA modeling capability that provides for increased flexibility and more efficient implementation of fundamental representations of multi-physics processes and their couplings within a computational framework that is compatible with high-performance computing technologies. The goal of this advanced modeling capability is to provide a robust total system approach by balancing the development of a conceptual model framework that can represent a range of multi-physics processes for specific subsystems with the development of a computational framework that can facilitate adequate multi-physics couplings across the entire disposal system. Specific activities related to advanced modeling capabilities included:

- Preliminary development of some advanced multi-physics modeling components,
- Systematic development of conceptual models and architecture for the engineered barrier system (EBS) and natural barrier system (NBS) PA submodels,
- Continuing development of an advanced approach for treating diffusion in clay or shale to account for heterogeneity and the impact of electrochemical processes, and
- Design and partial implementation of a parameter database and configuration management strategy to support the PA modeling capability.
- Identification of existing code development efforts having the best combination of multi-physics modeling and computational framework capabilities to support the development of an advanced PA model framework and common GDSM architecture.

Because the GDSM architecture and the advanced modeling capability are still under development, simplified PA models developed prior to FY 2012 were maintained and revised as appropriate. These simplified PA models – the salt GDS model, the granite GDS model, the clay GDS model, and the deep borehole GDS model – were used for the following disposal system performance simulations:

- Probabilistic sensitivity analyses – Some parameter values and model components were updated from prior (FY 2011) versions of the models to examine the sensitivity of system performance to various parameters and submodels.
- Deterministic baseline scenario analyses and sensitivity analyses – Some parameter values and model components were further revised from the versions used for the FY 2012 probabilistic analyses to create more consistency between the four individual models. This set of consistent simulations was used to support a preliminary generic deep geologic disposal safety case.

The results from these simplified PA models provide insights into processes and parameters that could influence disposal system performance, and support a conclusion that all four of the disposal options – salt, granite, clay, and deep borehole – show promise with respect to providing acceptable containment of UNF and HLW under undisturbed conditions. These model insights can inform research needs for each of the disposal options; however, these simplified disposal system models and results are generic and are

likely to change in the future as site-specific information is used, disturbed scenarios are evaluated, and more advanced models are implemented. Due to this limited pedigree, the simplified PA model results are not intended to screen and/or prioritize specific disposal options, designs, and sites for their suitability for a geologic disposal facility.

This work supports the Used Fuel Disposition Campaign within the U.S. Department of Energy, Office of Nuclear Energy, Fuel Cycle Technologies (FCT) Program.

CONTENTS

1 INTRODUCTION 1-1
1.1 Programmatic Objectives 1-1
1.2 Report Content and Organization 1-2

2 GDSM ARCHITECTURE DEVELOPMENT 2-1
2.1 GDSM Overview 2-1
2.1.1 GDSM Conceptual Model Framework Overview 2-2
2.1.2 GDSM Computational Framework Overview 2-6
2.2 PA Model Framework Development 2-7
2.2.1 Development of a Simplified PA Model Framework 2-8
2.2.2 Development of an Advanced PA Model Framework 2-9
2.3 EBS Conceptual Model and Numerical Implementation 2-15
2.3.1 Generic EBS Conceptualization 2-15
2.3.2 Generic EBS FEP Analysis 2-18
2.3.3 Numerical Implementation 2-34
2.4 NBS Conceptual Model and Numerical Implementation 2-35
2.4.1 Generic NBS Conceptualization 2-35
2.4.2 Generic NBS FEP Analysis 2-39
2.4.3 Numerical Implementation 2-41
2.5 Database Development and Configuration Management 2-46
2.5.1 Introduction 2-46
2.5.2 Role of the GDSM Computational Parameter Database in Overall Data Management Structure for the UFDC 2-46
2.5.3 GDSM Computational Parameter Database Requirements 2-49
2.5.4 Modeling/Database Architecture 2-51
2.5.5 Database User Experience 2-54
2.5.6 GDSM Configuration Management Strategy 2-55

3 SIMPLIFIED PA MODEL APPLICATION 3-1
3.1 Salt GDS Model 3-2
3.1.1 Model Description 3-2
3.1.2 Probabilistic Sensitivity Analyses 3-3
3.2 Granite GDS Model 3-9
3.2.1 Model Description 3-9
3.2.2 Probabilistic Sensitivity Analyses 3-11
3.3 Clay GDS Model 3-16
3.3.1 Model Description 3-16
3.3.2 Probabilistic Sensitivity Analyses 3-17
3.4 Deep Borehole GDS Model 3-52
3.4.1 Model Description 3-52
3.4.2 Probabilistic Sensitivity Analyses 3-56
3.5 Deterministic GDS Safety Assessments 3-62
3.5.1 Model Descriptions 3-62
3.5.2 Deterministic Baseline Analyses 3-67
3.5.3 Deterministic Sensitivity Analyses 3-77

4 CONCLUSIONS 4-1

5 REFERENCES 5-1

Appendix A Summary of the Preliminary Generic FEP Evaluation for the EBS A-1

Appendix B Summary of the Preliminary Generic FEP Evaluation for the NBS B-1

Appendix C Documentation of Deterministic GoldSim Parameter Inputs C-1

Appendix D Diffusion Modeling in a Generic Clay Repository D-1

FIGURES

Figure 2-1. Schematic Illustration of GDSM Conceptual Model Components with Mapping to FEP Numbering Hierarchy 2-2

Figure 2-2. Computational Framework Components 2-6

Figure 2-3. Detailed Representation of GDSM Conceptual Model Components 2-17

Figure 2-4. Alternative Implementation Methods of Conceptual Flow Models 2-44

Figure 2-5. Architecture of UFDC Data Management System 2-48

Figure 3-1. A Schematic Showing the Conceptual Model for Radionuclide Release and Transport from a Salt Generic Repository 3-2

Figure 3-2. Mean Advective and Diffusive Mass Flux from the Near-Field Salt DRZ with Revised UNF Inventory for Waste Inventory Case 1 of the Undisturbed Scenario 3-6

Figure 3-3. Mean Annual Dose with Revised UNF Inventory for Waste Inventory Case 1 of the Undisturbed Scenario 3-7

Figure 3-4. Mean Mass Flux from the Repository with Revised UNF Inventory for Waste Inventory Case 1 of the Human Intrusion Scenario 3-8

Figure 3-5. Model Results with Corrected UNF Inventory for Waste Inventory Case 1 of the Human Intrusion Scenario: Mean Annual Dose 3-8

Figure 3-6. Flow Scaling Factors for One Glacial Cycle 3-12

Figure 3-7. Groundwater Velocity Adjusted by Flow Scaling Factors during One Glacial Cycle 3-12

Figure 3-8. ^{237}Np K_d Variation, Affected by Oxidizing Conditions during Glacial Flushing Periods 3-13

Figure 3-9. ^{129}I Mass Flux Out into the Far-Field Granite during One Glacial Cycle 3-13

Figure 3-10. ^{237}Np Mass Flux into the Far-Field Granite during One Glacial Cycle with Flow Rate Change, but no K_d Change 3-14

Figure 3-11. ^{237}Np Mass Flux into the Far-Field Granite during One Glacial Cycle with Flow Rate Change and K_d Change 3-14

Figure 3-12. ^{129}I Mean Annual Dose during One Glacial Cycle 3-15

Figure 3-13. ^{129}I Mean Annual Dose Comparison for Glacial and Temperate Climate Conditions 3-15

Figure 3-14. ^{129}I Diffusion—Inventory Sensitivity 3-22

Figure 3-15. ^{36}Cl Diffusion—Inventory Sensitivity 3-23

Figure 3-16. ^{99}Tc Diffusion—Inventory Sensitivity 3-24

Figure 3-17. ^{237}Np Diffusion—Inventory Sensitivity 3-25

Figure 3-18. ^{129}I Diffusion—Vertical Advective Velocity Sensitivity 3-28

Figure 3-19. ^{36}Cl Diffusion—Vertical Advective Velocity Sensitivity 3-29

Figure 3-20. ^{99}Tc Diffusion—Vertical Advective Velocity Sensitivity 3-30

Figure 3-21. ^{237}Np Diffusion—Vertical Advective Velocity Sensitivity 3-31
Figure 3-22. ^{79}Se Diffusion—Vertical Advective Velocity Sensitivity 3-32
Figure 3-23. Solubility Factor Sensitivity 3-33
Figure 3-24. Solubility Limit Sensitivity 3-34
Figure 3-25. K_d Factor Sensitivity 3-35
Figure 3-26. K_d Sensitivity 3-36
Figure 3-27. ^{129}I Inventory—Waste Form Degradation Rate Sensitivity 3-42
Figure 3-28. ^{36}Cl Inventory—Waste Form Degradation Rate Sensitivity 3-43
Figure 3-29. ^{99}Tc Inventory—Waste Form Degradation Rate Sensitivity 3-44
Figure 3-30. ^{237}Np Inventory—Waste Form Degradation Rate Sensitivity 3-45
Figure 3-31. ^{129}I Diffusion—Waste Package Failure Time Sensitivity 3-47
Figure 3-32. ^{36}Cl Diffusion—Waste Package Failure Time Sensitivity 3-48
Figure 3-33. ^{99}Tc Diffusion—Waste Package Failure Time Sensitivity 3-49
Figure 3-34. ^{237}Np Diffusion—Waste Package Failure Time Sensitivity 3-50
Figure 3-35. Schematic Illustration of Deep Borehole Disposal 3-53
Figure 3-36. Vertical Groundwater Fluxes at Center of Corner Borehole at 3,000-m Depth as a Function of Time for all Permeability Combinations Considered 3-55
Figure 3-37. Vertical Groundwater Fluxes at Center of Corner Borehole at 4,000-m Depth as a Function of Time for all Permeability Combinations Considered 3-55
Figure 3-38. Vertical Groundwater Fluxes at Center of Corner Borehole at 5,000-m Depth as a Function of Time for all Permeability Combinations Considered 3-56
Figure 3-39. Mean Total Dose for Various Rock and Disturbed Zone Permeability Cases 3-57
Figure 3-40. Mean Dose for Dominant Radionuclides for the Base Case Rock and Disturbed Zone Permeability Values 3-58
Figure 3-41. Mean Dose for Dominant Radionuclides for the Upper Bounding Case Rock and Disturbed Zone Permeability Values and the Iodine Getter Case 3-58
Figure 3-42. Partial Rank Correlation Coefficients on Total Dose over Time including Uncertainties in Rock and DZ Permeability Values 3-60
Figure 3-43. Partial Rank Correlation Coefficients on Total Dose Over Time with Iodine Getter and for the Upper Bounding Case Rock and Disturbed Zone Permeability Values. 3-61
Figure 3-44. Salt Baseline Scenario Annual Dose for a Receptor 5,000 m from the Repository 3-67
Figure 3-45. Distribution of ^{129}I in the Salt GDS Model Components 3-68
Figure 3-46. Granite Baseline Scenario Annual Dose for a Receptor 5,000 m from the Repository 3-69
Figure 3-47. Distribution of ^{129}I in the Granite GDS Model Components 3-71
Figure 3-48. Clay Baseline Scenario Annual Dose for a Receptor 150 m from the Repository 3-72

Figure 3-49. Distribution of ^{129}I in the Clay GDS Model Components 3-74

Figure 3-50. Deep Borehole Baseline Scenario Annual Dose for a Receptor Directly Above the Borehole 3-75

Figure 3-51. Distribution of ^{129}I in the Deep Borehole GDS Model Components 3-76

Figure 3-52. Effect of Waste Form Degradation Rate on Annual Dose from ^{129}I in the Salt GDS Model 3-79

Figure 3-53. Effect of Near-Field DRZ Integrity on Annual Dose from ^{129}I in the Salt GDS Model 3-80

Figure 3-54. Effect of Brine Flow Rate on Annual Dose from ^{129}I in the Salt GDS Model 3-82

Figure 3-55. Effect of Diffusion Coefficient on Annual Dose from ^{129}I in the Salt GDS Model 3-83

Figure 3-56. Effect of Interbed Sorption on Annual Dose from ^{129}I in the Salt GDS Model 3-84

Figure 3-57. Effect of Distance to Receptor on Annual Dose from ^{129}I in the Salt GDS Model 3-85

Figure 3-58. Effect of Waste Form Degradation Rate and Gap Fraction on Annual Dose from ^{129}I in the Granite GDS Model 3-87

Figure 3-59. Effect of Waste Package Lifetime on Annual Dose from ^{129}I in the Granite GDS Model 3-88

Figure 3-60. Effect of Sorption in Bentonite Buffer on Annual Dose from ^{129}I in the Granite GDS Model 3-89

Figure 3-61. Effect of Flow Rate on Annual Dose from ^{129}I in the Granite GDS Model 3-90

Figure 3-62. Effect of Diffusion Coefficient on Annual Dose from ^{129}I in the Granite GDS Model 3-91

Figure 3-63. Effect of Sorption in Granite on Annual Dose from ^{129}I in the Granite GDS Model 3-92

Figure 3-64. Effect of Fracture Spacing in Granite on Annual Dose from ^{129}I in the Granite GDS Model 3-93

Figure 3-65. Effect of Distance to Receptor on Annual Dose from ^{129}I in the Granite GDS Model 3-94

Figure 3-66. Effect of Waste Form Degradation Rate on Annual Dose from ^{129}I in the Clay GDS Model 3-96

Figure 3-67. Effect of Waste Package Lifetime on Annual Dose from ^{129}I in the Clay GDS Model ` 3-97

Figure 3-68. Effect of Buffer and DRZ Integrity on Annual Dose from ^{129}I in the Clay GDS Model 3-98

Figure 3-69. Effect of Flow Rate on Annual Dose from ^{129}I in the Clay GDS Model 3-99

Figure 3-70. Effect of Diffusion Coefficient on Annual Dose from ^{129}I in the Clay GDS Model 3-100

Figure 3-71. Effect of Clay Sorption on Annual Dose from ^{129}I in the Clay GDS Model 3-101

Figure 3-72. Effect of Overlying Clay Thickness on Annual Dose from ^{129}I in the Clay GDS Model 3-102

Figure 3-73. Effect of Waste Form Degradation Rate on Annual Dose from ^{129}I in the Deep Borehole Model 3-104

Figure 3-74. Effect of Sorption in the Disposal Zone on Annual Dose from ^{129}I in the Deep Borehole GDS Model 3-105

Figure 3-75. Effect of Sorption in the Seal Zone on Annual Dose from ^{129}I in the Deep Borehole GDS Model 3-106

Figure 3-76. Effect of Diffusion Coefficient on Annual Dose from ^{129}I in the Deep Borehole GDS Model 3-107

TABLES

Table 2-1. Functional Requirements of the GDSM Computational Parameter Database....2-50
Table 2-2. Summary of Roles and Responsibilities for GDSM Configuration Management....2-57
Table 3-1. Salt GDS Model Components and Features....3-3
Table 3-2. Revised Isotopic Mass Inventory for Commercial UNF for the Salt GDS Model....3-4
Table 3-3. Granite GDS Model Components and Features....3-9
Table 3-4. Revised Parameter Values for the Granite GDS Model....3-10
Table 3-5. Duration of Each Climate Period in a Simplified 120,000-Year Glacial Cycle....3-11
Table 3-6. Clay GDS Model Components and Features....3-16
Table 3-7. Simulation Group Structure for Individual and Dual Parameter Sensitivity Analyses....3-18
Table 3-8. Diffusion Coefficient and Mass Factor Simulation Groupings....3-20
Table 3-9. Vertical Advective Velocity and Diffusion Coefficient Simulation Groupings....3-27
Table 3-10. Safety Indicators for the Actinides and Their Daughters....3-38
Table 3-11. Safety Indicators for Soluble, Non-Sorbing Radionuclides....3-39
Table 3-12. Safety Indicators for Solubility-Limited and Sorbing Radionuclides....3-40
Table 3-13. Simulation Groupings for Vertical Path Length Sensitivity Analysis....3-51
Table 3-14. Deep Borehole GDS Model Components and Features....3-53
Table 3-15. Host Rock and Disturbed Zone Permeability Values Used in TH Simulations....3-54
Table 3-16. Stepwise Rank Regression Analysis over Total Dose at 1 Million Years, for Combined Results Including Uncertainties in Rock and DZ Permeability Values....3-59
Table 3-17. Stepwise Regression Analysis over Total Dose at 1 Million Years with Iodine Getter (Sorbent) and for the Upper Bounding Case Rock and DZ Permeability Values....3-61
Table 3-18. Summary of the Salt Baseline Scenario Model....3-63
Table 3-19. Summary of the Granite Baseline Scenario Model....3-64
Table 3-20. Summary of the Clay Baseline Scenario Model....3-65
Table 3-21. Summary of the Deep Borehole Baseline Scenario Model....3-66
Table 3-22. Summary of the Baseline Brine Flow....3-81
Table A-1. Included FEPs for Outer EBS Components (Upstream and Downstream)....A-3
Table A-2. Included FEPs for Interior EBS Components (Upstream and Downstream)....A-4
Table A-3. Included FEPs for Waste Package Components (Diversion and Containment)....A-6
Table A-4. Included FEPs for Waste Form and Waste Package Internals Components....A-8
Table B-1. Included FEPs for the Natural Barrier System....B-2
Table C-1. Summary of the Deterministic Approximations for the Salt GDS Model....C-3

Table C-2. Summary of the Deterministic Approximations for the Granite GDS Model C-5
Table C-3. Summary of the Deterministic Approximations for the Clay GDS Model C-9
Table C-4. Summary of the Deterministic Approximations for the Deep Borehole GDS Model..... C-12

ACRONYMS

1D	one dimensional
2D	two dimensional
3D	three dimensional
ADSM	Advanced Disposal System Modeling
Andra	Agence Nationale pour la gestion des Déchets Radioactifs (French National Radioactive Waste Management Agency)
ANL	Argonne National Laboratory
APAC	Advanced Performance Assessment Code
BSC	Bechtel SAIC Co.
DLL	dynamic link library
DOCR	document repository
DOE	U.S. Department of Energy
DOE-NE	U.S. Department of Energy Office of Nuclear Energy
DRZ	disturbed rock zone
DZ	disturbed zone (specific to the deep borehole GDS model)
EBS	engineered barrier system
ECN	External Collaboration Network
EDZ	excavation disturbed zone
ERB	example reference biosphere
F&T	flow and transport
FCT	Fuel Cycle Technologies
FEHM	Finite Element Heat and Mass Transfer
FEP	feature, event, and process
FY	fiscal year
GDS	generic disposal system (specific to individual, simplified PA models known as GDS models)
GDSM	Generic Disposal System Model or Modeling
GPAM	generic performance assessment model
GUI	graphical user interface
HLW	high-level radioactive waste
HPC	high performance computing

HTO	tritiated water
IAEA	International Atomic Energy Agency
ID	Identification
IPSC	Integrated Performance and Safety Codes
IT	information technology
KBS	KärnBränsleSäkerhet (Nuclear Fuel Safety)
LANL	Los Alamos National Laboratory
LBNL	Lawrence Berkeley National Laboratory
MIC	microbially influenced corrosion
MIT	Massachusetts Institute of Technology
MTHM	metric tons of heavy metal
MTU	metric tons of uranium
Nagra	Nationale Genossenschaft für die Lagerung Radioaktiver Abfälle (Swiss National Cooperative for the Disposal of Radioactive Waste)
NBS	natural barrier system
NE	Office of Nuclear Energy
NEAMS	Nuclear Energy Advanced Modeling and Simulation
ODBC	open database connectivity
PA	performance assessment
PADB	performance assessment database
PWR	pressurized water reactor
R&D	research and development
SCC	stress corrosion cracking
SciDAC	Science Discovery through Advanced Computing
SKB	Svensk Kämbränslehantering AB (Swedish Nuclear Fuel and Waste Management Company)
SNF	spent nuclear fuel
SNL	Sandia National Laboratories
TDB	technical database
TH	thermal-hydrologic
THC	thermal-hydrologic-chemical
THCM	thermal-hydrologic-chemical-mechanical
THCMBR	thermal-hydrologic-chemical-mechanical-biological-radiological

THM	thermal-hydrologic-mechanical
TSPA-LA	Total System Performance Assessment for the License Application
UFDC	Used Fuel Disposition Campaign
UNF	used nuclear fuel
UZ	unsaturated zone
V0	version 0
V1	version 1
WIPP	Waste Isolation Pilot Plant
WP	waste package
YMP	Yucca Mountain Project

GENERIC DISPOSAL SYSTEM MODEL: ARCHITECTURE, IMPLEMENTATION, AND DEMONSTRATION

1 INTRODUCTION

This report summarizes generic disposal system modeling (GDSM) activities performed in fiscal year (FY) 2012 for the evaluation of disposal system performance for a variety of geologic disposal system options to support the Used Fuel Disposition Campaign (UFDC). The UFDC operates under the U.S. Department of Energy (DOE) Office of Nuclear Energy (NE) Fuel Cycle Technologies (FCT) Program.

UFDC GDSM activities are managed within the GDSM work package. The GDSM work package activities are focused on the development of disposal system modeling capabilities to support the evaluation of a range of generic geologic disposal options at varying levels of complexity. GDSM activities are augmented by Advanced Disposal System Modeling (ADSM) work package activities that are focused on the acquisition or development of a performance assessment (PA) model framework for implementing the GDSM capabilities.

This report satisfies DOE Level 2 Milestone Number M2FT-12SN0808042. It describes FY 2012 activities managed within the GDSM work package and integrates the content of the following GDSM Level 4 Milestone reports that were completed throughout FY 2012:

- M4FT-12SN0808044: Generic Performance Assessment Model: Architecture, Implementation, and Demonstration
- M4FT-12SN0808045: Generic Natural System Conceptual Model and Numerical Architecture
- M4FT-12SN0808046: Generic Engineered Barrier System Conceptual Model and System Architecture
- M4FT-12SN0808047: GDSM Database and Computation Environment Description and Implementation
- M4FT-12AN0808011: Clay GDSM Model Development, Demonstration, Analysis
- M4FT-12LA0808021: Generic System Model Refinement: (Granite)
- M4FT-12LB0808032: Diffusion Modeling in a Generic Clay Repository: Impacts of Heterogeneity and Electro-chemical Process

This report also incorporates relevant information from the ADSM FY 2012 Level 3 Milestone report (Freeze and Vaughn 2012).

The FY 2012 GDSM activities involved scientists from Sandia National Laboratories (SNL), Argonne National Laboratory (ANL), Los Alamos National Laboratory (LANL), and Lawrence Berkeley National Laboratory (LBNL) and are a continuation of FY 2011 activities (Clayton et al. 2011).

1.1 Programmatic Objectives

The mission of the UFDC is to identify alternatives and conduct scientific research and technology development to enable storage, transportation, and disposal of used nuclear fuel (UNF) and wastes generated by existing and future nuclear fuel cycles (DOE 2010, Section 3.7.1). To support this mission, the UFDC has established a number of near-term (i.e., 5-year) and long-term objectives. UFDC objectives specific to disposal system modeling include (DOE 2010, Section 3.7.1):

- **Short-Term Objective 1—**Provide technical expertise to inform policy decision-making regarding the transportation, storage, and disposal of UNF and radioactive waste that would be generated under existing and potential future nuclear fuel cycles.
- **Short-Term Objective 4—**Develop a comprehensive understanding of the current technical bases for disposing of UNF, low-level nuclear waste, and high-level nuclear waste in a range of potential disposal environments to identify opportunities for long-term research and development.
- **Short-Term Objective 5—**Continue model development for the evaluation of disposal system performance in a variety of generic media and generic disposal system concepts.
- **Long-Term Objective 3—**Develop a fundamental understanding of disposal system performance in a range of geologic media for potential wastes that could arise from future nuclear fuel cycle alternatives through theory, simulation, testing, and experimentation.
- **Long-Term Objective 4—**Develop a computational modeling capability for the performance of storage and disposal options for a range of fuel cycle alternatives, evolving from generic models to more robust models of performance assessment.

In addition, DOE (2010, Section 3.7.3) identifies the following five-year research and development (R&D) activity relevant to disposal system modeling:

- Develop a framework of computational models for disposal system performance, including both process-level models for the performance of specific component of engineered and natural barrier systems and system-level models of generic disposal concepts.

The objective of the GDSM work package activities, augmented by ADSM activities, is to create a disposal system modeling capability that (1) facilitates science-based evaluation of disposal system performance for a range of fuel cycle alternatives in a variety of geologic media and generic disposal system concepts, and (2) takes advantage of high performance computing (HPC) technologies, as needed. This capability will facilitate PA model development, execution, and evaluation consistent with the UFDC near-term and long-term objectives and will support the evolving needs of the UFDC to produce risk information throughout the potential future phases of the mission including: identification and prioritization of R&D needs; evaluation of disposal option viability; site selection and screening; and licensing support.

1.2 Report Content and Organization

This report summarizes activities to develop a UFDC GDSM capability. The following definitions are provided to ensure consistent understanding of terminology used throughout the report:

- **Used nuclear fuel (UNF)—**Irradiated fuel withdrawn from a nuclear reactor and stored pending reprocessing, recycling, or for which the manner of disposition has not been determined. In the U.S. (i.e., within the UFDC) this term is preferred, where appropriate, and is used extensively in this report.
- **Spent nuclear fuel (SNF)—**Irradiated fuel withdrawn from a nuclear reactor that is intended for permanent disposal without further reuse. In non-U.S. programs, the distinction between UNF and SNF is not made, and SNF is used to refer to all irradiated fuel from reactors. In this report, the term SNF is used where necessary to retain its original meaning.
- **High-level radioactive waste (HLW)—**Highly radioactive material resulting from the reprocessing of UNF.
- **Conceptual model—**A representation of the behavior of a real-world process, phenomenon, or object as an aggregation of scientific concepts, so as to enable predictions about its behavior. Such a model

consists of concepts related to geometrical elements of the object (size and shape); dimensionality (one-, two-, or three-dimensional (1D, 2D, or 3D)); time dependence (steady-state or transient); applicable conservation principles (mass, momentum, energy); applicable constitutive relations; significant processes; boundary conditions; and initial conditions (NRC 1999, Appendix C).

- **Mathematical model—**A representation of a conceptual model of a system, subsystem, or component through the use of mathematics. Mathematical models can be mechanistic, in which the causal relations are based on physical conservation principles and constitutive equations. In empirical models, causal relations are based entirely on observations (NRC 1999, Appendix C).
- **Numerical model—**An approximate representation of a mathematical model that is constructed using a numerical description method such as finite volumes, finite differences, or finite elements. A numerical model is typically represented by a series of program statements that are executed on a computer (NRC 2003, Glossary).
- **Computer code—**An implementation of a mathematical model on a digital computer generally in a higher-order computer language such as FORTRAN or C (NRC 1999, Appendix C).
- **Disposal options—**Combinations of disposal concept (e.g., waste type, repository and emplacement geometry, engineered components) and geologic setting (e.g., salt, clay/shale, crystalline rock) that describe the disposal system. The UFDC is actively evaluating four concepts for the long-term disposal of UNF and HLW: mined geologic disposal in three media (salt, clay, and crystalline rock); and deep borehole disposal in crystalline rock. For each of these options, the rock type is identified at a broad level: salt includes both bedded and domal formations; clay includes a broad range of fine-grained sedimentary rocks including shales, argillites, and claystones as well as soft clays; and crystalline rock includes granite, granitic gneiss, and other felsic igneous and metamorphic rock types.
- **Generic disposal system model (GDSM) —**A conceptual description of the generic disposal system components for a specific disposal option. For each GDSM, the disposal system is represented by the conceptual models (and, in some cases, mathematical models) of the system components and their interactions. As will be described in Section 2, there are some component conceptual models common to all four of the GDSMs. The term GDSM is also sometimes used to collectively refer to the set of four UFDC generic disposal system (GDS) models. Finally, the term GDSM is also used when referring to the Generic Disposal System Modeling work package.
- **Performance assessment (PA) model—**A PA model derives from the steps of a PA methodology (Meacham et al. 2011, Section 1): feature, event, and process (FEP) analysis; scenario construction; uncertainty quantification; and development of an integrated system model (incorporating conceptual, mathematical, and numerical model considerations). The terms PA model and GDSM are used somewhat interchangeably in this report, but a PA model typically includes greater specification of the mathematical and numerical implementation. Furthermore, to perform calculations with a PA model, a computer code that implements the numerical model must be specified.
- **GDSM architecture—**The overarching structure that facilitates the development of GDSMs, their implementation in PA models, and the associated data management. The goal of the UFDC GDSM architecture is to provide a single common structure that is applicable to all UFDC disposal options.
- **PA model framework—**The combination of conceptual model and computational components that facilitate PA model development, execution, and evaluation within a formal PA methodology.

The report is organized into the following sections and appendices:

- **Section 1: Introduction**
- **Section 2: GDSM Architecture Development—**Describes the continuing development of the GDSM architecture, which includes: a PA model framework; an engineered barrier system (EBS) conceptual submodel; a natural barrier system (NBS) conceptual submodel; and parameter database and configuration management components. The description includes development of both simplified and advanced PA model frameworks.
- **Section 3: Simplified PA Model Application—**Describes the FY 2012 application of simplified individual GDS models for salt, clay, granite, and deep borehole. The description includes refinements from the FY 2011 GDS models (Clayton et al. 2011, Section 3) and results that demonstrate the current model capabilities and identify processes and parameters expected to be important to disposal system performance. These results can provide insights to guide future research needs.
- **Section 4: Conclusions**
- **Appendix A: Summary of the Preliminary Generic FEP Evaluation Results for the EBS**
- **Appendix B: Summary of the Preliminary Generic FEP Evaluation Results for the NBS**
- **Appendix C: Documentation of Deterministic GoldSim Parameter Inputs**
- **Appendix D: Diffusion Modeling in a Generic Clay Repository**

2 GDSM ARCHITECTURE DEVELOPMENT

This section describes the continuing development of the GDSM architecture that can provide a single common structure that is applicable to all UFDC disposal system models. Following a GDSM overview (Section 2.1), refinements to the components the GDSM architecture from FY 2011 (Clayton et al. 2011, Section 4) are summarized, including: the PA model framework (Section 2.2); the EBS conceptual submodel (Section 2.3); the NBS conceptual submodel (Section 2.4); and parameter database and configuration management functions (Section 2.5).

2.1 GDSM Overview

As described in Section 1.1, the objective of the GDSM work package activities is to create a GDSM capability for the science-based evaluation of disposal system performance for a range of generic disposal system options. The GDSM capability is managed through an overarching GDSM architecture that facilitates:

- Examination of multiple generic and site-specific geologic disposal options at levels of complexity that are expected to increase as the UFDC matures
- Evaluation of system- and subsystem-level performance
- Uncertainty and sensitivity analyses to isolate key subsystem processes and components
- Modular integration of representations of subsystem processes and couplings, where the level of complexity of the representation may vary with intended use or relative importance to the total system
- Data and configuration management functions

The GDSM architecture will be implemented through a PA model framework. The two main components of a PA model framework are (Freeze and Vaughn 2012, Section 2):

- A *conceptual multi-physics model framework* that facilitates development of
  - a conceptual model of the important FEPs and scenarios that describe the multi-physics phenomena of a specific UFDC disposal system and its subsystem components, and
  - a mathematical model (e.g., governing equations) that implements the representations of the important FEPs and their couplings.
- A *computational framework* that facilitates integration of
  - the system analysis workflow (e.g., input pre-processing, integration and numerical solution of the mathematical representations of the conceptual model components, output post-processing), and
  - the supporting capabilities (e.g., mesh generation, input parameter specification and traceability, matrix solvers, visualization, uncertainty quantification and sensitivity analysis, file configuration management, compatibility with HPC environments).

The conceptual multi-physics model framework supports conceptual model development of the various GDSM submodels. Conceptual model framework considerations are described in Section 2.1.1. The computational framework supports the numerical model and computer code implementation, including advanced modeling and HPC considerations. Computational framework considerations are described in Section 2.1.2. Development of the simplified and advanced PA model frameworks is described in Section 2.2.

2.1.1 GDSM Conceptual Model Framework Overview

A detailed discussion of conceptual model framework considerations and components is provided in Freeze and Vaughn (2012, Section 2.2) and provides a basis for the overview presented here.

The GDSM conceptual model framework is organized around three disposal system regions, illustrated schematically in Figure 2-1: the EBS, the NBS, and the Biosphere. These three regions are common to all UFDC generic disposal options. Each region, in turn, consists of one or more common generic features, although not all of the disposal options necessarily contain all of the generic features. Collectively, these regions and features are the GDSM conceptual model framework components.

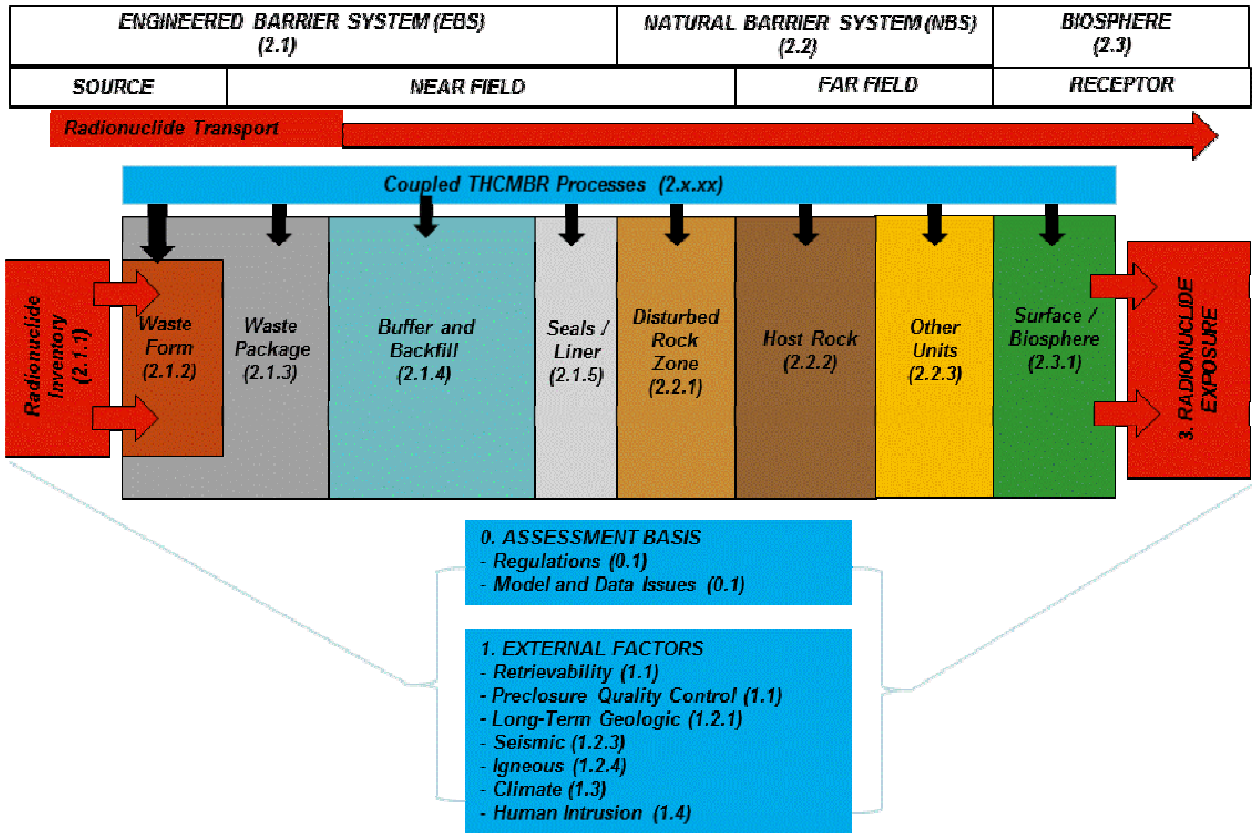

NOTE: THCMBR = thermal-hydrologic-chemical-mechanical-biological-radiological

Figure 2-1. Schematic Illustration of GDSM Conceptual Model Components with Mapping to FEP Numbering Hierarchy

The generic EBS features include: Waste Form (including radionuclide inventory), Waste Package, Buffer and Backfill, and Seals and Liner. The generic NBS features include: Disturbed Rock Zone (DRZ), Host Rock, and Other Geologic Units (above and below the repository, and including any aquifers, if present). The DRZ is the portion of the host rock adjacent to the EBS that experiences durable (but not necessarily permanent) changes due to the presence of the repository. Immediately adjacent to the EBS, these repository-induced changes are more likely to be permanent (e.g., mechanical alteration due to excavation), whereas further from the EBS the repository-induced changes are more likely to be time-dependent but not permanent (e.g., thermal effects due to radioactive decay of waste). The DRZ is sometimes referred to as the excavation damaged zone or the excavation disturbed zone (EDZ). However, in this report, DRZ is preferred because it more accurately represents the fact that the disturbed zone includes effects from excavation and waste emplacement. The generic Biosphere is represented by a

human receptor. The effects of radionuclide releases from the NBS to the receptor, located in the Biosphere, are dependent on assumptions about behaviors and characteristics of the receptor and the physical location and evolution of the Biosphere. The relationship between the GDSM components and alternate terms that are commonly used to describe a disposal system, near field and far field, are also shown in Figure 2-1. The near field encompasses the EBS and the DRZ (i.e., the components influenced by the presence of the repository). The far field encompasses the remainder of the NBS (i.e., beyond the influence of the repository).

Figure 2-1 also illustrates schematically how radionuclide movement from the waste form to the receptor is influenced by multi-physics phenomena that can act upon and within each of the GDSM components. These multi-physics phenomena include, at a high level, the thermal-hydrologic-chemical-mechanical-biological-radiological (THCMBR) processes and external events (e.g., seismicity) that describe (1) waste form and waste package degradation, (2) radionuclide mobilization from the waste form and radionuclide release from the waste package (identified as the radionuclide source in Figure 2-1), (3) radionuclide transport through the near field and far field, and (4) radionuclide transport, uptake, and health effects in the biosphere. In addition to their direct effects on radionuclide transport, the THCMBR processes also influence the physical and chemical environments (e.g., temperature, fluid chemistry, biology, mechanical alteration) in the EBS, NBS, and Biosphere, which in turn affect water movement, degradation of EBS components, and radionuclide transport. Further discussion of the generic EBS processes is provided in Section 2.3 and in Hardin (2012, Sections 2 and 3). Further discussion of the generic NBS processes is provided in Section 2.4 and in Arnold et al. (2012, Sections 2 and 3).

It should be noted that the schematic illustration in Figure 2-1 is 1D. In reality, a disposal system consists of a set of nested 3D components. For example, the NBS completely surrounds the EBS and radionuclides can be transported from the EBS to the NBS along multiple flow pathways; these details are not shown in Figure 2-1.

A geologic disposal system generally relies on the performance attributes of multiple barriers (i.e., the EBS and NBS) to isolate waste from the environment and limit the migration of materials that could be released from the disposal facility. These barriers have different performance attributes for the different disposal options and depend, in part, on the inventory and waste forms being disposed and the natural and perturbed characteristics of the disposal option environment. The barrier capabilities of the EBS and NBS also vary with time. In general the EBS provides a shorter-term barrier capability than the NBS. They work in unison to provide the overall disposal system with effective isolation and containment performance.

The generic GDSM components, and the associated THCMBR processes and events, are consistent with the generic features defined in the UFDC FEP list (Freeze et al. 2010; Freeze et al. 2011). As described in Freeze et al. (2010, Section 2), the UFDC FEP list derived from an international FEP list that included phenomena from 10 different national radioactive waste disposal programs covering a wide range of waste forms, disposal concepts, and geologic settings. As a result, the UFDC FEP list represents a comprehensive set of phenomena potentially relevant to a wide range of disposal system options. Correspondingly, the generic GDSM components are a comprehensive set of disposal system components applicable to a wide range of potential disposal options, including the four UFDC disposal options mentioned previously and three additional open emplacement concepts identified by Hardin (2012, Section 2). The UFDC FEP list contains 208 FEPs that are classified using a hierarchical numbering scheme that associates each FEP with a specific feature. In Figure 2-1 the FEP classification and numbering hierarchy is overlain on the schematic illustration of the GDSM components.

The combination of generic disposal system components and THCMBR phenomena forms the basis of the GDSM conceptual multi-physics model framework. The GDSM is modular such that, for a specific disposal system option, relevant system components and FEPs can be identified and formed into scenarios

– combinations of important FEPs that represent possible future states of the system. The goal of scenario development is to construct a set of scenarios that (1) represent all of the important (i.e., included) FEPs, and (2) cover the spectrum of possible future states of the disposal system. Scenario development typically results in the creation of an undisturbed scenario (sometimes referred to as nominal or expected or reference) and one or more disturbed scenarios (sometimes referred to as alternative or disruptive). The nominal scenario is typically, but not necessarily, considered to represent the most likely or expected evolution of the disposal system. Disturbed scenarios describe the evolution of the system if altered by phenomena such as human intrusion, seismicity, volcanism, or unexpected component failures.

The development of a conceptual model for a specific disposal option thus involves performing FEP identification and screening, and then constructing plausible scenarios. Based on preliminary generic FEP analyses for the EBS (Section 2.3.2 and Appendix A) and NBS (Section 2.4.2 and Appendix B), the GDSM conceptual model should have the capability to represent, at a minimum, the following spatially variable and time-dependent multi-physics processes:

- *Source (Inventory and Waste Form)*
  - Radionuclide inventory (heat generation, decay and ingrowth)
  - Waste form degradation (dissolution processes)
  - Gas generation
  - Radionuclide release and transport (mobilization, early release [e.g., from gap and grain boundaries], precipitation/dissolution)

- *Near Field (Waste Package, Buffer, Backfill, Seals/Liner, and DRZ)*
  - Waste package degradation (corrosion processes, mechanical damage, early failures)
  - Evolution/degradation of EBS components and DRZ
  - Effects from rockfall, drift collapse (e.g., salt creep)
  - Fluid flow and radionuclide transport (advection, dispersion, diffusion, sorption, decay and ingrowth)
  - Chemical interactions (aqueous speciation, mineral precipitation/dissolution, reaction with degraded materials, surface complexation, radiolysis)
  - Thermal effects on flow and chemistry
  - Effects from disruptive events (seismicity, human intrusion)

- *Far Field (Host Rock and Other Units)*
  - Fluid flow and radionuclide transport (advection, dispersion, diffusion, sorption, decay and ingrowth)
  - Effects of fracture flow (e.g., dual porosity/permeability, discrete fracture)
  - Groundwater chemistry

- *Receptor (Biosphere)*
  - Dilution due to mixing of contaminated and uncontaminated waters
  - Receptor characteristics (basis for converting radionuclide concentrations in groundwater to dose)

Processes in the EBS are likely to differ from NBS processes in several aspects. The EBS contains the waste form, and therefore the greatest concentrations of radionuclides. Concentration-dependent chemical

transport processes such as precipitation of radionuclide bearing solid phases, and proximity-dependent processes such as sorption on corrosion products of man-made materials, are typically included in the EBS model but may be neglected in the NBS model. Materials used in the EBS such as metals, alloys, and glass are man-made and subject to degradation in the disposal environment, whereas natural geologic media comprising the NBS have been subject to the natural environment for millions of years, and have achieved more stable forms. Heating can affect the EBS and the near-field portion of the NBS, and should be included consistently in both parts of the system model. The EBS configuration may be changed by disruptive events (e.g., seismic ground motion and faulting), whereas the state of the NBS reflects cumulative effects from past natural events and is less likely to change significantly or permanently from future events. However, disruptions of the NBS such as changes in the groundwater system associated with glaciation or seismicity can be significant, depending on site-specific system responses.

To perform a quantitative evaluation of the specific disposal option, mathematical representations of the conceptual model FEPs and scenarios need to be developed. The complexity of the representation of these FEPs in a disposal system PA model is dependent on their importance to the performance and safety of the disposal system. Simpler process representation may be sufficient in early PA model iterations, with more complex representations introduced, as needed, during later iterations. For example, flow and transport may initially consider only single-phase, fully saturated conditions. However, for some disposal options (e.g., salt) gas generation processes may be important, and the capability to evaluate unsaturated and multi-phase flow and transport will eventually be needed.

The modularity of the generic conceptual model framework permits the mathematical representations of the FEPs to range from simple abstractions with uni-directional linkages to complex coupled multi-physics processes with implicit bi-directional couplings. While the generic disposal system components and FEPs described above provide a useful basis for developing a disposal system conceptual model, the development of mathematical models (and subsequent computational models) for a specific disposal system option requires a number of additional modeling details to be addressed. These modeling details, which generally are dependent on the level of complexity of the conceptual model and/or the desired mathematical models, include:

- **Spatial Representation of the Disposal System—**The number of features, regions, and/or components and the corresponding spatial discretization
- **Mathematical Representations of the FEPs and Scenarios—**Governing equations describing the geometry (e.g., 1D or 3D), representation of the key THCMBR processes (ranging from simplified to very detailed), and degree of multi-physics process coupling
- **Numerical Implementation of the Mathematical Models—**Numerical methods and solution techniques (which may include the application of HPC capabilities) to solve the governing equations deriving from the multi-physics processes and couplings

These modeling details, which are inter-related, provide an interface between the conceptual model framework (via the governing equations describing the coupled multi-physics) and the computational framework (via the numerical model implementation). HPC capabilities can enhance the efficiency of the numerical solution and thus allow for more complex and/or fundamental multi-physics representations, as needed. HPC capabilities include: object oriented design, advanced numerical methods (e.g., spatial and temporal integration methods, linear and nonlinear solvers), parallel execution, agile code development, software reuse (e.g., Trilinos and Sierra Tool Kit libraries), and ability to use new computer hardware architectures, embedded uncertainty quantification, and 3D animated graphics.

2.1.2 GDSM Computational Framework Overview

A detailed discussion of computational framework considerations and components is provided in Freeze and Vaughn (2012, Section 2.3) and provides a basis for the overview presented here.

A computational framework controls the flow of information among the PA model components (i.e., the system analysis workflow) and between the PA model components and the supporting capabilities. The computational framework is not concerned with the physics that is modeled in the various PA model components, only with the linkages and interfaces. Computational framework capabilities are implemented through integrated computer codes.

To facilitate the integration of system analysis workflow and supporting capabilities, the GDSM computational framework includes the following components, also shown in Figure 2-2:

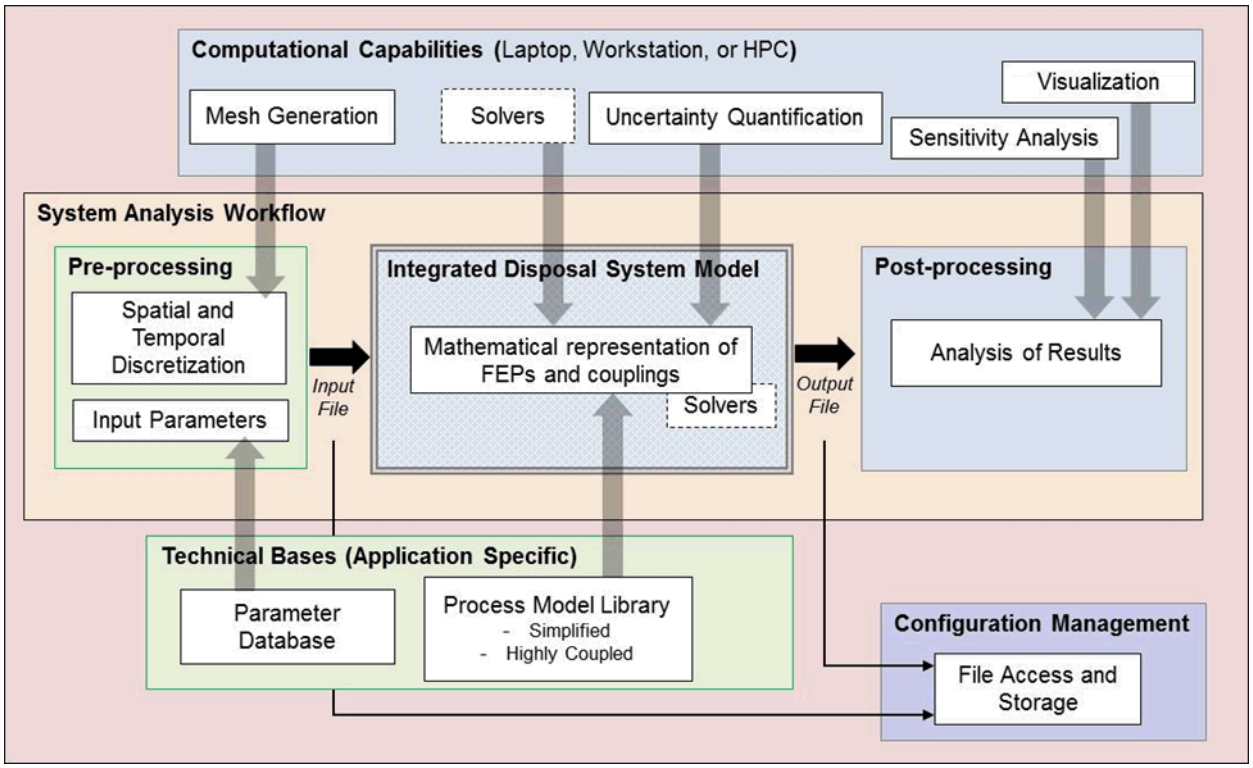

Source: Freeze and Vaughn 2012, Figure 2-6.

Figure 2-2. Computational Framework Components

System Analysis Workflow—This component controls the development and execution of the integrated system model through the following:

- Pre-processing (spatial and temporal discretization, input parameter specification and traceability)
- Integrated system model implementation and execution (mathematical representations of FEPs and couplings)
- Post-processing (analysis of results)

Computational Capabilities—This component enables the System Analysis Workflow by supporting the following:

- Input development (mesh generation)
- System model development and execution (data structure and matrix solvers, uncertainty quantification)
- Output management (visualization, sensitivity analyses)

Configuration Management and Technical Bases—This component enables the System Analysis Workflow by supporting the following:

- Input development (parameter database, file access and storage)
- System model development and execution (process model/governing equation library, data structure and matrix solvers, uncertainty quantification)
- Output management (file access and storage)

As shown in Figure 2-2, the integrated disposal system model is central to the System Analysis Workflow component, which in turn is the central component of the computational framework. Within the computational framework, the integrated disposal system model is the integrated set of numerical representations of the subsystem components and multi-physics phenomena (i.e., the governing equations describing the included FEPs) for a specific disposal system option. More specifically, the integrated disposal system model is defined by the governing equations, initial and boundary conditions, and input parameters that describe the integrated disposal system FEPs and scenarios.

The Computational Capabilities component enables the numerical solution of the integrated set of governing equations by providing capabilities for mesh generation, uncertainty quantification, and numerical solution techniques. The Computational Capabilities component also enables analyses of model results by providing capabilities for visualization and sensitivity analysis.

The Configuration Management and Technical Bases component supports the development of the integrated disposal system model by providing capabilities for specification of input parameters and distributions, and of the multi-physics submodel components to be used, e.g. (from the process model library). This component also controls the flow of information throughout the calculation through configuration management.

2.2 PA Model Framework Development

As described in Section 2.1, the GDSM architecture that provides a structure for the UFDC GDSM capability is implemented in the form of a PA model framework. The development of the PA model framework involves two major efforts: (1) the identification and implementation of conceptual multi-physics models describing the FEPs occurring in each of the disposal system components, and (2) the identification and implementation of a computational framework for integrating the conceptual model components together into a cohesive system and managing the flow of information and execution of calculations. These two efforts are addressed by the conceptual model framework (Section 2.1.1) and the computational framework (Section 2.1.2), respectively.

The challenge in developing a disposal system PA modeling capability is one of balancing these two efforts. An over-emphasis on computational framework development can result in a very robust framework code with extensive functionality, but may fail to provide adequate capabilities to address the range of multi-physics needed to represent the system being modeled. The result is an elegant computational framework tool that cannot be used to address issues regarding disposal system performance because of a lack of multi-physics modeling capabilities. This over-focus on computational

framework development is a common cause leading to the cessation or failure of system modeling framework development projects, because the ultimate objective should be to solve a multi-physics problem. Conversely, an over-emphasis on the development of specific process modeling capabilities can result in very accurate conceptual and numerical representations of independent subsystem processes, but may fail to provide a mechanism to integrate those subsystem processes into a robust total system model or to integrate the multi-physics within or across subsystems. The result is a good representation of subsystem processes, but a limited ability to address issues related to integrated disposal system performance. The ongoing development of the GDSM PA modeling capability for UFDC attempts to balance these two efforts; it aims to provide an adequate range of process models while facilitating adequate multi-physics couplings across the entire disposal system.

This section describes the following activities, related to the development of a GDSM PA modeling capability:

- Continued development of a simplified PA model framework (Section 2.2.1)
- Initial development of components of an advanced PA model framework (Section 2.2.2)

2.2.1 Development of a Simplified PA Model Framework

In FY 2011, a first iteration of a simplified PA model framework, referred to as the generic performance assessment model (GPAM) version 0 (V0), was developed (Clayton et al. 2011, Section 4). GPAM V0 included a conceptual model framework and governing equations (Clayton et al. 2011, Section 4.1) and a computational implementation (Clayton et al. 2011, Section 4.2) using GoldSim software (GoldSim Technology Group 2010a). GPAM V0 consisted of a GoldSim model file (*Generic_PA_Model_R00.gsm*, dated 08/03/11 12:39 PM) (Clayton et al. 2011, Section 4.2.1) and a Microsoft Excel® parameter input spreadsheet (*GPAM_Model_Input.xlsx*) (Clayton et al. 2011, Section 4.2.2.1). In FY 2011, some simplified individual GDS models for salt, clay, granite, and deep borehole were developed and executed (Clayton et al. 2011, Section 3). These individual GDS models used GoldSim but were developed outside of the GPAM framework, meaning that there were some minor inconsistencies in various component submodels across the four disposal options.

In FY 2012 it was planned to bring the four individual GDS models into the common GPAM framework (Clayton et al. 2011, Section 4.3). A revised version of the framework, GPAM version 1 (V1) (*Generic_PA_Model_R01_001v.gsm*, dated 04/09/12 10:54 AM), was created to better accommodate the components of the individual GDS models. GPAM V1 included the following changes from GPAM V0:

- Implemented 8 solubility and 12 sorption data sets. These data sets capture the solubility and sorption (distribution coefficient, K_d) values needed to simulate all four UFDC disposal options (salt, clay, granite, and deep borehole) and are supported by corresponding changes to the Excel input file, *GPAM_Model_Input.xlsx*.
- Updated the results elements and added a mass balance calculation for results checking
- Added the capability to specify the available porosity in the Near-Field Host Rock Region separately from the available porosity in the Far-Field Host Rock Region and made corresponding changes to the Excel input file, *GPAM_Model_Input.xlsx*
- Corrected the dispersivity input for the Aquifer Region

GoldSim (GoldSim Technology Group 2010a) is a commercial system simulation framework. The GoldSim Contaminant Transport Module (GoldSim Technology Group 2010b) provides numerical solutions to simple mathematical representations of processes relevant to disposal system performance such as: waste degradation, radionuclide mobilization and release, radionuclide transport, and receptor health effects. However, the application of GoldSim to complex disposal system models has some

limitations. For example, for the Yucca Mountain Project (YMP) Total System Performance Assessment for the License Application (TSPA-LA), the computational burden of the underlying process models prevented direct coupling into the GoldSim-based TSPA-LA model because the resulting execution times were excessive (GoldSim has distributed processing, but not HPC). Therefore, most YMP process models were abstracted in one form or another, and then incorporated into the TSPA-LA model as response surfaces or look-up tables (SNL 2008d, Section 1.8.2.1). This abstraction-based approach using GoldSim is appropriate for a specific disposal system design and geologic setting such as the YMP, but is not very flexible to changes in design, geometry, or geology. For example, to accommodate different disposal system designs such as is required by UFDC, every process model abstraction has to be re-generated to be representative of the system differences. In addition, model abstractions can compromise transparency because they tend to have reduced dimensionality and reduced direct linkages to fundamental physics. Another limitation, specific to GoldSim, relates the representation of multi-dimensional geometry. There is a GoldSim capability to create 2D and 3D cell networks (grids), but it is quite labor intensive, especially to incorporate heterogeneity, which limits the flexibility of using a common GoldSim-based framework to represent the differing geometries in the four UFDC disposal options. There is also a GoldSim capability to link to external 3D codes, but the ability to couple multi-physics in cell networks or with external codes is limited. And finally, GoldSim cannot take advantage of HPC techniques, which could mitigate some of the computational burden associated with the desire to simulate coupled 3D multi-physics in a probabilistic fashion.

These limitations became apparent during attempts to incorporate the individual GDS model components into the common GoldSim-based GPAM framework. GoldSim is best used as a framework when the physics are simple and uncoupled, the size of numerical grids is small, the desired use is narrowly focused, and potential changes are limited. As a result, options for developing an advanced PA model framework that can better accommodate the needs of UFDC were examined (Section 2.2.2). Also, some additional disposal system simulations were performed with the individual GDS models; these are documented in Section 3.

2.2.2 Development of an Advanced PA Model Framework

To address the limitations of the simplified GoldSim-based PA model framework (Section 2.2.1) planning and initial development of an advanced PA modeling capability was performed in FY 2012. Considerations for an advanced PA model framework that provides for complex representations of THCMBR multi-physics processes and their couplings within a computational framework that is compatible with HPC technologies are summarized in Section 2.2.2.1. The preliminary development of some advanced multi-physics model and computational capabilities are summarized in Section 2.2.2.2.

2.2.2.1 Advanced PA Modeling Requirements

An advanced PA model framework includes the basic components – a conceptual multi-physics model framework and a computational framework – described in Section 2.1. However, in addition to the overarching objectives of the basic GDSM architecture (the five bullets listed in Section 2.1), an advanced PA model framework should also facilitate:

- New or alternative subsystem process representations, including the use of legacy codes
- Development and distribution in an open source environment
- Leveraging of existing utilities (e.g., meshing, visualization, matrix solvers)
- Implementation across a range of computing environments from laptops to HPC networks, including distributed code execution

As such, advanced disposal system modeling involves three main activities: (1) obtaining or developing a set of subsystem conceptual models that collectively represent the FEPs and scenarios comprising the

total disposal system, (2) obtaining or developing a computational framework for coupling the subsystem conceptual model components into an integrated representation of the disposal system, and (3) utilizing HPC, as needed, to enable the solution of complex probabilistic problems in acceptable runtimes. The flexibility of an advanced PA model framework to be applied to different disposal system options and multi-physics processes is dependent on its ability to integrate (conceptually, numerically, and computationally) different sets of governing equations from various sources (i.e., multi-physics codes and code objects, including legacy codes) contained in the process model library. Considerations and requirements for an advanced PA model are summarized below. Details are presented in Freeze and Vaughn (2012).

The considerations for an advanced PA model framework can be summarized through discussion of the inter-related modeling details introduced in Section 2.1.1: spatial representation of the disposal system; mathematical representations of the FEPs and scenarios; and numerical implementation of the mathematical models. The spatial and mathematical representations correspond to the conceptual model framework. The numerical implementation corresponds to the computational framework.

A key capability of the PA model framework is the representation of the multi-physics couplings, which provide an interface between the conceptual model framework and the computational framework. Multi-physics couplings can range from simple abstractions with uni-directional linkages to complex coupled multi-physics processes with implicit bi-directional couplings (Freeze and Vaughn 2012, Section 2.3). In general strongly coupled integration (e.g., implicit bi-directional coupling) provides greater flexibility to represent multiple disposal system processes. However, it also requires a robust computational framework, and greater computational resources, that may be offset by the application of HPC capabilities. Weakly coupled or uni-directional linkage provides greater computational efficiency for specific disposal system options. However, it may not be as flexible in representing the range of processes and couplings required, and may not be able to take full advantage of HPC capabilities. An advanced computational framework should provide the capability for both weakly and strongly coupled integration.

Section 2.3 provides an overview of considerations in developing a generic EBS model that can support an advanced disposal system PA modeling capability. These include both conceptual and numerical considerations. Section 2.4 provides a similar overview of considerations in developing a generic NBS model. These two sections collectively identify some high-level requirements for an advanced PA model framework.

Specific functions and requirements of an advanced PA model framework to address these considerations were developed by Freeze and Vaughn (2012). The function of the conceptual multi-physics model framework is to facilitate (Freeze and Vaughn 2012, Section 2.2):

- **FEP Analysis and Scenario Development—**The identification of important disposal system FEPs and scenarios that describe the multi-physics phenomena of a specific disposal system option
- **Conceptual and Mathematical Model Development—**The identification of governing equations that implement the mathematical representations of the important FEPs and their couplings
- **Use of Modular Integration—**Modular integration of representations of subsystem processes and couplings into a “science-based” disposal system model, in which the level of complexity of the representation may vary with intended use or relative importance to the total system

Conceptual model requirements, based on the above functions, are (Freeze and Vaughn 2012, Section 3.1):

- All potentially relevant FEPs and scenarios shall be included.
- The representation of the potentially relevant FEPs (e.g., as process or subsystem models) shall be based on fundamental models, wherever possible, rather than on highly abstracted models.

- The integration of the process/subsystem models into a disposal system model shall adequately represent the important THCMBR multi-physics and their couplings. A simple thermal-hydrologic-chemical (THC) representation (e.g., time-dependent radionuclide source term to fluid flow and radionuclide transport, with some capability for temperature and chemistry to affect the source, flow, and/or transport) is necessary.
- The mathematical models of the FEPs and their couplings shall adequately capture the necessary geometry, initial, and boundary conditions representing the source term, EBS, geosphere, and biosphere regions and the interfaces between regions.
- The numerical implementation of the mathematical models shall accommodate (see Sections 2.3 and 2.4 for details):
  - a spatially discretized geosphere region with 3D multi-phase fluid flow and radionuclide transport (e.g., using Eulerian, Lagrangian, or hybrid methods), including the capability to represent the effects of fractures,
  - an EBS region surrounded by (embedded within) the geosphere region, that provides a time-dependent, and possibly spatially variable, radionuclide source term at the EBS boundary with the geosphere, due to degrading waste forms, waste packages, and other engineered components in the EBS,
  - a biosphere region for calculating dose to a receptor, and
  - radionuclide decay and ingrowth.

The function of a computational framework is to facilitate (Freeze and Vaughn 2012, Section 2.3):

- **Computational Model Development—**The numerical implementation of the mathematical representations of the conceptual model components and the supporting capabilities (e.g., mesh generation, matrix solvers, uncertainty quantification, compatibility with HPC environments)
- **Construction and Execution of an Integrated Disposal System PA Model—**The integration of the system analysis workflow (e.g., input pre-processing, numerical solution of the governing equations, output post-processing) and the supporting capabilities (e.g., input parameter specification and traceability including uncertainty, file configuration management)
- **Sensitivity Analysis and Performance Evaluation—**The application of analysis techniques (e.g., sensitivity analyses, visualization) to evaluate system- and subsystem-level performance and isolate key processes and components

Specific requirements for each of the computational framework components identified in Section 2.1.2 (system analysis workflow, computational capabilities, and configuration management and technical bases) are outlined in Freeze and Vaughn (2012, Section 3.2).

2.2.2.2 Advanced PA Model Implementation

This section summarizes the preliminary development of some advanced multi-physics model and computational capabilities, which were completed in FY 2012. Details are presented in Mousseau et al. (2012). The work was a result of an integrated effort between GDSM, ADSM, and the DOE Nuclear Energy Advanced Modeling and Simulation (NEAMS) Waste Integrated Performance and Safety Codes (IPSC) model development activity. This advanced PA modeling work consisted of three thrusts; a 1D code development effort supporting high model fidelity, a 3D code development effort supporting low model fidelity, and an assessment of existing software to help design a path forward for obtaining a framework for future implementation of the disposal system model.

The advanced PA model development work focused on implementing the correct physics, coupling and parameter treatments, first in a 1D code where analysis and debugging are more straightforward and then

evolving to include 2D or 3D components. After determining an appropriate set of equations and how to solve them in 1D, the equations were moved to the 3D framework for parallel multi-dimensional simulation work. The strategy to implement and demonstrate the basic multi-physics capabilities of disposal system modeling is similar to many multi-scale methods and involves the development of a single system that uses numerical methods and physical properties that can be run either in a coarse-grid 1D mode or a fine-grid 3D mode. In this way, 1D abstractions can be constructed directly from more detailed 3D results for more rapid turn-around. The goal is to build a single framework that supports both detailed 3D simulations and coarse 1D simulations.

The advanced PA model development is summarized in the following subsections. Section 2.2.2.2.1 describes the 1D work, which produced a software package called the Advanced Performance Assessment Code (APAC). Section 2.2.2.2.2 describes the 3D effort, which produced a software package based on the Albany framework. Section 2.2.2.2.3 describes the software assessment work, which focused on the PFLOTRAN software package.

2.2.2.2.1 1D Advanced Performance Assessment Code

This subsection summarizes the progress made to date with the 1D APAC code. Additional details are available in Mousseau et al. (2012, Section 2).

The APAC code was the developed during the final year of the NEAMS Waste IPSC project. The goal was to provide a 1D grid-based capability to replace the existing capability provided by GoldSim. The main use of APAC was to examine application and solution methods and to provide a fast and extendable replacement for GoldSim. There was no effort given initially to multi-dimensional and parallel execution capabilities. Instead the focus was on 1D serial software as a logical first step to replace GoldSim as the PA workhorse. A graphical user interface (GUI) was also developed to increase the user-friendliness of the code and graphical output capabilities were included to better present results, including movie capabilities, in preparation for a 3D extension of APAC.

The APAC code provides a simple framework to represent the disposal system submodel components. It implements a simplified representation of Figure 2-1, where the EBS (consisting of a waste form and waste package), NBS (consisting of far-field host rock), and biosphere are sequentially linked together. Previously conducted FEP analyses (e.g., Clayton et al. 2011, Appendix B) were used to identify and prioritize the basic multi-physics capabilities to be included in the initial version of APAC. At a high level, these included FEPs representing (1) the release of radionuclides from the EBS to the NBS, dependent on waste form and waste package degradation and on radionuclide solubility constraints and precipitation, (2) subsequent radionuclide migration through the NBS to the biosphere by advection and diffusion, influenced by sorption and by radionuclide decay and ingrowth.

The fundamental equations in the initial version of APAC, which are the mathematical descriptions of the included FEPs, are quite simple and general, permitting increased realism in future versions (Mousseau et al. 2012). For example, waste package and waste form degradation in the initial version are linear in time. Eventually, waste form and waste package degradation will become functions of the groundwater chemistry and temperature. The initial version of APAC includes the following equations (Mousseau et al. 2012, Section 2.4):

- **Aqueous and Sorbed Phases Radionuclide Mixture Mass Conservation—**This equation describes the mass of radionuclides in the aqueous phase (dissolved in the groundwater) and the sorbed phase (attached to the rock surface) and accounts for advection, diffusion, dispersion, and precipitation resulting from solubility constraints on aqueous concentrations. The sorbed phase is in equilibrium with the aqueous phase. The dispersion term (referred to as hydrodynamic dispersion) includes the effects of both molecular diffusion in the water and mechanical dispersion caused by the tortuous

water flow in the porous medium. In 1D, the transverse dispersivity is assumed to be zero. Decay and ingrowth affect the concentration in the precipitate, aqueous and sorbed phases.

- **Solid Phase Radionuclide Mass Conservation—**This equation describes the mass of radionuclides in the solid phase (in the waste form) and accounts for decay and ingrowth and release to the aqueous phase.
- **Precipitate Phase Radionuclide Mass Conservation—**This equation describes the mass of radionuclides in the precipitate phase that results when solubility limits are exceeded and considers radioactive decay and ingrowth. The solubility limits are based on the elemental concentration, not the radionuclide concentration and requires summing radionuclide concentrations of the same element to produce elemental concentrations. Mass may move from the aqueous phase to the precipitate phase (precipitation) or vice versa (dissolution).
- **Waste Package Mass Conservation—**This equation describes the conservation of waste package mass that results from degradation. The current implementation uses a constant degradation rate. Degradation ceases after the mass is consumed. In the future, the degradation rate may be a function of temperature and chemistry.
- **Degraded Waste Package Mass Conservation—**This equation describes the conservation of degraded waste package mass that results from degradation. This equation is included as a place holder for future use when the degraded waste package mass could be accounted for in the EBS water chemistry. The current implementation uses a constant degradation rate. Degradation ceases after the mass is consumed.
- **Waste Form Mass Conservation—**This equation describes the conservation of waste form mass that results from degradation. The current implementation uses a constant degradation rate. Degradation ceases after the mass is consumed. In the future, the degradation rate may be a function of temperature and chemistry.
- **Degraded Waste Form Mass Conservation—**This equation describes the conservation of degraded waste form mass that results from degradation. This equation is included as a place holder for future use when the degraded waste package mass could be accounted for in the EBS water chemistry. The current implementation uses a constant degradation rate. Degradation ceases after the mass is consumed.
- **Groundwater Mass Conservation—**This equation describes the conservation of groundwater mass and includes the effect of changes in porosity should they occur. Currently, porosities are assumed to remain constant. In the future they could vary with time as a result of mechanical or chemical processes.
- **Groundwater Momentum Conservation—**This equation is derived from 1D Euler equations with a laminar model (linear in velocity) to account for viscous pressure drops. It represents an unsteady state version of Darcy's law and accounts for impacts due to changes in viscosity or density should they occur. Currently steady state conditions are assumed.
- **Groundwater Equation of State—**This equation relates groundwater density, pressure, and temperature. Currently it is assumed that isothermal conditions exist and that density varies linearly with pressure.

In addition to the above equations, the APAC includes a number of additional mathematical relationships, which define the equation parameters. These include rock properties (porosity, density, tortuosity, longitudinal dispersivity, transverse dispersivity, and permeability), radionuclide properties (decay constant, decay chain parent characteristic functions), chemical properties (linear sorption coefficients,

molecular diffusivity, solubility limits), water properties (reference density, reference pressure, compressibility, and viscosity), waste form degradation rate, and waste package degradation rate.

Finally, there are a number of peripheral processes that complete the mathematical formulation of the APAC disposal system model. These include (Mousseau et al. 2012, Section 2.54):

- **Molecular Diffusion—**This relationship describes the dependence of the molecular diffusion on temperature. Currently isothermal conditions are assumed.
- **Precipitation Model—**Two different precipitation models have been developed and coded. They are an equilibrium model and a kinetic model. In the equilibrium model we assume that the precipitate phase and the aqueous phase are in equilibrium.
- **Precipitation Mass Transfer Model—**The solubility limit is implemented as a kinetic mass transfer model and the radionuclide mass transfer rates are based on the radionuclide concentration of the phase it is coming from.
- **Precipitate Volume Fraction—**This relationship ensures the precipitate mass fraction is such that the aqueous concentration equals the solubility limit.
- **Biosphere Model—**This model converts radionuclide concentrations in the groundwater at the accessible environment into dose. The relationship between the individual effective dose and the bulk concentration of a radionuclide in drinking water is approximated using the International Atomic Energy Agency's (IAEA) BIOMASS Example Reference Biosphere 1A (ERB 1A) dose model (IAEA 2003) and considers flux to a pumping well and the radionuclide concentration within the well.

The 1D APAC code was exercised on a simplified but representative disposal system problem. Results are presented in Mousseau et al. (2012, Section 2.9).

2.2.2.2.2 3D Albany Framework

The 3D effort was performed to demonstrate how quickly a far-field modeling capability could be implemented in the Albany framework, run in parallel, and used to produce a 3D color animation. Albany was chosen as the implementing framework because it is open source, has existing capabilities consistent with the GDSM computational framework needs (Section 2.1.2), and is familiar to the GDSM personnel. The Albany framework (Freeze and Vaughn 2012, Section 4.1.3), developed at SNL, utilizes an Agile Components approach for code development and is based on a variety of existing packages, including:

- **Trilinos—**Parallel linear and non-linear solvers
- **Dakota—**Uncertainty quantification and optimization
- **Sierra Tool Kit—**Sierra (Freeze and Vaughn 2012, Section 4.1.2) capability in an open source format
- **ParaView—**Graphical support for 3D color animations

The 3D NBS capability implemented in Albany consists of a constant groundwater velocity (fixed advection) coupled to a 3D radionuclide advection/reaction/diffusion equation. The diffusivity is assumed to be a scalar. The conservation of mass for the radionuclide is the vector form of the 1D equation and it includes decay and ingrowth. A fixed groundwater velocity is assumed.

The 3D Albany-based code was exercised on a simplified but representative disposal system problem. Results from the 3D capability are presented in Mousseau et al. (2012, Section 3.2).

2.2.2.2.3 PFLOTRAN Evaluation

The PFLOTRAN code, funded by a DOE Office of Science project called Science Discovery through Advanced Computing (SciDAC), was examined for potential application supporting the multi-physics conceptual model capabilities (Section 2.1.1) of an advanced PA model framework. A representative 2D disposal system configuration was implemented in PFLOTRAN. Results and recommendations for continued work with PFLOTRAN are presented in Mousseau et al. (2012, Section 4).

The evaluation concluded that while PFLOTRAN is a good tool designed for chemistry in groundwater, there are a number of improvements or enhancements that are required to make it applicable to disposal system modeling. These include the following:

- The code is not designed for radionuclides. The radioactive decay (including decay chains) can be included in current chemistry but this is a stretch of the code capability. As long as there is only a single isotope (number of neutrons) of interest per element (number of electrons), then the code can simulate decay. However, if there are multiple isotopes of interest per element (e.g., ^{135}Cs and ^{137}Cs), then the code cannot properly simulate decay. The basic problem is the ability to include source/sink terms that depend both on the number of protons and the number of neutrons. Fixing this will require significant code modification.
- The code does not have the capability for multi-dimensional (greater than 1D) dispersion. Higher dimensional dispersion requires a tensor dispersivity that has both longitudinal and transverse components. Currently dispersivity is a scalar and only the longitudinal component is input (this is correct for 1D). This will require code modification.
- The current implementation of the distribution coefficient (K_d) for linear sorption uses units that seem inconsistent with units used in other work.
- The documentation and testing for PFLOTRAN is consistent with its purpose, which is a research code. Significant work needs to be done to bring it up to production code standards.
- Multi-phase flow is not considered. This is likely to be an important consideration for a number of the disposal options. Addition of multi-phase flow would be a significant effort.

It should be noted that these necessary enhancements were generated after only a short study and a more comprehensive study should be performed.

2.3 EBS Conceptual Model and Numerical Implementation

This section summarizes key considerations for the development of a generic EBS region within the GDSM architecture described in Section 2.1. It includes discussion of: reference disposal concepts (i.e. EBS designs) and corresponding generic EBS components consistent with current UFDC disposal options (Section 2.3.1); important EBS FEPs, based on key issues in evaluating the range of reference concepts (Section 2.3.2); and a proposed EBS numerical implementation compatible with the advanced PA model framework described in Section 2.2.2 (Section 2.3.3). Full details are presented in Hardin (2012).

2.3.1 Generic EBS Conceptualization

A basic set of EBS components are identified in Figure 2-1. These basic EBS components are sufficient to support simplified PA modeling of generic disposal systems. To identify a more detailed set of EBS components that might be necessary to support advanced disposal system modeling it is useful to examine potential disposal concepts in more detail. Reference disposal concepts for different prospective geologic settings have been identified based on international experience, previous experience in the U.S., and recent analyses of generic emplacement modes (Hardin et al. 2011). The following list includes the four enclosed emplacement modes currently under consideration by the UFDC as well as three open emplacement mode alternatives (Hardin 2012):

- **Crystalline Rock Repository (enclosed mode)—**Similar to the Swedish KBS-3 concept developed by the Swedish Nuclear Fuel and Waste Management Company (SKB) (SKB 2011), waste packages containing UNF or HLW are emplaced in vertical or horizontal boreholes at approximately 500-m depth in a crystalline rock mass. The rock is fractured but has low permeability at depth, and pathways for flow and transport in the host rock are chemically reducing. Waste packages are fabricated using materials that resist corrosion at expected in-situ chemical conditions, and are emplaced within a capsule of swelling clay-based buffer material.
- **Clay/Shale Repository (enclosed mode)—**Similar to the French Dossier 2005 Argile concept (Andra 2005a), in which waste packages containing SNF are emplaced in small-diameter horizontal borings or drifts, at approximately 500-m depth in a thick argillaceous sequence, surrounded by clay-based buffer material. A similar emplacement mode is proposed for HLW (Hardin et al. 2011). Waste packages are designed for handling and structural strength, but are not corrosion resistant.
- **Generic Salt Repository (enclosed mode)—**Waste packages containing UNF or HLW are emplaced on the floor of alcoves excavated in salt and covered with crushed salt backfill (Carter et al. 2011). Like the clay/shale concept, waste packages are designed for handling and structural strength, but are not corrosion resistant.
- **Deep Borehole Disposal (enclosed mode)—**Individual fuel assemblies are emplaced below a depth of approximately 3 km in low-permeability, crystalline basement rock (Brady et al. 2009). UNF would be contained in simple, small-diameter steel canisters, using rod consolidation to reduce volume. HLW glass is cast into similar, small-diameter canisters. The upper section (i.e., above 3 km) of each disposal borehole is sealed.
- **Hard Rock, Unsaturated Open Concept—**Waste packages are emplaced in open drifts and ventilated for decades to manage decay heat (e.g., as described for a specific geologic setting by DOE (2008). The repository is eventually closed, at which time any additional engineered barriers are installed, such as backfill, water diverters (e.g., drip shields), etc. Waste packages are corrosion resistant to limit damage from salts deposited by ventilation or evaporatively concentrated formation water. The host rock is fractured, with significant permeability, but unsaturated so that low-permeability backfill is not needed at repository closure to prevent water circulation through the repository.
- **Shale Open, Un-backfilled Emplacement Concept—**Waste packages are emplaced in small-diameter drifts in a thick, unfractured shale formation and ventilated for decades to manage heat. The host rock is protected from excessive desiccation and destabilization by ground support (e.g., shotcrete or steel liner). At closure, emplacement drifts are isolated from one another by plugs, and non-emplacement openings are completed with low-permeability backfill. Waste packages are designed for handling and containment integrity prior to repository closure, but are not corrosion resistant.
- **Sedimentary Open Concept, Backfilled at Closure—**Waste packages are emplaced in small-diameter drifts and ventilated for decades to manage heat. With installation of backfill at closure, a range of geologic settings could suffice (e.g., unsaturated alluvium). At closure, all emplacement and non-emplacement drifts are filled with low-permeability backfill. If the host medium has low permeability and reducing chemical conditions, the waste packages could be designed for handling and structural strength, but not necessarily for corrosion resistance. Alternatively, in an oxidizing, permeable formation the waste packages could be fabricated from corrosion resistant materials to enhance waste isolation performance.

The GDSM EBS conceptual models must be capable of discerning the relative advantages of these alternative disposal concepts, either generically or on a site-specific basis. Successful future implementation will allow waste isolation performance to be a meaningful discriminant for comparative evaluation of alternative disposal concepts at a specific site, or for comparing selected disposal concepts at alternative sites. To better enable this capability, Hardin (2012, Figure A-1) developed a more detailed set of GDSM conceptual model components for incorporation into the GDSM conceptual model. A modified version is shown schematically in Figure 2-3.

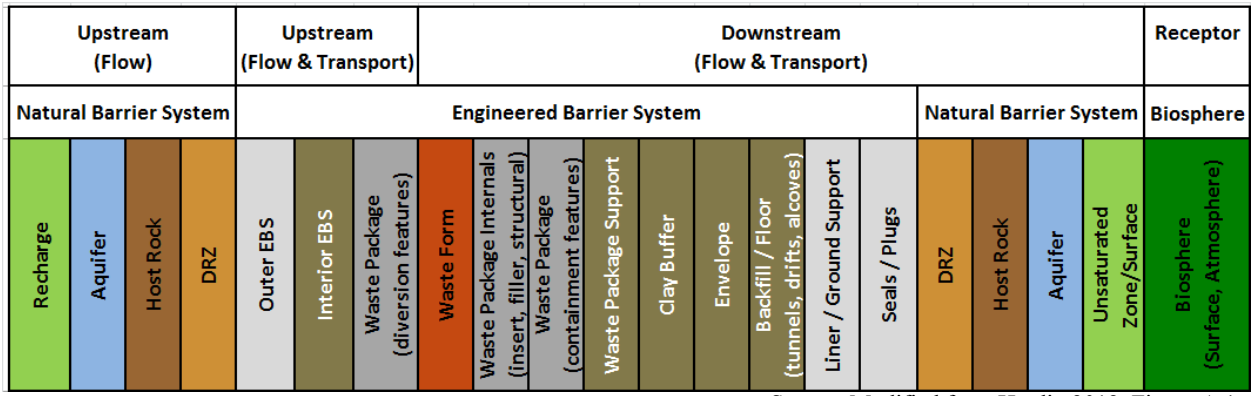

Source: Modified from Hardin 2012, Figure A-1.

Figure 2-3. Detailed Representation of GDSM Conceptual Model Components

Figure 2-3 provides additional detail in the EBS components beyond those identified in Figure 2-1. It also makes a distinction between the region upstream of the waste form (which provides for fluid flow into the waste form, and possible upstream diffusive transport of radionuclides from the waste form and the region downstream of the waste form (which provides for fluid flow and downstream advective and diffusive radionuclide transport from the waste form). For a specific representation of a disposal system option, the EBS and NBS components and features may be combined or further subdivided depending on the modeling needs.

The interface between the EBS and NBS will be established by embedding the EBS model within the NBS model (Hardin 2012, Section 1; Arnold et al. 2012, Section 4.1). The NBS model will represent heat transfer, groundwater flow processes, and aqueous transport of radionuclides (limited to radioactive decay and ingrowth, linear sorption, and matrix diffusion effects) and will provide boundary conditions for energy and mass transfers for the embedded EBS. Further details regarding the NBS model are presented in Section 2.4.

Two general modeling approaches, with differing complexity, are proposed for the embedded EBS (Hardin 2012, Section 3; Freeze and Vaughn 2012, Section 2.2.1):

- **Simple Lumped EBS**—The EBS around each waste package is embedded within the NBS, and is assigned to a subset of elements within the NBS simulation grid. Multiple waste packages can be embedded in a single lumped EBS representation, and mass and energy are conserved. This approach uses batch model concepts to represent the waste form, other waste package internals, the waste package itself, and the EBS features surrounding the waste package. Depending on the complexity of the NBS model, the lumped EBS might also explicitly include the DRZ. The NBS model would run as the "host" simulation and could have any defensible dimensionality including 1D. The embedded lumped EBS would be treated as a uniform source term (although it could vary over time in a stepwise fashion) for radionuclides released from a repository with homogeneous, average thermal,

hydrologic, chemical, and mechanical properties representative of the entire EBS for a given time step. Although simple, the lumped EBS would still rely on fundamental models to the extent possible to directly calculate the state of the EBS during simulations, thereby reducing the use of lookup tables or response surfaces. This results in a more transparent system model.

The lumped EBS approach is intended to use reduced dimensionality and limited multi-physics couplings to simplify and speed up the system model, and will have only limited feedback coupling from the NBS model. The lumped EBS approach resembles previous PA models but all components would be run simultaneously. It is a starting point for developing more complex and coupled generic PA models.

- **Complex High-Fidelity EBS—**The EBS features (and DRZ if necessary) are explicitly represented within the NBS simulation grid, and each element in the grid is associated with constitutive relationships that implement processes representing the physical and chemical evolution of the EBS. Explicit multi-physics couplings between EBS elements and NBS elements are supported.

  The complexity of the interface between the EBS and the NBS would be commensurate with the complexity, spatial resolution, and importance to disposal system performance of each subsystem. Explicit representation of individual repository drifts would require high-resolution gridding in both the EBS and NBS, and would probably require HPC for the numerical implementation of such a conceptual model (Arnold et al. 2012, Section 4.3).

Both approaches will evolve in the future as the constitutive relationships and numerical strategies improve, particularly fully coupled simulations involving novel processes like surface reactions, changes of state caused by degradation, containment failure, and reaction of water. The lumped approach may initially represent a simple mixing cell, but evolve to incorporate physical differentiation (e.g., 1D transport). Also, the boundary enclosing the region where lumped multi-physics are applied may shift as process modeling capabilities improve (e.g., shift inward from enclosing the buffer to enclosing the waste package, with higher-fidelity representation of buffer behavior for clay-based buffers).

2.3.2 Generic EBS FEP Analysis

A conceptual model of a specific EBS disposal concept must include representations of all important multi-physics processes. To identify important EBS processes that should be included in EBS conceptual models, a preliminary generic FEP screening was performed using generic EBS-related FEPs from the UFDC FEP list (Freeze et al. 2011). The FEP screening is described in detail in Hardin (2012, Section 3); a summary is provided here.

The generic FEP screening follows the approach taken by Clayton et al. (2011, Appendix B) to identify FEPs for inclusion in simplified PA models. The updated FEP screening described here aims to support a more widely applicable set of advanced PA models. Project technical staff were assembled in December, 2011 for a group review. First, the EBS-related FEPs were mapped to the detailed GDSM EBS components shown in Figure 2-3. Then, the group review by subject matter experts identified important EBS FEPs, and distinguished between relationships that are likely to be important to all reference disposal concepts and those that apply to only a subset. The screening decisions were based on expected base case evolution of the GDSM EBS components (Hardin 2012, Section 3), and on consideration of impacts on each EBS component from the following key EBS issues (Hardin 2012, Section 2):

- Thermal Management
- Waste Package Containment Lifetime
- Waste Form Degradation Rates
- Alteration of Host Rock by the Repository

- Alternative EBS Closure Concepts
- Gas Generation
- Liner/Reinforcement and Cementitious Materials
- Disruptive Events (Seismic)

The following subsections summarize the base case evolution and the associated key issues for each of the GDSM EBS components; relevant FEPs are noted parenthetically within the text. Additional details describing the key issues are presented in Hardin (2012, Section 2). The important (included) EBS FEPs, listed by EBS component, resulting from the preliminary generic FEP screening, are presented in Appendix A.

2.3.2.1 Outer EBS (Upstream and Downstream)

The outer EBS represents upstream flow paths for groundwater, and downstream flow and transport pathways for radionuclides. The flow and transport pathways are through repository openings that may be somewhat distant from where waste is emplaced, but may still be significantly influenced by waste heating. The outer EBS also includes plugs and seals. The FEPs included in the outer EBS components are listed in Table A-1. Including upstream modeling means that the NBS numerical simulation domain extends to natural hydrologic controlling boundaries such as watersheds, bodies of water, or hydrogeologic structures.

2.3.2.1.1 Base Case

The outer EBS potentially controls the interaction of groundwater flow with the waste package and interior EBS features, and it affects the dissipation of repository heat. Flows of groundwater and heat are included in the encompassing numerical simulation (FEPs 2.1.08.04 Flow Through Seals, 2.1.08.09 Influx/Seepage Into the EBS, 2.1.11.01 Heat Generation in EBS, 2.1.11.10 Thermal Effects on Flow in the EBS, and 2.1.11.11 Thermally-Driven Flow [Convection] in EBS). These coupled processes are represented using TH conceptual and mathematical constructions based on multi-phase Darcy flow and Fourier conduction (Wang et al. 2011; Bear 1972). Flow conditions depend on the repository geometry and hydrologic structure, so a numerical simulation approach is needed (e.g., a lumped or high-fidelity EBS approach).

For disposal in saturated geologic formations that contain faults or other hydraulically significant features, seals and low-permeability backfill will be used (in addition to other measures) to isolate waste emplacement areas of the repository. Points of inflow (FEP 2.1.08.09 Influx/Seepage into the EBS) will be represented by boundary conditions and hydrologic structure, which are conditioned on site data and input to the numerical simulation. Seals and backfill are assigned nominal hydrologic properties in such a simulation, based on analysis and measured data (FEP 2.1.08.04 Flow Through Seals). The evolution of seal properties is quite uncertain (FEP 2.1.05.01 Degradation of Seals) and is the focus of further discussion here.

Smectite clays are common ingredients in proposed seal materials (Hansen and Knowles 2000; SKB 2011). Dispersion of smectite as colloids in dilute, flowing groundwater is considered the most likely degradation mechanism in the SKB assessment, since alteration to illite occurs very slowly at repository temperatures (Gunnarsson et al. 2006). Backfill or seal erosion by dilute flowing groundwater may be insufficient to expose to produce advective conditions, by analogy to the SKB analysis of backfill erosion (SKB 2011, Section 10.4.8) if seal elements and backfilled drift segments are of sufficient size. Erosion can be represented by enhanced permeability caused by removal of the smectite, which increases bulk permeability to that of the sand or crushed rock used as the matrix (Gunnarsson et al. 2006, Figure 4-1).

EBS water chemistry is influenced by the composition of influent formation water, interaction with backfill and ground support materials, the extant oxygen and CO_2 fugacities, and temperature. A good approximation can be obtained using a geochemical model that allows interaction of formation waters with EBS materials along EBS flow pathways (following the lumped EBS approach). A geochemical modeling approach used to represent the composition of influent far-field water in described in SNL (2007c). A more complex, reactive transport model (high-fidelity EBS approach) can represent water composition in conjunction with other processes like backfill hydration (Weetjens et al. 2009) and groundwater flow between proximal waste packages.

2.3.2.1.2 Alteration of Host Rock by the Repository

This key issue refers to creation or expansion of a disturbed zone in the host rock around emplacement openings, caused by heating or desiccation or both. The issue is most relevant in shale, for both enclosed and open emplacement modes (desiccation may be more important in open modes with ventilation). Whereas the issue pertains to the DRZ that may form after emplacement, and therefore affects the NBS, the resulting impact on sealing function affects the outer EBS (FEP 2.1.08.06 Alteration and Evolution of EBS Flow Pathways). It is not possible to rigorously account for the dynamic development of the DRZ within the probabilistic disposal system model; however, because of the limited extent of these regions and the limited time over which the dynamics processes occur, it may be possible to define some "snap-shots" across time and space that capture the effects. These "snap-shots" would be based on the results from detailed dynamic simulations of the DRZ.

The major effect from desiccation caused by heating or ventilation is shrinkage and associated volume strain leading to increased porosity and permeability. For these processes to impact waste isolation performance in the outer EBS, they must allow formation water to flow around seals through the affected zone in the host rock. The permeability increase, caused initially by desiccation, would be at least partially reversed by swelling associated with the re-introduction of such formation water. In concept, the impact would be greatest in the interior EBS where temperatures are highest, but could also be expressed in the outer EBS where seals are installed.

Development of repository seals will be accompanied by demonstration and testing activities as was the case for WIPP (Hansen and Knowles 2000). Thus, there is a baseline level of performance that can be expected from seals, to prevent focusing of natural groundwater flow either within the EBS or in the DRZ around the sealed opening, for a repository subject to operating limitations to prevent alteration of host rock. This key issue refers to simulating the impact from exceeding typical temperature limits for sensitive host media, e.g., exceeding 90°C in shale (Andra 2005a, Section 6.1.1).

The importance of host rock alteration to waste isolation performance is therefore the residual effect on hydrologic structure from heating and/or desiccation followed by reentry of groundwater, which depends on coupled interactions between the water and rock in sensitive media. A numerical flow simulation is needed to discern effects from changes in flow properties, and thermal-hydrologic-chemical-mechanical (THCM) couplings need to be added to explicitly represent processes like rehydration. THCM interactions depend on many processes and their parameters, including the rock composition and fabric, water composition, and intrinsic constitutive behaviors of the medium (e.g., swelling in clays). The capability to simulate such interactions in the presence of gradients of stress and temperature is a desired endpoint of ongoing R&D (see status from Jove-Colon et al. 2012). While such capability is being developed and validated for use in PA models (e.g., by comparing predictions to site-specific data; see also De Windt et al. 2004) the potential impact can be represented using sensitivity studies that assign altered porosity and permeability to a region of elevated temperature (e.g., peak temperature greater than 90°C) in numerical simulations of groundwater flow. This requires separate calculations of volume strain and of the relationship between strain and permeability, both conditioned on measured data (see Hansen et al. 2010 for a review).

2.3.2.1.3 Alternative EBS Closure Concepts

This key issue refers to the possibility of not backfilling all emplacement openings, but using plugs and seals to isolate emplacement drift segments containing multiple waste packages. This would be done for open emplacement modes in massive low-permeability host rock formations (e.g., shale). It could avoid some of the complexity and risks associated with backfilling at closure, for emplacement openings that were maintained for decades of repository ventilation, and then left to collapse slowly around waste packages after closure. The affected region of rock and void space could allow transport of moisture. A corollary issue is whether there is any difference in waste isolation performance with larger waste packages containing more UNF, because failure of larger packages is analogous to simultaneous failure of adjacent, smaller waste packages that are in hydraulic communication.

For the outer EBS, the potential impacts to repository performance are associated with flow paths along un-backfilled drifts that connect adjacent parts of a repository (FEP 2.1.08.06 Alteration and Evolution of EBS Flow Pathways). In addition, there is the potential for TH interactions between heated, un-backfilled drifts and adjacent unheated, cooler regions after cessation of ventilation (FEPs 2.1.08.07 Condensation Forms in Repository, and 2.1.08.08 Capillary Effects in EBS). These are details of flow and transport that need to be represented numerically by the simulation, similar to previous studies (Birkholzer et al. 2008) and using separately estimated host rock properties around the collapsing drift to represent the DRZ.

2.3.2.1.4 Liner/Reinforcement and Cementitious Materials

Outer EBS features such as ground support (e.g., shotcrete, steel sets) and drift plugs (e.g., concrete) could impact water chemistry upstream of emplacement areas (FEP 2.1.09.07 Chemical Interaction of Water with Liner/Rock Reinforcement and Cementitious Materials in EBS). For the lumped EBS approach, alkaline leachates and other affected water compositions can be incorporated in a geochemical model, and reacted with intervening engineered materials or the host rock, to set the composition of groundwater entering the internal EBS. The geochemical model for this purpose would be similar to that presented by Jove-Colon et al. (2012, Part III, Section 1.1). For the high-fidelity approach, the leaching process and reaction with intervening materials would be represented using reactive chemical transport, which helps to ensure mass balance of gaseous, aqueous, and solid reactants. Carbonation of alkaline leachates is an important reaction that could affect the mass balance by depleting aqueous and gaseous CO_2 in the disposal environment.

Another potential impact from cementitious materials is their direct interaction with clay-based backfill or buffer, and degradation of clay properties causing increased permeability. Cement-clay interactions are being investigated (Jove-Colon et al. 2012) but model developers in the foreseeable future can assume that the potential for backfill degradation will be evaluated in separate analyses supporting selection of outer EBS materials.

2.3.2.1.5 Disruptive Events (Seismic)

Postclosure disruption by seismic ground motion or faulting (FEP 1.2.03.01 Seismic Activity Impacts EBS and/or EBS Components) could impact the outer EBS through fault displacement of intersected openings, and dynamic response of backfill, seals, and rock structures. Depending on site-specific conditions, faulting could change groundwater flow patterns that interact with EBS features. Such changes can be represented in the numerical simulator by postulating changes in hydrologic structure, properties, and boundary conditions.

Ground motion can affect the outer EBS, for example by jostling of rock blocks or settlement of backfill. Low permeability repository backfill is always specified to have swelling properties so that when hydrated it has low permeability, seals tightly to the host rock, and provides confinement. For these conditions ground motion is unlikely to affect backfill performance. Even for unconfined rock structures

and facilities underground, the effects from seismic ground motion are limited (Pratt et al. 1979; Sharma and Judd 1991).

Seismic disturbance occurs much more rapidly than degradation, flow, and transport processes in a repository although the effects may persist afterward. Effects from seismic ground motion can be represented by suspending a high-fidelity simulation of degradation, flow, and transport to perform a dynamic calculation on the same (or similar) grid, then resuming the previous simulation. Computational tools presently exist that map grids into different forms, for example from finite volume to finite difference (codes TOUGH2 and FLAC; Rutqvist et al. 2002).

2.3.2.2 Interior EBS (Upstream and Downstream)

The FEPs included in the interior EBS components for upstream and downstream processes are listed in Table A-2.

2.3.2.2.1 Base Case

Flows of groundwater and heat in the EBS are included in the numerical simulation (FEPs 2.1.08.01 Flow Through the EBS, 2.1.11.01 Heat Generation in EBS, 2.1.11.03 Effects of Backfill on EBS Thermal Environment, 2.1.11.10 Thermal Effects on Flow in the EBS, 2.1.11.11 Thermally-Driven Flow [Convection] in EBS, and 2.1.11.12 Thermally-Driven Buoyant Flow/Heat Pipes in EBS). These TH coupled processes are represented using conceptual and mathematical constructions based on multi-phase Darcy flow and Fourier conduction as discussed above. Points of inflow (FEP 2.1.08.09 Influx/Seepage Into the EBS) are represented by boundary conditions and hydrologic structure, as inputs to the numerical simulation, conditioned on site data. Evolution of backfill, and EBS water chemistry, are the focus of discussion here (FEPs 2.1.04.01 Evolution and Degradation of Backfill, 2.1.08.06 Alteration and Evolution of EBS Flow Pathways, 2.1.09.01 Chemistry of Water Flowing into the Repository, 2.1.09.03 Chemical Characteristics of Water in Backfill, 2.1.09.06 Chemical Interaction of Water with Backfill, and 2.1.11.13 Thermal Effects on Chemistry and Microbial Activity in EBS).

Dispersion of smectite as colloids in dilute, flowing groundwater is a possible backfill degradation mechanism in a recent assessment (SKB 2011). Direct, mechanistic simulation of backfill erosion would require modeling colloid generation, transport, and filtration, which are highly uncertain. Instead, bounding approximations are based on fracture flow rates, which can be obtained (high-fidelity approach) using explicit (Painter 2011) or approximate (Robinson et al. 2003) simulations of discrete fracture networks. Lower order approximations can be based on average specific discharge (Darcy flux) and characterization of flowing fractures.

Water chemistry in the interior EBS will be influenced by the composition of influent water, the interaction with engineered materials, the disposal environment including oxygen and CO_2 fugacities, and the temperature. Reactive transport is the preferred modeling approach to represent water composition in the interior EBS (high-fidelity EBS approach); available codes and their capabilities were surveyed by Wang et al. (2011, Section 4). Numerical model and code selection should address TH processes (e.g., multi-phase, non-isothermal) and thermal-hydrologic-mechanical (THM) coupling in addition to reactive chemical transport.

An alternative for the EBS is a lumped approach that extracts groundwater fluxes and potentials from the NBS simulation along a grid contour that encloses an appropriate subdomain, e.g., that includes the waste package and surrounding buffer. The composition of water in the NBS is assumed from consideration of NBS formation waters, reacted with materials encountered along outer EBS flow pathways. Water chemistry within the lumped EBS domain may be calculated assuming a stirred reactor, assuming local equilibrium or using a partial equilibrium assumption (i.e., dissolved species are in thermodynamic equilibrium), but interactions with solid phases may be kinetically limited. In an advection-dominated system, the resulting water composition is assigned to the water flowing out to the NBS; in a diffusion-

dominated transport situation it serves as the source concentration boundary condition for diffusive release to the NBS. The aqueous phase composition is also available for rapid, advective release if warranted (e.g., injection through the buffer by locally generated gas pressure). Mass balance can be preserved particularly with respect to radionuclides. This type of calculation can be repeated at successive time steps within the NBS simulation, and the state of the lumped domain modified and tracked. The approach is consistent with the "reactor network" capability discussed by Wang et al. (2011), integrated with a spatial-temporal numerical simulation of the overall domain.

The lumped EBS approach ("mixing cell") for EBS water chemistry is most appropriate for slowly advecting conditions with diffusive mixing of the aqueous phase composition within the subdomain. For advective systems the transport pathway may not interact with all nearby phases (e.g., radionuclides may not interact with sorbents) and a transport approach may be more appropriate. However, even for advective conditions within the EBS, a lumped EBS approach can still be implemented in reduced dimensionality compared to the NBS simulation, and with limited couplings (see Mousseau et al. 2012, Section 2). Thus, transport behavior within an EBS subdomain that is embedded within a 2D or 3D NBS simulation, can still be 1D, with EBS physical and chemical processes, and process couplings, different from the NBS. For example, the NBS simulator can represent chemical transport using linear sorption, while the EBS subdomain can include processes such as chemical precipitation and surface complexation.

While thermal energy, groundwater, and radionuclide mass balances are readily preserved with the lumped EBS approach, chemical mass balance may depend on specifying reactant mass fluxes at the upstream and downstream boundaries of the EBS domain. For example, formation of ferric iron corrosion products in the EBS may depend on influx of oxygen in some disposal environments, which would require more complex THC capability for the NBS simulator. The motivation here is to allow processes and couplings to be simpler in the NBS, and more complex in the EBS. Accordingly, approximate and conservative assumptions are used within the EBS subdomain to represent mass fluxes from the NBS that are not available directly from the NBS simulation.

A potentially important but developmental aspect of EBS modeling arises in the EBS, where surfaces are altering or corroding, for example a waste package or steel liner. Corrosion typically proceeds on one or both sides, and the feature is eventually penetrated so that diffusive and advective transport are possible. The process of penetration has typically been represented using corrosion rate calculations and conditional logic, implemented in simulators such as GoldSim (SNL 2008d). Within either a lumped or a high-fidelity EBS model, a submodel is needed to represent this type of degradation where the EBS component eventually changes from impermeable to permeable and corrosion products accumulate and participate in sorption of radionuclides. For example, the steel liner tube could react with available water on each side, to corrode at a fixed rate (BSC 2004a; see Section 2.3.2.3 below) producing corrosion products. When the full thickness is corroded, the permeability changes from zero to a fixed value and represents granular corrosion products, with associated hydrologic and chemical characteristics. This conceptual model for degrading metal surfaces can be used throughout the EBS, but especially for the waste package and its internals, and steel liners, to represent the onset of groundwater flow in a way that conserves reactant mass and is consistent with the NBS simulation.

Once radionuclides are released from waste packages by advection and/or diffusion, transport begins in the buffer and other interior EBS components (FEPs 2.1.01.02 Radioactive Decay and Ingrowth, 2.1.09.05 Chemical Interaction of Water with Corrosion Products, 2.1.09.13 Radionuclide Speciation and Solubility in EBS, 2.1.09.51 Advection of Dissolved Radionuclides in EBS, 2.1.09.52 Diffusion of Dissolved Radionuclides in EBS, and 2.1.09.53 Sorption of Dissolved Radionuclides in EBS). A lumped (mixing cell) approach could be appropriate for radionuclide accumulation in corrosion products and other debris outside the waste package. Corrosion products are inventoried in the model, and act as sorbents accessed by diffusing radionuclides (justifying mixed cell or stirred reactor assumption). However, for transport in porous media in the interior EBS, such as buffers and floors, a reactive transport

approach is preferable because it incorporates both advection and diffusion within the particular EBS geometry. An example of this approach is described in SNL (2007b) and SNL (2008d) with dimensionality that varies from 1D to 2D in different submodels.

A high-fidelity coupled simulation requires discretization of the buffer and other EBS components; thermal-hydrologic (TH) properties for representing multi-phase flow and buffer hydration; chemical data for dissolution/precipitation reactions and speciation; and transport properties (porosity, permeability, effective diffusivity and dispersivity, sorption constants, etc.).

2.3.2.2.2 Alteration of Host Rock by the Repository

As discussed above for the outer EBS, desiccation of argillaceous materials caused by heating or ventilation (e.g., an open, ventilated emplacement mode in shale) produces shrinkage and associated increased porosity and permeability. For these processes to impact waste isolation performance in the interior EBS, they must enhance radionuclide transport by channeling groundwater flow, or by increasing effective diffusion through the affected zone. The impact on a PA model could be as simple as not taking credit for radionuclide transport delay associated with diffusive transport across the zone (Hansen et al. 2010) or alteration could change the permeability structure and facilitate new advective pathways through the EBS and into the host rock (FEPs 2.1.08.03 Flow in Backfill, 2.1.08.05 Flow Through Liner/Rock Reinforcement Materials in EBS, and 2.1.08.06 Alteration and Evolution of EBS Flow Pathways). The permeability increase caused initially by desiccation, would be at least partially reversed by swelling associated with the re-introduction of such formation water. In concept, the impact would be greatest in the interior EBS (e.g., buffer) where temperatures are highest. As noted previously the importance of this issue to waste isolation performance is the residual effect in the presence of groundwater, which depends on multiple, coupled interactions between the water and rock. As described in Section 2.3.2.1.2, the potential impact can be represented parametrically by assigning altered porosity and permeability to a region of elevated temperature in the numerical simulation of groundwater flow, based on separate calculations of volume strain and a relationship between strain and permeability.

2.3.2.2.3 Alternative EBS Closure Concepts

Drift collapse (preceded by rockfall) will alter heat transport and groundwater flow paths in the interior EBS (2.1.07.01 Rockfall, 2.1.07.02 Drift Collapse, 2.1.08.06 Alteration and Evolution of EBS Flow Pathways, and 2.1.11.04 Effects of Drift Collapse on EBS Thermal Environment). The presence of unsaturated voids (until collapse is complete) will allow vapor movement, condensation, and capillary effects, although moisture may be very scarce for thousands of years in the interior EBS, after the desiccation caused by preclosure ventilation (FEPs 2.1.08.07 Condensation Forms in Repository, 2.1.08.08 Capillary Effects in EBS). These effects are readily simulated using available TH models (SNL 2008b, c); however, the interior EBS configuration that is analyzed depends on drift collapse, which is uncertain and challenging to simulate (SNL 2004). As a result, drift collapse simulations are likely to be separate calculations, abstracted or bounded for use in a PA model (lumped EBS approach). From these separate calculations the timing of collapse and the propagation of damage into the host rock can be estimated and used to frame numerical simulations of heat transfer and groundwater flow in the system model. For un-backfilled emplacement modes, the goal of this modeling work will be to understand the long-term, consolidated, stable configuration of the EBS, as input to simulation of radionuclide release and transport in a PA model (2.1.07.08 Mechanical Impact on Other EBS Components, and 2.1.07.10 Mechanical Degradation of EBS). The distinct element modeling approach (Cundall and Strack 1979; Lemos and Damjanac 2002) is amenable to this application since it can represent disintegration of EBS features, large displacements, and the dynamic interactions of free bodies.

Chemistry of the disposal environment will change because of drift collapse, as various EBS materials such as steel, shotcrete, waste packages, and waste forms are mechanically consolidated (FEP 2.1.09.12 Chemical Effects of Drift Collapse). A batch calculation can represent these interactions (lumped EBS

approach) in the presence of uncertain configuration from collapse and consolidation for use in the system model.

2.3.2.2.4 Gas Generation

Gas generation is directly related to corrosion of steels and other materials, and can be calculated by any submodel that represents hydrolytic corrosion reactions explicitly. The hydrogen gas produced does not carry radionuclides, but could interact with other EBS features, particularly clay buffers, in a manner that degrades waste isolation (FEPs 2.1.12.01 Gas Generation in EBS, and 2.1.12.02 Effects of Gas on Flow Through the EBS). Gas production to a limited waste package volume will increase the total pressure, with the potential to pressurize radionuclide bearing fluid until it can essentially "frack" a hydrated clay buffer (when local fluid or gas pressure exceeds the minimum compressive stress) and escape the EBS.

Gas production rates will depend on the availability of moisture, which requires buffer hydration, then moisture transport across the buffer (the water activity at equilibrium with dehydrated bentonite is much less than the threshold for steel corrosion; Jove-Colon et al. 2012). Inclusion of gas generation processes in the PA model involves the gas source (coupled to corrosion), and unsaturated, non-isothermal porous medium behavior of the subdomain inside the buffer (including the reservoir if present; see McKinley et al. 2006) with hydrogen as an additional gaseous component. The process of gas pressure buildup and dissipation in the EBS is sufficiently well matched to the capabilities of current porous medium simulators, to form the basis of FEP exclusion (Weetjens et al. 2009).

Whereas gas production is possible in any disposal setting where steel is used in chemically reducing conditions, gas generation is probably only important for disposal concepts that rely closely on buffer performance. For concepts that use clay buffers, such as the crystalline (enclosed) or clay/shale (enclosed) emplacement modes, an advanced multi-phase reactive transport (THCM) simulator can incorporate the availability of moisture and the reactions that produce gas, to calculate the pressure of that gas on the buffer (high-fidelity approach). The escape of gas or liquid from the buffer can be triggered in the simulation (with appropriate constitutive development), and the effect on flow and radionuclide transport outside the buffer can be examined. The simulation should represent the transport of moisture in the buffer, and the availability of moisture to corrode steel within, since the dehydrated clay buffer material can have equilibrium RH that is far less than the threshold for steel corrosion (Jove-Colon et al. 2012; Phipps and Rice 1979). These processes are currently the subject of an international R&D initiative (Weetjens et al. 2009).

A simpler, lumped EBS approach would involve calculating gas production using a batch geochemical model, calculating total pressure, and comparing to buffer failure criteria developed separately. This would then be used to inform the system model. To a first approximation, breach of the buffer can occur if the total pressure inside exceeds the swelling pressure. The amount of fluid released could be bounded, but will be limited by the rate of moisture transport through the buffer over time. Moisture movement in the buffer can be approximated using TH models (Weetjens et al. 2009), but additional changes in the clay properties are also likely from THCM coupled processes that are currently being investigated (Jove-Colon et al. 2012).

2.3.2.2.5 Liner/Reinforcement and Cementitious Materials

This issue refers to the interaction of leachate from metallic and cementitious materials used for ground support, emplacement drift floors, and other applications, with EBS features including backfill, waste packages, and waste forms (FEPs 2.1.09.07 Chemical Interaction of Water with Liner/Rock Reinforcement and Cementitious Materials in EBS, and 2.1.09.08 Chemical Interaction of Water with Other EBS Components). The effect on backfill is addressed here; the effects on waste packages and waste forms are discussed in Sections 2.3.2.3.5 and 2.3.2.4.5, respectively.

Depending on the disposal concept, these metallic and cementitious materials could be in direct contact with backfill, buffer, waste package supports, or other metallic features such as water diverters. Alternatively, leachate or affected groundwater can permeate the EBS and interact with these features. For disposal concepts involving backfill and buffer materials, the immediate upstream effect from leaching of cementitious ground support is the potential for degradation of hydrologic and chemical properties of clay-based materials. This is an area of active investigation in the U.S. and international programs (Jove-Colon et al. 2012). The types of possible reactions include ion exchange (with Ca^{2+}, and Fe^{2+} in reducing environments) and dissolution of silicate sheets in clay minerals, forming orthosilicic acid. The presence of silica tends to buffer the extreme alkalinity of cement leachates (Dole et al. 2004). Whereas some clay alteration can be expected, the effects on performance of buffer or backfill in the EBS could be limited because the overall mass of cement in shotcrete is much less than the clay in backfill or buffers. Study of these interactions is currently focused on geochemical modeling, experimental observation of reaction products, and measurements of thermodynamic data.

Coupled reactive transport simulations of effects from steel degradation and cement leaching on bulk porosity and permeability of backfill or buffer materials, have not been reported and would be well beyond current computational capabilities for use in routine probabilistic disposal system simulations. However, simpler models (lumped EBS approach) could be used to estimate the mass of clay affected. Such calculations lack spatial resolution and would not be bounding with respect to the possibility of buffer penetration by focused damage. Instead, a design decision to use steel or cementitious material proximal to clay-based backfill or buffer materials would likely be based on experimental analysis to examine the effects of interaction on flow and transport properties, and estimate their extent in repository applications. This type of understanding would be prerequisite to fully coupled, reactive transport calculations that simulate changes in flow and transport properties.

2.3.2.2.6 Disruptive Events

The possibility for rockfall and drift collapse into open drifts after permanent closure, determines whether this issue is important (FEPs 1.2.03.01 Seismic Activity Impacts EBS and/or EBS Components, and 2.1.07.10 Mechanical Degradation of EBS). For backfilled openings the effects from ground motion can be considered insignificant as discussed previously for the outer EBS. For the shale un-backfilled disposal concept and the hard-rock unsaturated disposal concept described above, emplacement drifts will remain open for some time after repository closure, ranging from a few years to hundreds of thousands of years. Where waste package containment lifetime is part of the performance strategy the effects from rockfall and drift collapse are modeled (e.g., DOE 2008, Section 2.3.4). Where waste package containment is not part of the performance strategy, the effects from collapse on the interior EBS are limited to those discussed above for alternative EBS closure concepts. Seismic initiation will increase the frequency of rockfall and drift collapse, depending on the site-specific hazard. The purpose for modeling or accounting for collapse, e.g. to find the stable, consolidated configuration for a collapsed repository where waste package containment longevity, is not a factor, and would be essentially the same with or without seismic initiation. Similar modeling approaches (e.g., distinct element; SNL 2004) can be used for static and dynamic (seismic initiation) analysis.

2.3.2.3 Waste Package Features (Diversion and Containment)

The FEPs included in the waste package EBS components (including upstream diversion and downstream containment subdomains) are listed in Table A-3.

2.3.2.3.1 Base Case

The following discussion focuses on waste package degradation. For some disposal concepts no performance credit may be taken for waste package longevity, but the waste package and its degradation products may be important in the transport of radionuclides released from the waste forms, e.g., changes

to the chemical environment and radionuclide retardation. For such concepts the additional, included, base-case transport FEPs are the same as those discussed below for waste forms (Section 2.3.2.4.1).

Waste package damage from general corrosion is expected for every disposal concept; FEP 2.1.03.02 General Corrosion of Waste Packages) so this mechanism is assigned to the base case. In addition, early waste package containment failures will occur either from defects in manufacture or handling, or because packages are not designed to provide long-term containment (2.1.03.01 Early Failure of Waste Packages). General corrosion is typically represented by a constant rate of surface retreat, accompanied by formation of corrosion products. Alternatively, it may be represented by a textbook kinetic rate law:

$$Rate = k_0[A]^a[B]^b[C]^c \cdots exp(E_a/RT) \qquad \text{Eq. 2-1}$$

where K_0 is an intrinsic rate constant; *A, B, C,…* are independent variables representing environmental conditions; *a, b, c,…* are fitting constants; E_a is an activation energy for the limiting reaction step; and RT is the product of absolute temperature and the gas constant (BSC 2004b). To obtain the parameters, various forms of this rate law are fitted to corrosion test data. Statistical and probabilistic methods are used to incorporate imperfect correlation behavior in these fits, into distribution functions that can be sampled by a PA model. Standard methods for modeling long-term corrosion for geologic disposal applications are available (ASTM 1998) and they produce corrosion rates as functions of temperature, pH, and other compositional variables (SNL 2007d). Accordingly, corrosion models typically require description of the temperature and chemical environment (FEPs 2.1.11.01 Heat Generation in EBS, 2.1.09.02 Chemical Characteristics of Water in Waste Packages, 2.1.09.05 Chemical Interaction of Water with Corrosion Products, and 2.1.11.13 Thermal Effects on Chemistry and Microbial Activity in EBS). For some applications the correlation behavior of measured data supports predictive models with limited functionality, such as temperature dependence only (SNL 2007d). For corrosion in humidity environments, experimental data show that general corrosion stops when the relatively humidity is too dry to support surface water films. Models based on environment-specific regressions can substantially increase model uncertainty depending on whether the test conditions match the corrosion environment. Corrosion submodels used in a PA model should include this type of uncertainty.

An alternative conceptual model for general corrosion is diffusion-controlled, transport-limited reaction in which the propagation of reactants such as oxygen and water through a layer of corrosion products is slower than the intrinsic reaction rate represented functionally by Equation 2-1. Diffusion control is evident from time-dependence, i.e., gradually decreasing corrosion rates, observed in long-term tests. This alternative was investigated for corrosion of low-alloy steel in a repository (SNL 2007c), and was evaluated for corrosion resistant materials (SNL 2007d).

General corrosion of low-alloy steels has a relative humidity threshold for onset (e.g., 70%; Phipps and Rice 1979) and the corrosion rate directly depends on oxygen partial pressure to first order, down to at least 10^{-2} atm (Jovancicevic and Bockris 1986). At some lower oxygen pressure the predominant corrosion mechanism changes to one involving hydrolysis and gas generation (SNL 2007c). The latter condition will be readily reached after closure in chemically reducing host media. Corrosion rates at reducing conditions are slow (on the order of 1 µm/yr for steels) or microbially influenced, so experimental data have limitations and simple rate laws or fixed corrosion rates are common. Other types of corrosion such as localized corrosion (used here to include pitting, crevice corrosion, or intergranular attack) and stress corrosion cracking, produce much smaller waste package penetrations and are addressed below in the discussion of containment lifetime.

The sizes of waste package penetrations, ranging from large “patches” produced by general corrosion, to arrays of small pits or cracks, controls interactions with groundwater flow and diffusive release of

radionuclides (FEPs 2.1.03.08 Evolution of Flow Pathways in Waste Packages, 2.1.08.01 Flow Through the EBS, 2.1.08.02 Flow In and Through Waste Packages, 2.1.08.06 Alteration and Evolution of EBS Flow Pathways, 2.1.09.51 Advection of Dissolved Radionuclides in EBS, and 2.1.09.52 Diffusion of Dissolved Radionuclides in EBS). Variations in waste package material composition, surface condition, mechanical stress, temperature, and corrosion chemistry will produce spatially variable corrosion rates on or within each package. This variability may be important in a PA model as it determines whether many waste packages undergo containment failure simultaneously, for disposal concepts that rely on waste package containment. Various approaches to quantifying this variability may be taken, for example, probabilistically assigning the residual variability from regression of laboratory corrosion test data, to subregions on each waste package (BSC 2002b). Note also that general corrosion can take place on both the inner and outer surfaces of the waste package, particularly after breach, generating corrosion products that can accumulate, and act as radionuclide sorbents.

Once the waste package is breached, groundwater can readily flow in and out, and radionuclides will be released by diffusion and advection. For diffusion-dominated transport (the objective in low-permeability host media) a diffusion area can represent partial or complete breach of the package wall in simple models (lumped EBS). Corrosion products and gas generated are inventoried in the model, and act as sorbents accessed by diffusing radionuclides (justifying mixed cell or stirred reactor assumption). Where advective transport is important, groundwater flow in and out of a region of the simulation grid corresponding to a breached waste package, can be calculated by the NBS simulation. This requires a non-zero permeability that can be assigned at closure (where containment lifetime is not important to performance) or at waste package breach during the simulation.

A high-fidelity coupled simulation requires chemical data for dissolution/precipitation reactions and speciation; discretization of the package and its contents; and transport properties (porosity, permeability, effective diffusivity and dispersivity, sorption constants, etc.). Reactive transport simulators are typically porous medium formulations with limited capability to represent processes that occur on surfaces, or at boundaries between regions with different composition or other properties. Hence, some numerical development or adaptation of existing models will be needed to incorporate these tools into a PA system model. Degradation of the waste package wall is an important application for the degrading metal surface concept described in Section 2.3.2.2.1 and below in the context of localized corrosion.

2.3.2.3.2 Waste Package Containment Lifetime

Where containment lifetime is an objective, waste package materials will be selected to provide ample margin against penetration by general corrosion. That leaves localized corrosion, and possibly microbially influenced corrosion (MIC), as the most important modes of degradation. Localized corrosion mechanisms and MIC mechanisms are focused on small areas of attack, and can penetrate waste packages made from corrosion resistant, passive materials much more quickly than general corrosion (FEPs 2.1.03.03 Stress Corrosion Cracking of Waste Packages, 2.1.03.04 Localized Corrosion of Waste Packages, and 2.1.03.06 Microbially Influenced Corrosion of Waste Packages). These processes depend on temperature, the chemical environment (pH, chloride, etc.), the condition of the metal surface, and the presence of initiation sites such as surface damage or contact crevices. The following discussion focuses on localized corrosion of passive metals, and briefly considers modeling of MIC.

Localized corrosion requires steep gradients of composition in an aqueous phase contacting the metal surface, and it is sustained where those gradients persist as corrosion proceeds. In other words, the process initiates and then persists if the local conditions for initiation continue, even as corrosion damage accumulates. Models for localized corrosion distinguish the electrochemical conditions for initiation, from the rate of propagation (and the eventual penetration of a waste package layer). Imitation is defined to occur when the long-term, open-circuit corrosion potential (E_{corr}) exceeds a critical potential (E_{crit})

defined by electrochemical testing. Each of these potentials is represented by a regression of an empirical equation over experimental data, for example (SNL 2007d):

$$E_{corr} = C_0 + C_1 T + C_2 pH + C_3 \frac{[NO_3^-]}{[Cl^-]} + C_4 T \frac{[NO_3^-]}{[Cl^-]} + C_5 pH \frac{[NO_3^-]}{[Cl^-]} + C_6 \ln[Cl^-] + \varepsilon_{corr} \quad \text{Eq. 2-2}$$

where E_{corr} is the long-term corrosion potential, T is the temperature (°C), $[Cl^-]$ is the molal chloride-ion concentration, $[NO_3^-]$ is the molal nitrate-ion concentration, and $c_0, c_1, c_2, \ldots c_6$ are fitting parameters. The error term (ε_{corr}) represents data variance not explained by the fitting procedure (SNL 2007d). Once initiation occurs ($E_{corr} > E_{crit}$) the rate of localized propagation is highly uncertain, and has been treated as a fixed, independent parameter with an uncertainty distribution based on various reported measurements (SNL 2007d).

Regressions can be applied at sites where heating, flow, or other initiating conditions occur (SNL 2008d). They can be applied within a simulation grid (lumped and high-fidelity EBS approaches) subject to the limitation discussed above that the capability to embed penetration processes has not been demonstrated. Also, localized corrosion initiation, once it occurs, is a permanent state change that must be tracked in any EBS simulation.

Embedded models of localized corrosion can be used to further enhance the representation of degrading metal surfaces (Section 2.3.2.2.1) such that simulation grid elements representing the waste package wall can have permeability after breach, but are not completely degraded as with general corrosion. This is important because the size of breaches can become an important factor in the source term release rate for system performance, if radionuclides released from waste packages are not significantly attenuated by other EBS features (SNL 2008d). The cross-sectional diffusion or advection area of penetrations from localized corrosion is millimeter-scale, whereas that from general corrosion is potentially at the meter-scale. Unless millimeter-scale grid elements are to be used, an expression of partial permeability is needed to define the state of elements penetrated by localized corrosion processes.

The existence of MIC indicates that microbes are capable of mediating metal degradation reactions that might otherwise be limited by intrinsic kinetics or mass transport. The occurrence of MIC and the resulting rate of metal degradation are highly uncertain because of the ranges of microbe types, environmental conditions, and metabolic pathways possible in the repository environment. A humidity threshold for onset (e.g., 90%) has been identified and is subject to uncertainty (SNL 2007d). Waste package damage from MIC may resemble abiotic general or localized corrosion, but if both abiotic modes occur, then the greatest effect from MIC may be acceleration of general corrosion because it produces larger breaches.

2.3.2.2.3.3 Alternative EBS Closure Concepts

This issue represents a deliberate strategy to allow collapse of un-backfilled openings containing waste packages, in a low permeability medium (e.g., massive shale) for disposal option where there is no practical need to consider long-term waste package containment lifetime (beyond repository closure) Waste isolation performance in this situation is allocated to the waste form and natural barriers. As a result, the potential for mechanical impact and degradation of waste packages and other EBS components is not a modeling priority (FEPs 2.1.07.05 Mechanical Impact on Waste Packages, and 2.1.07.10 Mechanical Degradation of EBS).

2.3.2.2.3.4 Gas Generation

Waste packages made from low-alloy steel will be a major source of generated gas (FEP 2.1.12.01 Gas Generation in EBS) in anaerobic disposal environments, while those made from stainless steel or

corrosion resistant materials (e.g., copper, nickel alloys, titanium) will corrode more slowly allowing gas to dissipate. The potential significance of gas generation to system performance is summarized above (Section 2.3.2.2.4). To extend the porous medium analysis approach (Weetjens et al. 2009) to include multi-phase flow in waste package penetrations (and gas generation within the package (2.1.12.02 Effects of Gas on Flow Through the EBS) requires some development of constitutive behavior for grid elements as well as characteristic curves that describe the capillary effect and interference that one phase places on the other phase.

2.3.2.3.5 Liner/Reinforcement and Cementitious Materials

Interaction of leachate from cementitious materials with waste packages will not be significant, because for disposal concepts that use shotcrete or concrete, the waste packages are low-alloy steel, or the cementitious materials are removed at closure. Low-alloy steel could actually be protected by alkaline leachate (Weetjens et al. 2009). The possible exceptions for mined disposal concepts are the hard-rock unsaturated open mode and the backfilled open mode. For the hard-rock unsaturated mode cementitious materials would not be used in emplacement areas of the repository, and their use in adjacent areas would not affect performance (Ziegler 2004; SNL 2008a). For the backfilled open mode, the package and its support may be of low-alloy steel or corrosion resistant materials (depending on the geologic setting) but in either case a low-permeability backfill intervenes between the roof and the package (FEPs 2.1.09.07 Chemical Interaction of Water with Liner/Rock Reinforcement and Cementitious Materials in EBS, and 2.1.09.08 Chemical Interaction of Water with Other EBS Components). Interaction of cementitious materials with waste package materials is not a modeling priority for the disposal concepts under consideration.

2.3.2.3.6 Disruptive Events

As discussed in Section 2.3.2.2.6 for the interior EBS, the possibility for rockfall and drift collapse into open drifts determines whether this issue is important (FEPs 1.2.03.01 Seismic Activity Impacts EBS and/or EBS Components, and 2.1.07.10 Mechanical Degradation of EBS). For backfilled openings the effects from ground motion can be considered insignificant. For the shale un-backfilled disposal concept and the hard-rock unsaturated disposal concept described above, emplacement drifts will remain open for some time after repository closure, ranging from a few years to hundreds of thousands of years. For the hard-rock unsaturated concept where waste package containment lifetime is part of the performance strategy, the effects from rockfall and drift collapse on waste packages have been modeled (e.g., DOE 2008, Section 2.3.4).

Where waste package containment is not part of the performance strategy, the purpose for collapse modeling, to find the stable, consolidated postclosure configuration for the repository, would be essentially the same with or without seismic initiation. Seismic initiation will increase the likelihood of rockfall and drift collapse, depending on the site-specific hazard. Modeling approaches similar to those used in the past for the hard-rock unsaturated concept (e.g., distinct element; SNL 2004) can be used for static and dynamic (seismic initiation) analysis.

Extensive calculations of seismic response performed for the YMP EBS concept (SNL 2007e) showed that (1) waste packages in open drifts can accumulate damage (e.g., residual stress) from repeated impacts with falling rocks or other EBS components; and (2) waste packages surrounded by fill (e.g., rockfall debris, or engineered buffer or backfill) sustain little or no damage from seismic ground motion.

2.3.2.4 Waste Form and Waste Package Internals

The FEPs included in the waste form and waste package internals EBS components are listed in Table A-4.

2.3.2.4.1 Base Case

The numerical simulation must have sufficient capacity to handle the range of radionuclides present in UNF and HLW waste forms, and radioactive decay of each, and ingrowth of daughters (FEPs 2.1.01.01 Waste Inventory, and 2.1.01.02 Radioactive Decay and Ingrowth). Several criteria for including radionuclides have been used in previous studies (BSC 2002a): regulatory requirements (e.g., gross alpha), abundance and long half-life, mobility in the host geologic setting, relative radiotoxicity, and projected measures of dose. Other criteria include heat generation and radioactive precursors to important daughter radionuclides. The minimum number of radionuclides is approximately 10, which allows for most heat generation and might be appropriate for some problems, for example if actinides are immobilized and do not contribute to dose. Larger sets have been used in previous PA models (up to 32; see BSC 2002a).

In general, the zirconium-alloy cladding on UNF is resistant to corrosion; however, an uncertain fraction has cladding damage. Cladding penetrations admit water and other reactants, and act as loci for the assumed initiation of fuel rod failure after waste package breach. UNF cannot be readily inspected for damage before disposal, but a percentage of rods can be assumed to have perforated cladding at emplacement (SNL 2008a, App. C). For previous PA models cladding has conservatively assumed to be 100% failed at the time of waste package breach (SKB 2011; SNL 2008a). Taking performance credit for integrity of cladding in a PA model requires attention to the initial condition, and to mechanical damage from seismic ground motion and other causes.

Radionuclide releases from UNF are generally modeled as a sequence of mechanisms starting with the most labile constituents released when cladding is first breached (an uncertain "fast release" fraction, consisting mainly of fission products present as gases or condensed phases, in gaps or grain- boundaries). With further degradation, most constituents are released congruently as the uranium oxide matrix dissolves, leaving an insoluble phase containing certain metallic fission products (Sassani 2011).

Matrix dissolution has been represented: (1) by simple fractional release models conditioned on measured release data for representative disposal environments (SKB 2011; Clayton et al. 2011), and (2) by functions derived from regression of a kinetic rate expression to measured data (BSC 2004b). Kinetic rate functions are derived by fitting generic rate laws (Equation 2-1) to measured data, and choosing independent variables, for example (BSC 2004b):

$$log_{10}R_d = a_0 + {}^{a_1}/_{T} + a_2 pCO3 + a_3 pO2 + a_4 pH \qquad \text{Eq. 2-3}$$

where R_d is the degradation rate (contaminant mass/area/time); T is temperature; $a_0, a_1, \ldots a_4$ are fitting constants; and $pCO3$, $pO2$, and pH are independent variables (negative $\log_{10}$ values of total carbonate, oxygen fugacity, and solution hydrogen ion molar concentration, respectively). Separate regressions may be used for different ranges of environmental conditions, e.g., acidic and alkaline. These modeling approaches were built into the previous PA models and can be readily embedded as source terms in a NBS simulation (FEPs 2.1.02.01 SNF [Commercial, DOE] Degradation, and 2.1.02.06 SNF Cladding Degradation and Failure). The kinetic functions for matrix dissolution can also be used with various simplifications (e.g., fixed temperature and solution chemistry) so they essentially reduce to fractional release models.

An alternative approach could be based on general rate laws for heterogeneous reactions that use the activities of reactant species chemisorbed on degrading solid surfaces (Lasaga et al. 1994; Stout and Leider 1998). Such formulations are more mathematically complex and could include cross-terms or quadratic terms in the independent variables (BSC 2004b).

Radionuclide releases from borosilicate HLW glass can similarly be modeled using either a kinetic rate function (regression to measured data) or a fractional release approach (Clayton et al. 2011). The rate function assumed for defense HLW glass at YMP was based on a rate law of the form:

$$R_d = k_0 10^{\eta \cdot pH} \exp\left(\frac{-E_a}{RT}\right)\left(1 - \frac{Q}{K}\right) + k_{long} \qquad \text{Eq. 2-4}$$

where the intrinsic rate constant k_0, constant η, activation energy E_a, and long-term residual rate k_{long} are fitted by regression to measured data. The affinity factor $\left(1 - \frac{Q}{K}\right)$ has a range from zero to 1 and expresses the slowing of glass degradation as degradation proceeds and the solution loads up in dissolved silica. It may be set to 1 (i.e., $Q = 0$) as a conservative simplification or to accommodate strongly advective disposal environments (BSC 2004b). The extent of surface area due to cracking of HLW glass is an important parameter. Similar approaches can be taken for modeling degradation of other HLW forms, such as glass-bonded zeolite (BSC 2004b). These modeling approaches have been used previously and can be readily embedded in a NBS simulation (FEP 2.1.02.02 HLW [Glass, Ceramic, Metal] Degradation).

Migration of released radionuclides from the waste form, through the degraded waste package, to the outside EBS has typically been modeled using a mixing cell approach (SNL 2008a; SKB 2011). Radionuclides are released into solution by degrading waste forms, while waste package internals also degrade, and equilibrium calculations determine the extent of precipitation and radionuclide attenuation that occurs (FEPs 2.1.09.02 Chemical Characteristics of Water in Waste Packages, 2.1.09.13 Radionuclide Speciation and Solubility in EBS, 2.1.09.05 Chemical Interaction of Water with Corrosion Products, and 2.1.09.53 Sorption of Dissolved Radionuclides in EBS). The resulting solution serves as the effluent composition for advective release, and/or the upgradient concentration boundary condition for diffusive release from the waste package (FEPs 2.1.09.51 Advection of Dissolved Radionuclides in EBS, and 2.1.09.52 Diffusion of Dissolved Radionuclides in EBS). Temperature dependence has typically been provided by a NBS numerical simulator that considers the waste package as an undifferentiated solid (SNL 2008a; FEPs 2.1.11.01 Heat Generation in EBS, and 2.1.11.13 Thermal Effects on Chemistry and Microbial Activity in EBS). However, the timing of waste package breach and flooding is such that the rates of heat generation have decayed, so that temperatures within and at the surface of the breached waste package are similar.

The foregoing description corresponds to a lumped EBS approach. A high-fidelity approach that accounts for the developing permeability structure, chemical heterogeneity within a degrading waste package, and heat generation, has not been reported (for example, SNL 2008a or SKB 2010a). Hence there is little difference in how waste form degradation and in-package chemistry would be implemented in lumped EBS and high-fidelity approaches using currently available tools, and neither approach would represent the modification of in-package flow structure (FEPs 2.1.03.08 Evolution of Flow Pathways in Waste Packages, 2.1.08.02 Flow In and Through Waste Packages, and 2.1.08.06 Alteration and Evolution of EBS Flow Pathways).

2.3.2.4.2 Waste Form Degradation Rates

This key issue refers to the need to evaluate waste isolation performance with new waste forms, such as ceramic or metallic waste forms from reprocessing UNF. The potential benefit from hypothetical waste forms that degrade very slowly over the performance period of a repository was pointed out by Swift et al. (2010). A description of ongoing waste form R&D that is directed to increasing longevity was provided by Sassani (2011). The system model needs the capability to evaluate the impact of delayed or diminished radionuclide releases form waste forms, and the processes such as radiolysis or radiation

damage that could affect waste form stability over very long times (FEP 2.1.02.02 HLW [Glass, Ceramic, Metal] Degradation, 2.1.13.01 Radiolysis, and 2.1.13.02 Radiation Damage to EBS Components).

To evaluate chemical and physical stability of the waste form, a lumped EBS approach such as that described above could be used if the needed environmental parameters (e.g., temperature, pH, silica) are provided. To evaluate other types of enhancements to the waste form such as getters, fillers, etc. a high-fidelity approach is needed to represent changes in porosity and permeability, and the associated mechanical boundary conditions such as confinement.

2.3.2.4.3 Alternative EBS Closure Concepts

As discussed in Section 2.3.2.3.3, this issue represents a deliberate strategy to allow collapse of un-backfilled openings containing waste packages, in a low permeability medium (e.g., massive shale). Waste isolation performance is allocated to the waste form and natural barriers, but UNF cladding failure will be assumed (consistent with current models), and the un-backfilled shale emplacement mode is not proposed for HLW. As a result, the potential for mechanical impact and degradation of UNF and other EBS components is not a modeling priority (FEPs 2.1.07.05 Mechanical Impact on Waste Packages, and 2.1.07.10 Mechanical Degradation of EBS).

2.3.2.4.4 Gas Generation

Anaerobic corrosion of waste package internals is a potentially important source of hydrogen gas, for disposal concepts that use low-alloy steel or cast iron for packaging (e.g., crystalline reference concept). Filler materials consisting of steel shot or similar materials, that would occupy interstices in the waste package after loading of the basket and UNF, have also been proposed (CRWMS M&O 1999). Analysis of gas generation effects needs to account not only for steel waste packages as discussed above, but also for steel/cast iron internals (FEPs 2.1.12.01 Gas Generation in EBS, and 2.1.12.02 Effects of Gas on Flow Through the EBS). Note that hydrolysis reactions are not thermodynamically favored in the oxidative alteration of UO_2 fuel, and UO_2 degrades slowly under anaerobic conditions and does not produce significant hydrogen. As discussed above, to extend the porous medium analysis approach (Weetjens et al. 2009) to include multi-phase flow in waste package penetrations (and gas generation within the package requires some development of constitutive behavior for grid elements. Waste isolation performance may be degraded by gas pressurization or enhanced, for example, gas pressure may prevent water entering the waste package due to phase interference (SKB 2010a).

2.3.2.4.5 Liner/Reinforcement and Cementitious Materials

Degradation of UNF and HLW is sensitive to environmental conditions including pH, pO_2, carbonate concentration, and temperature (BSC 2004b). One of the strongest associations is the pH dependence of dissolution rates for borosilicate glass, which dominates the dissolution of silica at alkaline conditions. Cementitious materials such as shotcrete or concrete, if used in construction of emplacement areas, are sources of alkaline leachate (FEPs 2.1.09.07 Chemical Interaction of Water with Liner/Rock Reinforcement and Cementitious Materials in EBS, and 2.1.09.08 Chemical Interaction of Water with Other EBS Components). Interaction of such leachate with UNF or HLW is uncertain, and has driven past design decisions whether to use cementitious materials in ground support (e.g., shotcrete) and other applications (e.g., floor construction). Whereas low-pH cement formulations have been proposed (Dole et al. 2004), the capability to model the effects on repository performance, in a framework that represents other disposal system elements and imposes mass and energy balances, has not been established.

The environmental conditions for waste form degradation can be evaluated using the lumped EBS or high-fidelity approaches discussed above. Both approaches incorporate the effects from dissolved constituents, for example, precipitation of secondary phases and speciation of released radionuclides. For most of the reference concepts addressed here the approaches need to take reducing chemical conditions into account, because the mobility of many important radionuclides (e.g., Tc, U, Np, Pu) is profoundly

affected. Past approaches that have assumed oxidizing conditions (BSC 2005; SNL 2007a) may be appropriate for the hard-rock unsaturated and the backfilled open mode concepts presented above, but not for other concepts that are specific to low permeability, chemically reducing host media. Batch simulators such as EQ3/6 and PHREEQC, and published accounts of their application to redox problems, are more common than reactive transport simulations with dynamic redox conditions (Wang et al. 2011). The understanding of, and capability for predictive modeling of dynamic redox conditions in reactive transport simulations of waste form degradation and radionuclide transport, is an acknowledged gap area in PA modeling.

2.3.2.4.6 Disruptive Events

Whereas dynamic calculations have been performed for waste packages in an un-backfilled repository (see above), they have generally not included in-package structural response (FEPs 1.2.03.01 Seismic Activity Impacts EBS and/or EBS Components, and 2.1.07.10 Mechanical Degradation of EBS). For intact waste packages, the fuel basket and other internals may retain the known initial configuration that can be used for dynamic simulation of seismic response. However, after waste package degradation and breach the configuration and physical condition of the package vessel, basket, and other elements is highly uncertain. For the clay/shale and salt reference concepts, waste packages will be made from corrosion allowance materials and will be breached relatively soon after repository closure (compared with the waste isolation performance period). Moreover, after breach the condition of the UNF cladding is assumed to be fully degraded (see above) so a consistently pessimistic assumption would be needed to represent the condition of other internals. Simulation of response to ground motion at that point would produce uncertain and unrealistic results, and is not a modeling priority.

2.3.3 Numerical Implementation

The numerical implementation of the GDSM EBS model is dependent on the selection of either a simple lumped EBS or a complex high-fidelity EBS, embedded within the NBS model as described in Section 2.3.1. Previous studies (Wang et al. 2011) assessed the state of the art in numerical simulation of coupled processes, including numerical simulation codes, with discussion of how such simulations would be applied. Hardin (2012, Section 4) recommends the initial numerical implementation of a simple lumped EBS model that can then be successively improved, evolving toward a fully coupled, fully discretized (spatial and temporal) numerical simulation (i.e., a complex high-fidelity EBS). The flexibility to implement a PA analysis using either simpler or more complex component models, as needed during future repository siting, characterization, design, and licensing activities, should be maintained because many issues can be addressed adequately by simpler calculations. Even for the simple lumped EBS, it is preferred that no lookup tables or response surfaces be used, and to the extent possible, all model elements (e.g., code modules) run together simultaneously to maintain modularity and flexibility.

In this approach the PA model always uses a numerical simulator for the NBS, which avoids the labor and limitations associated with abstraction of transport behavior (e.g., avoids compiling libraries of breakthrough curves that become increasingly complex with radioactive decay). Numerical considerations for the NBS model are discussed in Section 2.4.3. The EBS grid detail can be varied within the NBS numerical grid, with commensurate EBS process fidelity. A simple lumped EBS model may require only temperature and groundwater inflow/outflow as inputs, and these could be calculated by the NBS simulation using coarsely gridded EBS components. EBS process kernels representing the included EBS FEPs (Section 2.3.2 and Appendix A) should be developed that have increasing detail, such as a corrosion of metallic components, evolution of EBS flow paths, gas generation, sorption on corrosion products, etc. Process kernels for a lumped EBS approach are flexible and scalable, and can be used with runtime uncertainty management shells such as DAKOTA. Maintaining the modularity of EBS process kernels (e.g., specifying a standard set of inputs/outputs at the EBS boundary within a numerical grid, for use with alternative EBS models) will help to maintain modularity.

A conceptual model for degrading metal surfaces was presented in Section 2.3.2.2.1 that would represent corrosion, onset of groundwater flow commensurate with breach size, and corrosion products. This concept supports the capability for a mechanistic disposal system PA model that does not use abstraction in the form of lookup tables or response surfaces. It can be used throughout the EBS, but especially for the waste package and its internals, and steel liners, to represent the onset of groundwater flow in a way that conserves mass of EBS components, and is consistent with the NBS simulation. The foregoing discussion would change the properties of grid elements as corrosion advanced. An alternative approach would use adaptive gridding to create new elements representing corrosion products, and eventually eliminate the original elements when they are fully consumed. While plausible, this alternative would produce successively smaller elements (e.g., representing penetration by localized corrosion). A more approximate approach that recalculates the effective permeability and other properties for grid elements, based on the extent of corrosion, could be more numerically tractable. This capability has not yet been reported in the literature in a form that is embedded in a numerical flow and transport simulation grid for a geologic repository.

2.4 NBS Conceptual Model and Numerical Implementation

This section summarizes key considerations for the development of a generic NBS region within the GDSM architecture described in Section 2.1. The NBS architecture must be comprehensive in the conceptual and numerical representation of FEPs that are relevant to the four disposal options (mined geologic disposal in salt, clay, and crystalline rock; deep borehole disposal in crystalline rock). In addition, the GDSM NBS components must be sufficiently flexible to accommodate differences among the disposal options, while using a common, numerically efficient architecture. This section includes discussion of: geologic media and generic NBS components consistent with current UFDC disposal options (Section 2.4.1); important NBS FEPs, based on key issues in evaluating the range of geologic media (Section 2.4.2), and; a proposed NBS numerical implementation compatible with the advanced PA model framework described in Section 2.2.2 (Section 2.4.3). Full details are presented in Arnold et al. (2012).

2.4.1 Generic NBS Conceptualization

A basic set of NBS components are identified in Figure 2-1. This basic NBS representation (DRZ, host rock, other geologic units) is sufficient to support simplified PA modeling of generic disposal systems. To identify a more detailed EBS representation that might be necessary to support advanced disposal system modeling it is useful to examine potential geologic media associated with the four disposal options in more detail. The geological media and conditions for each of the four disposal system options are defined in a broad sense, but are not specific with regard to detailed local geological or hydrogeological conditions. For example, a mined repository in salt could be in bedded salt or in a salt dome. Crystalline rock refers to a range of mineralogy and petrology among igneous and metamorphic rock types. Nonetheless, the basic characteristics of the four disposal systems are based on typical geological conditions associated with the corresponding host media and experience in these media in the United States and international repository science programs.

The following discussion of considerations and reference concepts for the four disposal options is summarized from Arnold (2012, Section 1.3):

- **Mined Geologic Disposal in Salt—**A salt repository disposal system consists of a mined repository excavated in bedded salt at a nominal depth of 500 m, similar to the Waste Isolation Pilot Plant (WIPP) disposal system. Although numerous alternatives exist for the details of waste emplacement, the reference concept consists of multiple, approximately horizontal galleries in a bedded salt formation. The natural system surrounding the repository is composed of the DRZ in the salt, the bedded salt, underlying sedimentary strata, overlying sedimentary strata, and unconsolidated near-surface deposits. Groundwater in salt formations is generally present within intercrystalline porosity

or fluid inclusions rather than as a continuous phase. Interconnected porosity may be present in fissures, faults and/or interbeds. Under natural stratification conditions, the permeability of rock salt is extremely low. Rock salt also exhibits a high level of specific thermal conductivity. Rock salt reacts to mechanical load with a slow, flowing movement that is known as "salt creep". This particular property of rock salt causes cavities and fissures to be self-sealed over time. Bedded salt that has formed as evaporites in a sedimentary basin is geologically associated with fine-grained clastic sedimentary rocks. Underlying and overlying sedimentary rocks may consist of a wide range of sedimentary rock types originating from active basinal filling, including shales, sandstones, and carbonates. Safe disposal of non-heat-generating radioactive waste has been demonstrated by WIPP in the U.S. (DOE 1996) and research continues on UNF disposal in salt domes in Germany.

- **Mined Geologic Disposal in Crystalline Rock—**A crystalline rock repository disposal system entails a mined repository excavated in crystalline rock at a nominal depth of 500 m. Favorable crystalline rock types include granite, granitic gneiss, and other felsic igneous and metamorphic rock types. As with other mined repository alternatives, the repository layout consists of multiple, approximately horizontal drifts. The natural system surrounding the repository includes the DRZ in the host rock, the underlying and overlying crystalline rock, and unconsolidated near-surface deposits. Naturally occurring fractures, faults, and shear zones constitute important features in crystalline rock with regard to groundwater flow and radionuclide transport. An example of a proposed UNF repository in saturated granite is the Swedish KBS-3 concept (SKB 2011). Disposal in crystalline rocks is under scientific investigation in Switzerland, Japan, and Korea, and has advanced to the stage of site selection and licensing in Sweden and Finland.
- **Mined Geologic Disposal in Clay—**A clay repository disposal system consists of a mined repository in clay, shale or argillite at a nominal depth of 500 m. The repository layout would consist of multiple, horizontal drifts in the clay host rock. The natural system includes the DRZ, the host rock, underlying and overlying sedimentary rocks, and unconsolidated near-surface deposits. Clay/shale formations have low permeability, plasticity, fracture sealing or healing, and high sorption capacity. Clay-rich deposits appropriate for UNF and HLW disposal may be associated with a wide range of other overlying or underlying sedimentary rock types, including sandstones and carbonate rocks. Examples of proposed UNF and HLW repositories in saturated clays are the Swiss project in Opalinus Clay (Nagra 2002) and the French project in Callovo-Oxfordian argillites (Andra 2005b). An active research program for disposal in clay also exists in Belgium.
- **Deep Borehole Disposal in Crystalline Rock—**The deep borehole disposal concept involves drilling a borehole to a nominal depth of 5,000 m into crystalline basement rocks, with disposal of waste in the lower 2,000 m of the borehole. The upper 3,000 m of the borehole would be sealed in a manner similar to the sealing of boreholes and shafts in the shallower mined repository disposal systems. An array of multiple disposal boreholes would be developed at a given site. A summary of deep borehole disposal is presented in Brady et al. (2009) and reference conceptual design of the disposal system is described in Arnold et al. (2011a). Favorable crystalline host rock types include granite, granitic gneiss, and other felsic igneous and metamorphic rock types. The natural system for the borehole disposal system is composed of the DRZ, the crystalline host rock, overlying crystalline rock and sedimentary strata, and unconsolidated near-surface deposits. Overlying sedimentary strata in stable, intracontinental geological settings favorable for deep borehole disposal would likely consist of a wide variety of generally horizontal strata, including shales, sandstones, and carbonates. Investigation of the deep borehole disposal alternative generally has been limited to conceptual design studies, modeling, and literature investigations, but active research programs exist at the Massachusetts Institute of Technology (MIT) and at SNL.

To represent these different geologic media and disposal concepts in an advanced modeling framework, the GDSM NBS conceptual models should consist of a 3D domain that has sufficient spatial extent to

contain all significant THCMBR perturbations caused by the presence of the repository. The NBS conceptual model domain must also contain the assumed interfaces with the EBS and biosphere. These interfaces must be defined conceptually, geometrically, and with regard to the exchange of information on radionuclide transport. The nature of these interfaces has important implications for consistency among the GDSM conceptual model components and for the overall disposal system modeling capabilities. Considerations in conceptualizing the interfaces are discussed in Section 2.4.1.1. Ideally, the NBS model domain would extend to natural groundwater flow boundary conditions, such as no-flow groundwater divides and surface discharge locations, zero-flux confining units at the lower boundary, and natural recharge conditions at the topographic surface. Considerations in describing the boundary conditions are discussed in Section 2.4.1.2.

Figure 2-3 provides a schematic illustration of the generic NBS and EBS components desirable for an advanced disposal system model. The generic NBS components include: the DRZ, the host rock, the aquifer system, and the surface/unsaturated zone and atmospheric system. These component subdomains may be subdivided or combined in terms of hydrogeologic units depending on the disposal system option or site-specific geology. For example, the host rock, aquifer system, and unsaturated zone system may all be a single fractured granite bedrock hydrogeologic unit in the case of a mined repository in crystalline rock. For a clay or salt repository, the aquifer system may consist of several distinct hydrogeologic units that correspond to multiple aquifers and aquitards in the stratified sedimentary system overlying the repository.

Specifics of the hydrogeologic conceptualization for NBS modeling, including stratigraphy, lithology, and structural geology, are highly variable and site specific. Nonetheless, meaningful generalizations can be made about the hydrogeologic framework for the four disposal system options, for the purposes of the GDSM NBS conceptual model. These generalizations are made on the basis of geological associations between the genesis of the host rock and other geological units, and further support the specification of reference concepts for the four disposal options (Arnold et al. 2012, Section 4.1.1):

- **Mined Geologic Disposal in Salt—**Bedded salt forms by the evaporation of seawater on the shallow margins of sedimentary basins, in which the circulation of seawater was restricted enough to allow the precipitation of evaporite minerals. Such low-energy depositional environments also result in the sedimentary deposition of fine grained clastic sediments such as clay and silt, so bedded salt deposits are generally interspersed with shales and siltstones. Continuing evolution of the sedimentary basin eventually leads to greater circulation of seawater along the basin margins, and evaporite deposits are often overlain by carbonate rocks, sandstone, and additional fine-grained strata. The generic hydrogeologic framework for the salt repository thus consists of underlying shales and siltstones, salt host rock, overlying shales, and an upper fractured carbonate rock aquifer. This conceptual model approximately corresponds to the geology of the WIPP site in the Permian Basin of New Mexico.
- **Mined Geologic Disposal in Crystalline Rock—**The crystalline rock repository concept encompasses a range of potential rock types; however, most sites that have been investigated for a crystalline rock repository have consisted of felsic igneous and metamorphic rocks, such as granite and granitic gneiss. Such Precambrian rocks are widespread, typically moderately to sparsely fractured, and include widely spaced fracture or shear zones of enhanced permeability. The hydrogeologic framework for the crystalline rock repository option consists of fractured granite or granite gneiss, with a relatively thin (<100-m thick) alluvial aquifer overlying the granite. This conceptual hydrogeologic framework approximately corresponds to the geology of the KBS-3 concept (SKB 2011).
- **Mined Geologic Disposal in Clay—**Clay, shale, or argillite rocks that are appropriate for the clay repository disposal system can form in a variety of sedimentary environments, ranging from a deep marine setting to lake beds. While the depositional environment for these fine-grained sediments is

very low energy, underlying and overlying strata may be coarser grained clastic sediments from near shore and terrestrial depositional environments, and it is difficult to draw generalized conclusions about their lithology. The hydrogeologic framework for the clay repository consists of an underlying sandstone unit, a thick clay-shale host rock, overlying siltstone, and uppermost sandstone unit.

- **Deep Borehole Disposal in Crystalline Rock—**The assumed hydrogeologic framework for the deep borehole disposal concept extends to a much greater depth than the mined repository concepts and consists of deeper crystalline basement rocks and sedimentary rocks in the upper 1,000 m of the model. The crystalline rock consists of fractured granite or granite gneiss with widely spaced fracture zones of enhanced permeability. The sedimentary section consists of alternating sandstones, shales, and carbonate units.

2.4.1.1 Interfaces with the EBS and Biosphere

As described in Section 2.3.1, the interface between the EBS and NBS will be established by embedding the EBS model within the NBS model. The geometry of the interface between the EBS model and the NBS model can be abstracted as a simplified representation or as a geometrically realistic representation of the repository design. For mined repository systems a simplified representation would be a lumped EBS (Section 2.3.1) embedded within the NBS model, where the lumped EBS is treated as a uniform source term for radionuclides released from the repository. A geometrically more realistic interface between the EBS model and the NBS model would include individual waste disposal drifts of the repository. The radionuclide source term would include releases from specific locations at the interface, based on detailed simulation results from a more complex EBS model. The complexity of the interface between the EBS model and the NBS model would be commensurate with the complexity and spatial resolution of both component models. Explicit representation of individual repository drifts would require high-resolution gridding in both the EBS model and the NBS model, and would probably require HPC for the numerical implementation of such a conceptual model. Routine probabilistic calculations with the GDSM do not require this level of fidelity.

The interface between the EBS and NBS models must also be defined in terms of groundwater flow, radionuclide transport, heat flux, and mechanical stress or displacement. Groundwater flow between the EBS and the NBS should be fairly limited as long as the buffer materials, grouting, and repository seals remain effective in the mined repository systems. For the deep borehole disposal system there would be more interaction between fluids in the host rock and the EBS in the disposal zone. In either case, the interface should allow for groundwater flow between the EBS and the NBS. Radionuclide transport between the EBS and the NBS could be either advective or diffusive, with diffusive transport dominating for the undisturbed scenario in the mined repository systems. Uni-directional transport from the EBS to the NBS is a justifiable simplification and could be implemented with a specified radionuclide flux coupling between the EBS and NBS. Thermal coupling between the EBS model and the NBS model should be bi-directional to obtain accurate estimates of the near-field temperature history. In the case of the deep borehole disposal system bi-directional coupling of heat transport at the interface between the EBS and the NBS is particularly important because of the role of TH effects in driving groundwater flow. Mechanical and thermo-mechanical effects are probably less important for the NBS model and could be implemented in a simplified, uni-directional fashion.

Numerous potential scenarios are plausible for the release of radionuclides from the NBS to the biosphere. Releases could occur at natural groundwater discharge locations, such as springs, rivers, lakes, or the ocean. More directly, radionuclide releases could occur in a hypothetical pumping well that supplies groundwater for drinking, household use, and/or agriculture. For simplicity and given current regulations, the pumping well release scenario to a human receptor is assumed for the GDSM conceptual model. This form of the interface between the NBS and biosphere avoids the technical uncertainties and

numerical limitations associated with accurately simulating in-situ radionuclide concentrations in groundwater or in surface water bodies that have received contaminated discharge.

2.4.1.2 Boundary Conditions

Defining the boundary conditions for any model of the natural system is important to the development of the conceptual model because the overall behavior of the model is largely determined by those boundary conditions. Typically, site-specific information and inferences about groundwater flow systems in general, for example, are used in defining the boundary conditions. Boundary conditions for the NBS model are arbitrary in the sense that the model does not correspond to any specific site. Nonetheless, reasonable assumptions about the boundary conditions can be made on the basis of "typical" natural system characteristics and assuming that a site with generally favorable characteristics would be chosen for a repository disposal system.

Groundwater boundary conditions for the three mined repository concepts are defined for the NBS model by assuming a subregional flow system with dimensions of 20 km by 30 km and significant active groundwater flow extending to a depth of 1 km. Subregional flow, which may be confined or unconfined, is assumed to have a relatively low average horizontal hydraulic gradient of 0.001, resulting from an unconfined regional groundwater flow system driven by distributed recharge on the topographic surface and surface water discharge at one end of the flow system. Such a groundwater flow system corresponds to an area with limited topographic relief, low-permeability rocks below 1 km, and lack of large-scale, regional groundwater driving forces.

Groundwater boundary conditions for the deep borehole disposal system are defined for a flow system with no vertical fluid driving forces (i.e., without overpressured or underpressured conditions at depth). Lateral boundaries consist of specified hydrostatic pressure, allowing inflow and outflow of groundwater in response to thermally-induced convection resulting from waste heat. No significant horizontal hydraulic gradient is assigned to the shallow part of the model domain. These boundary conditions correspond to a stable continental interior location with stagnant groundwater in the deep crystalline basement and no significant flow in the overlying sedimentary rock cover.

Thermal and mechanical boundary conditions assigned to the NBS model are the same for all four disposal system options. The thermal and mechanical boundary conditions are assumed to be far enough from the repository or disposal boreholes that they have little impact on the temperature and stress calculations related to waste heat. These boundary conditions correspond to a location with low to moderate heat flow in a tectonically stable environment without a large differential in ambient horizontal stress.

2.4.2 Generic NBS FEP Analysis

To identify important processes that should be included in NBS conceptual models, a preliminary generic FEP screening was performed using generic NBS-related FEPs from the UFDC FEP list (Freeze et al. 2011). The FEP screening is described in detail in Arnold et al. (2012, Section 2); a summary is provided here.

The generic FEP screening follows the approach taken by Clayton et al. (2011, Appendix B) to identify FEPs for inclusion in simplified PA models. In preparation for screening, 51 NBS-related FEPs (Arnold et al. 2012, Table A-1) were identified through a review of the UFDC FEP list in Freeze et al. (2011) and each of the NBS-related FEPs was mapped to the relevant NBS components (DRZ, host rock, other units). Some FEPs apply to just one NBS component; other FEPs apply to all NBS components.

The preliminary NBS FEP screening was based on (1) the judgment of a small group of NBS subject matter experts, (2) FEP evaluations documented in Freeze et al. (2010, Appendix B), and (3) prioritization analyses in the UFDC R&D Roadmap (DOE 2011). Each of the 51 NBS-related FEPs was evaluated for

importance in each of the four disposal system options. The screening process categorized each NBS FEP (for each disposal option) as "very important" or "somewhat important" or "low consequence/not applicable". The very important FEPs are those that need to be implemented in the GDSM NBS conceptual model. The importance is defined based on the capability of the process to facilitate or delay radionuclide transport and/or to enhance or diminish the NBS component performance. The somewhat important FEPs may or may not need to be implemented in the GDSM NBS conceptual model. In the latter case, these FEPs may instead be addressed in an alternative model or in an in-depth evaluation. In both cases, adequate justification for ultimately excluding a somewhat important FEP would be needed.

The preliminary generic NBS FEP screening summarized here only considers undisturbed conditions. The importance of external factors (e.g., seismic disruption, human intrusion) will be evaluated at a later time. The generic screening decisions were based on the conceptual assumptions outlined in Section 2.4.1 and on further assumptions about nominal scenarios, initial conditions, and transience summarized in the following subsections. This screening information is presented on a FEP-by-FEP basis in Arnold et al. (2012, Section 2.2). The important (included) NBS FEPs resulting from the preliminary generic FEP screening are listed in Appendix B.

Screening decisions will need to be re-evaluated in conjunction with site selection and the availability of site-specific information. However, this preliminary screening can be used to guide preliminary identification of necessary model capabilities.

2.4.2.1 Generic Scenarios

The NBS model includes both undisturbed and disruptive generic scenarios. The undisturbed scenarios for each of the four disposal options correspond to the conceptual model descriptions presented in Section 2.4.1 and to the important nominal FEPs described in Section 2.4.2 and listed in Appendix B. The anticipated disruptive scenarios (e.g., human intrusion, seismic) can be accommodated with modifications of the undisturbed NBS model.

A human intrusion scenario typically entails hypothetical future drilling into the repository and creating a mechanism for radionuclide release that bypasses some or all of the barriers in the EBS and NBS. The NBS model could be modified to include direct release of radionuclide mass into the NBS at any location along the drillhole to represent the human intrusion scenario.

A seismic disruption scenario could include activation of faults in the natural system and enhanced permeability in fracture networks and along faults following an earthquake. The seismic disruption scenario could be accommodated in the NBS model by changing values of permeability and the nature of heterogeneities in the natural system.

If continental glaciation is a plausible disruptive event at a particular site, impacts on the natural system would include increased fluid pressures, alteration of groundwater boundary conditions, increased vertical mechanical stress, and suppressed temperatures in the geothermal gradient. Modifications to the undisturbed NBS model could include these changes, although complex THM coupling would probably require more advanced numerical simulation methods.

2.4.2.2 Initial Conditions

Steady-state, equilibrium conditions for groundwater flow, heat flow, and mechanical stress are justifiable as the initial conditions for the NBS model for the four alternative disposal system options, with some possible exceptions for some sites. Ambient conditions in the natural system may be altered somewhat by dewatering within or stress redistribution around the repository excavation, but such perturbations generally occur only very near the EBS. Non-equilibrium conditions may have persisted to the present day following continental glaciation in very low permeability units, such as overpressured conditions in clay or shale. Post-glacial rebound would also lead to non-steady-state hydrologic and mechanical

conditions for slowly rising landscapes. Variations in past climatic conditions can also result in non-equilibrium temperature profiles with depth. None of these transient effects would have significant impacts on the generic natural system model with regard to simulations of radionuclide transport from repository systems.

2.4.2.3 Transience in the Natural System

The natural system may experience transient conditions for different features and processes over a range of time scales. Groundwater flow conditions change at short time scales in response to individual precipitation events, seasonal variations in precipitation and evapotranspiration, and variations in river stage, lake levels, or marine tidal conditions. In addition, the presence of a mined repository and dewatering of the excavation may impact local groundwater flow rates and directions in the natural system. Such short-term transience in groundwater flow is generally limited to the shallowest parts of the flow system or near the repository for a short period of time, has little relevance to radionuclide transport from a deep repository, and can be neglected by assuming steady-state flow conditions for undisturbed natural system analysis. At longer time scales the groundwater flow conditions may be altered by climate change (including glaciation), anthropogenic influences via groundwater pumping, and geomorphic evolution (at very long time scales). Analysis of disturbed scenarios for changes to the groundwater flow system is often determined by policy and regulatory decisions. Generally, the impacts on groundwater flow of disturbed conditions can be evaluated by changing the boundary conditions of the undisturbed scenario model and allowing transient changes to propagate through the system.

The natural system would also experience transient conditions for heat flow and mechanical stress due to the presence of the repository. Temperature perturbations may extend for significant distances from the repository into the natural system and persist for hundreds or thousands of years; however, the magnitude of change in temperature declines rapidly with distance from the repository. Mechanical effects may also impact the natural system, but have significant impacts only very near the repository. Coupled TH processes can produce transient groundwater flow conditions in the natural system, but have limited impact on groundwater flow and radionuclide transport for the three mined repository systems. For the deep borehole disposal concept coupled TH flow would be the primary process driving fluid flow and radionuclide transport for a deep hydrogeological system that lacks significant ambient gradients in fluid potential.

2.4.3 Numerical Implementation

As summarized in Section 2.4.1, the GDSM NBS should consist of a 3D model domain that has sufficient spatial extent to contain all significant THCMBR perturbations caused by the presence of a repository. The NBS model domain must also contain the assumed interfaces with the EBS and biosphere. Mathematical models and the associated governing equations describing the important NBS FEPs provide the basis for the numerical implementation of the NBS model. At a high level, these governing equations describe coupled fluid flow and mass and energy transport through the subsurface, where the subsurface is represented as a porous medium with spatially variable properties. A detailed discussion of considerations for the numerical implementation of flow and transport in an NBS model is presented in Arnold et al. (2012, Section 5). A summary is provided here.

Governing equations for the following THCMBR processes are provided by Arnold et al. (2012, Section 3):

- **Groundwater Flow**—Compressible, multi-component, multi-phase flow, including alternate representations of the heterogeneity in permeability (e.g., dual porosity, dual continuum, multiple interacting continuum) and relative permeability
- **Heat Transport**—Based on conservation of energy

- **Mass Transport**—Based on conservation of mass, with transport influenced by advection, hydrodynamic dispersion, diffusion, matrix diffusion (for fractured media), sorption, and colloids
- **Biochemical and Geochemical Reactions**—Equilibrium and kinetic reactions, mineral precipitation and dissolution
- **Geomechanics**

Several numerical methods using spatial discretization or gridding of the problem domain are commonly used in the numerical implementation of the governing equations for groundwater flow, heat transport, mass transport, and geomechanics. These methods include finite difference, finite element, finite volume, and integrated finite difference techniques. These methods use an Eulerian frame of reference in which flow and transport are analyzed from a spatially rigid perspective. Alternatively, flow and transport can be analyzed from a Lagrangian frame of reference in which individual parcels of fluid or solute mass are tracked through space.

Eulerian numerical methods like the finite element method are very successful for simulating generally highly diffusive properties of the natural system such as fluid pressure in groundwater flow, temperature in heat transport, and stress in solid mechanics, particularly in homogeneous or mildly heterogeneous media. The grid resolution and the associated computational burden required to accurately model these processes is related to the magnitude of the gradients in the dependent properties and the degree of heterogeneity in the media. As examples, the grid resolution near a pumping well must be higher to accurately represent the gradient in hydraulic head and the grid resolution near the EBS must be higher to accurately simulate the gradients in temperature associated with repository heat. A moderate amount of heterogeneity in permeability within the medium can be accurately represented with a uniform grid; however, highly heterogeneous media and explicit representation of discrete fractures require extremely high grid resolution in the strictly Eulerian approach.

For solute transport in systems that are advectively dominated, strictly Eulerian numerical methods are less successful. Very high grid resolution, particularly at the front of an advancing solute plume is required to obtain an accurate numerical solution. This is because numerical dispersion inherent in Eulerian methods overwhelms physical dispersion, leading to "smearing" of the simulated solute plume and unrealistically low simulated solute concentrations. Solute mass balance errors can also be a problem in Eulerian methods.

Lagrangian numerical methods have the advantage in solute transport simulations of limited numerical dispersion that is generally independent of grid resolution (e.g., see Zheng 1990). Often implemented as a particle tracking method, the Lagrangian approach also enforces solute mass balance in solute transport modeling. In addition, Lagrangian numerical methods are numerically much more efficient than Eulerian methods for solute transport.

Hybrid methods that combine the respective strengths of the Eulerian and Lagrangian numerical approaches can be used to model the NBS for PA analyses. 3D Eulerian modeling of groundwater flow, thermal processes, and mechanics could be used in combination with particle tracking to define paths for radionuclide transport through the generic natural system model. Essentially 1D modeling could then be used to simulate radionuclide transport from the EBS to the biosphere. The 1D modeling of transport can be directly coupled to the 3D modeling of other processes to capture transient effects in flow and heat transport or time-invariant flow paths can be extracted for simplified, decoupled simulation of radionuclide transport. Examples of numerical methods using hybrid approaches that are relevant to UNF and HLW disposal and natural system modeling include Arnold et al. (2003), Robinson et al. (2010), and Painter et al. (2008).

Furthermore, numerical methods applied to numerical models of groundwater flow, solute transport, heat transport, and solid mechanics are dependent on the conceptual simplifications applied to the media in the

natural system. These alternative implementation methods of conceptual flow models are summarized in Altman et al. (1996) and shown in Figure 2-4 and include the following alternatives, listed from least to most complex:

- **Equivalent Porous Medium Continuum—**All processes and material properties treated as a porous medium in a single continuum. Equivalent material properties are based on effective characteristics of the medium.
- **Composite Porosity Continuum—**All processes and material properties treated as a porous medium in a single continuum. Some material properties (e.g., relative permeability – capillary pressure relationships) are altered to reflect the effects of fractures.
- **Dual Porosity—**Processes and materials are represented by two collocated continua, the fracture continuum and the matrix continuum. Flow occurs only in the fracture continuum, but fluid and solute exchange occurs between the fracture continuum and the matrix continuum.
- **Dual Permeability—**Processes and materials are represented by two collocated continua, the fracture continuum and the matrix continuum. Flow occurs both in the fracture continuum and in the matrix continuum. Fluid and solute exchange also occur between the fracture continuum and the matrix continuum.
- **Discrete Fracture Network—**Individual fractures are discretely represented. Flow and transport only occur in the fractures.
- **Discrete Fracture Network with Matrix—**Individual fractures are discretely represented. Flow and transport occur in both the fractures and matrix. Fluid and solute exchange also occur between the fractures and the matrix.

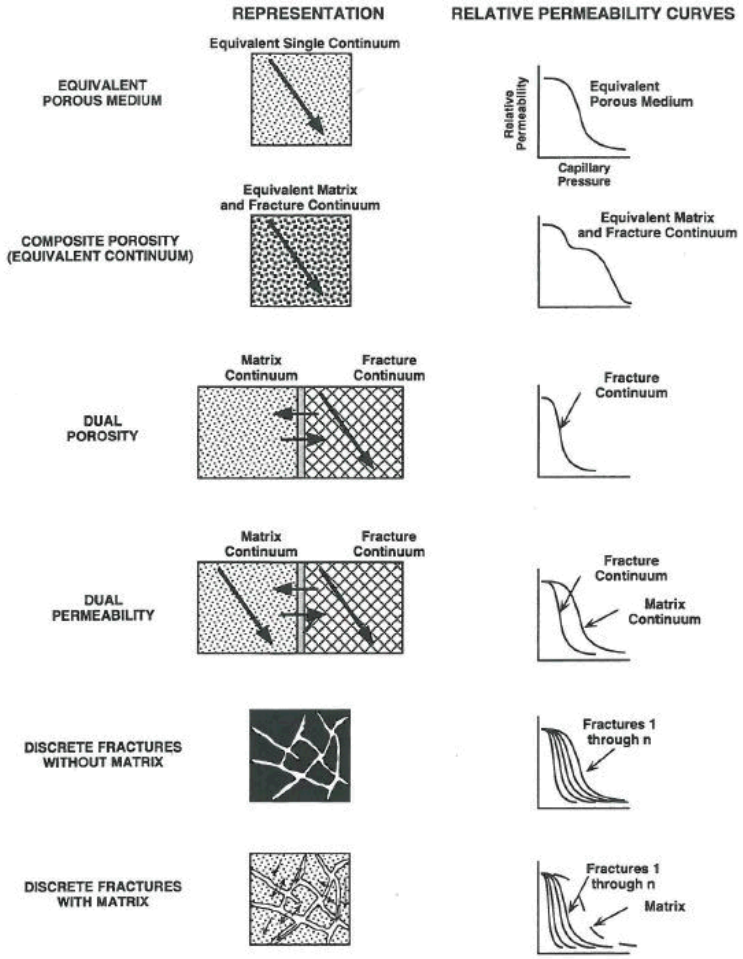

Source: Altman et al. 1996.

Figure 2-4. Alternative Implementation Methods of Conceptual Flow Models

Different alternative implementation methods may be appropriate for different units within the generic NBS model and for different disposal system options. The equivalent porous medium approach is valid for aquifers consisting of granular media and probably for low-permeability host rock such as clay. The dual-porosity approach is appropriate for densely fractured units, such as fractured carbonate aquifers and for fractured crystalline rock as some sites. The discrete fracture network with matrix approach may be required for granite host rock at some sites.

The appropriate implementation method may also be a function of spatial scale. For example, radionuclide transport of a few hundred meters through fractured crystalline rock from a mined repository may require a discrete fracture network approach, whereas transport of a few thousand meters through fractured crystalline rock from deep borehole disposal might appropriately use a continuum dual-porosity approach. Computationally efficient methods have also been developed that effectively upscale solute transport behavior in discrete fracture networks for implementation with a continuum approach (e.g., Painter and Cvetkovic 2005).

Based on the preceding discussion, the following recommendations can be made for the numerical implementation of the GDSM NBS model (Arnold et al. 2012, Sections 5.2 and 5.3; Freeze and Vaughn 2012, Section 2.2.2):

- Groundwater flow can be simulated using a 3D model based on Eulerian methods. An equivalent porous medium representation may be sufficient for some units, but a dual-porosity, dual-permeability, or discrete fracture representation may be required in other units. Large-scale discrete fracture network representations with matrix participation for the entire natural system model are generally beyond the computational reach of standard finite-element formulations. However, advanced finite-element gridding methods to explicitly include discrete fracture networks at large scales are under development.
- Heat transport and geomechanics can be simulated using a 3D model based on Eulerian methods. Heat transport and mechanics can be accommodated using a continuum representation for all units in the natural system. The option will exist to turn off the heat transport and geomechanics processes in the model (completely or at specified times and/or subdomains), which may be acceptable for many GDSM applications, and will lead to significantly greater computational efficiency. The dynamics of mechanical coupling to the host rock is not likely to be considered in the NBS model at this time or in the foreseeable future; however, detailed process level mechanics modeling will be needed to inform the approach to be taken.
- Radionuclide transport (including advection, dispersion, diffusion, sorption, matrix diffusion in fractured media, colloid-facilitated transport, and radionuclide decay and ingrowth) can be simulated using Lagrangian methods or Eulerian methods.

  Eulerian methods can be applied to preserve an implicit coupling between flow and transport processes, as long as numerical dispersion can be minimized. The corresponding fine grid resolution may require numerical solutions that take advantage of HPC to produce acceptable runtimes. Eulerian methods are more straightforward than Lagrangian methods and, as a result, can be more desirable, if these numerical limitations can be overcome.

  Lagrangian methods can be applied along essentially 1D pathways through the NBS using multiple stochastically generated particle tracks representing packets of radionuclide mass. The 1D nature of the solute transport solution would be computationally efficient. However, particle tracking can require a very large number of particles to obtain an accurate solution for contaminant concentrations in groundwater, particularly for very low concentrations at the margins of a plume. Simulating decay chains directly may also require a large number of particles and/or very small time steps. These limitations may be partially overcome by extending simple particle tracking to the method-of-characteristics numerical method.

  Numerical solution techniques that are appropriate for local conditions could be applied to different segments of the transport pathway through the system to improve computational efficiency. For example, for those portions of the flow path in which diffusion dominates, a simplified equivalent porous medium, diffusion-only solution would be implemented. For locations along the particle path in which groundwater flow dominates transport, an advection-dispersion solution would be applied, with potentially dual-porosity mass transfer applied in fractured units. An additional option, if needed, could allow the groundwater flow solution to be "frozen" under steady-state conditions. Radionuclide transport would be simulated along 1D flow paths that have been determined using particle tracking methods in the 3D model.

In summary, the 3D NBS model will be capable of simulating the processes of groundwater flow, heat transport, and mass transport, with a possible inclusion of geomechanics, if needed. The NBS model will consist of simplified, but reasonable representations of hydrogeologic units, specific to each disposal

system option. Input to the NBS model from the embedded EBS model will include radionuclide mass release, thermal output, and possibly mechanical stress. As noted above, the inputs of thermal output and mechanical stress would be disabled for simulations that do not include heat transport and geomechanics. Other inputs may include initiating events that would change the boundary conditions or material properties within the natural system, such as climate change, seismic events, or continental glaciations. Output of the NBS model to the biosphere will be radionuclide mass release for each time step. Actual numerical implementation of the model is subject to the availability and limitations of software codes, a list of potential codes is provide in Freeze and Vaughn (2012, Section 4).

2.5 Database Development and Configuration Management

2.5.1 Introduction

Recognizing the importance of a controlled computational environment, the development of a GDSM Computational Parameter Database was initiated in parallel with the development of the simplified GoldSim GPAM model capability (Section 2.2.1). The relational parameter database serves two important functions: (1) it is the controlled source of parameter information for GDSM calculations, and (2) it is a key element of the GDSM configuration management strategy (Section 2.1.2), and as such the database design helps to ensure that the performance analyses are traceable, transparent, and reproducible.

The GDSM Computational Parameter Database was initially developed to interface with the GoldSim-based simplified GPAM framework (Clayton et al. 2011, Section 4.2.2). Because current PA model development has moved away from the simplified GPAM framework and is focused on an advanced framework (Section 2.2.2), further development of the centralized database is being deferred until the path forward for the advanced framework is established (Freeze and Vaughn 2012, Section 5), sometime in FY 2013. The current design of the GDSM Computational Parameter Database is flexible and can accommodate the transition to any advanced PA model framework ultimately selected to implement the GDSM architecture. Currently the database contains some specific interfaces to provide integration with GoldSim. These interfaces can be readily modified without compromising the main structure of the database. Additionally, configuration control is being maintained during this period using previously established protocols (Clayton et al. 2011, Section 4.3).

The following subsections summarize the progress made on the GDSM Computational Parameter Database, both in terms of the conceptual design and its preliminary implementation. They describe how the GDSM Computational Parameter Database fits into the overall data management structure for the UFDC and then discuss the database itself, addressing the identification of database requirements, the architecture, the user experience, and the GDSM configuration management strategy.

2.5.2 Role of the GDSM Computational Parameter Database in Overall Data Management Structure for the UFDC

The GDSM Computational Parameter Database is one of multiple efforts to collect and manage data in the UFDC. An integration plan (Wang 2011) was developed to promote effective coordination of these multiple efforts across the UFDC. This plan identifies four sets of data to be collected and managed: natural system evaluation, EBS evaluation, interim storage and transportation, and PA models. The use of data and parameter values in the following text should be taken in general to include descriptions of parameter uncertainty such as distribution types and ranges of values. The three data sets of particular interest to GDSM activities are shown below (PA model modified from Wang (2011)):

Natural System Evaluation

- Spatial distributions of relevant geologic media (e.g., salt, clay/shale, granite)
- Demographic information for site screening and selection

- Regional flow information
- Physical configuration of geologic repositories
- Hydrologic properties of geologic media
- Thermal properties of geologic materials
- Mechanical properties of geologic materials
- Chemical/mineralogical compositions of relevant geologic media
- Groundwater chemistry
- Radionuclide speciation information
- Radionuclide sorption properties
- Information on colloid-facilitated radionuclide transport
- Biological attributes
- Others

EBS Evaluation

- Waste inventory
- Physical configuration of EBS
- Waste form degradation information
- Waste package degradation information
- Thermal properties of introduced materials
- Mechanical properties of introduced materials
- Chemical properties of introduced materials
- Radionuclide speciation information (especially for elevated temperatures)
- Radionuclide sorption on engineered materials or their corrosion products
- Information on colloid generation and transport
- Others

PA Model

- Submodel parameter values, e.g. porosities, solubilities, decay rates
- Submodel interface parameter values, e.g. radionuclide mass flux from EBS to geosphere
- System-model-related parameter values, e.g. spatial extent, duration, grid generation information
- Numerical control parameter values, e.g. convergence criteria, time step control
- PA model results, e.g. system and subsystem calculated results

The integration plan recognizes the need for a UFDC data management system to store, control, and provide access for the various data sets. The system must also facilitate the use of the information in the system-level PA model. As seen in Figure 2-5, Wang (2011) suggests that the UFDC data management system be comprised of two major databases—a performance assessment database (PADB) and a

supporting technical database (TDB)—as well as a document repository (DOCR). The GDSM Computational Parameter Database is intended to perform the functions of the PADB discussed in Wang (2011).

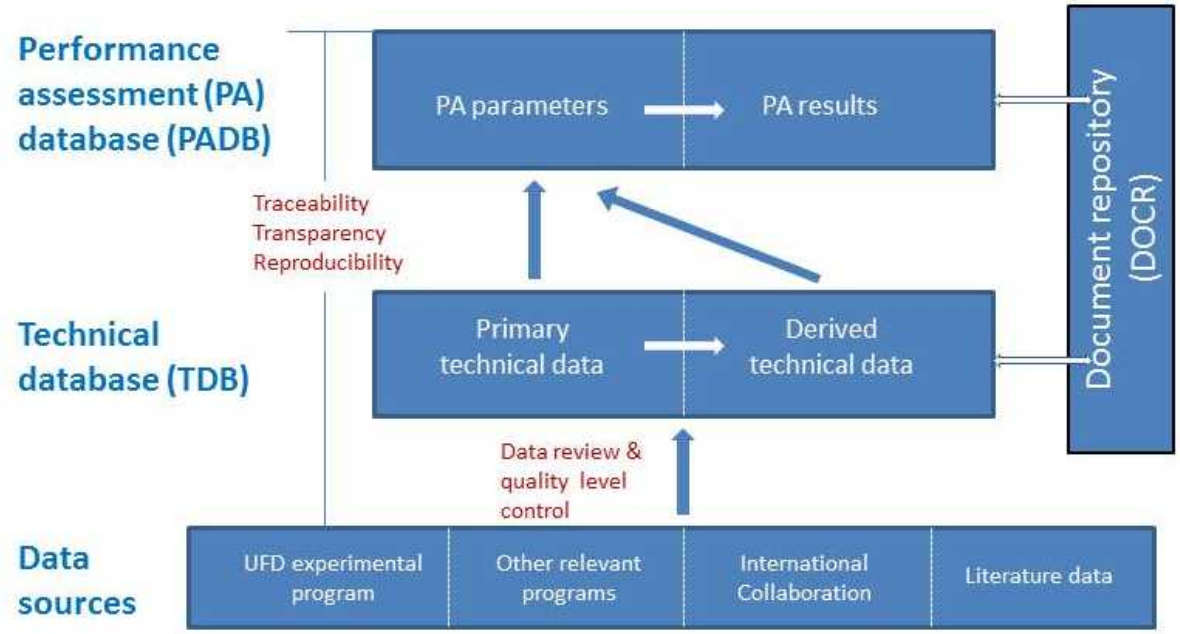

Source: Wang 2011, Figure 1.

NOTE: The PADB referred to above is the GDSM Computational Parameter Database.

Figure 2-5. Architecture of UFDC Data Management System

The GDSM Computational Parameter Database and the TDB have different functions, but must be closely coordinated. Wang (2011) identifies the function of the TDB as storing "all technical data, both primary and derived, that support PA model parameter development." The functions of the GDSM Computational Parameter Database include maintaining configuration control of all the parameters required by the disposal system model. This includes the subsystem model parameters, which in general require a synthesis of information residing in the TDB in order to be used directly by the disposal system model.

Close coordination is required to ensure that the parameter information in the GDSM Computational Parameter database is consistent with the technical data in the technical database. Part of this coordination involves the synthesis of the primary and derived technical data into parameter values for disposal system PA model. A simple example of this synthesis is units conversion; however, this synthesis will also involve an assessment of the adequacy of the technical data, relevancy for intended use in the system model, and other factors such as uncertainty strategy. The subject matter experts provide the expertise for this synthesis with the guidance from the GDSM team. The latter group defines the needs, the purpose, and the specification of the data for use in the disposal system PA model.

Future data management work will focus on developing a structure to support achieving the appropriate integration and coordination between the GDSM Computational Parameter Database and the TDB. Of particular importance is the characterization of parameter uncertainty and integration across all data providers, which is required in order to characterize uncertainty in a consistent and appropriate fashion for use in the disposal system model. Previous experience from WIPP (DOE 1996, 2004, 2009) and YMP (DOE 2008) suggests that formal documentation is useful. Interactions between the EBS and Natural Systems groups and the GDSM team have been and will continue to be conducted. These interactions are expected to produce formal documentation summarizing the results of the interactions along with evidence, such as signatures, to verify agreement between all parties.

2.5.3 GDSM Computational Parameter Database Requirements

The broad objectives for the GDSM Computational Parameter Database are as follows:

- Maintain and control information on the parameters used in disposal system models
- Serve as a controlled source of input for all disposal system and subsystem calculations
- Support and document the verification of information in the database
- Produce reports including listing of parameters by parameter name and parameter attributes
- Support downloading database information to a framework model file

Table 2-1 provides the specific functional requirements that form the basis for the GDSM Computational Parameter Database development. These requirements are driven by the anticipated needs of disposal system modeling and the associated demonstration of pedigree and control of information. PA calculations are a key part of the safety evaluation of a geologic repository. The data used to support these calculations must meet high standards. Traceability, transparency, and reproducibility must be maintained for all calculations and supporting information.

A significant first step towards maintaining traceability, transparency, and reproducibility is to ensure configuration control of information related to parameters used in the PA models developed by the GDSM team. There are several requirements that have been established for the database with the intention of maintaining this configuration control. There are requirements for controls on who may enter and/or change information that is contained in the database. There are requirements for check and verification of information entered and/or changed in the database. There are also requirements for identifying and maintaining references to support technical information in the database. Additional details regarding the configuration management strategy are discussed in Section 2.5.6.

An important aspect of maintaining traceability, transparency, and reproducibility is to ensure that inputs for model calculations are controlled. There is a requirement for the system to maintain information on all parameter values used in an individual model calculation. Also, as discussed in Section 2.5.5, there will likely be a need to store the database in more than one location to provide access for both on-site and off-site users. If multiple versions (i.e., mirror images or copies of the controlled database) are made available, configuration management must ensure that all such versions contain exactly the same parameter information.

Table 2-1. Functional Requirements of the GDSM Computational Parameter Database

1. The software shall be a stand-alone software application. The software shall be developed using a commercial database manager.
2. The system shall store information in a series of tables. Included are three tables: GS_Parameter, GS_Parameter_Value, and GS_Value_Component, as defined in Appendix F of the GoldSim User's Guide (GoldSim Technology Group 2010a), for a "Yucca Mountain Database", which are directly accessed by GoldSim model simulation runs.
3. The system shall provide the capability to edit all input fields (including data values).
4. Parameter names cannot be duplicated.
5. The system shall assign each parameter entered a parameter code corresponding to the parameter type (e.g., Type: 1-d Table Code: 5100). Parameter types and associated codes are specified in Appendix F of the GoldSim User's Guide (GoldSim Technology Group 2010a).
6. The database shall be capable of storing network paths and audit tracking signature numbers for external files and dynamic link libraries (DLLs) located on a controlled network drive.
7. The system shall retain a history of users that have made changes to a parameter, including the date, time, and name of the user that made the change.
8. For data validation the system shall record the date, time, and name of the user performing data verifications.
9. In addition to the minimum parameter data shown above, the system shall store model location and input type for each parameter.
10. The system shall allow multiple references for each parameter.
11. The system shall indicate a verification status of "unverified" if reference information or data values are changed for a parameter, except for the following fields which will not affect verification status: model location and input type.
12. The system shall prevent incidental changes to parameter names and data values by requiring the user to enter "edit" mode before changes can be made.
13. The system shall be capable of handling a minimum of 20 columns for 2D tables.
14. The system shall take text inputs and numeric values that range from single constants to 2D tables.
15. Inputs shall be manually entered into the database using forms with input fields for the information to be entered. (Note that drop-down lists and list boxes should be used to the extent possible.)
16. The software shall present parameter values and information in a format that is viewable for auditing and verification.
17. The system shall be capable of defining and maintaining references (for example, documents, diagrams, and reports) for parameter values and other information.
18. The system shall provide the capability to comment on data changes (for example, explain rationale for change).
19. The system shall maintain the capability to add input fields in the future (if needed).
20. The software shall display and print reports containing parameter information sorted alphabetically and by model location and input type.
21. The system shall maintain the capability to record parameter information used for individual calculations and make this information available to future users, i.e., a run log.

Table 2-1. Functional Requirements of the GDSM Computational Parameter Database (continued)

22. If multiple versions, or copies, of the database are needed to provide access to multiple users, then the system shall maintain configuration control with all such versions containing exactly the same parameter information.
23. The database shall be open database connectivity (ODBC) compliant.
24. The system shall provide a “data entry” level of access to permit add and update privileges.
25. The system shall provide a “checker” level of access to permit verification and review privileges.
26. The system shall provide a “read-only” level of access to permit viewing privileges.

2.5.4 Modeling/Database Architecture

The plan for the database architecture is summarized in Walkow (2012). Much of the database architecture plan has been implemented and a working version has been available for testing and evaluation. Completion of the plan is on hold pending definition of the GDSM framework path forward, discussed in Section 2.2.3. In the database architecture, the SNL External Collaboration Network (ECN) serves as the entry point for all users. Users must log into the ECN in order to access other components of the architecture. All users must have SharePoint user IDs and passwords. The hardware supporting the architecture—the database server, GoldSim Cluster, terminal server, and reporting server—is transparent to the database users.

The GDSM Computational Parameter Database is maintained as a SharePoint site on the ECN. The database hardware and software that stores the data values is housed on a SQL server. The preliminary version of this SharePoint site is operational. The initial implementation of the site includes 15 user-interface lists designed to allow users to enter information on model parameters. The task of populating the GDSM Computational Parameter Database with information on parameters and parameter values has begun. As discussed below (Section 2.5.4.1), two types of parameter sets are contained within the database: framework parameters and GDSM parameters. An initial listing of names for framework parameters has been used to populate the appropriate list on the site. In addition, information related to approximately 400 GDSM system and subsystem parameters has been entered. Some lists are also used to establish categories of information that are stored for the GDSM Parameters. These categories can be used as filters to facilitate organizing and searching information stored in the database.

Initial reporting capabilities have also been developed. Reports can be generated for both GDSM and framework parameters. Reports for these parameters can be sorted by parameter name to identify types of parameters, e.g., sorption coefficients. In the future, the reporting capabilities will be expanded. Among the capabilities envisioned is the generation of a report based on filters developed to help users navigate the database.

2.5.4.1 Structure of Parameter Sets within the Database

The GDSM Computational Parameter Database is designed to allow users to create input files that the implementing GPAM framework reads to perform and manage the calculations. Within the database, the relevant information is organized into two parameter sets:

- **Framework Parameter Set**—The framework parameters are preprogrammed (i.e., hardwired) because they are required to implement the PA model framework, currently GoldSim-based GPAM V1 (Section 2.2.1). As a result, they are fixed and will be changed only to support a formal revision of PA model framework. Such a revision is expected when the new advanced framework is identified (Section 2.2.2). At that time, the framework parameter set will be modified for

compatibility with the new PA model framework. A PA model framework revision could also result from a new or improved submodel that uses different parameters because of a different treatment of, for example, a feature or phenomenon. The GDSM Computational Parameter Database stores framework parameters as shells, or placeholders, with the parameter name and, perhaps, some other limited information. The process by which the empty shells are filled with technical information from the GDSM parameter set to create input files is described in more detail below.

- **GDSM Parameter Set**—This parameter set is independent of the framework parameters. It contains a suite of technical information about parameters, parameter values, and their uncertainties that can be used in the multi-physics models to represent the GDSM conceptual components and FEPs. The GDSM parameters have fixed names and values that will not change unless (1) an error was made when the parameter information was entered into the database or (2) the subsystem models have changed and require additional or different parameter support. The number of GDSM parameters is expected to increase with time, as new or refined system or subsystem models are used. The current suite of technical information has been gathered by the GDSM team, in consultation with subject matter experts, to support model development activities and current disposal system analysis capabilities. Sources include the scientific literature as well as basic observations and measurements in field and laboratory settings by subject matter experts at DOE laboratories or other entities. While adequate for present GDSM activities, ultimately the parameter information and their pedigrees will be "owned" and justified by UFDC EBS and NBS subject matter experts. As discussed in Section 2.5.2, this effort will be aided by the development of the TDB. The purpose of the TDB is to store the primary and derived technical data that subject matter experts can use to synthesize and develop parameter values in the GDSM parameter set stored in the GDSM Computational Parameter Database.

Within the GDSM Computational Parameter Database, the framework parameter set and the GDSM parameter set can be thought of as representing two different conceptual levels in the process used for creating PA model input files. The process begins at the framework parameter level. The framework parameter set supplies the shells with specific parameter names needed to support a particular calculation. The shells are essentially placeholders waiting to be populated with values. The focus then shifts to the GDSM parameter level. The GDSM parameter set provides a suite of potential parameter values, from which specific values are selected to "feed" or populate the framework parameter shells in the input file.

This dual-level structure was developed for several reasons. The most obvious reason is to provide the flexibility to support multiple frameworks without having to manipulate or alter the underlying computational parameters and parameter values describing the physics of generic disposal. The simplest and most transparent way to provide for the flexibility needed to generate the input files for the implementing framework is to have the placeholders for the framework parameters explicitly identified by name in the database.

The structure also facilitates interactions between the PA analysts and the process model developers and data collectors. The structure allows everyone to see how GDSM parameters are utilized and how they relate to the PA model framework. It is also possible to define supporting information requirements for the GDSM parameters. The supporting information can provide valuable insights about the way in which primary data are used in the PA model.

2.5.4.2 Generic Features of the Database

The GDSM Computational Parameter Database has important features that are generic in nature. These features are required to address the challenges of generic disposal modeling, but are not dependent on the details of the system model, subsystem models, the implementing framework, or the hardware used for calculations and analysis.

The two parameter sets described in Section 2.5.4.1 are required for any configuration of numerical models and hardware. Any configuration will have to use parameter names, even if some specific details depend on the implementing framework. The database structure has the capability of accommodating the use of parameter names.

The database has the capability to store supporting information related to input parameters. For example regardless of the configuration, there will be a need for information on items such as rock type, design type, and model location along with a justification of the pedigree or a pointer or reference to the justification. The database needs to be able to store, or link to, reference information in all cases. Important work has been done to support this requirement. These aspects of the database will provide a significant starting point for work on the new modeling system.

2.5.4.3 Framework-Specific Features of the Database

As indicated above, the GDSM Computational Parameter Database has been designed to accommodate multiple implementing PA model frameworks through the use of parameter sets representing dual levels: framework parameters and GDSM parameters. Currently the implementing PA model framework is GoldSim; therefore, there are elements of the database that are GoldSim specific and will need to be changed when a new implementing framework is selected. For example, GoldSim uses "parameter codes" to quantify uncertainty in GDSM parameters values. The GoldSim user's manual (GoldSim Technology Group 2010a) includes a listing of "parameter codes" relating to parameter distribution types that can be implemented within the GoldSim software. A numerical code is assigned to each distribution type and this parameter code is a required input for all parameters used in a GoldSim model file.

Another example is the list of GoldSim parameter names. These names are specific to the implementation of GPAM in the GoldSim software. Of course, the new implementing framework will similarly require parameter names and will also require a mechanism for identifying parameter distribution types. The specific information in the database will need to be replaced or supplemented, and the database will need to be able to handle this type of information regardless of the implementing framework that is ultimately chosen.

2.5.4.4 General Attributes of GDSM Parameters

The database has been designed to include supporting information about general attributes of the GDSM parameters. The purpose of this supporting information is to facilitate the use of the GDSM parameter values by the PA analysts and to provide guidance to the subject matter experts on the needs and uses of the GDSM parameters. This information is also designed to assist reviewers of the information.

Supporting information is provided through a number of categories or fields. Examples include rock type, design type, waste type, property type, and model location. The rock type selected to represent the repository host rock is one of the distinguishing characteristics of a disposal system calculation. Potential rock types include salt, clay, and granite. There are many parameters that are determined by rock type (e.g., sorption coefficients, permeability, and porosity). Design type (e.g., mined or deep borehole) is an important determinant for some parameters. Waste Type l determines the values for parameters associated with inventory and source term. Property type helps to designate general types of parameters (e.g., physical, geometric, or hydrologic). Model location defines which component or subsystem within the disposal system model is relevant to specific sets of parameters. For example, there are several parameters (e.g., solubility limits) that may have different values for different model subsystems or locations. These categories will be used, principally, to sort data within the database and facilitate examination of the information. Several libraries of information have also been designated to assist in sorting parameters:

- Solubility Library
- Sorption Library

- Inventory Library
- Rock Properties Library
- Available Porosity Library
- Design Characteristics
- Natural System Characteristics

As the UFDC repository program matures, the database will expand to include a potentially very large amount of information. The PA analyst will need tools to help navigate this large suite of data values. The above categories and libraries fill this need by providing filters to sort the database. This capability should greatly aid analysts in generating input files by making it easier to sort through and select values from the GDSM parameter set to populate the shells from the framework parameter set. These library categories also facilitate description of the model in reports.

2.5.5 Database User Experience

The GDSM activities involve modelers and subject matter experts from multiple national laboratories and associated contractors. Additionally, it is important to provide access to other stakeholders and in particular to the DOE customer. To facilitate access for this diverse group of users, the GDSM Computational Parameter Database is internet based. While many of the users are located within the SNL physical facilities, there are also users located at a variety of other off-site locations. This situation creates challenges for access and for configuration management, which are addressed by the architecture of the GDSM Computational Parameter Database (Section 2.5.4).

The database utilizes the SNL ECN in order to facilitate access for all of these users. In addition, the database maintains all of the information for configuration control of GDSM PA analyses that are reviewed, developed, and used by the off-site users. As a result, the off-site users will have to have access to a controlled mirror image of the database that resides on the SNL SQL server. The database also needs to maintain a record of the parameters used in each GDSM PA calculation that is performed by the off-site user. The database is being developed to meet these requirements; however, it is not currently available to these off-site users.

2.5.5.1 Database Controls—User Levels

Configuration management requires strict control on changes that are made to the GDSM Computational Parameter Database. One control mechanism is to establish user levels with different access privileges. Three user levels have been established to control access and to facilitate management of the database. User Level 1 is the database manager level. Anyone with User Level 1 access can enter and/or modify all parameter information, including data values. User Level 1 access also allows changes to be made to the lists on the SharePoint site. User Level 2 is the checker level. Anyone with User Level 2 access can review all parameter information. User Level 2 access will allow the checker to document verification of the parameter information and/or any comments that the checker may have related to the parameter information. User Level 3 access is general “read only” access. User Level 3 access will be available to anyone on request.

In the future a fourth user level may be established. This user level would be designed for the GDSM PA analysts who also use the database to support investigative calculations and evaluations. The reason for considering this additional user level is that analysts may need to make a large number of trial or sensitivity analyses. It could be useful to have a user level for analysts who could enter information into the database for a sensitivity or trial analysis, but without privileges for changing the baseline information.

Mechanisms to support the three user levels have been incorporated into the preliminary implementation of the GDSM Computational Parameter Database. However, users for the different levels have not yet been identified. The exception is User Level 1 which is currently in use to enter the initial parameter values discussed above.

2.5.5.2 Run Controls—Log with Parameters

To support configuration management objectives, the GDSM Computational Parameter Database has been structured to include a Model Runs list. This list is designed to provide documentation for all calculations that are performed using the database as a source. The list documents all parameter values used in a calculation.

SharePoint lists have been established for "Model Runs" and "Model Run Status." Model Run Status includes the following steps:

- Input in Progress
- Input Complete
- Run Complete
- Run Failed
- Cancelled

The Model Runs list provides a means for quickly preserving and accessing information related to specific analyses. For each GDSM PA calculation, the Model Runs list identifies a run ID number, a run name, and a run description, along with the run author. A run is initiated by a PA analyst by obtaining a run ID number and completing the information required for this list.

When a run is initiated the run status is assigned as Input in Progress. The PA analyst must select a suite of GDSM parameters to assign to the framework parameters used by the PA model. The analyst may select a previous run and use the GDSM parameters from this previous run as a template, or starting point, to generate the list of framework parameters for the new run. If no template is selected then the PA analyst must assign a GDSM parameter to each framework parameter individually. When all of the assignments have been made the run status is changed to Input Complete.

The modifications have been made to the database to support the Model Runs list. However, changes are required to PA model framework to support importing parameter values directly from the database into the model at run time. These changes are not expected until the transition to the new PA model framework has occurred. Consequently, the database-supported Model Runs list is not available at this time.

2.5.6 GDSM Configuration Management Strategy

2.5.6.1 Configuration Management Role of the GDSM Computational Parameter Database

The GDSM Computational Parameter Database is a major part of the GDSM configuration management strategy. The database addresses four elements of the strategy:

- Maintain configuration control of parameters and parameter values
- Document calculations performed using the PA model framework
- Ensure reproducible results
- Establish management controls (Model Runs list)

The GDSM Computational Parameter Database provides an effective tool for maintaining configuration control of parameters and parameter values. The database allows the initial input of parameter information and subsequent changes to that information to be strictly controlled. Changes to the information contained in the database are documented within the database. As a result, the database maintains a complete record of the history of parameters and parameter values.

The Model Runs list (Section 2.5.5.2) along with the other associated documentation, ensures the reproducibility of results for GPAM calculations. The GDSM Computational Parameter Database includes documentation that identifies all parameters and parameter values that are used for each GDSM PA calculation. The results of the calculations are also maintained, but these may be stored outside of the database itself. This documentation also facilitates the planning and execution of future PA calculations. Complete documentation of PA calculations allows runs contained on the Model Runs list to be used as a starting point for future analyses. This capability contributes to the ability to define new analyses efficiently.

Given the current stage of database development, some of the desired configuration management capabilities are not yet available, e.g., the automatic storage and control of results from calculations and analyses. Therefore, an interim configuration management policy has been adopted until the database can fulfill its intended role. Discussed below, this policy provides many of the needed functionalities, but does so in a non-automated fashion.

2.5.6.2 Interim Configuration Management Policy

During the development of the GDSM Computational Parameter Database, interim tools have been developed to maintain configuration control. These interim tools have been developed using Excel and SharePoint. Excel spreadsheets have been used to document parameters and parameter values. SharePoint has been used to store versions of the models, parameter lists, results, and analysis descriptions.

Parameters—While the GDSM Computational Parameter Database is under development, configuration control will be maintained using parameter lists in a spreadsheet format. Parameter lists are available for all four individual GDS models (Clayton et al. 2011, Section 3) on the GDSM site on SharePoint. An Excel-based input file is also being used for GPAM V1 until the GDSM Computational Parameter Database is operational. These parameter lists provide a tool for establishing a baseline, in the absence of a relational database. While the Configuration Management Lead is responsible for maintaining the parameter lists on the GDSM site, the content is ultimately the responsibility of the model developers.

The parameter lists were developed for each of the four individual GDS models. The lists were developed by manually extracting information on individual parameters from the models and recording them in Excel files. The parameter lists were developed by the Configuration Management Lead and were subsequently reviewed and approved by the individual generic process model leads.

The parameter lists identify the PA model framework (currently GoldSim) parameter name, as used in the implemented model. For each parameter name, the list provides information on the representation type, i.e., discrete or stochastic. If the parameter is included in the model as a stochastic type, then the parameter list identifies the type of stochastic used. The parameter list provides the value of the parameter that is used in the individual GDS models reported by Clayton et al. (2011, Section 3). The list also provides any descriptive information about the parameter that is included in the implemented model file and any additional comments that the model developer wants to include. The list also includes traceability information to help anyone using the list find the parameter in the model file.

The parameter lists for the models reported by Clayton et al. (2011, Section 3) define the baseline for the four individual GDS models. Changes to this initial parameter information, due to error correction or evaluation of new information, will be documented in revisions to the parameter lists. The revised parameter lists will be stored on SharePoint. The database is intended as a living repository of

information, in which historical versions are preserved along with a history of the changes. It will be important to use the parameter lists as documentation of inputs for individual calculations. A copy of the parameter list, with changes from the Clayton et al. (2011, Section 3) version noted, is part of the documentation of individual calculations (discussed in more detail below).

Models—The Clayton et al. (2011, Section 3) versions of the four individual GDS models provide a partial baseline for the GDSM numerical models. The version of GPAM that incorporates these GDS models completes the initial model baseline for GDSM. Version control of these models is maintained as the GDSM efforts move forward. The Configuration Management Library on the GDSM SharePoint site is used to store the baseline versions of the models. The individual model developers are responsible for maintaining the most current version of their model on the GDSM site. A standard versioning convention is used: Version x.yz.

Calculations—As part of the configuration management strategy, the calculations made during the interim period are documented. In particular, documentation is required for calculations and analyses that are reported in a publication. Documentation is also needed for calculations completed to test or evaluate a particular model or submodel. Examples include validation calculations, baseline calculations, and sensitivity analyses.

An analysis documentation package is developed for each calculation. This package contains the model file (currently the GoldSim model file), a copy of the parameter list developed for the model, and a GDSM Analysis Description. The GDSM Analysis Description includes the following: (1) identification of the purpose of the calculation, (2) a description of the calculation, (3) identification of changes to baseline parameter values, and (4) a description of the uncertainty characterization. The completed calculation documentation package is stored in the Configuration Management Library on the GDSM site.

Table 2-2 identifies the roles and responsibilities for the Configuration Management Lead and the model developers and/or PA analysts producing calculations.

Table 2-2. Summary of Roles and Responsibilities for GDSM Configuration Management

Roles	Responsibilities
Configuration Management Lead	• Maintain Configuration Management library on GDSM Site. As needed, help others post files to appropriate areas in timely manner. Move or delete files if needed to properly maintain library. • Maintain parameter lists for the initial baseline • Maintain Model Runs list (interim version) • Serve as principal contact with the Information Technology (IT) Group for the GDSM Computational Parameter Database.
Model Developers or PA Analysts (i.e., anyone producing calculations)	• Working with Configuration Management Lead as needed, – Ensure updated versions of parameter lists are available on the GDSM site (Parameters folder) – Ensure updated versions of models are available on the GDSM site (Models folder) – Produce the documentation packages for calculations and ensure they are available on the GDSM site (Calculations folder) • Goal is to post within 5 days of completion. • Provide input for the Model Runs list to Configuration Management Lead

3 SIMPLIFIED PA MODEL APPLICATION

As noted in Section 2.2.1, simplified individual GDS models for salt, clay, granite, and deep borehole were developed and executed (Clayton et al. 2011, Section 3). These simplified models, referred to as the GDS models, used GoldSim but were developed outside of the GPAM framework, meaning that there were some minor inconsistencies in various component submodels across the four disposal options. In FY 2012, continued development of the individual GDS models was planned to (1) incorporate the four individual GDS models into a common GoldSim-based PA model framework, GPAM V1 (Section 2.2.1), and (2) maintain a simplified PA modeling capability to support (a) sensitivity analyses of various disposal system components, (b) the development of conceptual reference cases for each of the four disposal options, and (c) short-turnaround generic PA model needs.

However, some limitations of GoldSim became apparent during attempts to incorporate the individual GDS model components into the common GoldSim-based GPAM framework. GoldSim is best used as a framework when the physics are simple and uncoupled, the size of numerical grids is small, the desired use is narrowly focused, and potential changes are limited. As a result, attempts to develop a GoldSim-based simplified PA model framework were abandoned, in favor of the development of an advanced PA model framework (Section 2.2.2).

Nonetheless, some advancement of the simplified PA modeling capability was made in FY 2012. This included:

- **Salt GDS Model (Section 3.1)—**Probabilistic sensitivity analyses using parameter values updated from the FY 2011 salt GDS model (Clayton et al. 2011, Section 3.1)
- **Granite GDS Model (Section 3.2)—**Probabilistic sensitivity analyses using parameter values and model components updated from the FY 2011 granite GDS model (Clayton et al. 2011, Section 3.2)
- **Clay GDS Model (Section 3.3)—**Probabilistic sensitivity analyses using parameter values updated from the FY 2011 clay GDS model (Clayton et al. 2011, Section 3.3)
- **Deep Borehole GDS Model (Section 3.4)—**Probabilistic sensitivity analyses using parameter values updated from the FY 2011 deep borehole GDS model (Clayton et al. 2011, Section 3.4)
- **Deterministic Safety Assessments (Section 3.5)—**Deterministic simulations and sensitivity analyses using revised versions of the four individual GDS models. Revisions included updating some parameter values and model components for more consistency between the four individual models. This set of consistent simulations can be used to support a preliminary generic deep geologic disposal safety case.

Where possible, these individual GDS models try to represent the important EBS and NBS FEPs identified in Sections 2.3.2 and 2.4.2, respectively. The sensitivity analysis results from these simplified models provide insights into the relative importance of processes and parameters that affect the long-term performance attributes of salt, clay, granite, and deep borehole generic disposal environments. These results can inform the development of generic reference cases and R&D for each of the disposal options, however, the results are not intended to screen and/or prioritize specific disposal options, designs, and sites for their suitability for a geologic disposal facility.

These simplified PA modeling activities support the continued UFDC capability to perform short-turnaround PA modeling until an advanced PA modeling capability is developed.

3.1 Salt GDS Model

3.1.1 Model Description

The salt GDS model used for the FY 2012 sensitivity simulations described in this section derives from the FY 2011 salt GDS model (Clayton et al. 2011, Section 3.1). The salt GDS conceptual model, shown schematically in Figure 3-1, includes an undisturbed reference scenario and a disturbed (human intrusion) scenario.

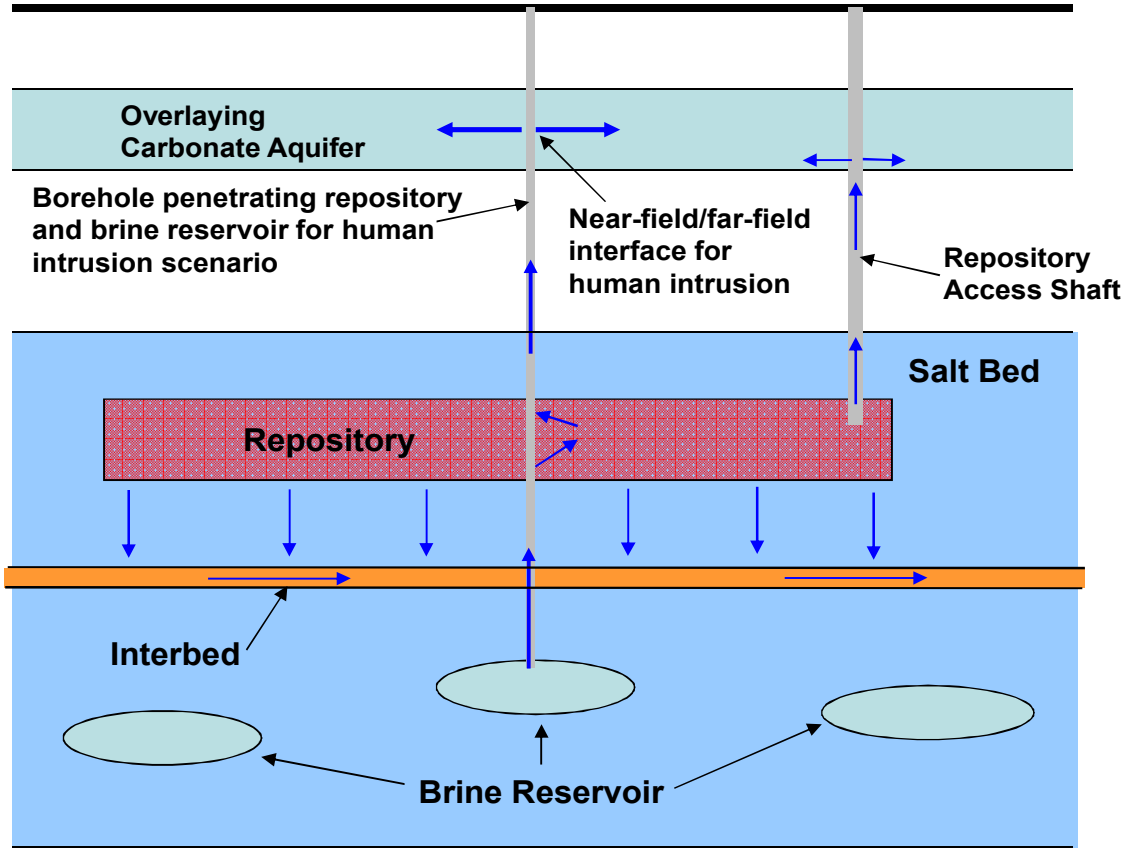

Figure 3-1. A Schematic Showing the Conceptual Model for Radionuclide Release and Transport from a Salt Generic Repository

The undisturbed scenario assumes that repository is located in a bedded salt formation in a saturated, chemically reducing environment. The waste package is assumed to be placed horizontally in an emplacement alcove and backfilled with crushed salt. The waste package does not provide any containment capability, it is assumed to fail instantaneously. Over a period of time following the emplacement, the confined space of the waste disposal area would be slowly closed by creep deformation of the salt host rock, and the crushed salt backfill undergo consolidation. This will result in close contact of the waste package with the consolidated salt rock and potential encapsulation of the waste package by salt rock. A horizontal interbed with a reasonable thickness of relatively more permeable anhydrite is assumed to exist below the repository, and runs in parallel with the repository horizon to an extended distance. Radionuclides released from the repository may be transported downward through a DRZ in the

near-field salt to the interbed, which is assumed to provide the primary pathway for radionuclide transport to the biosphere.

The disturbed scenario represents a "stylized" human intrusion scenario, which assumes that a single borehole penetrates a small number of waste packages (between 1 and 5) at 1,000 years after repository closure. A large pressurized brine reservoir is assumed to exist below the repository and is also penetrated by the intrusion borehole. The pressurized brine moves dissolved radionuclides from the breached waste package up through the borehole, resulting in the direct release of radionuclides into an overlying carbonate aquifer.

The FY 2012 GoldSim representation of the salt GDS conceptual model is summarized in Table 3-1, with mapping to the GDSM conceptual model components (Figure 2-1).

Table 3-1. Salt GDS Model Components and Features

GDSM Component	GDSM Feature	Salt GDS Model
Source	Inventory	UNF
	Waste Form	UNF
Near Field	Waste Package	Waste Package (no performance credit)
	Buffer / Backfill	Not modeled
	Seals / Liner	Not modeled
	DRZ	Salt – interface rock block (5 m)
Far Field	Host Rock	Salt – underlying interbed (5,000 m)
	Other Units	Aquifer (included in Biosphere)
Receptor	Surface / Biosphere	IAEA BIOMASS ERB1B (IAEA 2003)

Changes from the FY 2011 salt GDS model (Clayton et al. 2011, Section 3.1.4.1.1) common to all probabilistic salt analyses in Section 3.1.2 include the following:

- A revised radionuclide inventory was analyzed for both the undisturbed and disturbed (human intrusion) scenarios. Details are provided in Section 3.1.2.

Additional model details and input parameter values are found in Clayton et al. (2011, Section 3.1).

Probabilistic sensitivity analyses were performed using the FY 2012 salt GDS model. The sensitivity analyses, described in Section 3.1.2, included the impact of

- Revised UNF inventory for the undisturbed scenario (Section 3.1.2.1)
- Revised UNF inventory for the human intrusion scenario (Section 3.1.2.2)

3.1.2 Probabilistic Sensitivity Analyses

The isotopic inventory of commercial UNF in the FY 2011 salt GDS model (Clayton et al. 2011, Section 3.1.2.2 and Table 3.1-1) was calculated based on data for pressurized water reactor (PWR) fuel with a burn-up of 60 GWd per metric ton heavy metal (MTHM), 4.73% enrichment, and 30 years of aging after discharge from a reactor documented in Carter and Luptak (2010, Table C-1). The total UNF inventory was reported to be 140,000 MTHM in 32,154 waste packages. However, an implementation error in the calculation of isotope mass per waste package resulted in an actual total UNF inventory of only ~97,200

MTHM. This error, due to a missing factor of 1.4402 MT of isotope mass per waste package, was not discovered until after the FY 2011 results had been published. This error does not invalidate the FY 2011 salt GDS model results; it simply changes the total UNF inventory basis from 140,000 MTHM to ~97,200 MTHM. The total HLW inventory remains at ~1,750 MTHM, unchanged from FY 2011, and relatively insignificant compared to the UNF inventory. To examine the effect of ~140,000 MTHM in a single salt repository, the FY 2012 salt GDS model was run with the Waste Inventory Case 1 (Clayton et al. 2012, Section 3.1.4.1.1), which includes the revised, corrected UNF inventory (Table 3-2) and the unchanged HLW inventory.

The FY 2012 model with the revised Waste Inventory Case 1 was run probabilistically, with 100 realizations for each scenario and over a time period of 1,000,000 years. The results from the undisturbed scenario (Section 3.1.2.1) and the human intrusion scenario (Section 3.1.2.2) provide an indication of sensitivity to UNF inventory when compared to the corresponding FY 2011 salt GDS model results.

Table 3-2. Revised Isotopic Mass Inventory for Commercial UNF for the Salt GDS Model

Isotope	Half-life (yr)	Fractional Mass Inventory	Isotope Mass per Waste Package (g)
^{227}Ac	2.18E+01	2.7469E-13	1.7225E-06
^{241}Am	4.32E+02	8.7003E-04	5.4557E+03
^{243}Am	7.37E+03	1.8796E-04	1.1787E+03
^{14}C	5.71E+03	3.1524E-07	1.9768E+00
^{36}Cl	3.01E+05	3.4808E-07	2.1827E+00
^{245}Cm	8.50E+03	6.6221E-06	4.1526E+01
^{135}Cs	2.30E+06	5.3570E-04	3.3592E+03
^{137}Cs	3.01E+01	7.2561E-04	4.5501E+03
^{129}I	1.70E+07	2.1754E-04	1.3642E+03
^{93}Nb	1.36E+01	4.9591E-04	3.1097E+03
^{237}Np	2.14E+06	8.5892E-04	5.3861E+03
^{231}Pa	3.25E+04	7.1103E-10	4.4586E-03
^{210}Pb	2.26E+01	7.8324E-15	4.9115E-08
^{107}Pd	6.50E+06	2.8663E-04	1.7974E+03
^{238}Pu	8.77E+01	3.4170E-04	2.1427E+03
^{239}Pu	2.41E+04	5.1487E-03	3.2286E+04
^{240}Pu	6.54E+03	2.8427E-03	1.7826E+04
^{241}Pu	1.44E+01	2.6198E-04	1.6428E+03
^{242}Pu	3.76E+05	5.6750E-04	3.5586E+03
^{226}Ra	1.60E+03	2.2081E-12	1.3846E-05
^{228}Ra	6.70E+00	1.4339E-18	8.9913E-12

Table 3-2. Revised Isotopic Mass Inventory for Commercial UNF for Salt GDS Model (continued)

Isotope	Half-life (yr)	Fractional Mass Inventory	Isotope Mass per Waste Package (g)
^{126}Sb	3.61E-05	1.6470E-12	1.0328E-05
^{79}Se	6.50E+04	7.2769E-06	4.5631E+01
^{126}Sn	1.00E+05	3.4663E-05	2.1736E+02
^{90}Sr	2.91E+01	3.0809E-04	1.9319E+03
^{99}Tc	2.13E+05	8.8739E-04	5.5646E+03
^{229}Th	7.90E+03	4.4252E-12	2.7749E-05
^{230}Th	7.54E+03	1.5838E-08	9.9318E-02
^{232}Th	1.41E+10	4.2412E-09	2.6595E-02
^{232}U	6.89E+01	3.1642E-09	1.9842E-02
^{233}U	1.59E+05	9.7002E-09	6.0827E-02
^{234}U	2.45E+05	2.1220E-04	1.3306E+03
^{235}U	7.04E+08	3.7329E-03	2.3408E+04
^{236}U	2.34E+07	4.3349E-03	2.7183E+04
^{238}U	4.46E+09	6.3215E-01	3.9640E+06
^{93}Zr	1.53E+06	1.0193E-03	6.3919E+03

3.1.2.1 Undisturbed Reference Scenario

The salt GDS model undisturbed reference scenario results with the revised Case 1 inventory (~ 142,000 MTHM of UNF and HLW) are shown in Figure 3-2 (mean mass flux from the near-field salt DRZ) and Figure 3-3 (mean annual dose). An indication of the sensitivity of these salt GDS model results to UNF inventory can be seen by comparing these two results to the corresponding FY 2011 salt GDS model results for the Waste Inventory Case 1 of the Reference Scenario (Clayton et al. 2011, Section 3.1.4.1.1 and Figures 3.1-5 and 3.1-8).

The FY 2012 model results for the revised UNF inventory are similar or identical to those of the FY 2011 inventory for all radionuclides that have a solubility constraint and abundant inventory (i.e., ^{238}U). The dissolved concentrations for those radionuclides are constrained by their elemental solubility; therefore their dissolved concentrations near the source are same as for the lower FY 2011 inventory. However, for the radionuclides with no solubility constraint (i.e., ^{129}I), with a high solubility (i.e., ^{36}Cl), or with a solubility constraint but a small inventory (i.e., ^{239}Pu, not constrained by the solubility limit), the mean mass flux rates and mean annual doses are approximately 1.4 times higher with the revised inventory, consistent with 1.4 times larger total inventory. Because these radionuclides are the dominant contributors to mean annual dose for the undisturbed scenario, the mean annual dose is about 1.4 times higher with the revised inventory. This represents an approximately linear increase in mean annual dose with increasing inventory.

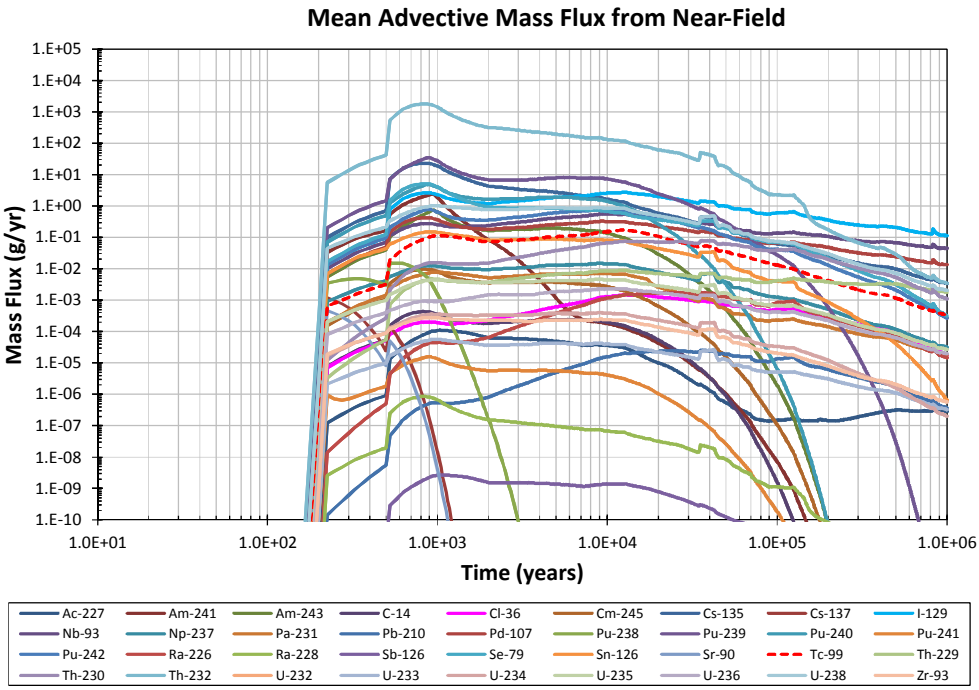

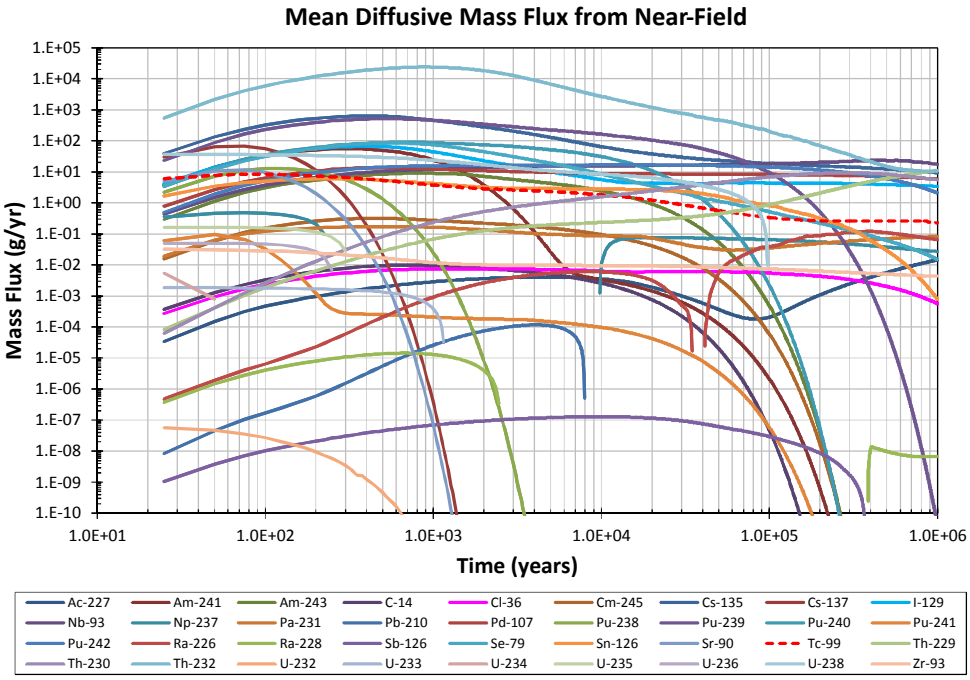

NOTE: Compare with Clayton et al. (2011, Figure 3.1-5).

Figure 3-2. Mean Advective and Diffusive Mass Flux from the Near-Field Salt DRZ with Revised UNF Inventory for Waste Inventory Case 1 of the Undisturbed Scenario

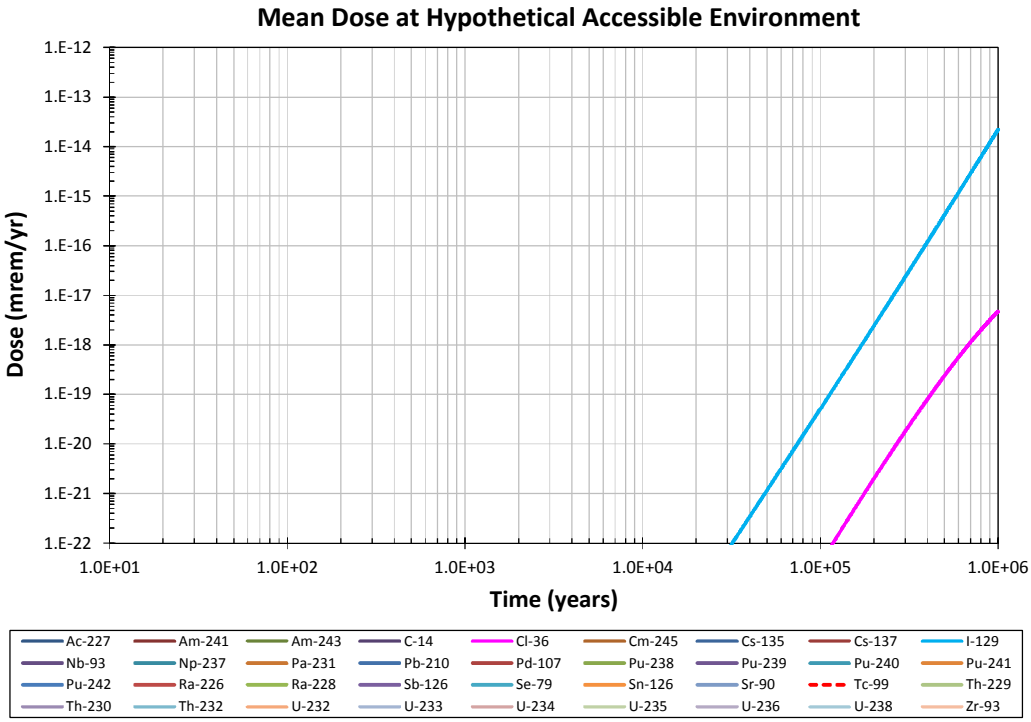

NOTE: Compare with Clayton et al. (2011, Figure 3.1-8).

Figure 3-3. Mean Annual Dose with Revised UNF Inventory for Waste Inventory Case 1 of the Undisturbed Scenario

3.1.2.2 Human Intrusion Scenario

The salt GDS model human intrusion scenario results with the revised Case 1 inventory are shown in Figure 3-4 (mean mass flux from the near-field salt DRZ) and Figure 3-5 (mean annual dose). An indication of the sensitivity of these salt GDS model results to UNF inventory can be seen by comparing these two results to the corresponding FY 2011 salt GDS model results for the Waste Inventory Case 1 of the Human Intrusion Scenario (Clayton et al. 2011, Section 3.1.4.2.1 Figures 3.1-13 and 3.1-15). For simplicity, only the commercial UNF waste packages are affected by human intrusion; between 1 and 5 (a sampled parameter) UNF waste packages are assumed to be impacted in each realization.

The effects of the increased inventory are the same in the human intrusion scenario as for the undisturbed scenario (described in Section 3.1.2.1). For radionuclides with a solubility constraint and abundant inventory (e.g., ^{238}U and ^{237}Np), there is negligible change in the mean mass flux rate and mean annual dose. However, for radionuclides with no solubility constraint (e.g., ^{129}I and ^{14}C), with a high solubility (e.g., ^{36}Cl), or with a solubility constraint but a small inventory (i.e., ^{239}Pu and ^{242}Pu, not constrained by the solubility limit), the mean mass flux rates and the mean annual doses are approximately 1.4 times higher with the revised inventory, consistent with the 1.4 times larger total inventory.

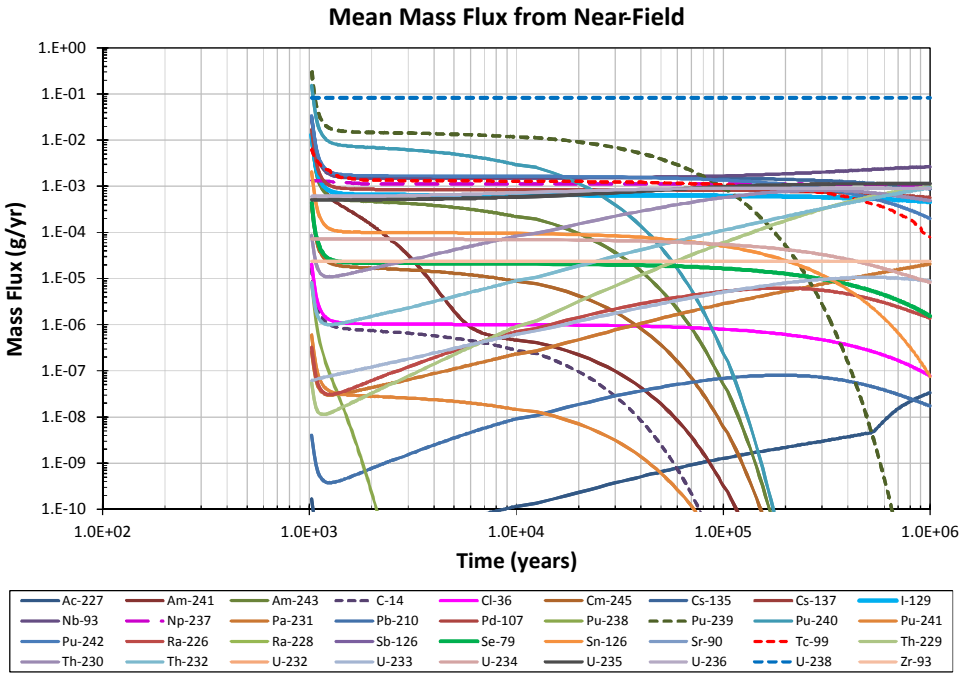

NOTE: Compare with Clayton et al. (2011, Figure 3.1-13).

Figure 3-4. Mean Mass Flux from the Repository with Revised UNF Inventory for Waste Inventory Case 1 of the Human Intrusion Scenario

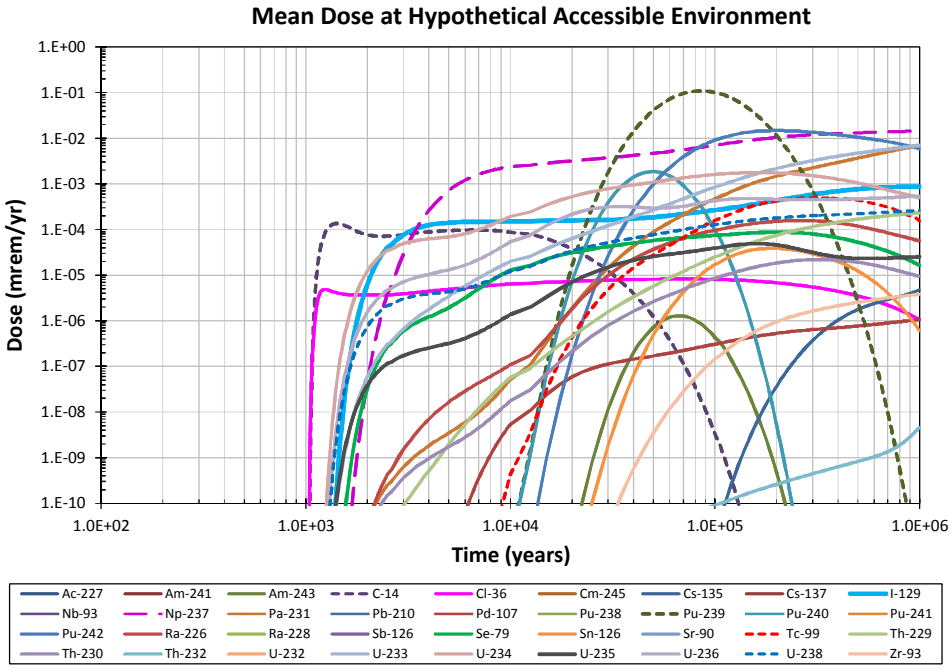

NOTE: Compare with Clayton et al. (2011, Figure 3.1-15).

Figure 3-5. Model Results with Corrected UNF Inventory for Waste Inventory Case 1 of the Human Intrusion Scenario: Mean Annual Dose

3.2 Granite GDS Model

3.2.1 Model Description

The granite GDS model used for the FY 2012 sensitivity simulations described in this section derives from the FY 2011 granite GDS model (Clayton et al. 2011, Section 3.2). The granite GDS conceptual model includes a base case scenario and a disturbed (human intrusion) scenario, however for FY 2012 only the base case scenario was simulated. The development and application of the FY 2012 granite GDS model is described in detail in Chu (2012). A summary is presented here.

The base case scenario assumes that the repository is located in a saturated, chemically reducing environment below the water table. The repository is assumed to have a square footprint with 25-m spacing between emplacement tunnels and 6 m between waste packages. The waste packages do not provide any containment capability, they are assumed to fail instantaneously. This is a conservative assumption that is contrary to typical granite repository designs (e.g., SKB 2011) which rely on waste package longevity. Radionuclides are transported away from the waste packages by diffusion with sorption through a bentonite buffer. The transport pathways from some of the waste packages are assumed to directly intersect fractures in the surrounding granite. The number of waste packages with direct buffer pathways to granite fractures is treated with uncertainty and is sampled between 0.1% and 1% of the total number of waste packages. The radionuclides transported through the buffer pathways that do not intersect granite fractures are assumed to enter and remain in the granite matrix. The small fraction of waste packages with direct pathways to granite fractures in consistent with analyses performed by SKB (SKB 2010b). Radionuclide transport through the far-field fractured granite to the biosphere includes advective transport with sorption in the fractures and matrix diffusion. Transport through the far-field fractured granite is modeled with the Finite Element Heat and Mass Transfer (FEHM) code (version 3.0) (Zyvoloski et al. 1997; Zyvoloski 2007). The FEHM code is externally linked into the GoldSim-based granite GDS model (Chu et al. 2008).

The FY 2012 GoldSim representation of the granite GDS conceptual model is summarized in Table 3-3, with mapping to the GDSM conceptual model components (Figure 2-1).

Table 3-3. Granite GDS Model Components and Features

GDSM Component	GDSM Feature	Granite GDS Model
Source	Inventory	UNF and HLW
	Waste Form	UNF and HLW
Near Field	Waste Package	Waste Package (no performance credit)
	Buffer / Backfill	Bentonite (0.36 m)
	Seals / Liner	Not modeled
	DRZ	Fractured Granite (0.42 m)
Far Field	Host Rock	Fractured Granite (5,000 m)
	Other Units	Aquifer (included in Biosphere)
Receptor	Surface / Biosphere	IAEA BIOMASS ERB1B (IAEA 2003)

Probabilistic analyses performed in FY 2012 with the granite GDS model are described in Chu (2012). These included an evaluation of a multiple fracture pathways capability, and a sensitivity analysis of the

potential impacts of glaciations. Several changes were made to the FY 2011 granite GDS model (Clayton et al. 2011, Section 3.2.3.2.1) to accommodate these probabilistic granite analyses. These changes, some of which of are listed in Table 3-4, include:

- Solubilities more representative of granite pore waters are used, based on Mariner et al. (2011, Table 2-5) for granite at 25°C. These solubility values are summarized in Table C-3. Note that C, Cs, I, Sr, and Pb have unlimited solubility.
- Groundwater flow rates more representative of fractured granite systems were used, corresponding to mean groundwater velocities on the order of 1m/yr (SKB 2010b, Table 3).
- Waste package porosity and dimensions were revised to be consistent with waste packages used in other GDS models (Table 3-4).
- Water flow rate to a fracture intersecting a waste package was changed to be more representative of a fractured granite system (Table 3-4).
- Bentonite buffer properties were updated to be consistent with those documented in SKB (2010b) (Table 3-4).

Additional model details and input parameter values are found in Clayton et al. (2011, Section 3.2).

Table 3-4. Revised Parameter Values for the Granite GDS Model

Parameter	Stochastic Parameter Type	Base Case Value	Distribution Parameters
Porosity, inside waste package	Constant	0.175	N/A
Waste package size outer diameter (m)	Constant	0.863	N/A
Waste package size outer length (m)	Constant	5.096	N/A
Water flow rate to fracture intersecting waste package in undisturbed scenario (m^3/yr per waste package (WP))	Normal	5.1×10^{-4}	Mean = $5.1\text{x}10^{-4}$ Stdv = $0.2\text{x}10^{-4}$
Bentonite density (kg/m^3)	Triangular	1562	1484, 1562, 1640
Bentonite porosity	Triangular	0.435	0.41, 0.435, 0.46

Source: Mariner et al. 2011, Table 4-1; SKB 2010b.

Additional changes made to support the glaciation sensitivity analysis are the following:

- K_d values for uranium (U), thorium (Th), technetium (Tc), and neptunium (Np) were reduced during the flushing periods to represent decreased sorption due glacial conditions.
- Time dependent groundwater velocity and flow rates are used to represent the different phases of the glaciation process.
- Use a 1D GoldSim pipe model with matrix diffusion to model flow and transport through the far-field fractured granite instead of the externally linked 3D FEHM model.

The probabilistic sensitivity analyses for glaciation are described further in Section 3.2.2.

3.2.2 Probabilistic Sensitivity Analyses

This section discusses the sensitivity studies carried out addressing the effect of future glaciation events on the performance of a generic repository sited in a granite environment. Glaciation has been identified in studies in Sweden, Finland and Canada as a potentially important process affecting repository performance. Based on detailed flow modeling studies of glaciation effects by SKB (2010b), large groundwater flow velocities are expected for brief periods as the ice front passes groundwater recharge points. Between these brief glacial flushing periods, the flow velocities are expected to be smaller because the ice sheet will block recharge. The model abstraction for these glaciation sensitivity analyses assumes the groundwater flow paths to be fixed and only considers changes in groundwater velocity within the fixed pathways.

Glaciation can also produce changes to water chemistry due to the increased flow during the glacial flushing periods. During these flushing periods, oxygen-rich water may be present over much of the transport pathways, which can reduce the sorption of redox-sensitive radionuclides (e.g., U, Th, Tc, and Np) (SKB 2010b). To account for these changes in the sensitivity analyses, the equilibrium K_d values for uranium U, Th, Tc, and Np were reduced during the flushing periods. The relationship between K_d value, retardation factor, and radionuclide transport is discussed in Section 3.3.2.4. An additional effect of the influx of oxidizing water is the potential for higher solubilities. However, this effect of solubility was not modeled.

A number of probabilistic analyses for the effects of single and multiple glacial cycles considering UNF and HLW inventories are presented in Chu (2012). Results from a single glacial cycle are summarized here.

An additional consequence of glaciation is deterioration of the bentonite buffer from repeated exposure to dilute glacial melt water, causing loss of buffer material and eventually to partial buffer failure. The effect was not included in the sensitivity analyses described here, but was examined by Chu (2012).

3.2.2.1 Representation of a Single Glacial Cycle

For this study, a simplified 120,000-year glacial cycle is simulated that includes one temperate period, one periglacial period, one glacial period, one submerged period, and advancing before and retreating after the glacial period. Table 3-5 lists the time periods for each flow change in the first 120,000-year cycle.

Table 3-5. Duration of Each Climate Period in a Simplified 120,000-Year Glacial Cycle

Climate Period	Time (yrs after present)	Duration (yrs)
Temperate	0 – 35,000	35,000
Periglacial	35,000 – 89,000	54,000
Advancing phase	89,000 – 90,800	1,800
Glacial	90,800 – 110,700	19,900
Retreating phase	110,700 – 111,000	300
Submerged	111,00 – 120,000	9,000

To calculate radionuclide transport, the flow rates in the near-field granite DRZ and far-field granite host rock are scaled by the values in Figure 3-6 (flow scaling factor) to obtain corresponding values for the different climate periods in the glacial cycle. The flow scaling factors are defined relative to the Darcy flux in the temperate period. Also, K_d values for the redox-sensitive radionuclides are adjusted to account

for oxidizing conditions in the near-field and far-field granite during ice front passages (i.e., during the advancing phase and retreating phase time periods when the flow scaling factors are greater than 10).

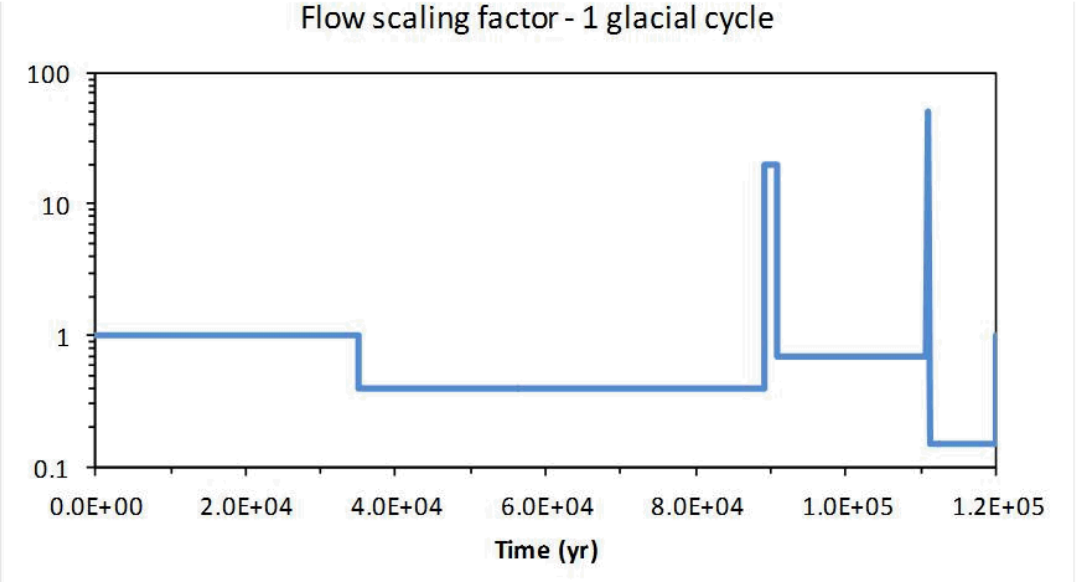

Figure 3-6. Flow Scaling Factors for One Glacial Cycle

Figures 3-7 and 3-8 show the granite groundwater velocity and K_d values adjusted by the flow scaling factor and oxidizing conditions, respectively, for use in the radionuclide transport simulation. The dominant effects are that during the brief advancing and retreating flushing phases, the groundwater velocities are large due to the ice front passages, and sorption-reducing oxygen-rich water may be present over much of the transport pathways.

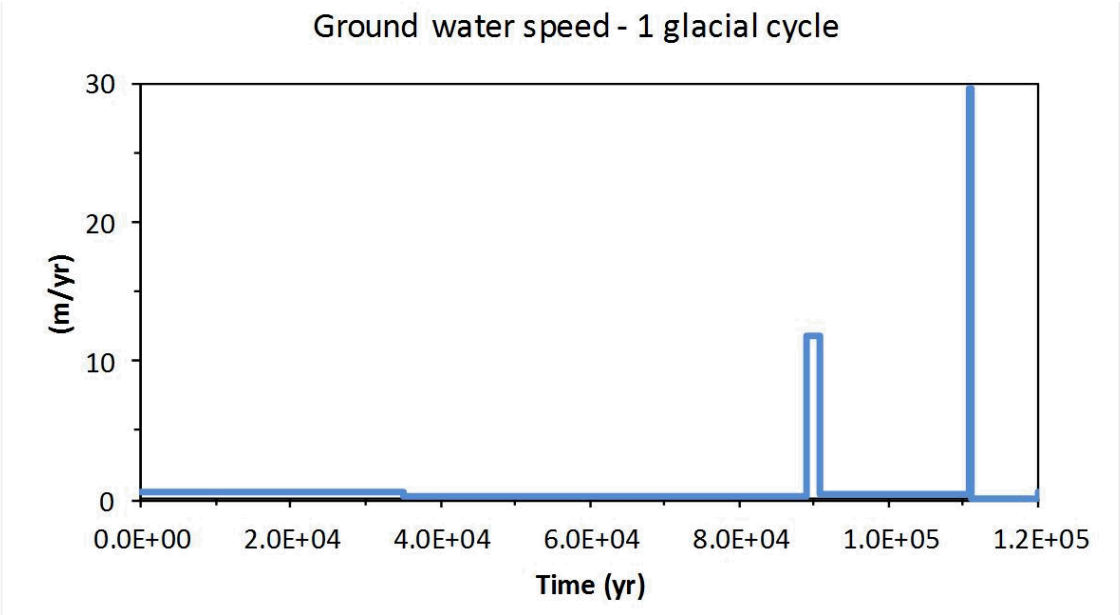

Figure 3-7. Groundwater Velocity Adjusted by Flow Scaling Factors during One Glacial Cycle

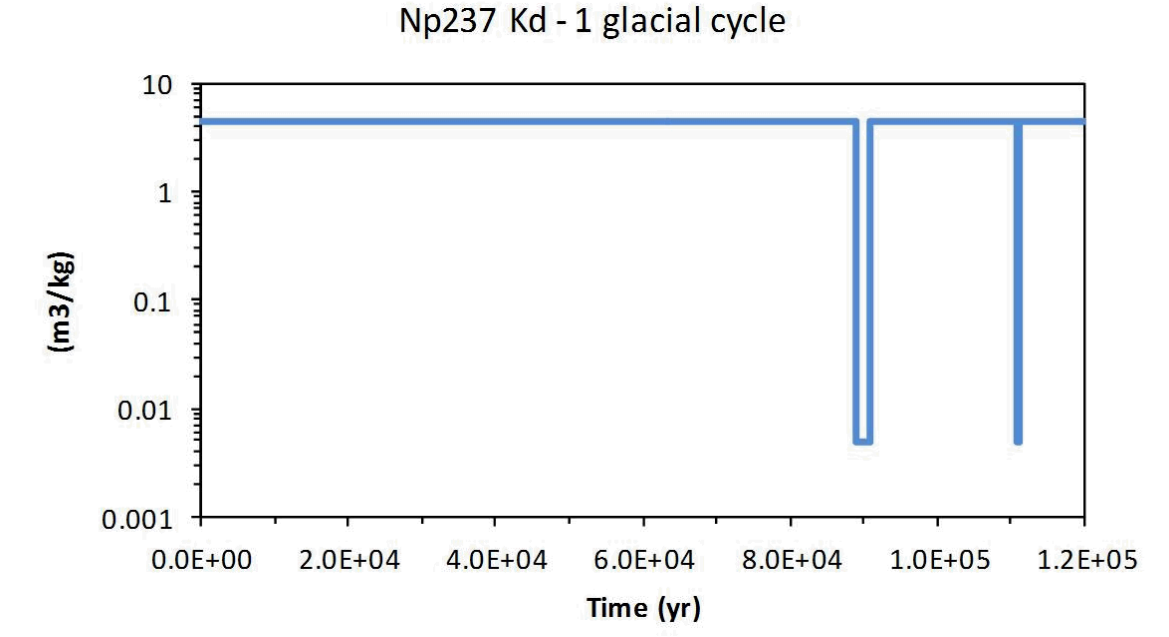

Figure 3-8. ^{237}Np K_d Variation, Affected by Oxidizing Conditions during Glacial Flushing Periods

Figure 3-9 shows the mass flux of ^{129}I (the largest contributor to mean annual dose) into the far-field granite over the duration of one glacial cycle. It shows a small decrease at 38,000 yrs when the climate changes from the temperate period to the periglacial period, and abrupt increase during the glacial flushing periods (advancing phase at ~90,000 yrs and retreating phase at ~110,000 yrs).

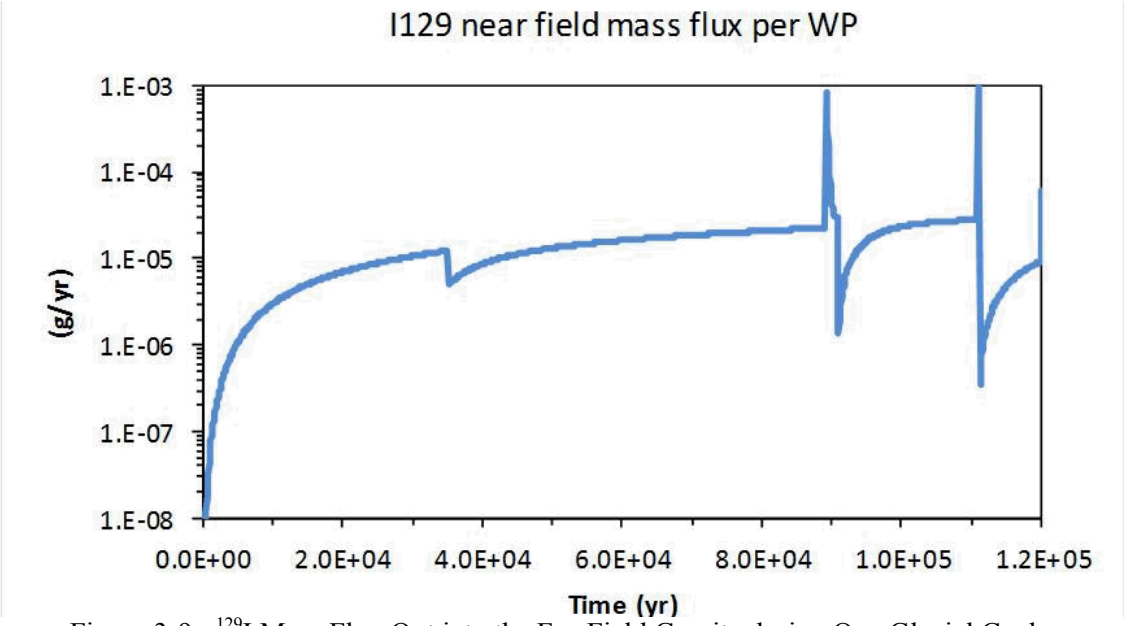

Figure 3-9. ^{129}I Mass Flux Out into the Far-Field Granite during One Glacial Cycle

Figures 3-10 and 3-11 show the effects of varying the K_d value during the glacial cycle. Figure 3-10 shows ^{237}Np mass flux per waste package into the far-field granite over one glacial cycle with flow rate

changes during ice front passages, but no corresponding K_d changes. Figure 3-11 shows ^{237}Np mass flux per waste package into the far-field granite over one glacial cycle with both flow rate and K_d changes during ice front passages. The mass flux is much larger during the advancing and retreating flushing periods when the K_d changes are included (Figure 3-11). For ^{237}Np, the oxidizing conditions decrease the K_d value from 4.38 m^3/kg to 0.0049 m^3/kg. However, even with the increased mass flux due to the smaller K_d values, the contribution of ^{237}Np to the total dose is very small.

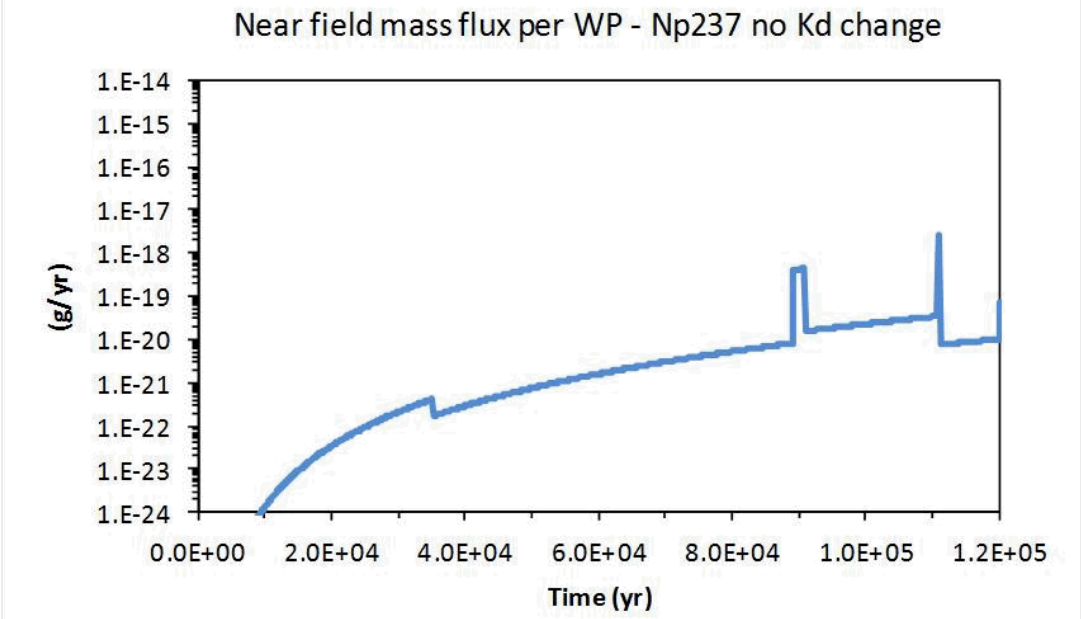

Figure 3-10. ^{237}Np Mass Flux into the Far-Field Granite during One Glacial Cycle with Flow Rate Change, but no K_d Change

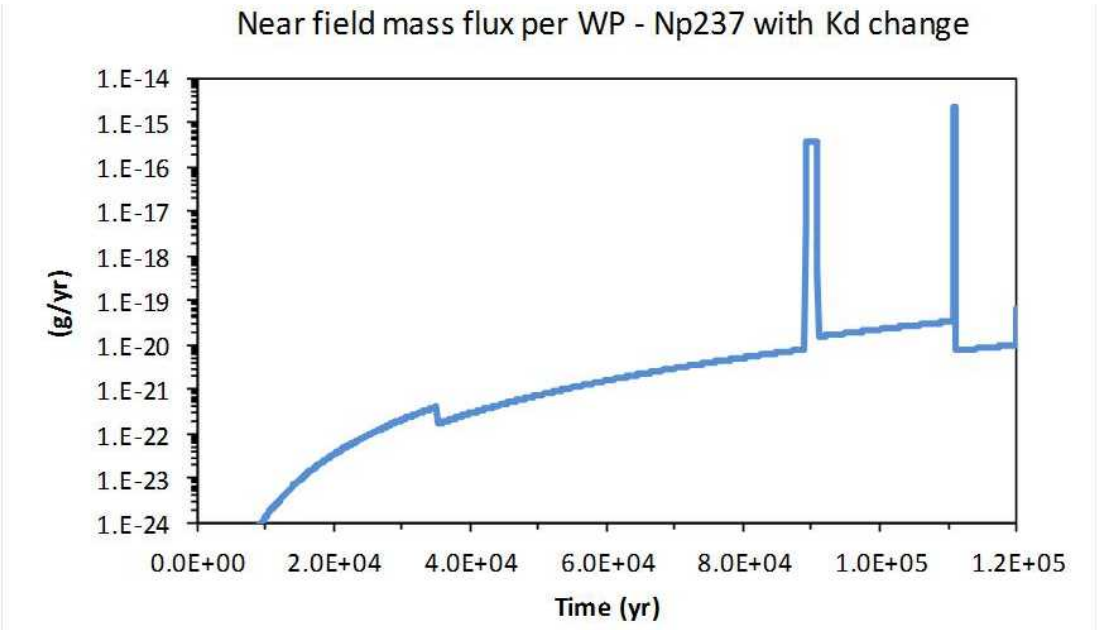

Figure 3-11. ^{237}Np Mass Flux into the Far-Field Granite during One Glacial Cycle with Flow Rate Change and K_d Change

Figures 3-12 shows ^{129}I mean annual dose for one glacial cycle. There is an abrupt increase in dose during the glacial flushing periods (advancing phase at ~90,000 yrs and retreating phase at ~110,000 yrs).

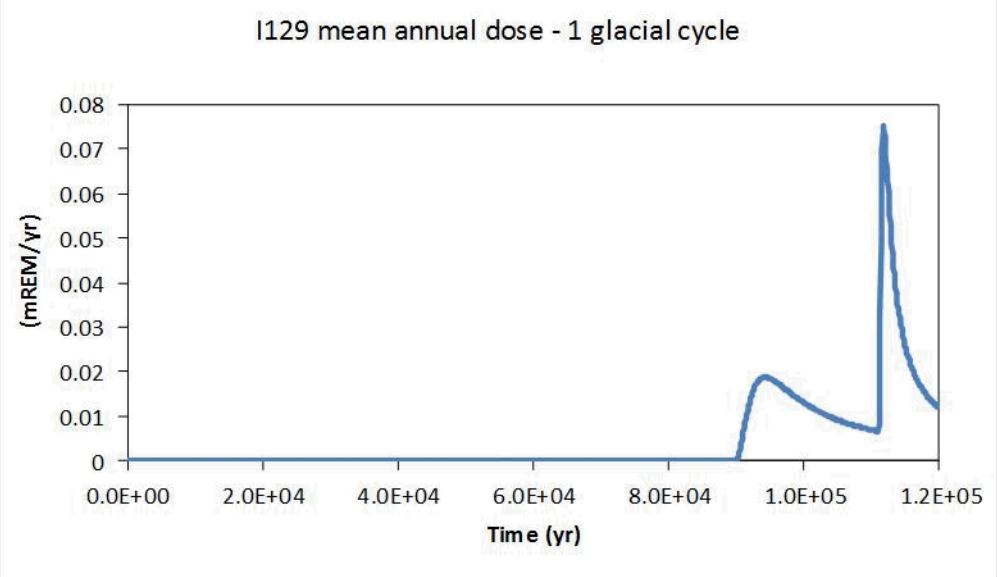

Figure 3-12. ^{129}I Mean Annual Dose during One Glacial Cycle

Figure 3-13 compares ^{129}I mean annual dose for one glacial cycle with the ^{129}I mean annual dose over the same time period if climate conditions are not assumed to vary (i.e., temperate conditions maintained for 120,000 yrs). Figure 3-13 shows the increased mean annual dose during the glacial period in comparison with temperate condition, due to the increased flow rates and decreased sorption.

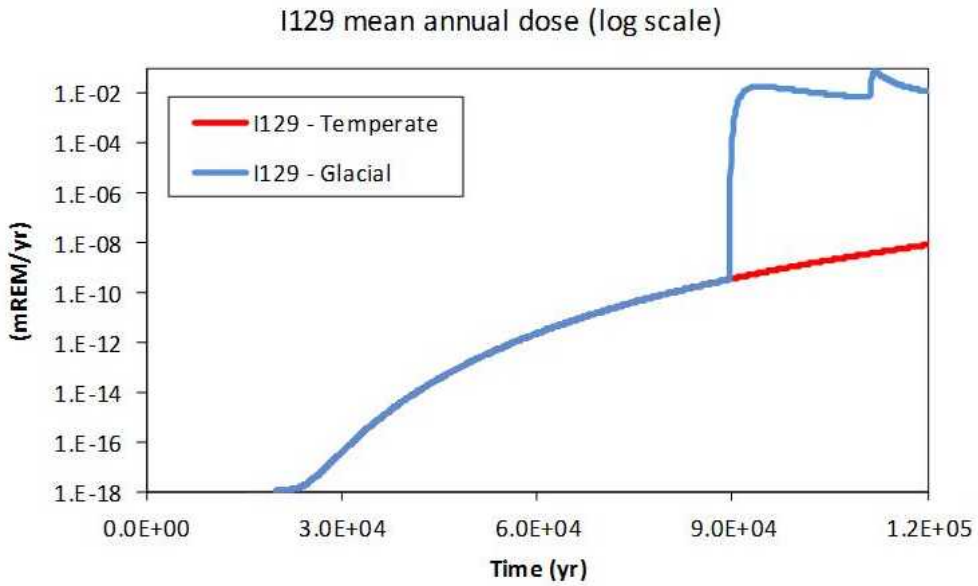

Figure 3-13. ^{129}I Mean Annual Dose Comparison for Glacial and Temperate Climate Conditions

The results of these glacial sensitivity analyses show that radionuclide transport may be significantly influenced by the effects future glacial cycles. The mean annual dose rates are most influenced by the flow rate changes during the glacial flushing periods. The associated changes in chemical conditions only influence the redox-sensitive radionuclides, which are not major contributors to the mean annual dose.

3.3 Clay GDS Model

3.3.1 Model Description

The clay GDS model used for the FY 2012 sensitivity simulations described in this section is unchanged from the FY 2011 clay GDS model (Clayton et al. 2011, Section 3.3.4.2.1). The clay GDS conceptual model includes the capability to represent two radionuclide release scenarios: an undisturbed pathway (i.e., nominal scenario) and a fast pathway (i.e., disturbed scenario). The development and application of the FY 2012 clay GDS model is described in detail in Huff and Nutt (2012). A summary is presented here.

The clay GDS models a single waste form, a waste package, an EBS buffer, a DRZ, and a far-field host rock using a batch reactor mixing cell framework. This waste unit cell is modeled with boundary conditions such that it may be repeated assuming an infinite repository configuration. The EBS components (waste form, waste package and buffer) are modeled as well-mixed volumes and radial transport away from the cylindrical base case unit cell is modeled as 1D. These EBS components can undergo rate-based dissolution and barrier failure. Radionuclide releases from the EBS enter the DRZ and subsequently the far-field host rock in which diffusive and advective transport can take place. Solubility limits, sorption, and dispersion phenomena can be modeled in the EBS components, DRZ, and far-field clay host rock.

Fast pathways can be included that directly intersect the waste form or directly intersect the EBS buffer. The fast pathway produces vertical advective transport through the far-field host rock.

The FY 2012 GoldSim representation of the clay GDS conceptual model is summarized in Table 3-6, with mapping to the GDSM conceptual model components (Figure 2-1). In these analyses, in order to isolate the effect of the far-field behavior, an instantaneous waste form degradation rate was assumed. In addition, solubility limits and the advective flow rate through the EBS were specified to produce immediate contaminant transport into the far field, leaving the far field as the only radionuclide transport barrier.

Table 3-6. Clay GDS Model Components and Features

GDSM Component	GDSM Feature	Clay GDS Model
Source	Inventory	UNF
	Waste Form	UNF
Near Field	Waste Package	Primary EBS Barrier - Waste Package
	Buffer / Backfill	Secondary EBS Barrier - Bentonite (1.025 m)
	Seals / Liner	Not modeled
	DRZ	Excavation Damage Zone - Fissured Clay (1.15 m)
Far Field	Host Rock	Far Field - Clay (150 m)
	Other Units	Aquifer (included in Biosphere)
Receptor	Surface / Biosphere	IAEA BIOMASS ERB1B (IAEA 2003)

Additional model details and input parameter values are found in Clayton et al. (2011, Section 3.3).

Probabilistic sensitivity analyses, described in Section 3.3.2, were conducted using the FY 2012 clay GDS model to examine the behavior of the following parameters:

- Far-field diffusion coefficient (Section 3.3.2.1)
- Far-field vertical advective velocity (Section 3.3.2.2)
- Far-field solubility coefficient (Section 3.3.2.3)
- Far-field sorption (K_d) (Section 3.3.2.4)
- Waste form degradation rate (Section 3.3.2.5)
- Waste package failure time (Section 3.3.2.6)
- Vertical path length (Section 3.3.2.7)

3.3.2 Probabilistic Sensitivity Analyses

The multiple barrier system modeled in the clay GDS model calls for a multi-faceted sensitivity analysis. The importance of any single component or environmental parameter must be analyzed in the context of the full system of barrier components and environmental parameters. Thus, this analysis has undertaken an analysis strategy to develop a many-dimensional overview of the key processes and parameters that can affect repository performance in generic clay media.

To address this, both individual and dual parametric studies were performed. Individual parameter studies varied a single parameter of interest in detail over a broad range of values. Dual parameter sensitivity studies were performed for pairs of parameters expected to exhibit some covariance. For each parameter or pair of parameters, forty simulation groups varied the parameter or parameters within the ranges under consideration. For each simulation group, a 100-realization simulation was completed. Table 3-7 shows examples the resulting forty simulation groups for individual and dual parametric study configurations. A sampling scheme developed in previous generic disposal media modeling was implemented in this model in order to ensure that the each 100-realization simulation sampled identical values for uncertain parameters (Clayton et al. 2011; Nutt et al. 2009).

Table 3-7. Simulation Group Structure for Individual and Dual Parameter Sensitivity Analyses

Individual Parameter Study

P	P_1	Group 1
	P_2	Group 2
	P_3	Group 3
	.	.
	.	.
	.	.
	P_{40}	Group 40

Dual Parameter Study

P	Q				
	Q_1	Q_2	Q_3	Q_4	Q_5
P_1	Group 1	Group 2	Group 3	Group 4	Group 5
P_2	Group 6	Group 7	Group 8	Group 9	Group 10
P_3	Group 11	Group 12	Group 13	Group 14	Group 15
P_4	Group 16	Group 17	Group 18	Group 19	Group 20
P_5	Group 21	Group 22	Group 23	Group 24	Group 25
P_6	Group 26	Group 27	Group 28	Group 29	Group 30
P_7	Group 31	Group 32	Group 33	Group 34	Group 35
P_8	Group 36	Group 37	Group 38	Group 39	Group 40

In these probabilistic sensitivity analyses, repository performance is quantified by radiation dose to a hypothetical receptor. Specifically, this sensitivity analysis focuses on parameters that affect the mean of the peak annual dose:

$$D_{MoP,i} = \frac{\sum_{r=1}^{N} \max \left[D_{r,i}(t)|_{\forall t} \right]}{N} \qquad \text{Eq. 3-1}$$

where:

$D_{MoP,i}$ = Mean of the peak annual dose due to isotope i [mrem/yr]

$D_{r,i}(t)$ = Annual dose in realization r at time t due to isotope i [mrem/yr]

N = Number of realizations

The mean of the peak annual dose is a conservative metric of repository performance. The mean of the peak annual dose should not be confused with the peak of the mean annual dose,

$$D_{PoM,i} = \max \left[\frac{\sum_{r=1}^{N} D_{r,i}(t)|_{\forall t}}{N} \right] \qquad \text{Eq. 3-2}$$

where:

$D_{PoM,i}$ = Peak of the mean annual dose due to isotope i [mrem/yr]

The mean of the peaks metric, $D_{MoP,i}$, was chosen in this analysis because it is more conservative since it is able to capture temporally local dose maxima and consistently reports higher dose values than the peak of the means, $D_{PoM,i}$.

The results described in the following subsections provide an overview of the relative importance of processes and parameters that affect the long-term performance attributes of generic clay disposal systems. This work is not intended to give an assessment of the performance of a specific disposal system. Rather, it is intended to generically identify properties and parameters expected to influence repository performance in generic clay geologic environments.

3.3.2.1 Far-field Diffusion Coefficient

In clay media, diffusion dominates far-field hydrogeologic transport due to characteristically low hydraulic head gradients and host rock permeability. Thus, the effective diffusion coefficient is a parameter to which repository performance in clay media is expected to be very sensitive.

The sensitivity of the mean of the peak dose to the reference diffusivity of the host rock was analyzed. In this analysis, the reference diffusivity of the medium was the input parameter used to vary the effective diffusivity in a controlled manner. In the GoldSim radionuclide transport module, the effective diffusion coefficient is defined as:

$$D_{eff} = n\tau D_{ref} D_{rel} \qquad \text{Eq. 3-3}$$

where:

D_{eff} = Effective diffusion coefficient [m^2/s]

D_{rel} = Relative diffusivity for each isotope in water [%]

D_{ref} = Reference diffusivity in water [m^2/s]

τ = Tortuosity [%]

n = Porosity [%]

In this sensitivity analysis the reference diffusivity was altered while the porosity and the tortuosity were both set to 1. Thus, the simulation rendered the effective diffusivity equal to the product of the reference diffusivity and the relative diffusivity (set to 1 for all isotopes). This allowed the diffusivity to be controlled directly for all isotopes.

The radionuclide inventory was also varied for each value of the reference diffusivity. The baseline radionuclide inventory considered in the clay GDS model is based on the disposal of four PWR assemblies in a waste 'unit cell', or the inventory associated with 2 MTHM of UNF (Clayton et al. 2011, Section 3.3.2.2.1). The radionuclide inventory was varied by multiplying this baseline radionuclide inventory by a scalar mass factor. It was expected that changing these two parameters in tandem would capture the importance of diffusivity in the far field to the repository performance as well as a threshold at which the effect of waste inventory dissolution is attenuated by solubility limits for those elements that are solubility controlled.

3.3.2.1.1 Parametric Range

The forty simulations executed corresponded to eight values of relative diffusivity and five values of inventory mass multiplier. That is, the reference diffusivity was varied over the eight magnitudes between 10^{-8} and 10^{-15} m^2/s. The mass factor, the dimensionless inventory multiplier discussed above, was varied over the five magnitudes between 10^{-4} and 10^{1}, which is expected to cover the full range of inventories in potential future waste forms. Table 3-8 shows the simulation grouping structure and the corresponding reference diffusivities and radionuclide inventories considered.

Table 3-8. Diffusion Coefficient and Mass Factor Simulation Groupings

Reference Diffusivity (m^2/s)	Mass Factor				
	0.001	0.01	0.1	1	10
	Groupings				
1×10^{-8}	1	2	3	4	5
1×10^{-9}	6	7	8	9	10
1×10^{-10}	11	12	13	14	15
1×10^{-11}	16	17	18	19	20
1×10^{-12}	21	22	23	24	25
1×10^{-13}	26	27	28	29	30
1×10^{-14}	31	32	33	34	35
1×10^{-15}	36	37	38	39	40

3.3.2.1.2 Results

The peak of the mean annual dose for highly soluble, non-sorbing elements such as I and Cl, are proportional to the radionuclide inventory and largely directly proportional to the relative diffusivity. This can be seen for ^{129}I and ^{36}Cl in Figures 3-14 and 3-15.

Long-lived ^{129}I and ^{36}Cl are assumed to be soluble, so in Figures 3-14a and 3-15a, the effect of a solubility-limited attenuation regime is not seen. Even for very low diffusivities, the diffusion length of the far field is the primary barrier. The flattening of the ^{129}I results shown in Figure 3-14a for a diffusion coefficient below 10^{-14} m^2/s is attributed to the very small vertical advective groundwater velocity assumed. For a diffusion coefficient below 10^{-14} m^2/s, diffusive transport becomes essentially negligible and very slow advective transport leads to releases from the far field.

In Figures 3-14b and 3-15b it is clear that in the absence of solubility limitation and sorption, the mean of the peak annual dose is directly proportional to the inventory of material disposed (recall, varied through the use of a scalar mass factor).

Both Cl and I are soluble and non-sorbing. The amount of ^{129}I in the UNF inventory is greater than the amount of ^{36}Cl, so a difference in magnitudes is expected; however, the trends should be the same. Since the half-life of ^{36}Cl, ~300,000 years, is much shorter than the half-life of ^{129}I, ~16 million years, a stronger proportional dependence on mass factor is seen for Cl due to its higher decay rate.

The peak of the mean annual dose for solubility-limited, sorbing elements such as Tc and Np, is much more complex as can be seen for ^{99}Tc and ^{237}Np in Figures 3-16 and 3-17. Two regimes with respect to the diffusion coefficient can be seen in for elements that are both solubility-limited and sorbing. In the low diffusion coefficient regime, the diffusive pathway through the homogeneous permeable porous medium in the far field is the dominant barrier to radionuclide transport. In the second regime, for very high diffusion coefficients, the effects of additional attenuation phenomena in the natural system can be seen. The dependence of peak of the mean annual dose on radionuclide inventory was consistently directly proportional for all isotopic groups.

The peak doses due to solubility-limited, sorbing elements such as Np and Tc demonstrate the two major regimes with respect to radionuclide inventory. In the first regime, for low radionuclide inventory, the mean of the peak annual dose rates is directly proportional to both reference diffusivity and inventory. For larger radionuclide inventories, the sensitivity to reference diffusivity and inventory are both attenuated at higher values due to both solubility limits and reversible sorption.

^{237}Np and ^{99}Tc exhibit a strong proportional relationship between diffusivity and peak of the mean annual dose as shown in Figures 3-16a and 3-17a. This relationship is muted as diffusivity increases. Both are directly proportional to mass factor until they reach the point of attenuation by their solubility limits, as can be seen in Figures 3-16b and 3-17b.

a) Sensitivity to Relative Diffusivity

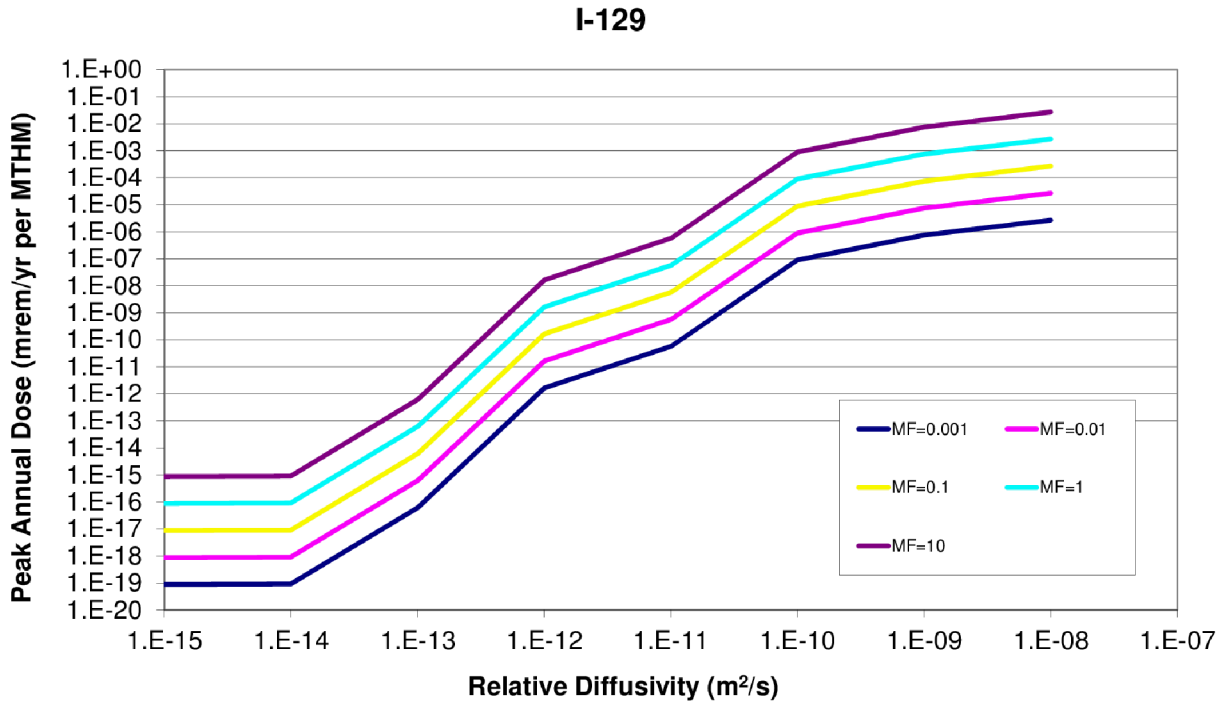

b) Sensitivity to Radionuclide Inventory

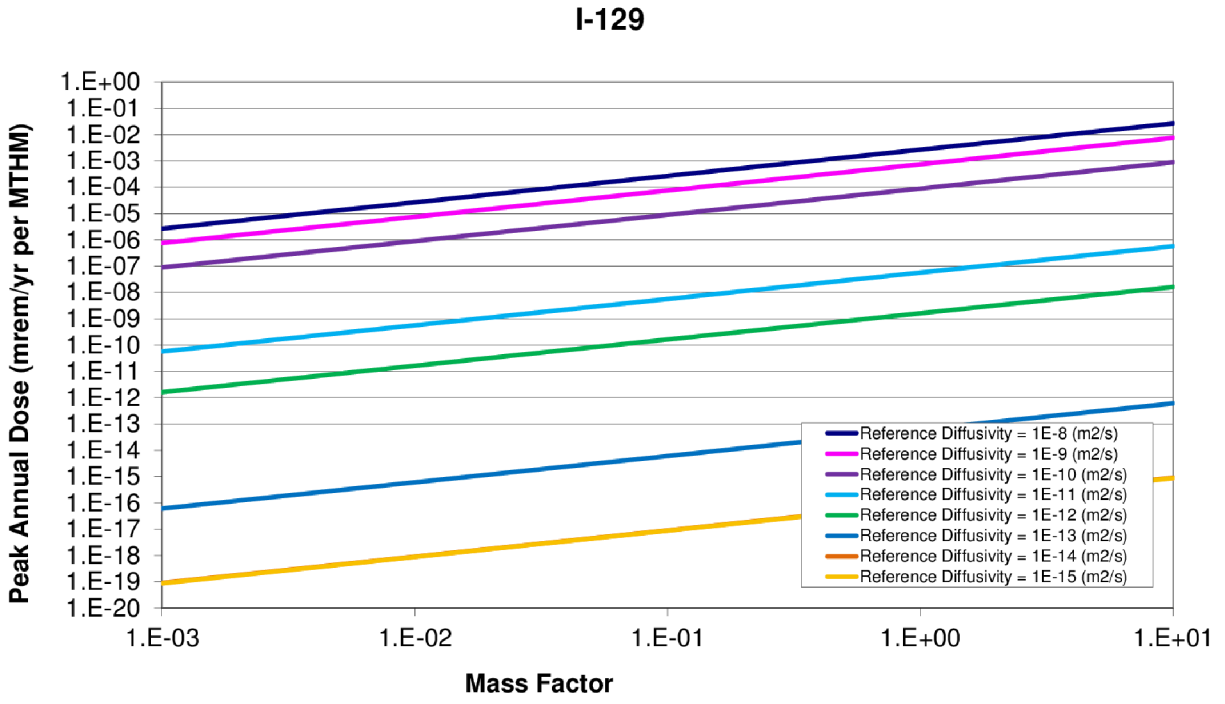

Figure 3-14. ^{129}I Diffusion—Inventory Sensitivity

a) Sensitivity to Relative Diffusivity

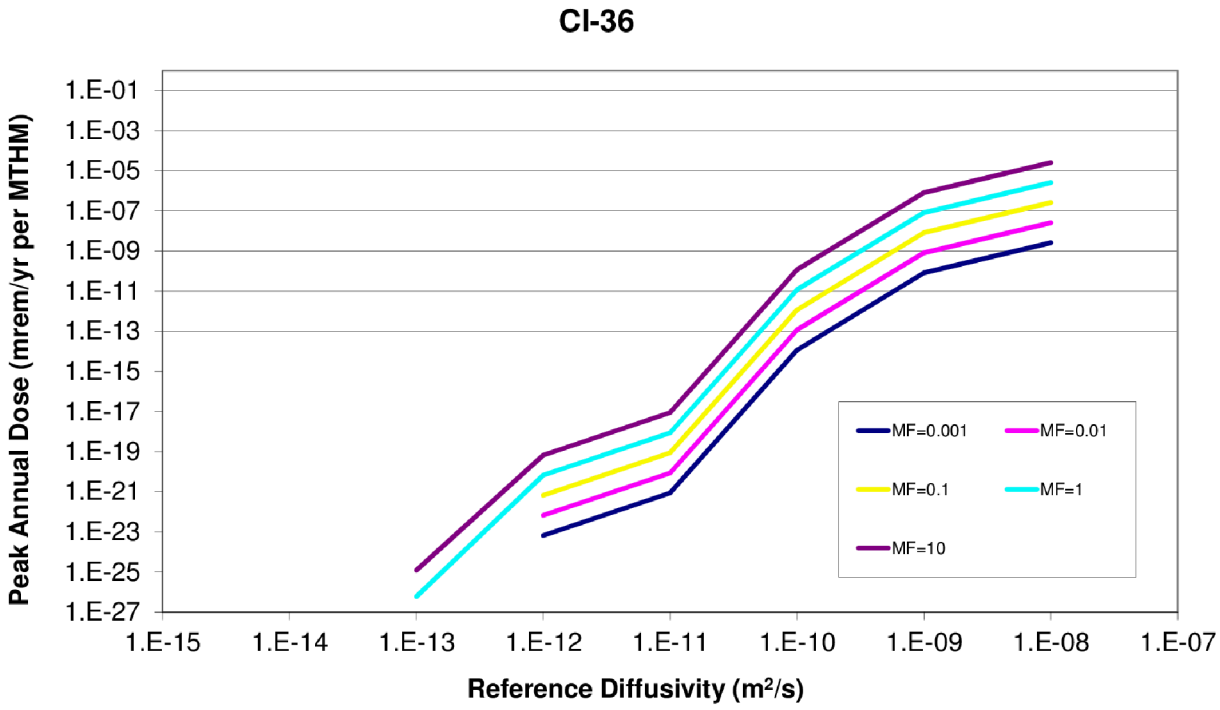

b) Sensitivity to Radionuclide Inventory

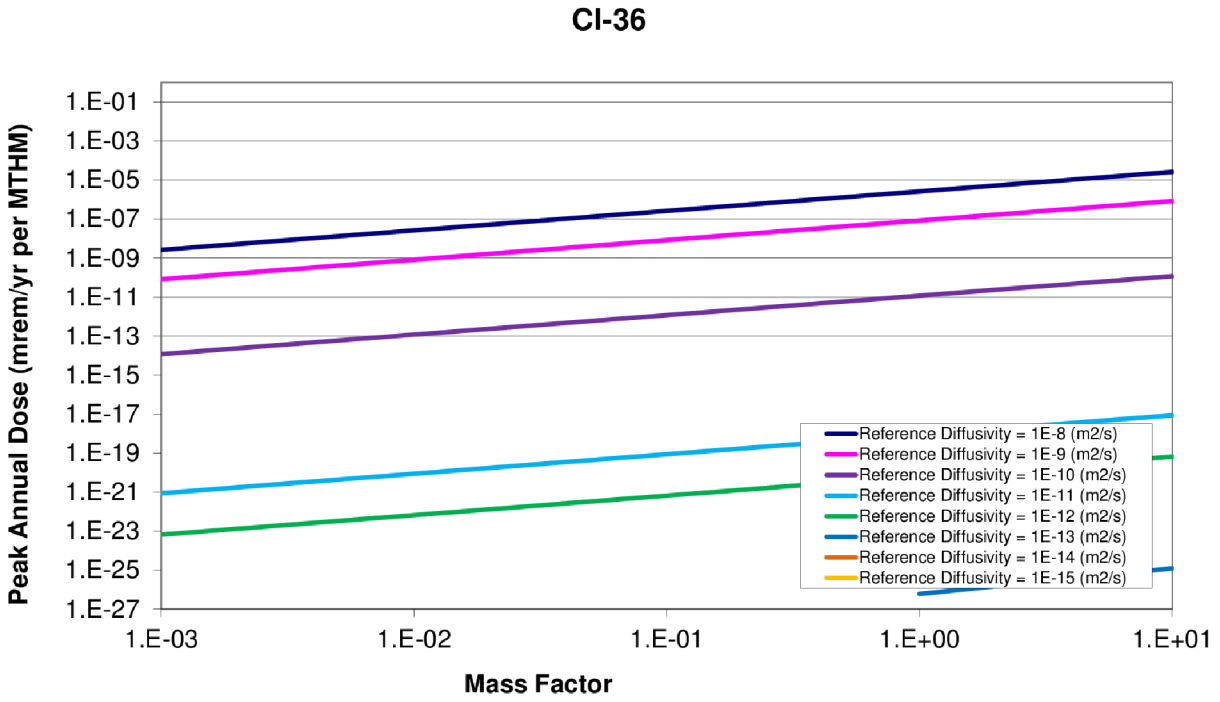

Figure 3-15. ^{36}Cl Diffusion—Inventory Sensitivity

a) Sensitivity to Relative Diffusivity

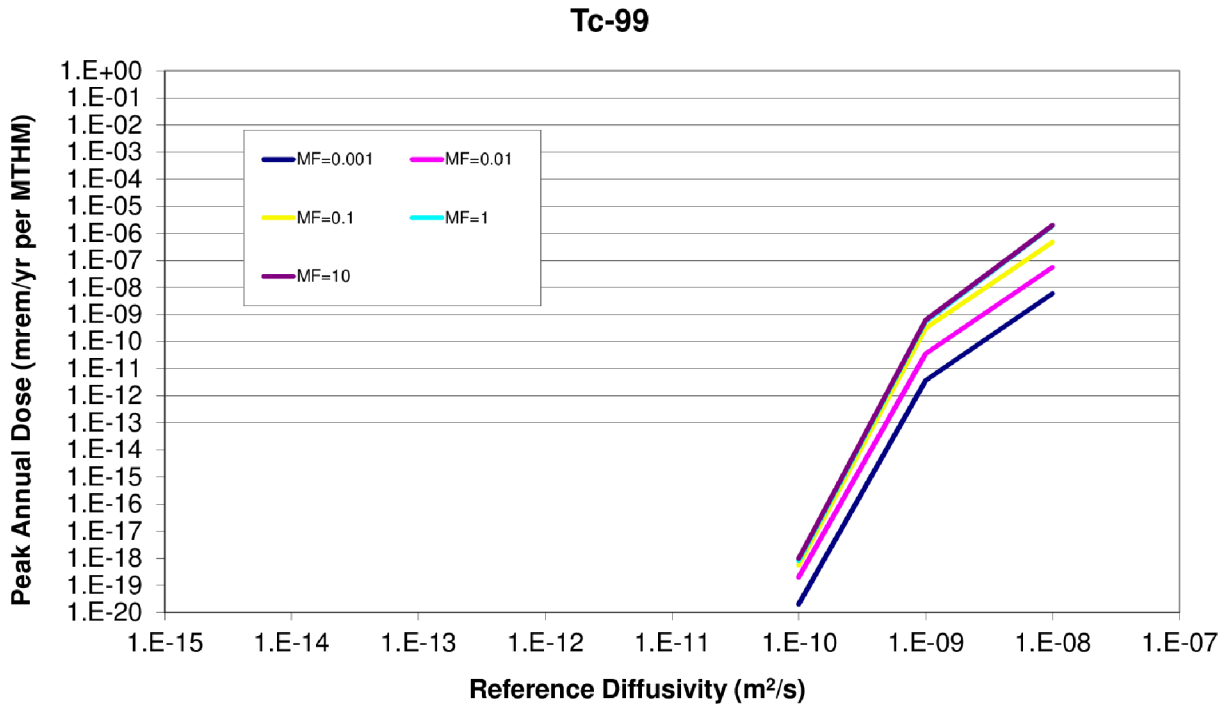

b) Sensitivity to Radionuclide Inventory

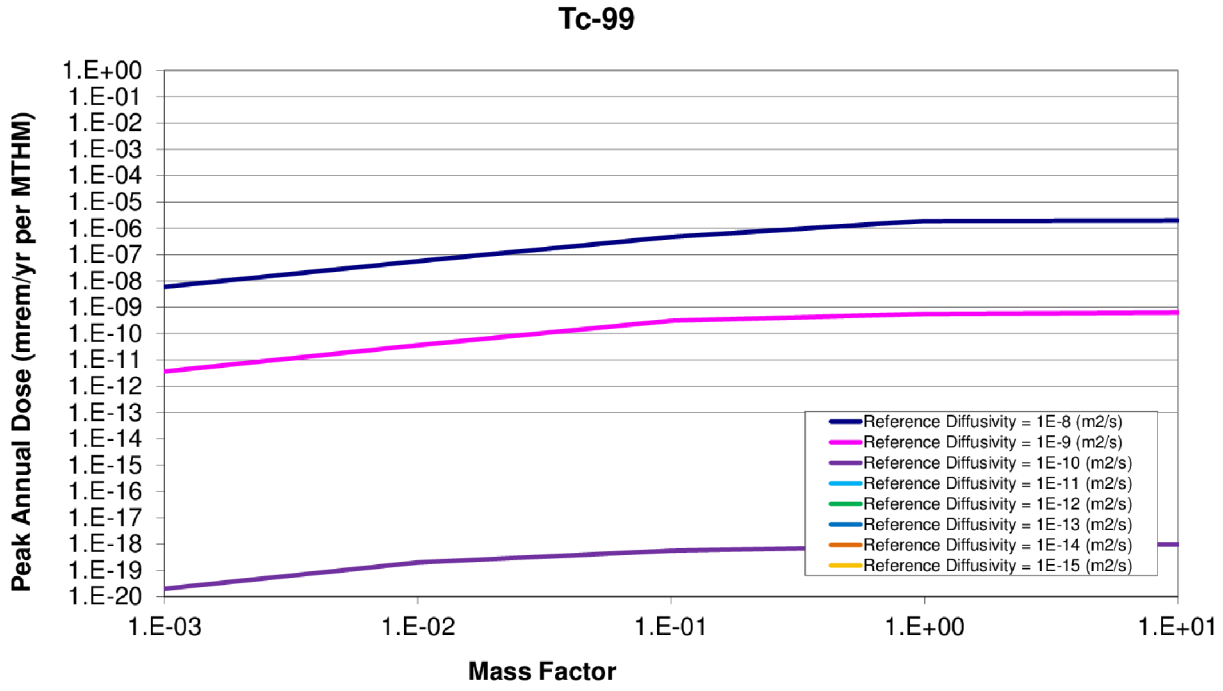

Figure 3-16. ^{99}Tc Diffusion—Inventory Sensitivity

a) Sensitivity to Relative Diffusivity

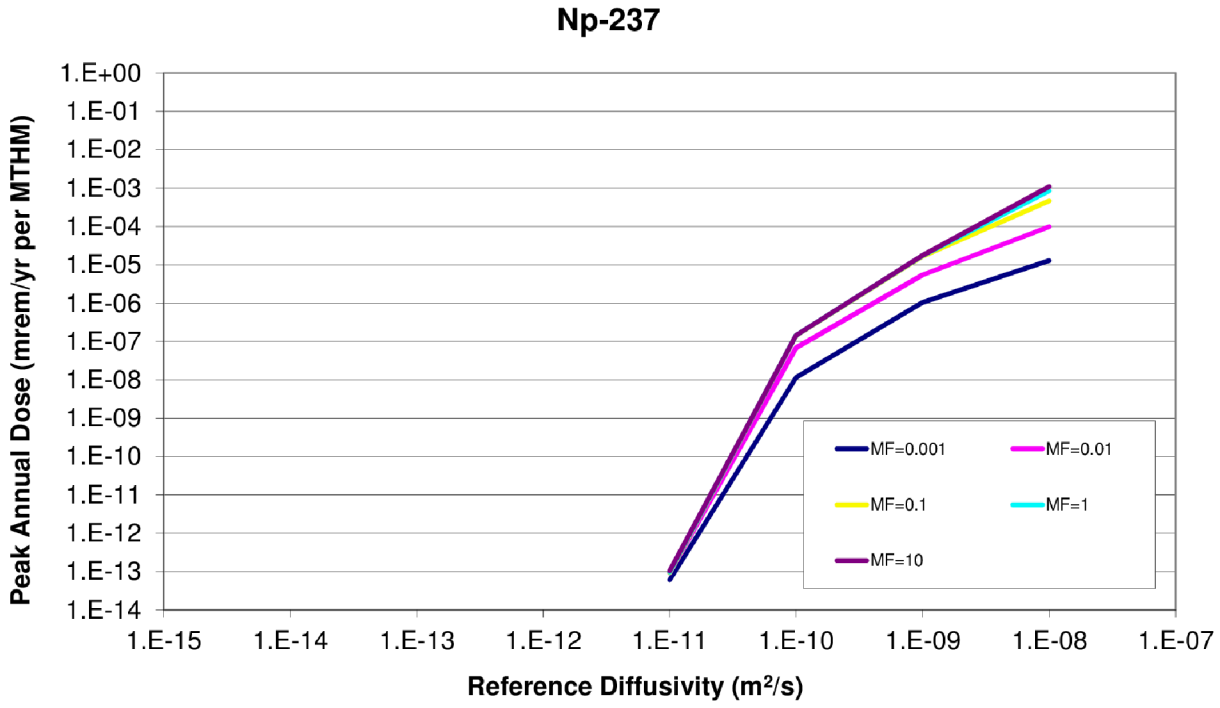

b) Sensitivity to Radionuclide Inventory

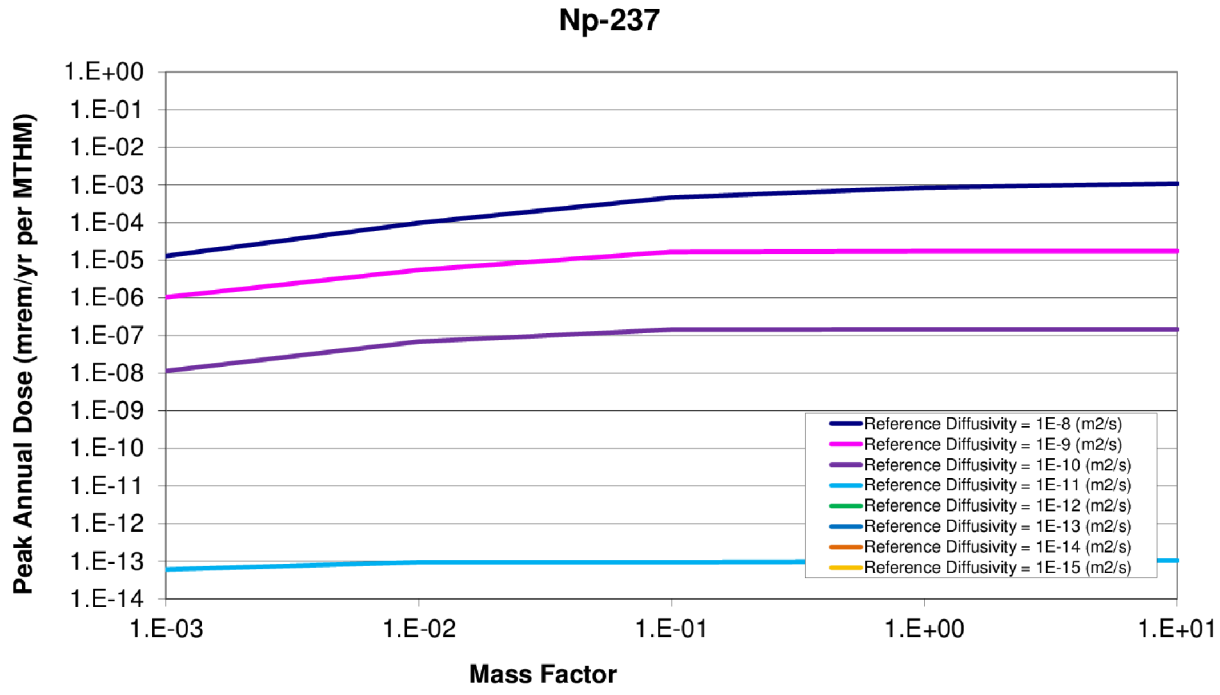

Figure 3-17. ^{237}Np Diffusion—Inventory Sensitivity

3.3.2.2 Vertical Advective Velocity

Transport out of the EBS and through the permeable, porous geosphere involves advection, diffusion, and hydraulic dispersion phenomena. Advection is transport driven by bulk water velocity, while diffusion is the result of Brownian motion across concentration gradients. The method by which the dominant solute transport mode (diffusive or advective) is determined for a particular porous medium is by use of the dimensionless Peclet number,

$$Pe = \frac{nvL}{\alpha nv + D_{eff}} = \frac{advective\ rate}{diffusive\ rate} \qquad \text{Eq. 3-4}$$

where:

n = Solute accessible porosity [%]

v = Advective velocity [m/s]

L = Transport distance [m]

α = Dispersivity [m]

D_{eff} = Effective diffusion coefficient [m^2/s]

For a high *Pe* number, advection is the dominant transport mode, while diffusive or dispersive transport dominates for a low *Pe* number (Schwartz and Zhang 2004).

In this analysis, the threshold between primarily diffusive and primarily advective transport was investigated by varying the vertical advective velocity in conjunction with the diffusion coefficient. It was expected that for the low diffusion coefficients and low advective velocities usually found in clay media, the model should behave entirely in the diffusive regime, but as the vertical advective velocity grows, system behavior should increasingly approach the advective regime.

3.3.2.2.1 Parametric Range

The diffusion coefficient was altered as discussed in Section 3.3.2.1 and the vertical advective velocity of the far field was altered as well. Based on Andra (2005a, Table 5.5-1), the vertical hydraulic gradient is 0.4, while the hydraulic conductivity is 5.0×10^{-14} m/s. The resulting vertical advective velocity is then 2.0×10^{-14} m/s, which is 6.31×10^{-7} m/yr (Andra 2005a).

The forty runs are a combination of the five values of the vertical advective velocity and eight magnitudes of relative diffusivity (Table 3-9).

Table 3-9. Vertical Advective Velocity and Diffusion Coefficient Simulation Groupings

Reference Diffusivity (m^2/s)	Vertical Advective Velocity (m/yr)				
	6.31×10^{-8}	6.31×10^{-7}	6.31×10^{-6}	6.31×10^{-5}	6.31×10^{-4}
	Groupings				
1×10^{-8}	1	2	3	4	5
1×10^{-9}	6	7	8	9	10
1×10^{-10}	11	12	13	14	15
1×10^{-11}	16	17	18	19	20
1×10^{-12}	21	22	23	24	25
1×10^{-13}	26	27	28	29	30
1×10^{-14}	31	32	33	34	35
1×10^{-15}	36	37	38	39	40

To capture the importance of the vertical advective velocity, a range was chosen to span a number of orders of magnitude between 6.31×10^{-8} and 6.31×10^{-4} m/yr. The relative diffusivity was simultaneously varied over the eight magnitudes between 10^{-8} and 10^{-15} m^2/s. It is worth noting that both the relative diffusivity and the vertical advective velocity are functions of porosity in the host rock and are therefore expected to vary together under actual geologic environments.

3.3.2.2.2 Results

For isotopes of interest, higher advective velocity and higher diffusivity lead to higher means of the peak annual dose. The highly soluble and non-sorbing elements, I and Cl were expected to exhibit behavior that is highly sensitive to advection in the system in the advective regime but less sensitive to advection in the diffusive regime.

In Figures 3-18 and 3-19, ^{129}I and ^{36}Cl are more sensitive to vertical advective velocity for lower vertical advective velocities. This demonstrates that for vertical advective velocities 6.31×10^{-6} m/yr and above, lower reference diffusivities are ineffective at attenuating the mean of the peak doses for soluble, non-sorbing elements.

The solubility-limited and sorbing elements, Tc and Np, in Figures 3-20 and 3-21 show a very weak influence on peak annual dose rate for low reference diffusivities, but show a direct proportionality between dose and reference diffusivity above a threshold. For ^{99}Tc, for example, that threshold occurs at 1×10^{-11} m^2/s.

Dose contribution from ^{99}Tc has a proportional relationship with vertical advective velocity above a regime threshold at 6.31×10^{-5} m/yr, above which the system exhibits sensitivity to advection.

The convergence of the effect of the reference diffusivity and vertical advective velocity for the cases above shows the effect of dissolved concentration (solubility) limits and sorption. Se is non-sorbing, but solubility limited. The results from ^{79}Se in Figure 3-22 shows that for low vertical advective velocity, the system is diffusion dominated. However, for high vertical advective velocity, the diffusivity remains important even in the advective regime as spreading facilitates transport in the presence of solubility-limited transport.

a) Reference Diffusivity Sensitivity

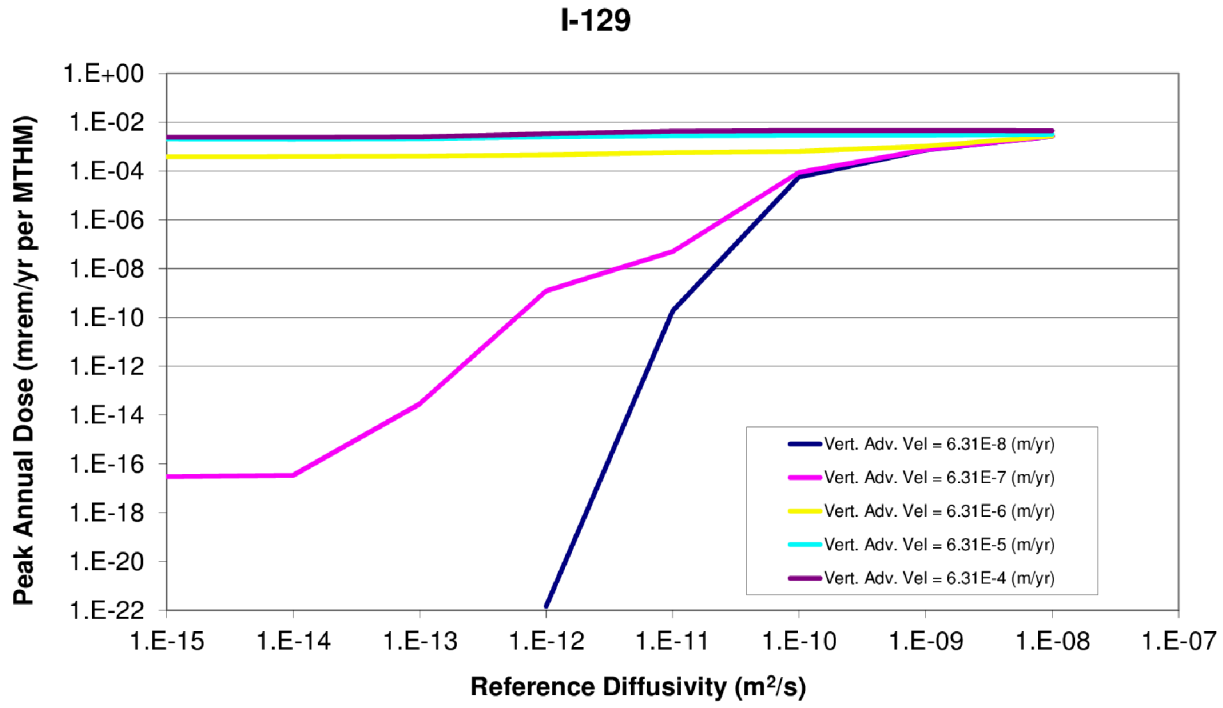

b) Vertical Advective Velocity

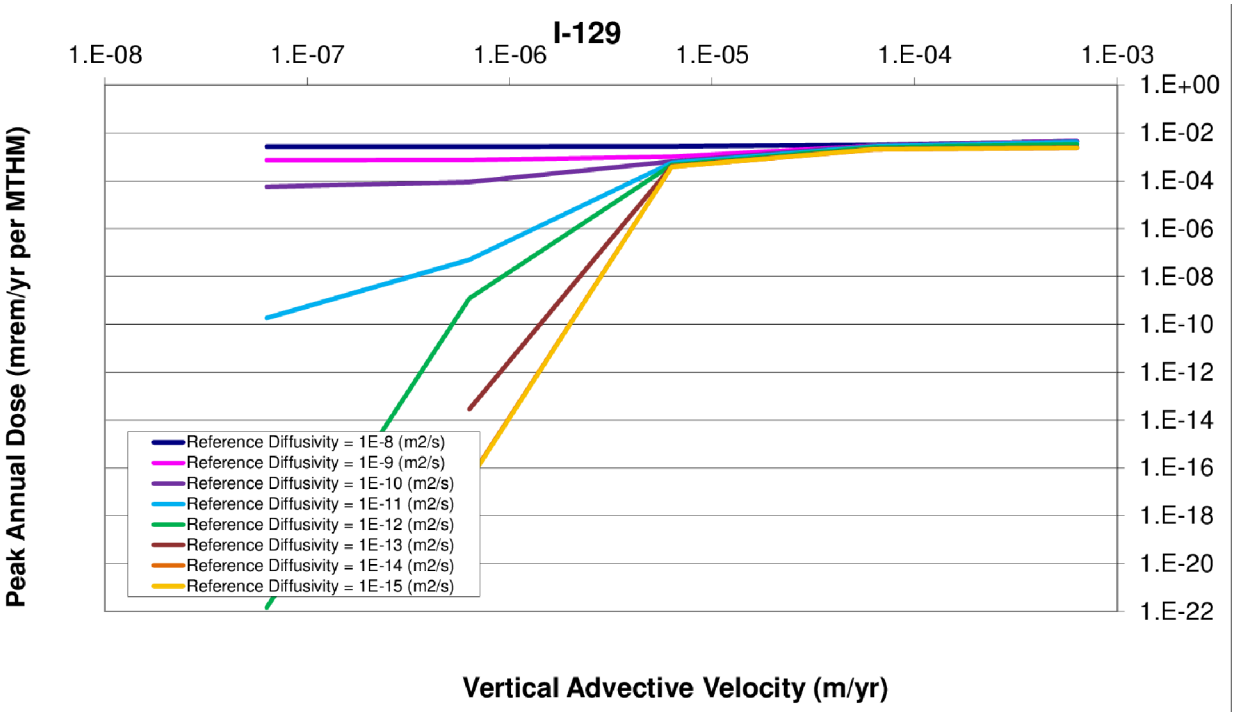

Figure 3-18. ^{129}I Diffusion—Vertical Advective Velocity Sensitivity

a) Reference Diffusivity Sensitivity

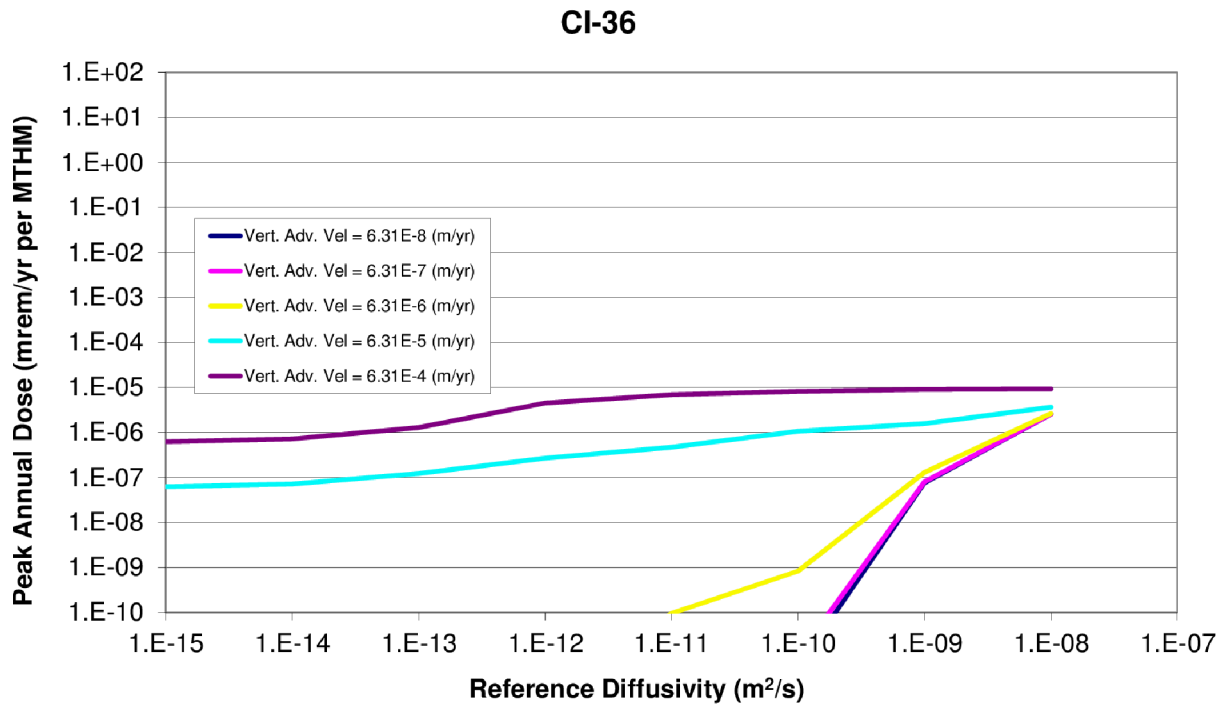

b) Vertical Advective Velocity

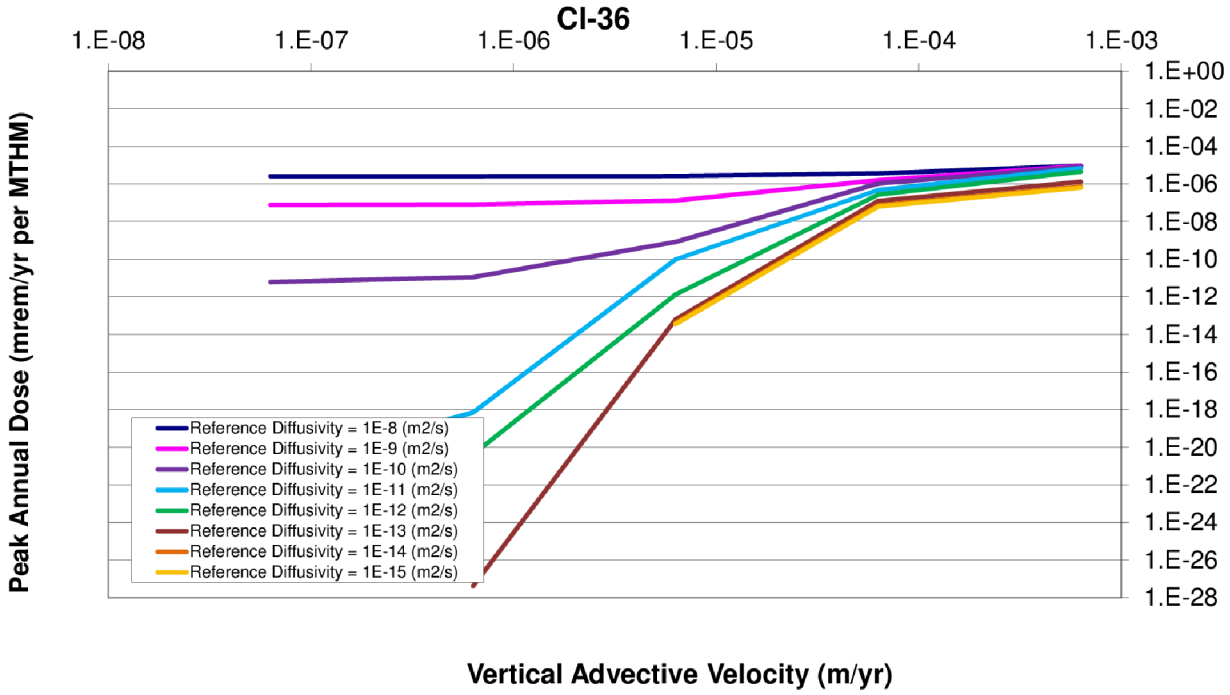

Figure 3-19. ^{36}Cl Diffusion—Vertical Advective Velocity Sensitivity

a) Reference Diffusivity Sensitivity

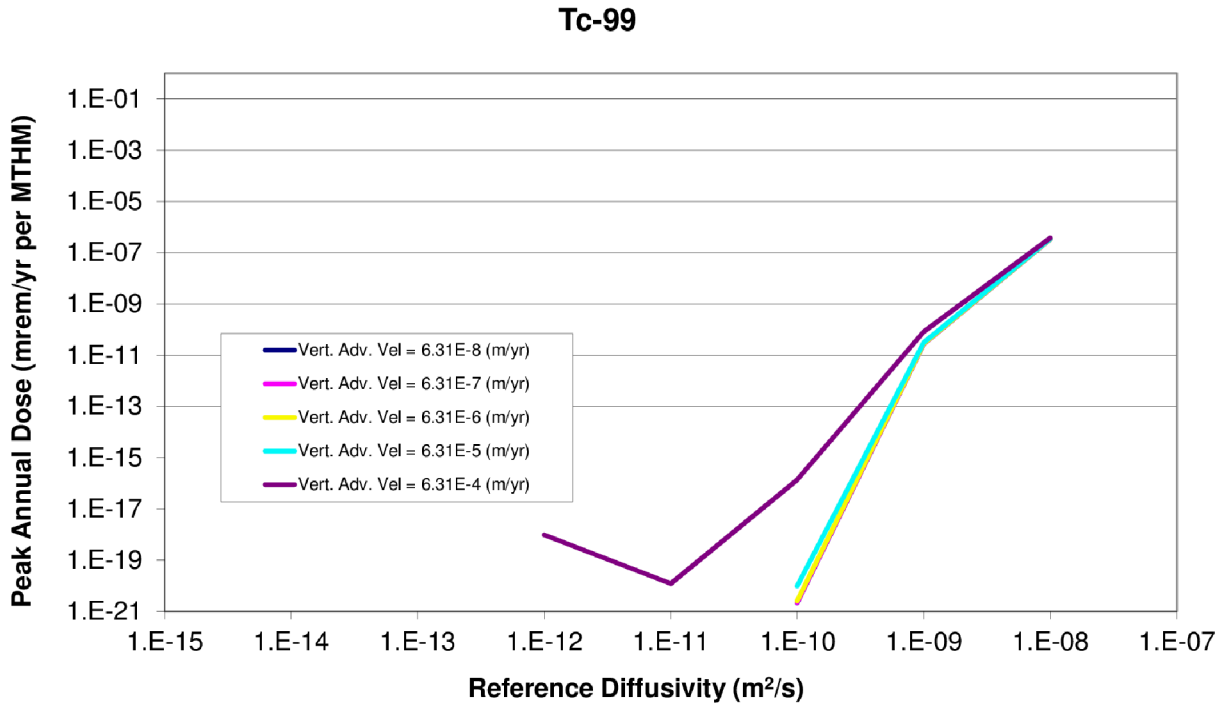

b) Vertical Advective Velocity

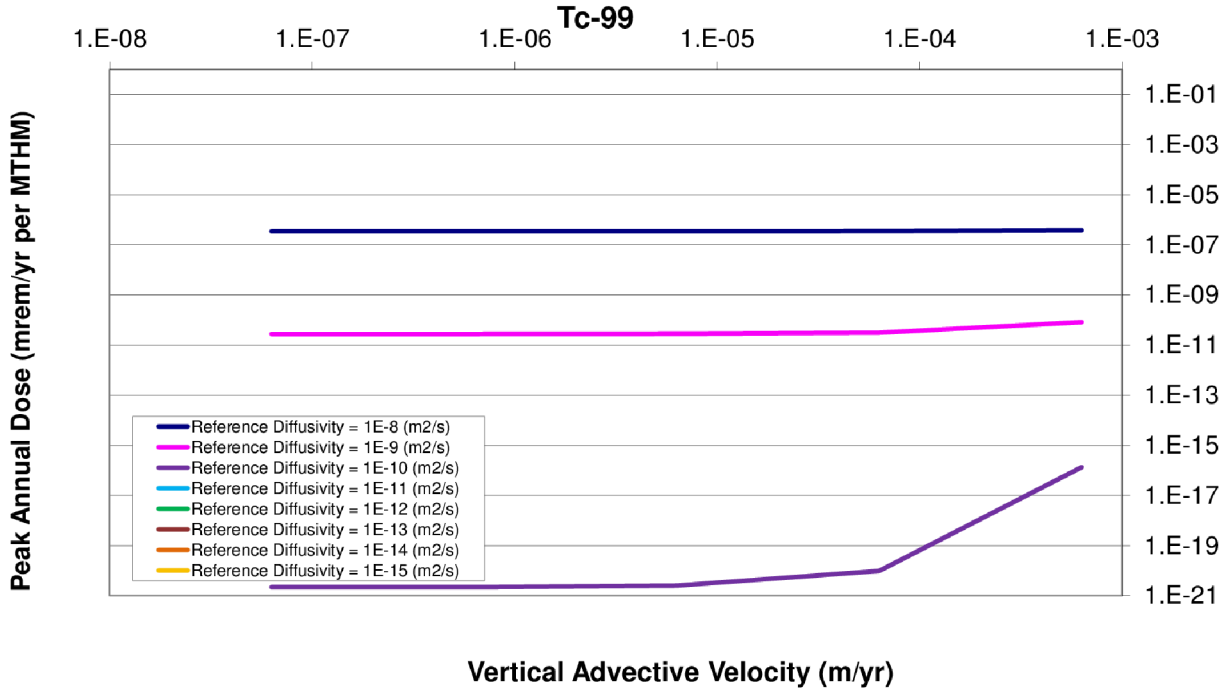

Figure 3-20. ^{99}Tc Diffusion—Vertical Advective Velocity Sensitivity

a) Reference Diffusivity Sensitivity

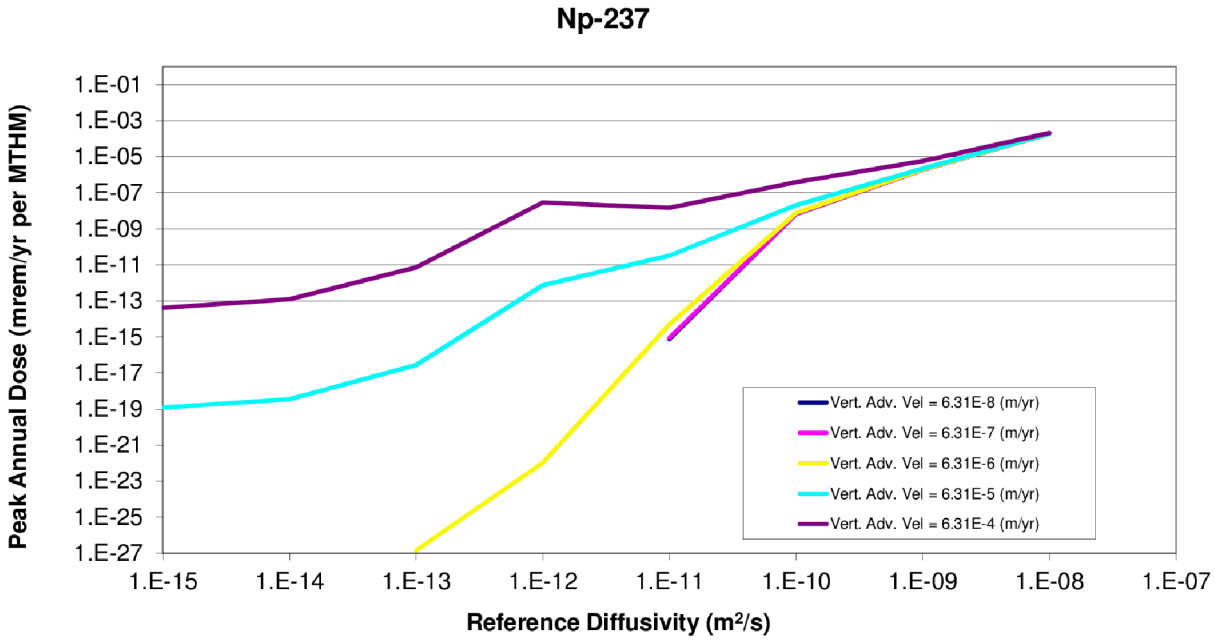

b) Vertical Advective Velocity

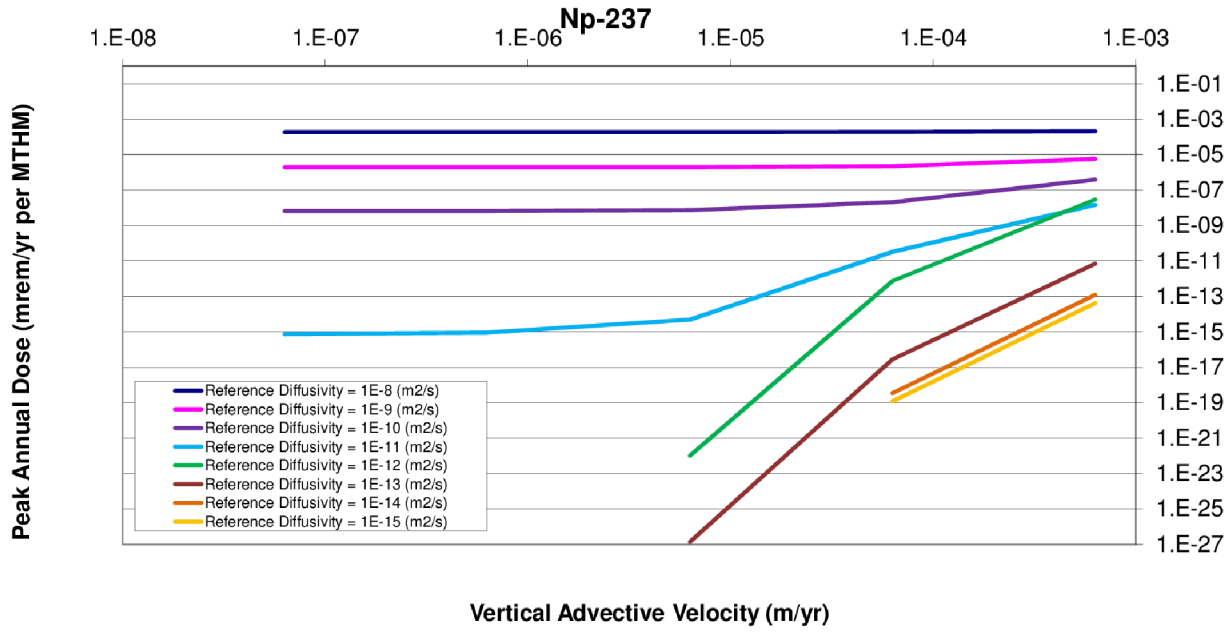

Figure 3-21. ^{237}Np Diffusion—Vertical Advective Velocity Sensitivity

a) Reference Diffusivity Sensitivity

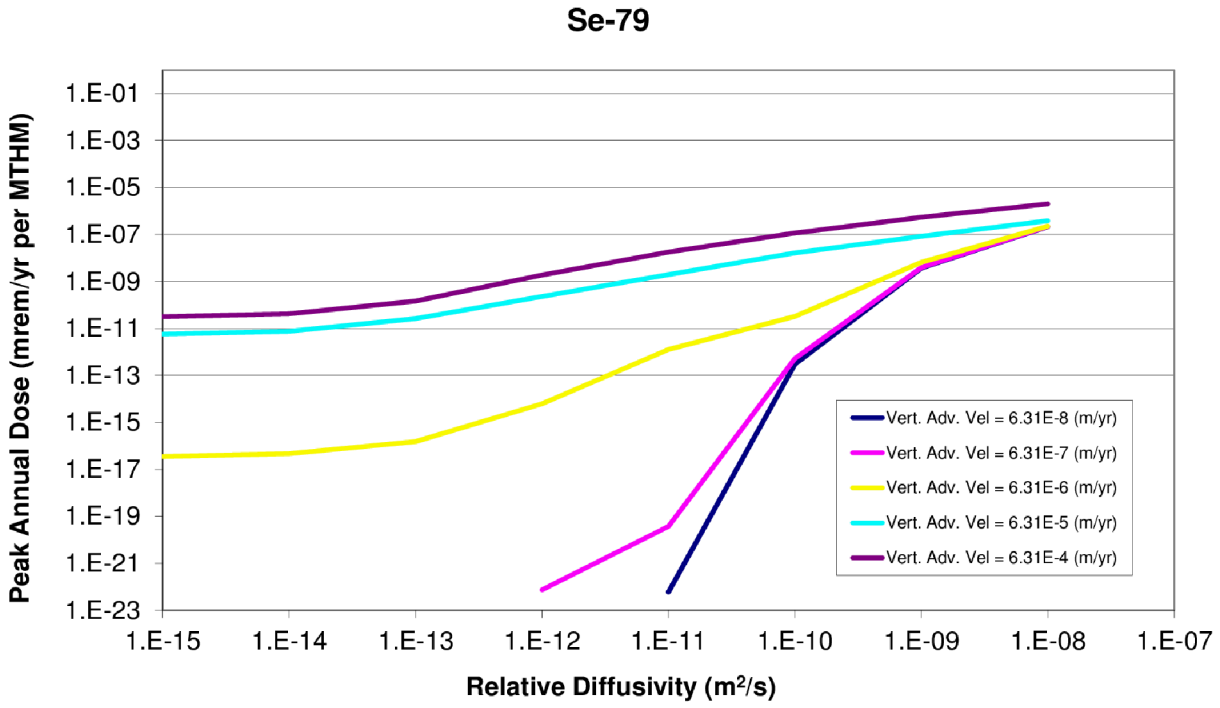

b) Vertical Advective Velocity

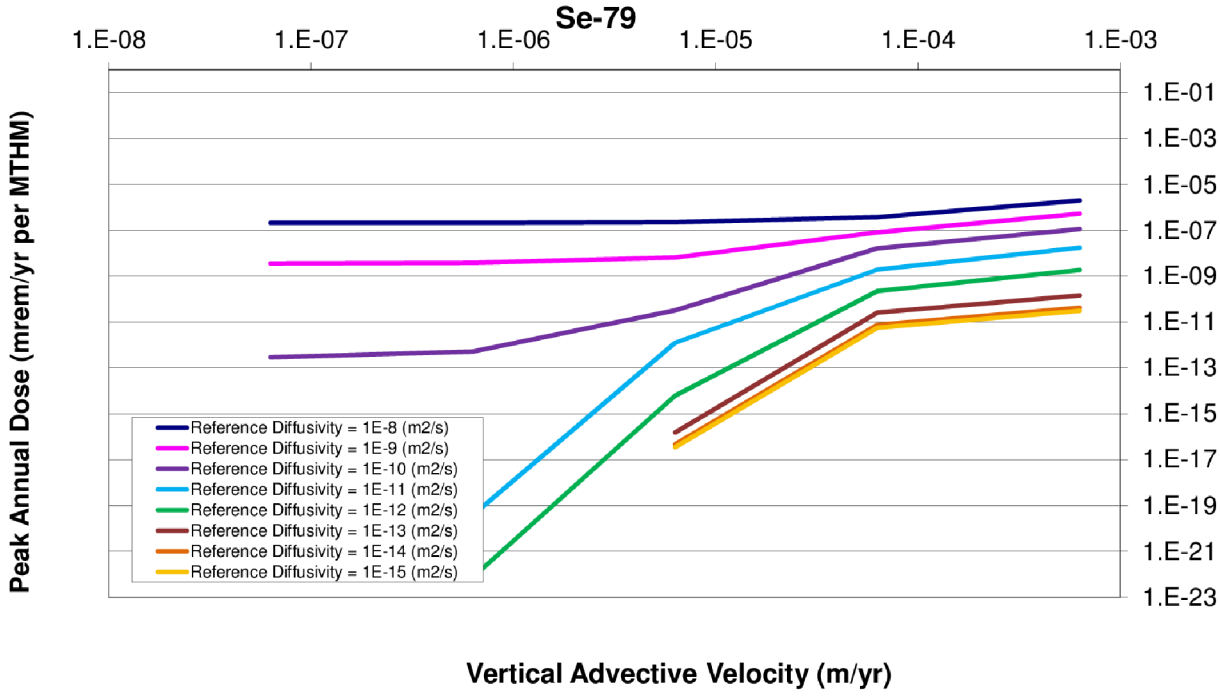

Figure 3-22. ^{79}Se Diffusion—Vertical Advective Velocity Sensitivity

3.3.2.3 Solubility Coefficients

3.3.2.3.1 Parametric Range

The solubility coefficients were varied in this simulation using a multiplier. The reference solubilities for each element were multiplied by the multiplier for each simulation group. This technique preserved relative solubility among elements. Forty values of solubility coefficient multiplier were used to change the far-field solubility.

The values of the solubility multiplier were varied over many orders of magnitude, from 1×10^{-9} through 5×10^{10}. This multiplier was applied to the most likely values of solubility for each element, so the relative solubility between elements was preserved.

3.3.2.3.2 Results

The results for varying the solubility coefficient were very straightforward. For solubility limits below a certain threshold, the dose releases were directly proportional to the solubility limit, indicating that the radionuclide concentration saturated the groundwater up to the solubility limit near the waste form. For solubility limits above the threshold, however, further increase to the limit had no effect on the peak dose. This demonstrates the situation in which the solubility limit is so high that even complete dissolution of the waste inventory into the pore water is insufficient to reach the solubility limit.

In Figures 3-23 and 3-24, it is clear that for solubility constants lower than a threshold, the relationship between peak annual dose and solubility limit is strong.

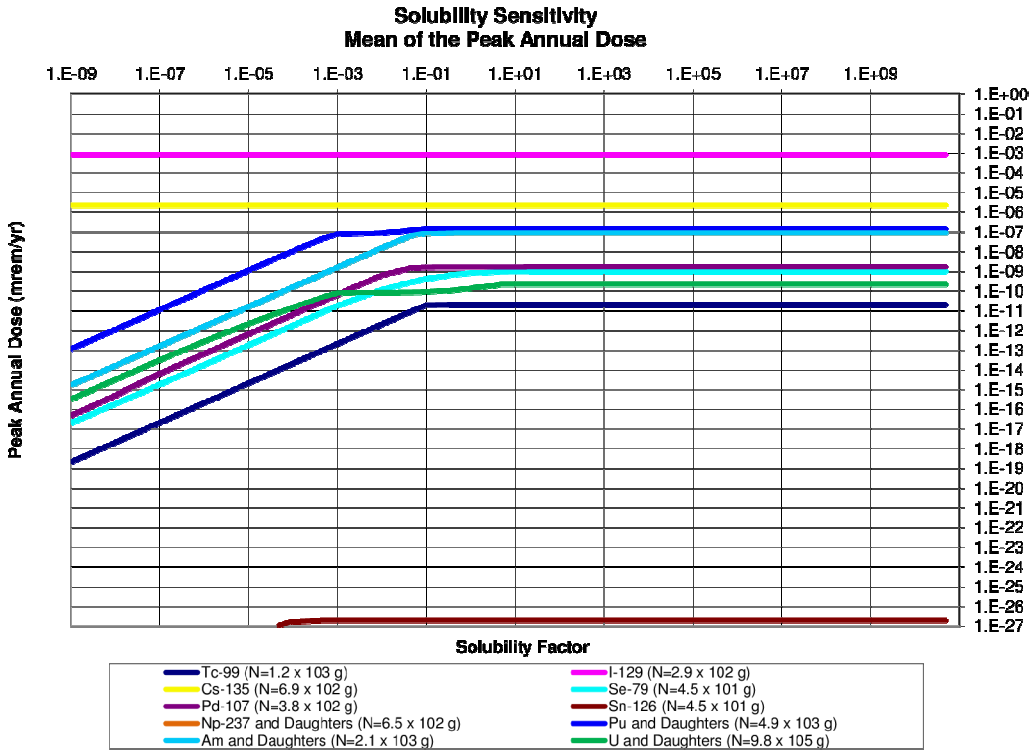

NOTE: The peak annual dose due to an inventory, *N*, of each isotope

Figure 3-23. Solubility Factor Sensitivity

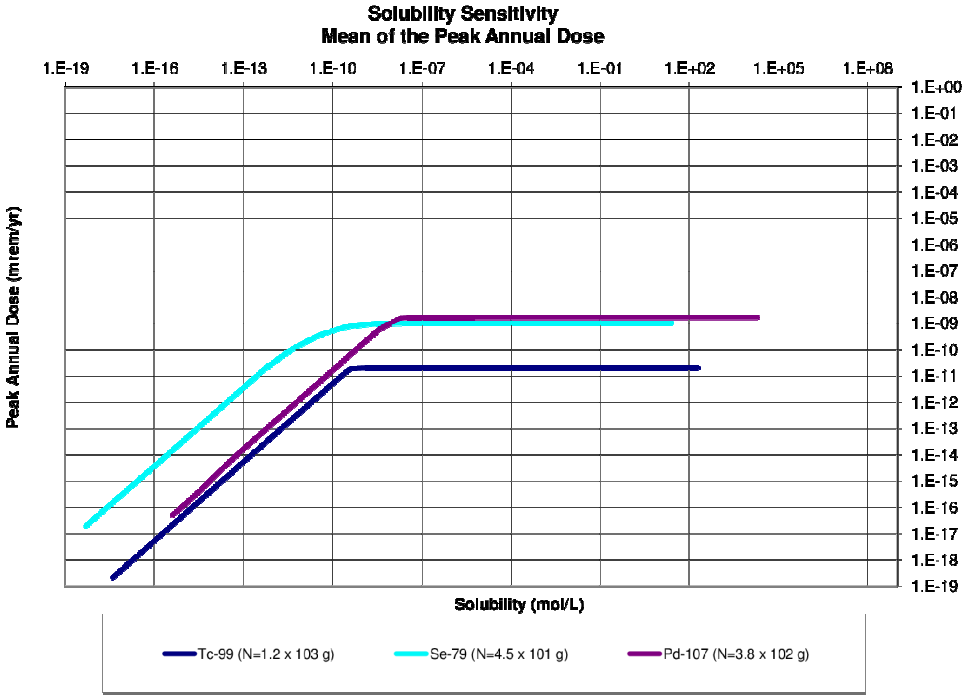

NOTE: The peak annual dose due to an inventory, N, of each isotope

Figure 3-24. Solubility Limit Sensitivity

3.3.2.4 Sorption Distribution Coefficient

This analysis investigated the peak dose rate contribution from various radionuclides to the distribution coefficient of those radionuclides. The distribution, or partition, coefficient, K_d, relates the amount of contaminant adsorbed into the solid phase of the host medium to the amount of contaminant adsorbed into the aqueous phase of the host medium. It is a common empirical coefficient used to capture the effects of a number of retardation mechanisms. The K_d, in units of m^3/kg, is the ratio of the mass of contaminant in the solid to the mass of contaminant in the solution.

The retardation factor, R_f, which is the ratio between velocity of water through a volume and the velocity of a contaminant through that volume, can be expressed in terms of the distribution coefficient (Freeze and Cherry (1979, Equation 9.14):

— Eq. 3-5

where

ρ_b = Bulk density [kg/m^3]

n_e = Effective porosity [-]

3.3.2.4.1 Parametric Range

The parameters in this model were all set to the default values except a multiplier applied to the distribution coefficients. The multiplier took the forty values 1×10^{-9}, 5×10^{-8}, …5×10^{10}. Only the far-field clay K_d values were altered by this factor. K_d's affecting the EBS, DRZ and fast pathway were not changed.

3.3.2.4.2 Results

The expected inverse relationship between the retardation factor and resulting peak annual dose was found for all elements that were not assumed to be effectively infinitely soluble. In the low retardation factor cases, a regime is established in which the peak annual dose is entirely unaffected by changes in distribution coefficient. For large values of retardation factor, the sensitivity to small changes in the retardation factor increases dramatically. In that sensitive regime, the change in peak annual dose is inversely related to the retardation factor. Between these two regimes is a transition regime which varies by radionuclide, but roughly corresponds to the K_d factor range from 1×10^{-5} to 5×10^{0}.

It is clear from Figures 3-25 and 3-26 that for retardation coefficients greater than a threshold, the relationship between peak annual dose and retardation coefficient is a strong inverse one.

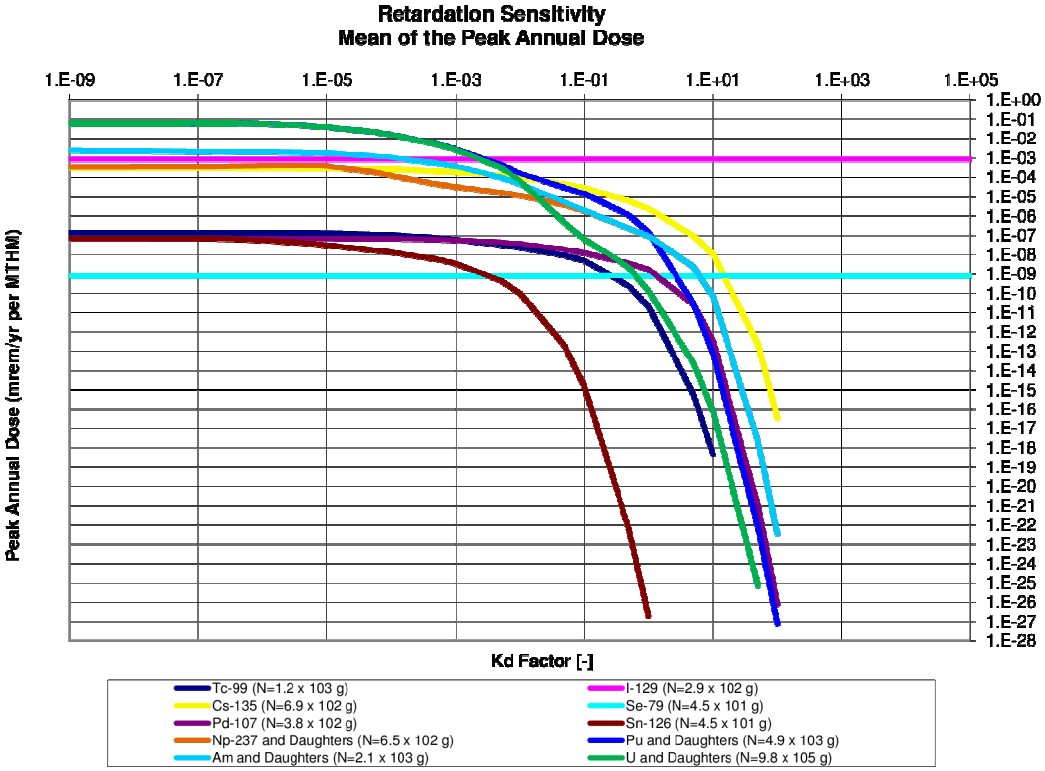

NOTE: The peak annual dose due to an inventory, N, of each isotope

Figure 3-25. K_d Factor Sensitivity

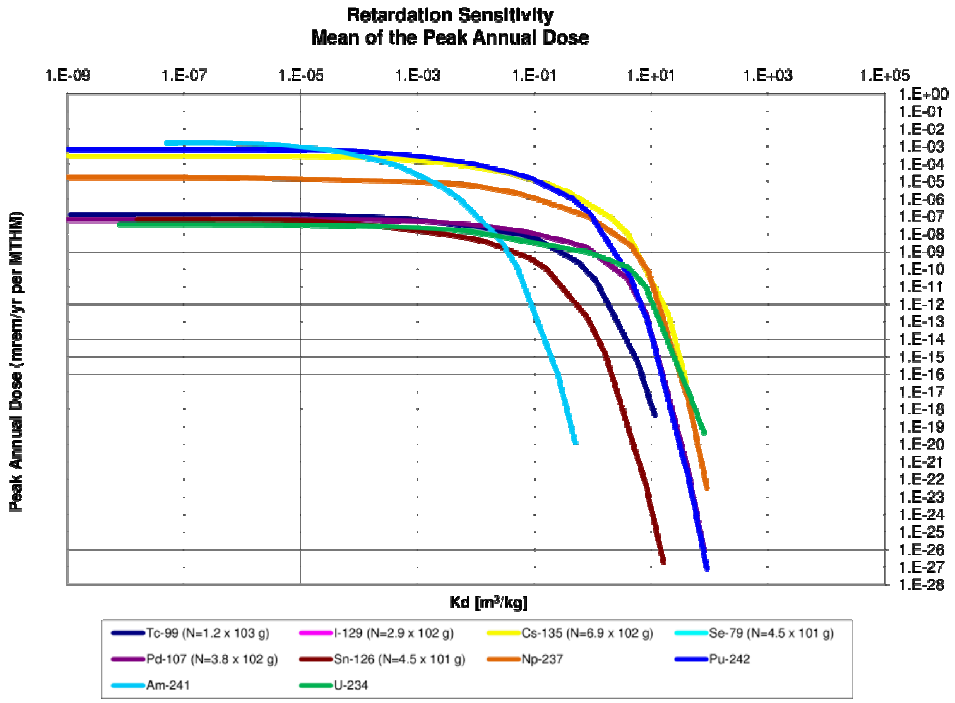

NOTE: The peak annual dose due to an inventory, N, of each isotope.

Figure 3-26. K_d Sensitivity

3.3.2.5 Waste Form Degradation Rate

The sensitivity of peak dose rate to the waste form degradation rate was determined with respect to varying inventories of waste.

The sensitivity of repository performance to waste form degradation rate was expected to vary according to the waste inventory. For cases in which the dominant dose contributing radionuclides have half-lives much shorter than the expected waste form lifetime, the waste form degradation rate is not expected to have an effect. So too, for cases in which the primary barrier to release, the slow diffusive pathway, dominates overall repository performance, the waste form engineered barrier was expected to have a negligible effect on repository performance in comparison.

In the case of a generic clay environment, the effect of the long time scale of the slow diffusive release pathway was to minimize the potential effect of high waste form degradation rates.

3.3.2.5.1 Parametric Range

For these sensitivity simulations both the waste form degradation rate and the waste inventory mass factor were varied. There were forty runs corresponding to eight values of the waste form degradation rate and five values of the mass factor. The waste form degradation rate was varied over the eight magnitudes between 10^{-9} and 10^{-2} yr^{-1}. The inventory mass factor was varied over the five magnitudes between 0.001 and 10.

3.3.2.5.2 Results

These results show two regimes. In the first regime, the mean of the peak annual dose rates is directly proportional to both the mass factor and the fractional waste form degradation rate. For some radionuclides, attenuation occurs for high values of both parameters as the release of radionuclides is limited by dispersion parameters. This phenomenon can be seen in the figures below in which transition between regimes for higher degradation rates happens at lower mass factors than transition between regimes for lower degradation rates.

Safety indicators for postclosure repository performance have been developed by the UFDC which utilize the inventory multiplier that was varied in this study (Nutt et al. 2009). These indicators are normalized by a normalization factor (100 mrem/yr) recommended by the IAEA as the limit to "relevant critical members of the public" (IAEA 1996). The functional form for this safety indicator for a single waste category, HLW, is just

$$SI_G = \left(\frac{\sum_{i=1}^{N} D_{G,i}(I_i, F_d)}{100\ mrem/yr} \right) [GWe/yr] \qquad \text{Eq. 3-6}$$

where

SI_G = Safety indicator for disposal in media type G [GWe/yr]
N = Number of key radionuclides considered in this indicator
$D_{G,i}$ = Peak dose rate from isotope i in media type G [mrem/yr]
F_d = Fractional waste form degradation rate [1/yr]

Tables 3-10 to 3-12 report the safety indicators for various independent isotopes and, where applicable, their daughters.

Table 3-10. Safety Indicators for the Actinides and Their Daughters

Degradation Rate	Inventory Factor				
	0.001	**0.01**	**0.1**	**1**	**10**
^{237}Np and Daughters (N = 6.5×10^{2} g)					
1×10^{-9}	3×10^{-13}	3×10^{-12}	3×10^{-11}	3×10^{-10}	9×10^{-10}
1×10^{-8}	3×10^{-12}	3×10^{-11}	3×10^{-10}	9×10^{-10}	9×10^{-10}
1×10^{-7}	3×10^{-11}	3×10^{-10}	9×10^{-10}	9×10^{-10}	9×10^{-10}
1×10^{-6}	1×10^{-10}	8×10^{-10}	9×10^{-10}	9×10^{-10}	9×10^{-10}
1×10^{-5}	2×10^{-10}	8×10^{-10}	9×10^{-10}	9×10^{-10}	9×10^{-10}
1×10^{-4}	2×10^{-10}	8×10^{-10}	9×10^{-10}	9×10^{-10}	1×10^{-9}
1×10^{-3}	2×10^{-10}	8×10^{-10}	9×10^{-10}	9×10^{-10}	1×10^{-9}
1×10^{-2}	2×10^{-10}	8×10^{-10}	9×10^{-10}	9×10^{-10}	1×10^{-9}
Pu and Daughters (N = 4.9×10^{3} g)					
1×10^{-9}	4×10^{-15}	4×10^{-14}	4×10^{-13}	3×10^{-12}	2×10^{-11}
1×10^{-8}	4×10^{-14}	3×10^{-13}	3×10^{-12}	2×10^{-11}	2×10^{-10}
1×10^{-7}	3×10^{-13}	2×10^{-12}	2×10^{-11}	2×10^{-10}	2×10^{-9}
1×10^{-6}	2×10^{-12}	2×10^{-11}	2×10^{-10}	1×10^{-9}	9×10^{-9}
1×10^{-5}	4×10^{-12}	4×10^{-11}	4×10^{-10}	3×10^{-9}	1×10^{-8}
1×10^{-4}	5×10^{-12}	5×10^{-11}	5×10^{-10}	3×10^{-9}	1×10^{-8}
1×10^{-3}	5×10^{-12}	5×10^{-11}	5×10^{-10}	3×10^{-9}	1×10^{-8}
1×10^{-2}	5×10^{-12}	5×10^{-11}	5×10^{-10}	3×10^{-9}	1×10^{-8}
Am and Daughters (N = 2.1×10^{3} g)					
1×10^{-9}	3×10^{-13}	3×10^{-12}	3×10^{-11}	3×10^{-10}	9×10^{-10}
1×10^{-8}	3×10^{-12}	3×10^{-11}	3×10^{-10}	9×10^{-10}	9×10^{-10}
1×10^{-7}	3×10^{-11}	3×10^{-10}	9×10^{-10}	9×10^{-10}	9×10^{-10}
1×10^{-6}	1×10^{-10}	8×10^{-10}	9×10^{-10}	9×10^{-10}	9×10^{-10}
1×10^{-5}	2×10^{-10}	8×10^{-10}	9×10^{-10}	9×10^{-10}	9×10^{-10}
1×10^{-4}	2×10^{-10}	8×10^{-10}	9×10^{-10}	9×10^{-10}	1×10^{-9}
1×10^{-3}	2×10^{-10}	8×10^{-10}	9×10^{-10}	9×10^{-10}	1×10^{-9}
1×10^{-2}	2×10^{-10}	8×10^{-10}	9×10^{-10}	9×10^{-10}	1×10^{-9}
U and Daughters (N = 9.8×10^{5} g)					
1×10^{-9}	2×10^{-15}	2×10^{-14}	1×10^{-13}	5×10^{-13}	6×10^{-13}
1×10^{-8}	2×10^{-14}	1×10^{-13}	5×10^{-13}	6×10^{-13}	7×10^{-13}
1×10^{-7}	1×10^{-13}	4×10^{-13}	6×10^{-13}	7×10^{-13}	2×10^{-12}
1×10^{-6}	3×10^{-13}	6×10^{-13}	7×10^{-13}	1×10^{-12}	7×10^{-12}
1×10^{-5}	4×10^{-13}	7×10^{-13}	8×10^{-13}	2×10^{-12}	9×10^{-12}
1×10^{-4}	4×10^{-13}	7×10^{-13}	9×10^{-13}	3×10^{-12}	9×10^{-12}
1×10^{-3}	4×10^{-13}	7×10^{-13}	9×10^{-13}	3×10^{-12}	9×10^{-12}
1×10^{-2}	4×10^{-13}	7×10^{-13}	9×10^{-13}	3×10^{-12}	9×10^{-12}

Table 3-11. Safety Indicators for Soluble, Non-Sorbing Radionuclides

Degradation Rate	Inventory Factor				
	0.001	**0.01**	**0.1**	**1**	**10**
^{129}I ($N = 2.9\times10^{2}$ g)					
1×10^{-9}	3×10^{-11}	3×10^{-10}	3×10^{-9}	3×10^{-8}	3×10^{-7}
1×10^{-8}	3×10^{-10}	3×10^{-9}	3×10^{-8}	3×10^{-7}	3×10^{-6}
1×10^{-7}	2×10^{-9}	2×10^{-8}	2×10^{-7}	2×10^{-6}	2×10^{-5}
1×10^{-6}	8×10^{-9}	8×10^{-8}	8×10^{-7}	8×10^{-6}	8×10^{-5}
1×10^{-5}	1×10^{-8}	1×10^{-7}	1×10^{-6}	1×10^{-5}	1×10^{-4}
1×10^{-4}	1×10^{-8}	1×10^{-7}	1×10^{-6}	1×10^{-5}	1×10^{-4}
1×10^{-3}	1×10^{-8}	1×10^{-7}	1×10^{-6}	1×10^{-5}	1×10^{-4}
1×10^{-2}	1×10^{-8}	1×10^{-7}	1×10^{-6}	1×10^{-5}	1×10^{-4}
^{36}Cl ($N = 1$ g)					
1×10^{-9}	1×10^{-15}	1×10^{-14}	1×10^{-13}	1×10^{-12}	1×10^{-11}
1×10^{-8}	1×10^{-14}	1×10^{-13}	1×10^{-12}	1×10^{-11}	1×10^{-10}
1×10^{-7}	1×10^{-13}	1×10^{-12}	1×10^{-11}	1×10^{-10}	1×10^{-9}
1×10^{-6}	9×10^{-13}	9×10^{-12}	9×10^{-11}	9×10^{-10}	9×10^{-9}
1×10^{-5}	3×10^{-12}	3×10^{-11}	3×10^{-10}	3×10^{-9}	3×10^{-8}
1×10^{-4}	4×10^{-12}	4×10^{-11}	4×10^{-10}	4×10^{-9}	4×10^{-8}
1×10^{-3}	4×10^{-12}	4×10^{-11}	4×10^{-10}	4×10^{-9}	4×10^{-8}
1×10^{-2}	4×10^{-12}	4×10^{-11}	4×10^{-10}	4×10^{-9}	4×10^{-8}

Table 3-12. Safety Indicators for Solubility-Limited and Sorbing Radionuclides

Degradation Rate	Inventory Factor				
	0.001	0.01	0.1	1	10
^{107}Pd (N = 3.8×10^{2} g)					
1×10^{-9}	2×10^{-16}	2×10^{-15}	2×10^{-14}	2×10^{-13}	2×10^{-12}
1×10^{-8}	2×10^{-15}	2×10^{-14}	2×10^{-13}	2×10^{-12}	1×10^{-11}
1×10^{-7}	2×10^{-14}	2×10^{-13}	2×10^{-12}	8×10^{-12}	3×10^{-11}
1×10^{-6}	5×10^{-14}	5×10^{-13}	3×10^{-12}	2×10^{-11}	3×10^{-11}
1×10^{-5}	5×10^{-14}	5×10^{-13}	4×10^{-12}	2×10^{-11}	3×10^{-11}
1×10^{-4}	5×10^{-14}	5×10^{-13}	4×10^{-12}	2×10^{-11}	3×10^{-11}
1×10^{-3}	5×10^{-14}	5×10^{-13}	4×10^{-12}	2×10^{-11}	3×10^{-11}
1×10^{-2}	5×10^{-14}	5×10^{-13}	4×10^{-12}	2×10^{-11}	3×10^{-11}
^{126}Sn (N = 4.5×10^{1} g)					
1×10^{-9}	0	0	0	0	0
1×10^{-8}	0	0	0	0	0
1×10^{-7}	0	0	0	0	2×10^{-29}
1×10^{-6}	0	0	0	2×10^{-29}	5×10^{-29}
1×10^{-5}	0	0	1×10^{-29}	3×10^{-29}	5×10^{-29}
1×10^{-4}	0	0	1×10^{-29}	3×10^{-29}	5×10^{-29}
1×10^{-3}	0	0	1×10^{-29}	3×10^{-29}	5×10^{-29}
1×10^{-2}	0	0	1×10^{-29}	3×10^{-29}	5×10^{-29}
^{93}Zr and ^{93}Nb					
1×10^{-9}	1×10^{-17}	1×10^{-16}	1×10^{-15}	1×10^{-14}	1×10^{-13}
1×10^{-8}	1×10^{-16}	1×10^{-15}	1×10^{-14}	1×10^{-13}	7×10^{-13}
1×10^{-7}	1×10^{-15}	1×10^{-14}	1×10^{-13}	6×10^{-13}	3×10^{-12}
1×10^{-6}	4×10^{-15}	4×10^{-14}	3×10^{-13}	1×10^{-12}	4×10^{-12}
1×10^{-5}	6×10^{-15}	6×10^{-14}	4×10^{-13}	2×10^{-12}	4×10^{-12}
1×10^{-4}	6×10^{-15}	6×10^{-14}	4×10^{-13}	2×10^{-12}	4×10^{-12}
1×10^{-3}	7×10^{-15}	6×10^{-14}	4×10^{-13}	2×10^{-12}	4×10^{-12}
1×10^{-2}	7×10^{-15}	6×10^{-14}	4×10^{-13}	2×10^{-12}	4×10^{-12}
^{99}Tc (N = 1.2×10^{3} g)					
1×10^{-9}	2×10^{-18}	2×10^{-17}	2×10^{-16}	2×10^{-15}	2×10^{-14}
1×10^{-8}	2×10^{-17}	2×10^{-16}	2×10^{-15}	2×10^{-14}	1×10^{-13}
1×10^{-7}	2×10^{-16}	2×10^{-15}	2×10^{-14}	1×10^{-13}	2×10^{-13}
1×10^{-6}	1×10^{-15}	1×10^{-14}	1×10^{-13}	2×10^{-13}	2×10^{-13}
1×10^{-5}	5×10^{-15}	5×10^{-14}	1×10^{-13}	2×10^{-13}	2×10^{-13}
1×10^{-4}	7×10^{-15}	5×10^{-14}	1×10^{-13}	2×10^{-13}	2×10^{-13}
1×10^{-3}	7×10^{-15}	5×10^{-14}	1×10^{-13}	2×10^{-13}	2×10^{-13}
1×10^{-2}	7×10^{-15}	5×10^{-14}	1×10^{-13}	2×10^{-13}	2×10^{-13}

Table 3-12. Safety Indicators for Solubility-Limited and Sorbing Radionuclides (continued)

Degradation Rate	Inventory Factor				
	0.001	0.01	0.1	1	10
^{135}Cs (N = 6.9×10^{2} g)					
1×10^{-9}	6×10^{-14}	6×10^{-13}	6×10^{-12}	6×10^{-11}	6×10^{-10}
1×10^{-8}	6×10^{-13}	6×10^{-12}	6×10^{-11}	6×10^{-10}	6×10^{-9}
1×10^{-7}	5×10^{-12}	5×10^{-11}	5×10^{-10}	5×10^{-9}	5×10^{-8}
1×10^{-6}	2×10^{-11}	2×10^{-10}	2×10^{-9}	2×10^{-8}	2×10^{-7}
1×10^{-5}	3×10^{-11}	3×10^{-10}	3×10^{-9}	3×10^{-8}	3×10^{-7}
1×10^{-4}	4×10^{-11}	4×10^{-10}	4×10^{-9}	4×10^{-8}	4×10^{-7}
1×10^{-3}	4×10^{-11}	4×10^{-10}	4×10^{-9}	4×10^{-8}	4×10^{-7}
1×10^{-2}	4×10^{-11}	4×10^{-10}	4×10^{-9}	4×10^{-8}	4×10^{-7}
^{79}Se (N = 4.5×10^{1} g)					
1×10^{-9}	2×10^{-14}	2×10^{-13}	2×10^{-12}	5×10^{-12}	8×10^{-12}
1×10^{-8}	2×10^{-13}	2×10^{-12}	5×10^{-12}	8×10^{-12}	8×10^{-12}
1×10^{-7}	2×10^{-12}	5×10^{-12}	8×10^{-12}	8×10^{-12}	8×10^{-12}
1×10^{-6}	5×10^{-12}	8×10^{-12}	8×10^{-12}	8×10^{-12}	8×10^{-12}
1×10^{-5}	6×10^{-12}	8×10^{-12}	8×10^{-12}	8×10^{-12}	8×10^{-12}
1×10^{-4}	6×10^{-12}	8×10^{-12}	8×10^{-12}	8×10^{-12}	8×10^{-12}
1×10^{-3}	6×10^{-12}	8×10^{-12}	8×10^{-12}	8×10^{-12}	8×10^{-12}
1×10^{-2}	6×10^{-12}	8×10^{-12}	8×10^{-12}	8×10^{-12}	8×10^{-12}

The peaks for highly soluble, non-sorbing elements such as I and Cl are directly proportional to mass factor for most values of waste form degradation rates. This effect can be seen in Figures 3-27 and 3-28.

Highly soluble and non-sorbing ^{129}I demonstrates a direct proportionality between dose rate and fractional degradation rate until a turnover where other natural system parameters dampen transport. Highly soluble and non-sorbing ^{129}I demonstrates a direct proportionality to the inventory multiplier.

The peaks for solubility-limited, sorbing elements such as Tc and Np, on the other hand, have a more dramatic turnover. For very high degradation rates, the dependence on mass factor starts to round off due to attenuation by solubility limits, as can be seen in Figures 3-29 and 3-30.

Solubility-limited and sorbing ^{99}Tc demonstrates a direct proportionality to fractional degradation rate until attenuation by its solubility limit and other natural system parameters.

a) Fractional Degradation Rate

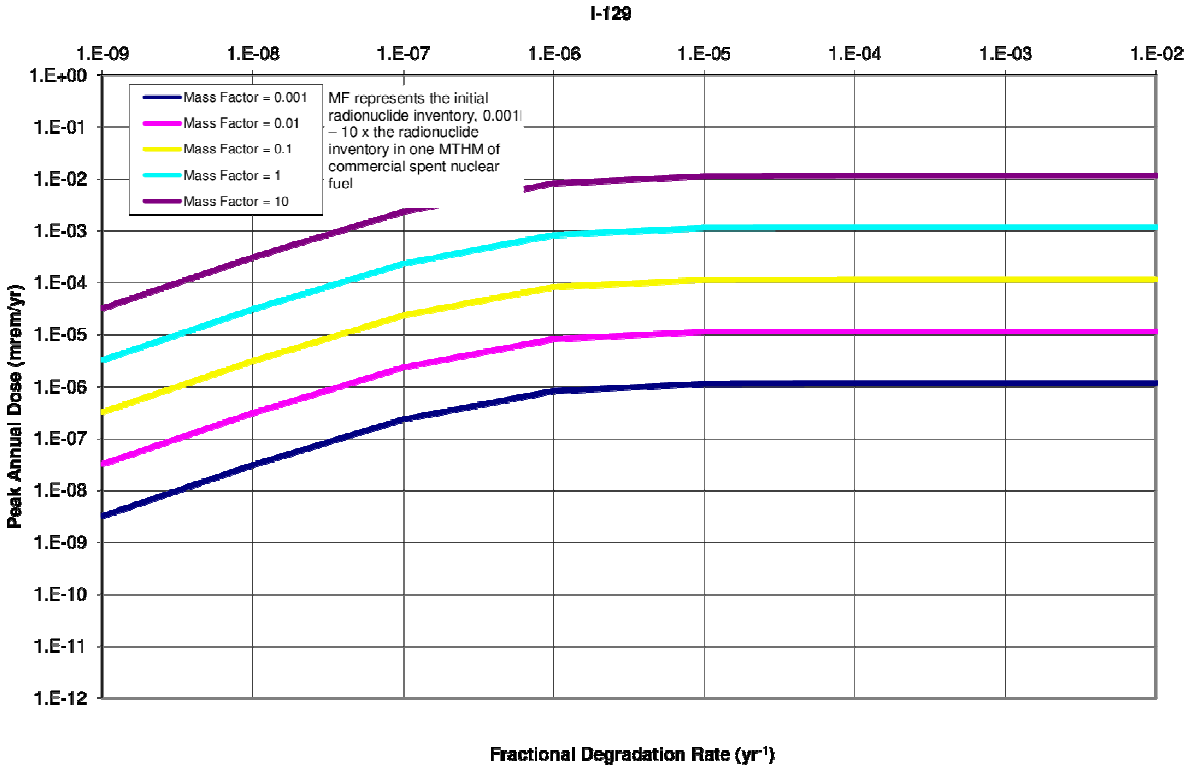

b) Inventory Sensitivity (Mass Factor)

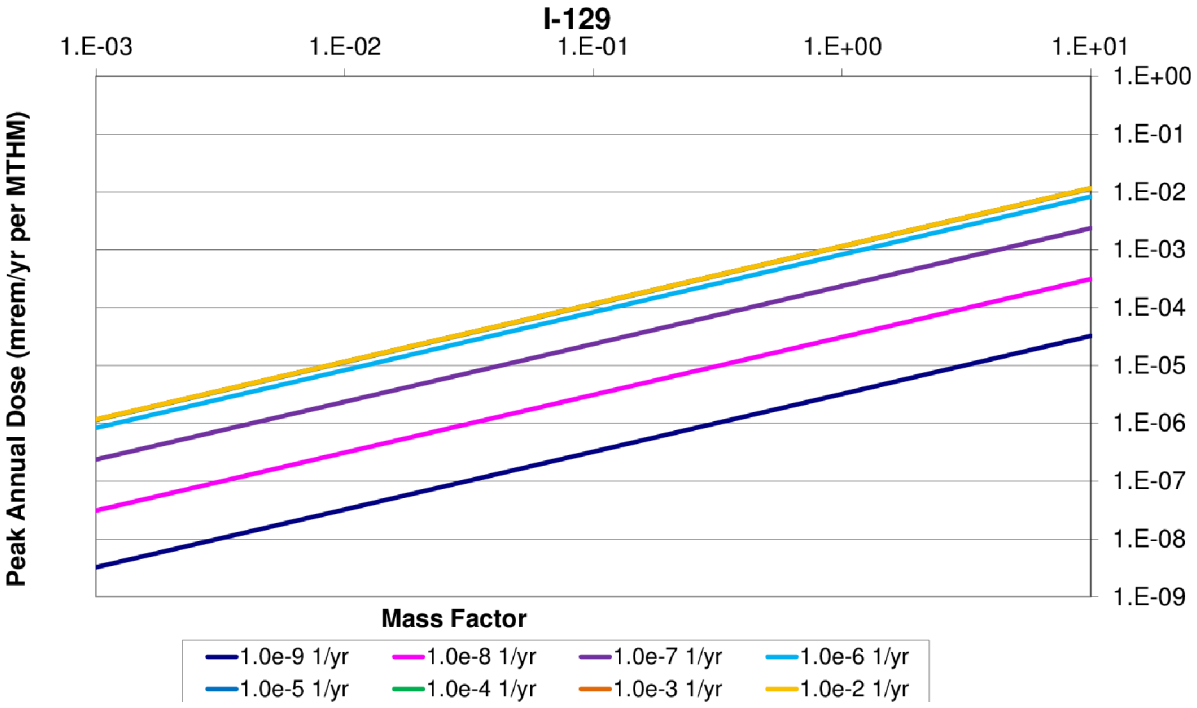

Figure 3-27. ^{129}I Inventory—Waste Form Degradation Rate Sensitivity

a) Fractional Degradation Rate

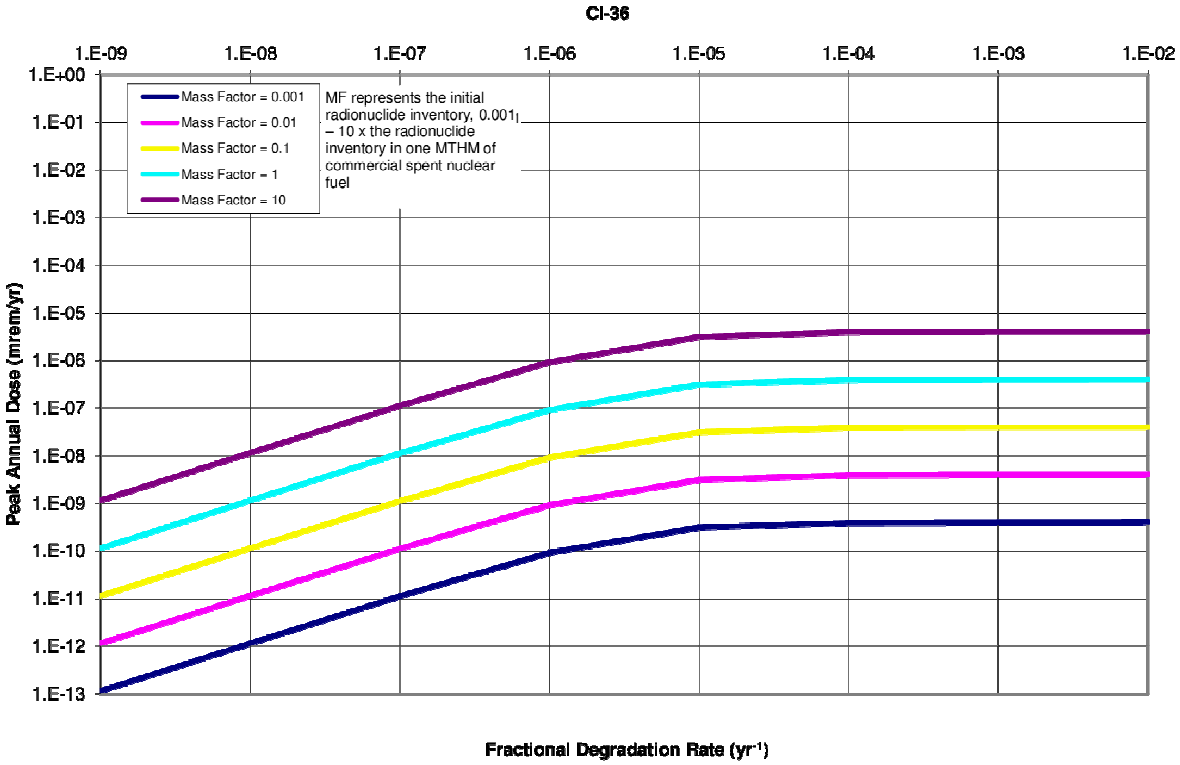

b) Inventory Sensitivity (Mass Factor)

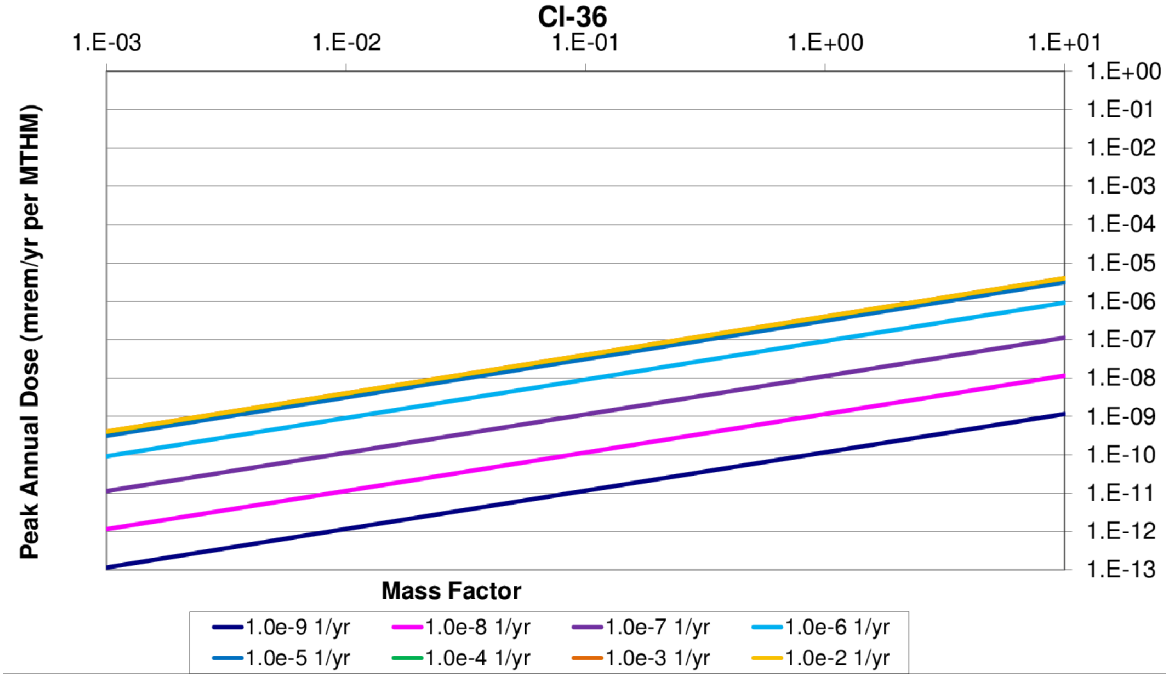

Figure 3-28. ^{36}Cl Inventory—Waste Form Degradation Rate Sensitivity

a) Fractional Degradation Rate

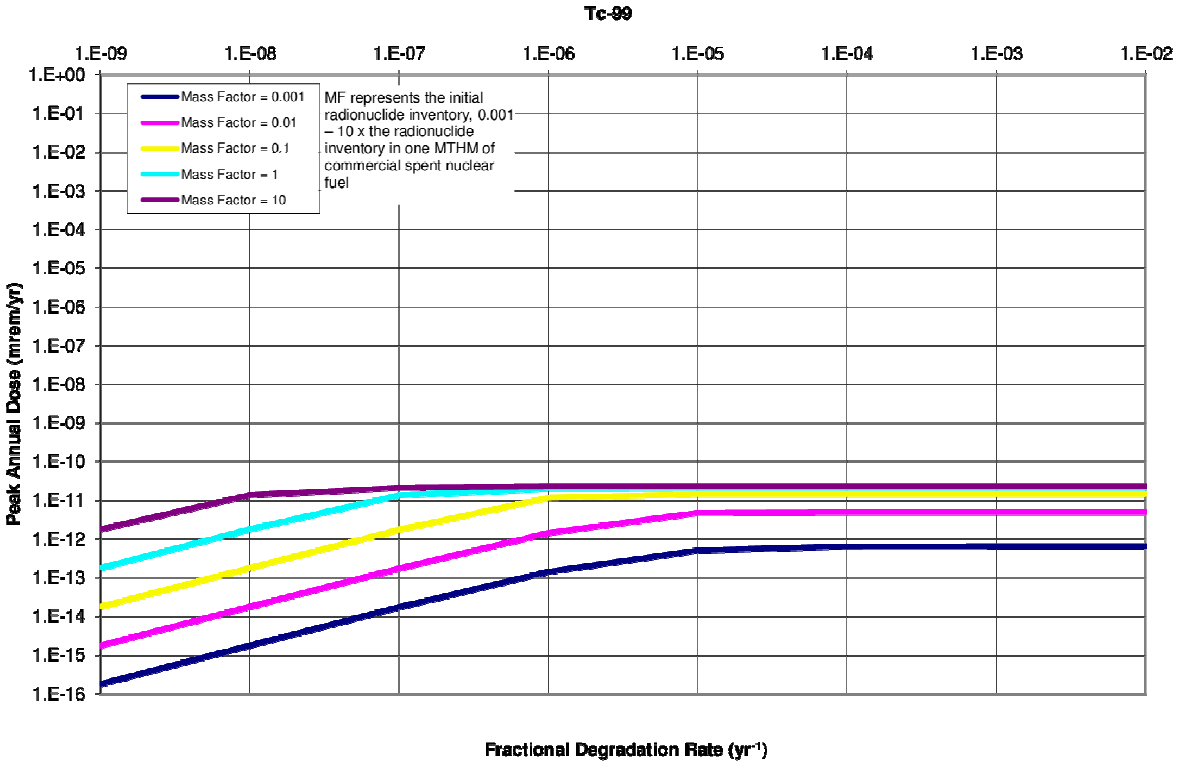

b) Inventory Sensitivity (Mass Factor)

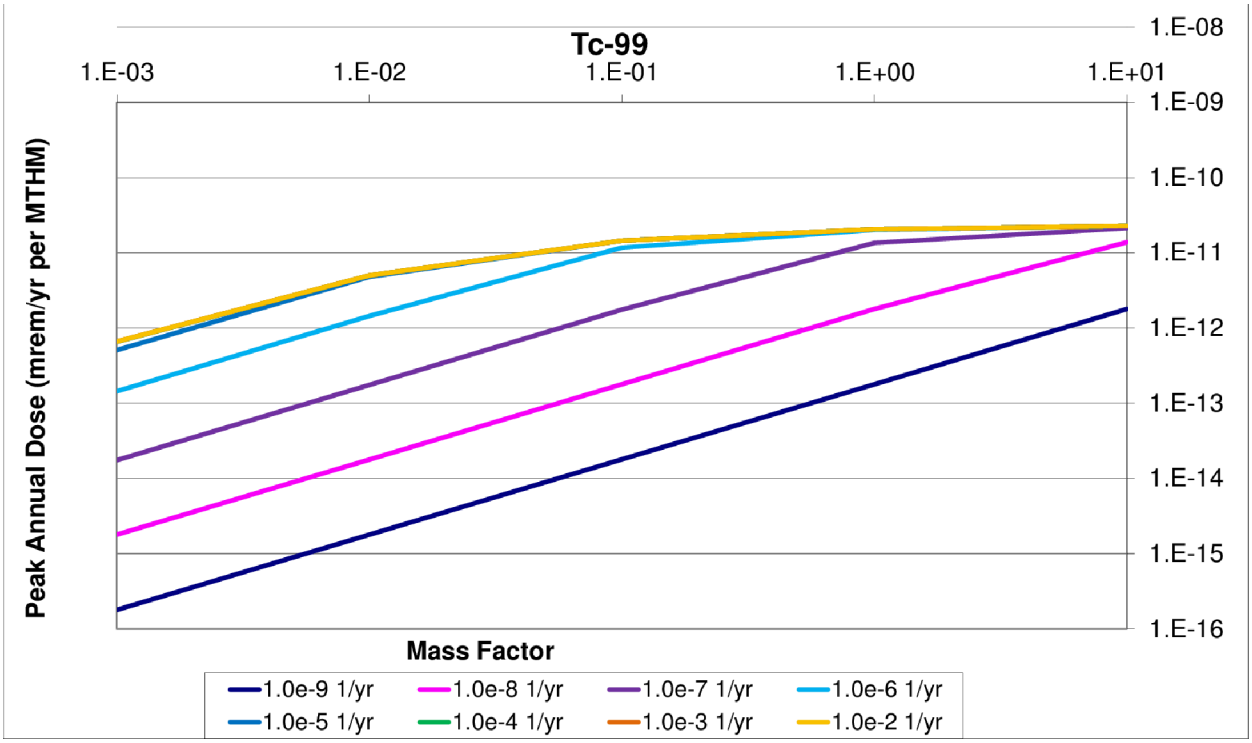

Figure 3-29. ^{99}Tc Inventory—Waste Form Degradation Rate Sensitivity

a) Fractional Degradation Rate

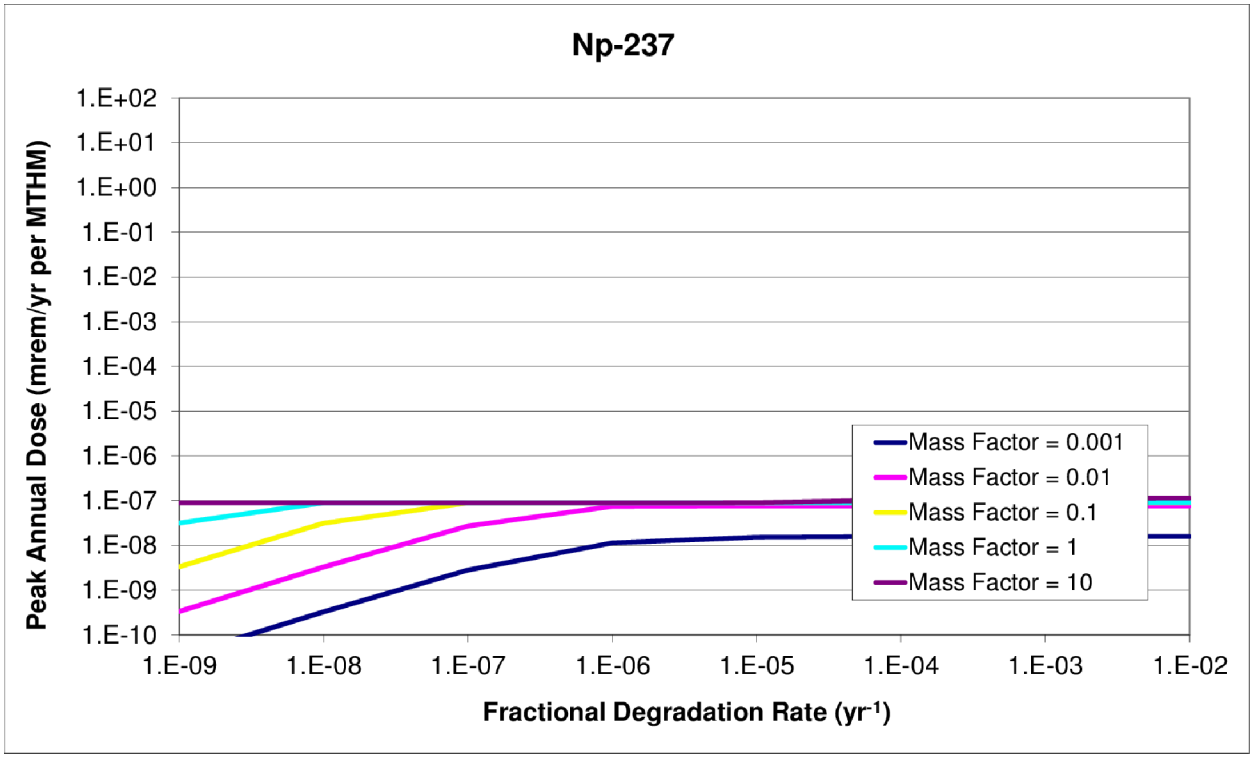

b) Inventory Sensitivity (Mass Factor)

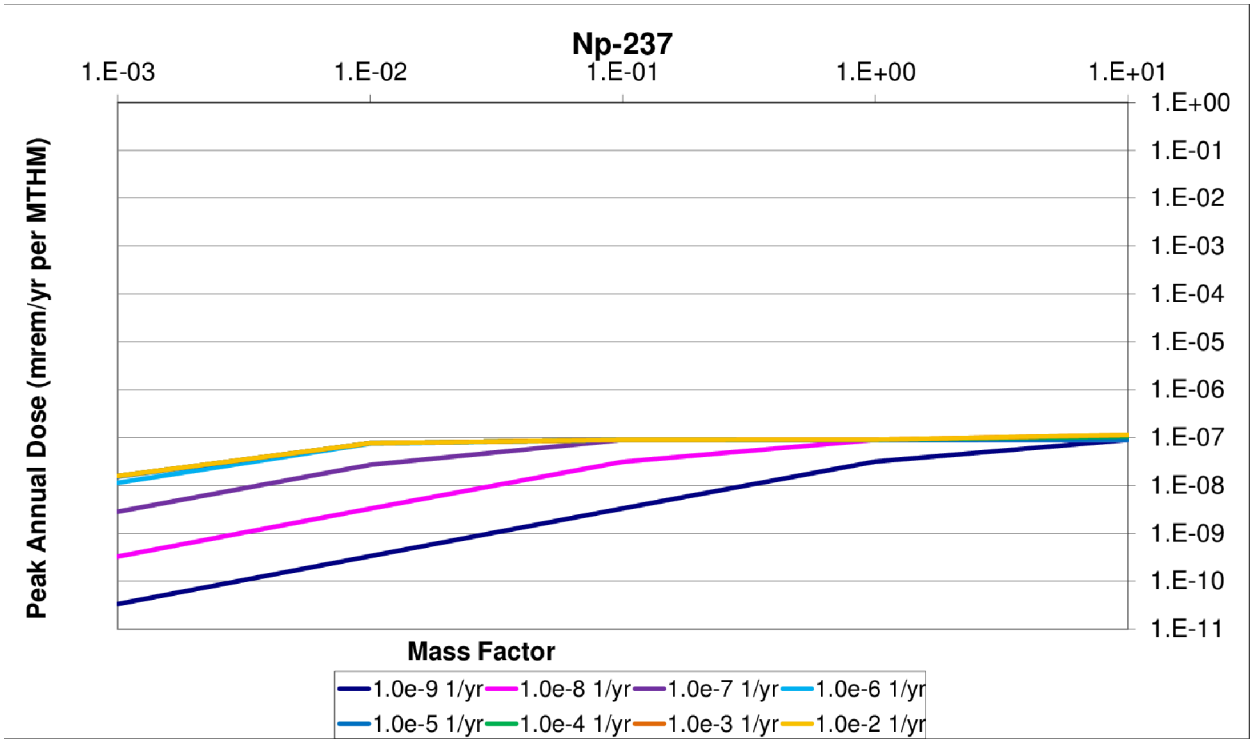

Figure 3-30. ^{237}Np Inventory—Waste Form Degradation Rate Sensitivity

3.3.2.6 Waste Package Failure Time

The time of waste package failure was not expected to greatly affect the magnitude of the mean of the peak doses except for cases in which waste package failure times exceeded the half-lives of dominant dose-contributing radionuclides. That is, since the dominant dose-contributing radionuclides for the reference case are quite long-lived (e.g., ^{129}I), all but the longest reasonable waste package containment lifetime is overwhelmed by the half-life of the dominant radionuclides. The long time scale of radionuclide release was expected to render the waste package lifetime irrelevant if it was shorter than a million years.

Though the model contains a unit-cell type waste package, it is possible to determine, in post-processing, the results of a simulation with temporally heterogeneous failures among waste packages. That is, by a weighted sum of the time histories of the no-fail case and the all-fail case, it is possible to mimic a time-varying failure among the many waste packages.

3.3.2.6.1 Parametric Range

To investigate the effect of the waste package failure time, it was varied over five magnitudes from one thousand to ten million years. Simultaneously, the reference diffusivity was varied over the eight magnitudes between 1×10^{-8} and 1×10^{-15} in order to determine the correlation between increased radionuclide mobility and the waste package lifetime.

3.3.2.6.2 Results

The results are shown in Figures 3-31 to 3-34 and demonstrate that for a generic clay environment repository performance is not affected by changes in the time that the waste package failures until the waste package failure times reach the million or ten million year time scale.

a) Relative Diffusivity

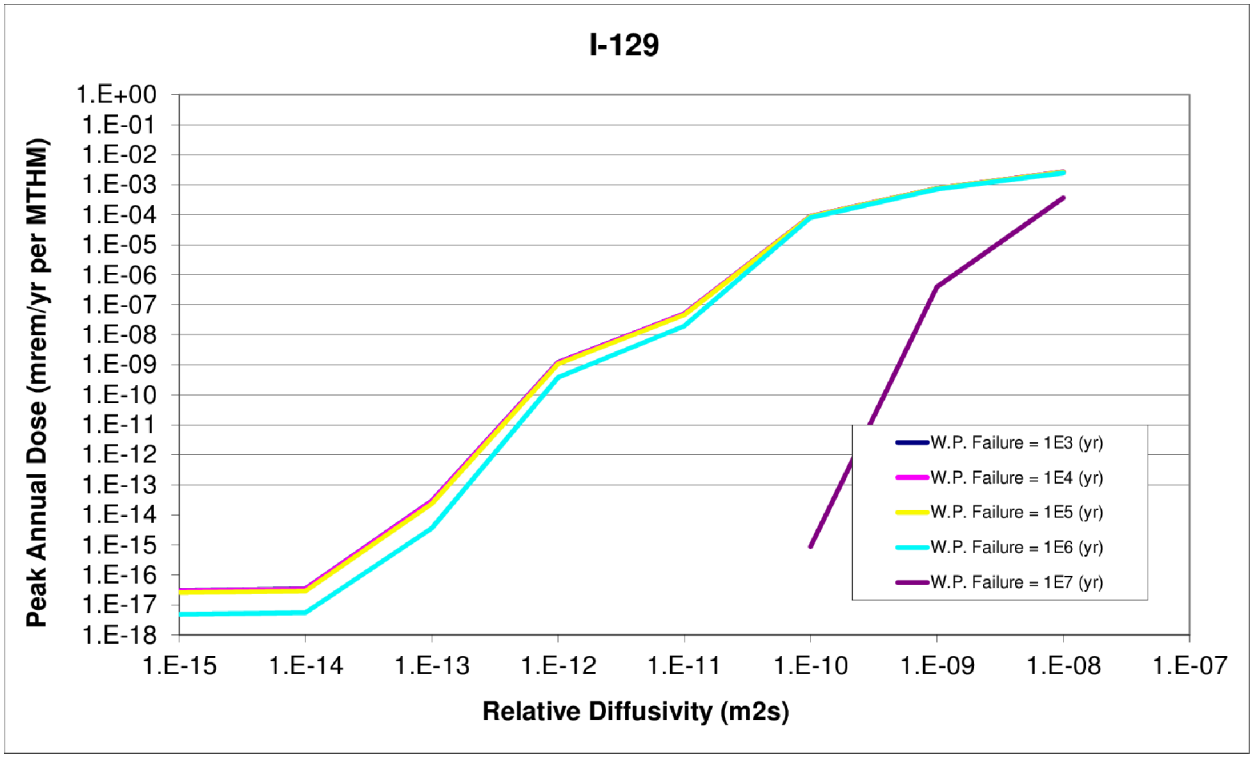

b) Waste Package Failure Time

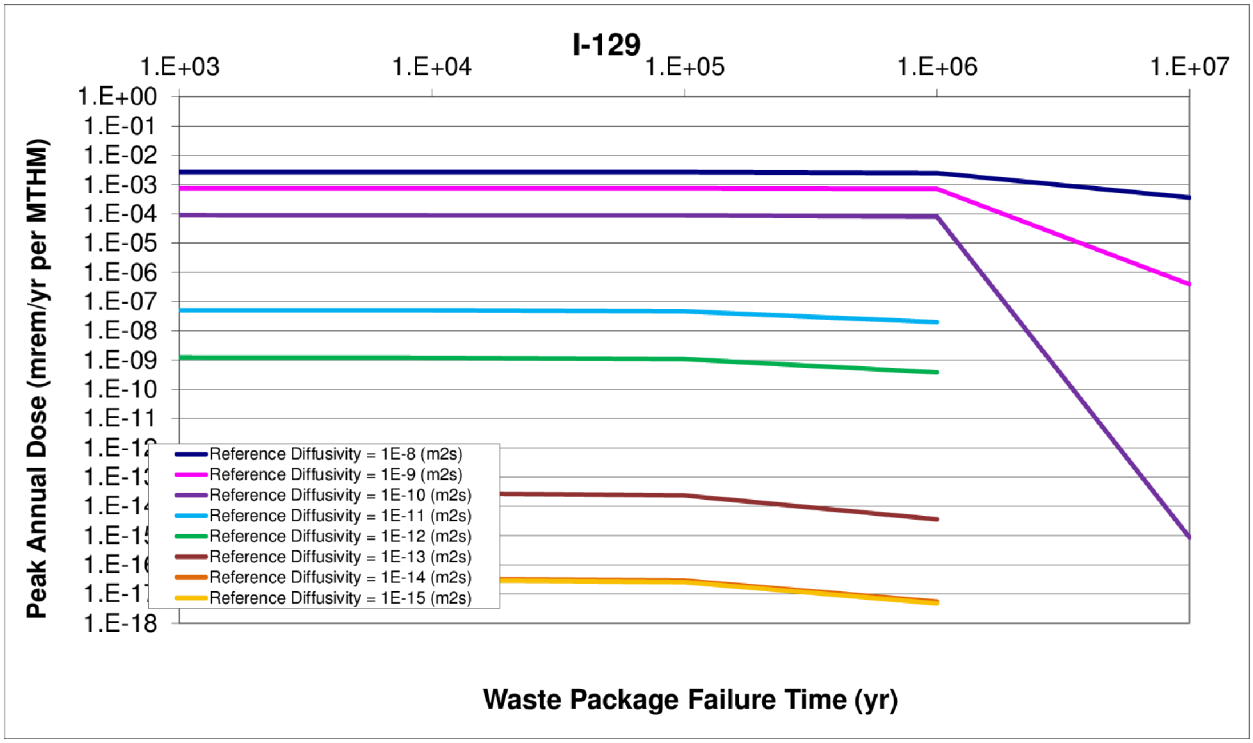

Figure 3-31. ^{129}I Diffusion—Waste Package Failure Time Sensitivity

a) Relative Diffusivity

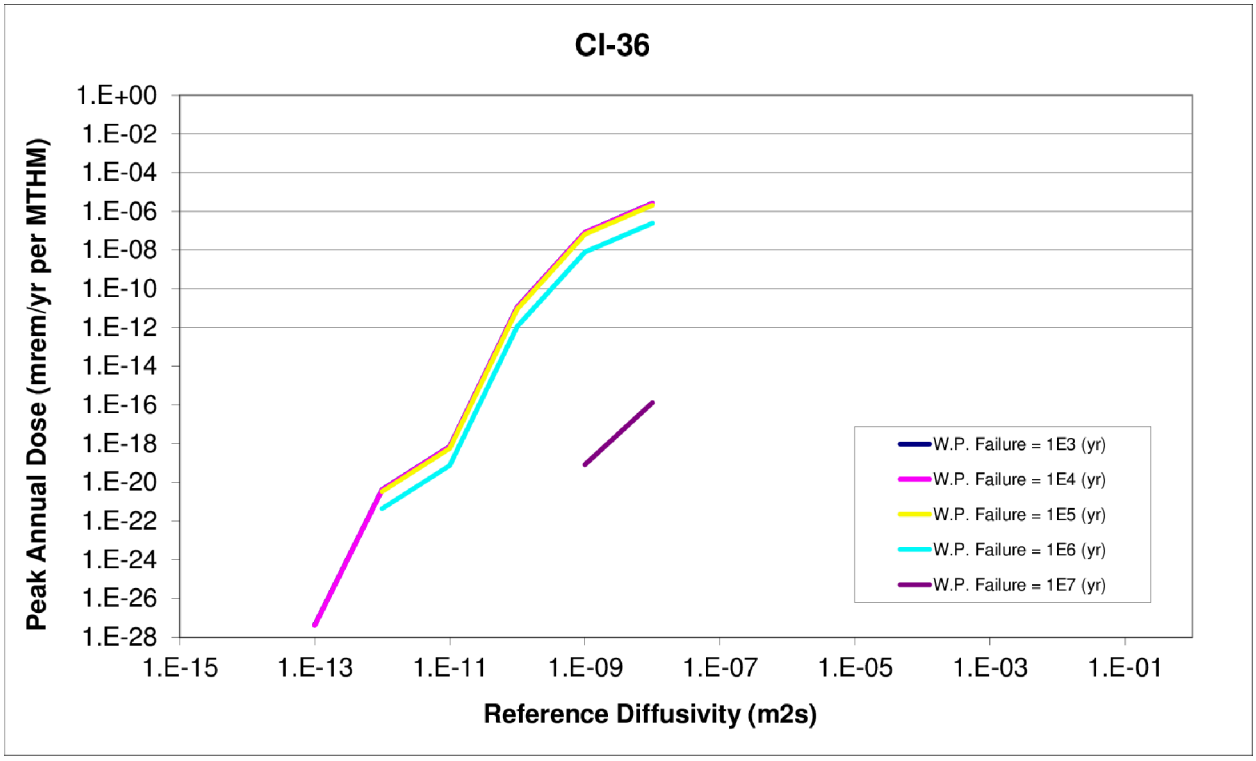

b) Waste Package Failure Time

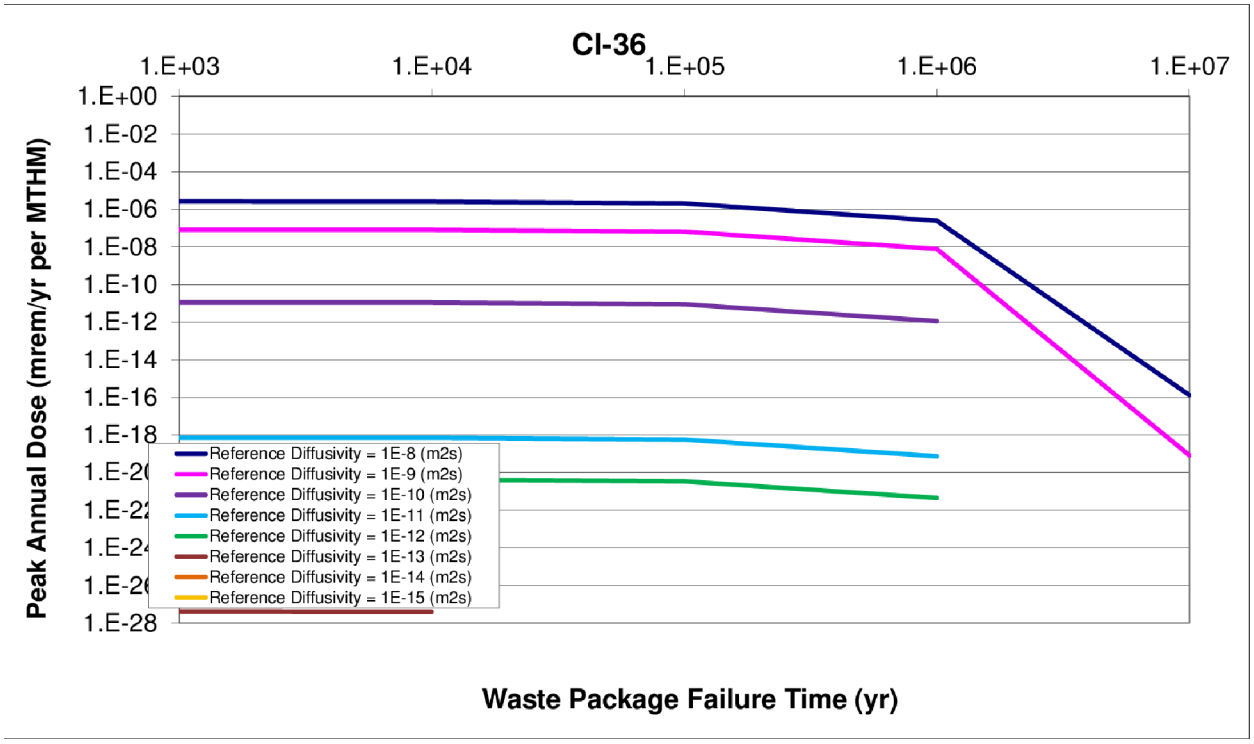

Figure 3-32. ^{36}Cl Diffusion—Waste Package Failure Time Sensitivity

a) Relative Diffusivity

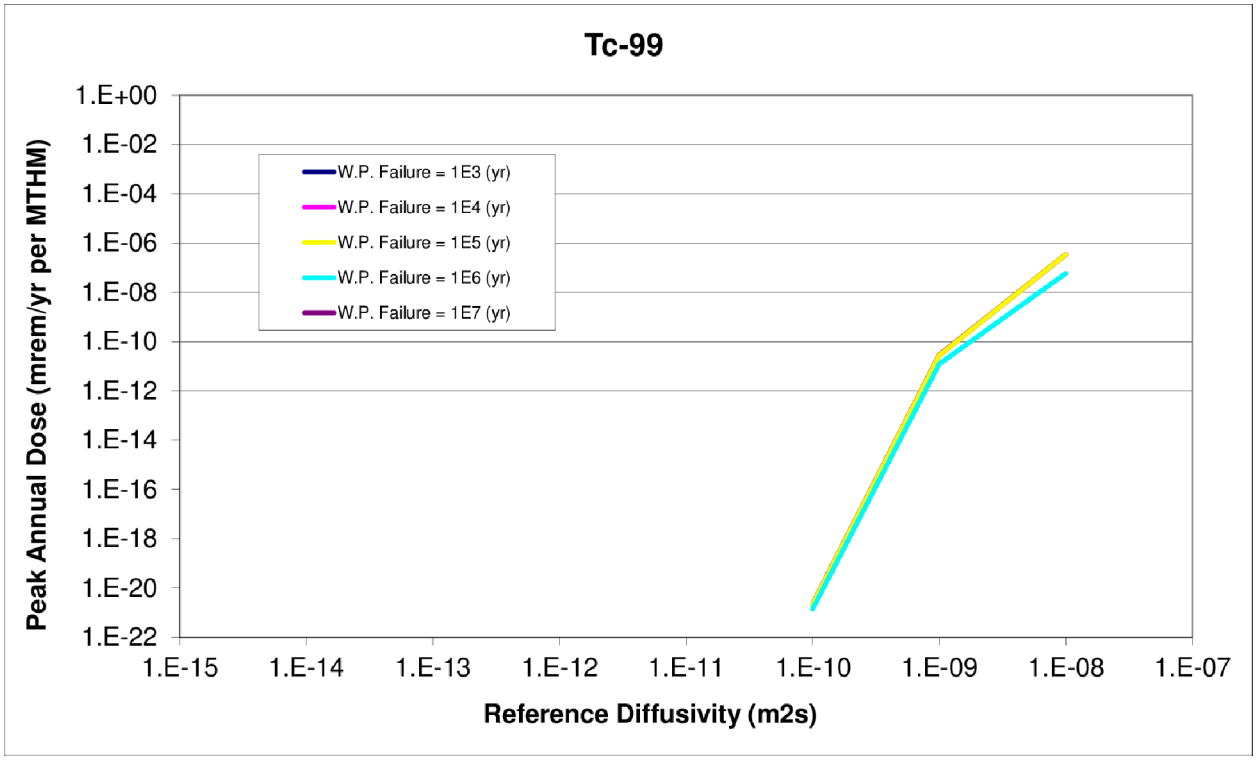

b) Waste Package Failure Time

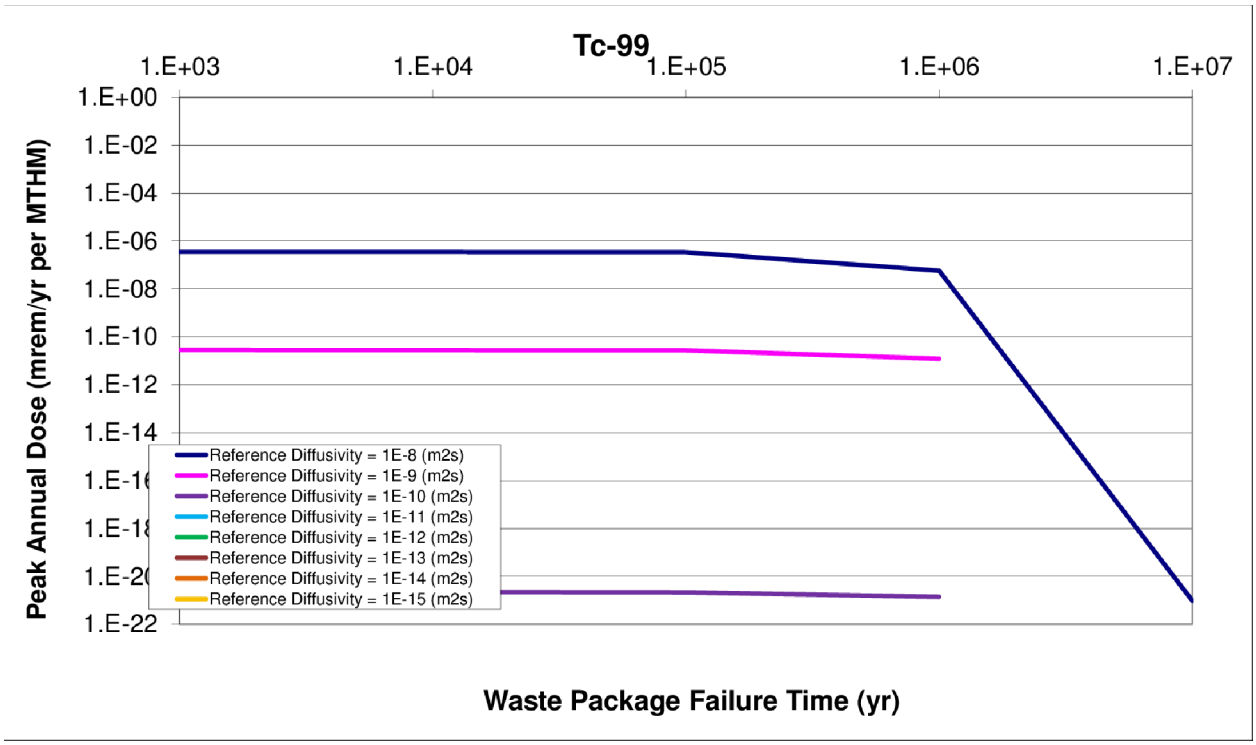

Figure 3-33. ^{99}Tc Diffusion—Waste Package Failure Time Sensitivity

a) Relative Diffusivity

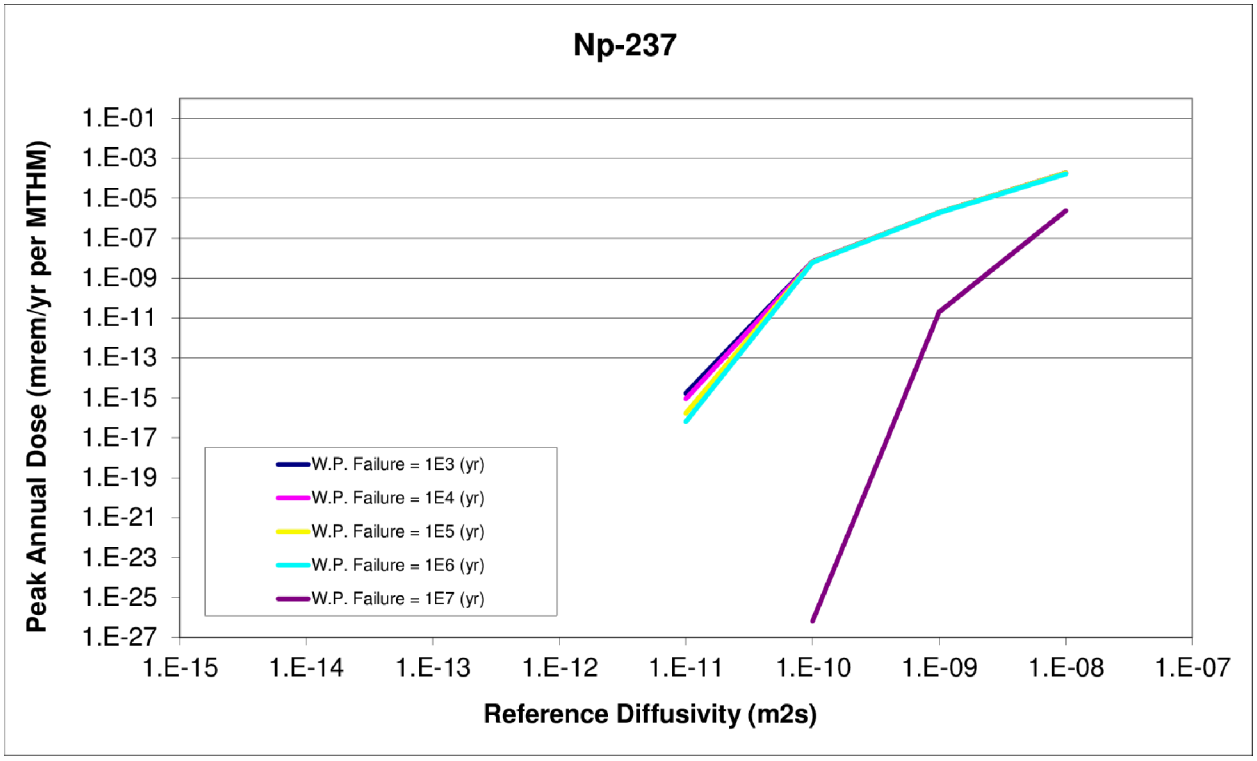

b) Waste Package Failure Time

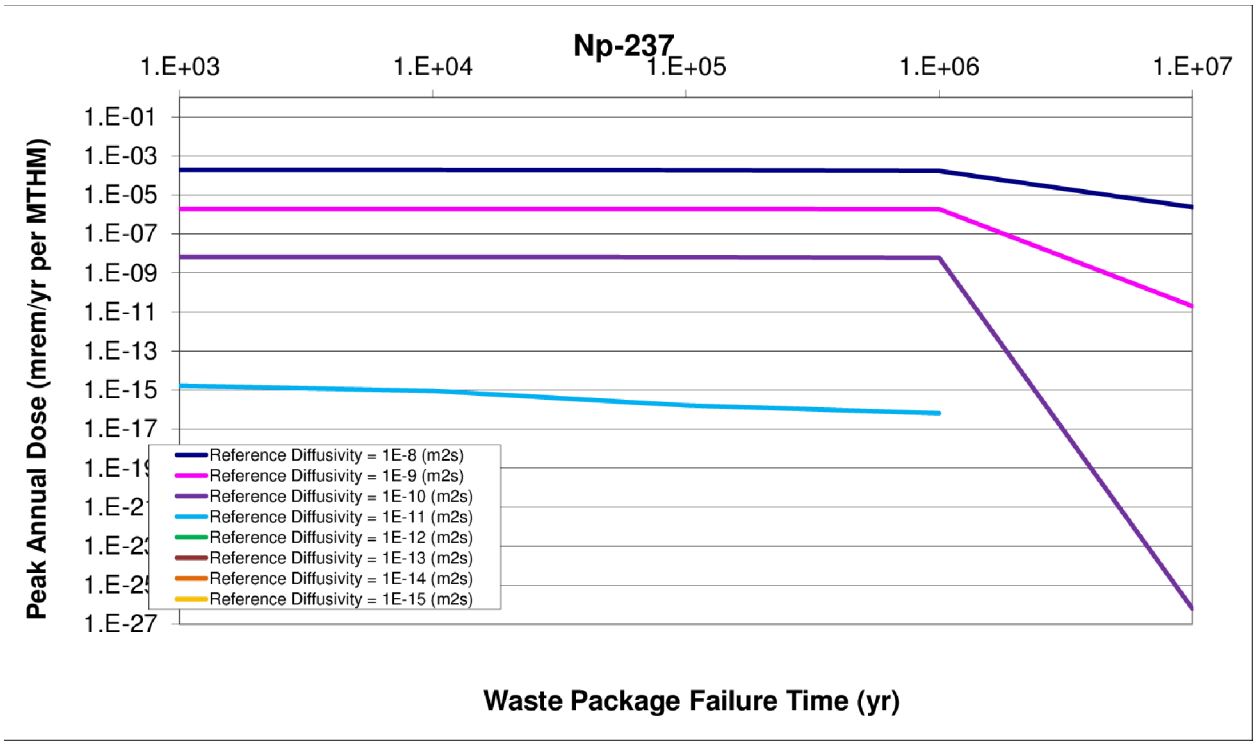

Figure 3-34. ^{237}Np Diffusion—Waste Package Failure Time Sensitivity

3.3.2.7 Vertical Path Length

The sensitivity of repository performance in a generic clay environment to the characteristics of a hypothetical advective vertical release pathway is examined in this section.

The model layout assumes that no vertical advective pathway intersects the waste packages. Rather, an optional vertical advective pathway with variable length can be modeled near the waste packages. This model feature addresses the concern that sufficient damage in the DRZ might provide a preferred horizontal pathway out of the confines of the repository that intersects a fast vertical pathway in which water flows advectively upward.

Comparing the effect of the length of the vertical advective path with the diffusion coefficient in the DRZ and the far field provides a notion of the importance of this release pathway. This analysis explores the effect of increasing the damage created by excavation, contributes to providing a higher source term at the base of a vertical advective pathway. In so doing, this analysis also provides some insight into the threshold between primarily diffusive and primarily advective contaminant movement.

3.3.2.7.1 Parametric Range

For each value of diffusion coefficient varied in the clay DRZ and far field clay, the vertical path length was varied from 10 to 500 m. Table 3-13 shows the sets of 100 realizations were run for each for vertical advective path length and diffusion coefficient in this dual sensitivity study.

Table 3-13. Simulation Groupings for Vertical Path Length Sensitivity Analysis

Reference Diffusivity (m^2/s)	Path Length				
	10	50	100	250	500
	Groupings				
1×10^{-8}	1	2	3	4	5
1×10^{-9}	6	7	8	9	10
1×10^{-10}	11	12	13	14	15
1×10^{-11}	16	17	18	19	20
1×10^{-12}	21	22	23	24	25
1×10^{-13}	26	27	28	29	30
1×10^{-14}	31	32	33	34	35
1×10^{-15}	36	37	38	39	40

3.3.2.7.2 Results

This analysis showed that varying advective pathway length within a reasonable range had negligible results on repository performance. It also showed that the importance of the length of the fast pathway was unaffected by reference diffusivities in the DRZ. That is, upon changing the reference diffusivity in those media simultaneously with the vertical advective pathway length, no effect was seen that could be attributed to variability in the advective path length. The only variability in the mean of the peak annual doses was due to changes in the diffusivity. For this reason it can be concluded that even in the case of significant damage to the DRZ, the dominant pathway in this scenario is the purely diffusive pathway rather than the vertical advective fast pathway.

3.4 Deep Borehole GDS Model

3.4.1 Model Description

The deep borehole GDS model used for the FY 2012 sensitivity simulations described in this section derives from the FY 2011 deep borehole GDS model (Clayton et al. 2011, Section 3.4). Disposal of radioactive waste in deep boreholes has been described in several recent publications and documents (Brady et al. 2009; Hadgu and Arnold 2010; Arnold et al. 2011a and 20011b; Swift et al. 2011; Lee et al. 2012; and Hadgu et al. 2012). The deep borehole concept consists of drilling boreholes into crystalline basement rocks to a depth of 5 km, emplacing waste canisters in the lower 2 km, and sealing the upper 3 km. The safety of deep borehole disposal is supported by low permeability and high-salinity in deep crystalline rocks, limited interaction of deep fluids with shallower groundwater, and geochemically reducing conditions at depth, which limit the solubility and enhance the sorption of many radionuclides.

A potential pathway for the release of radionuclides to the biosphere is up the borehole through the borehole seals and/or the DRZ around the borehole. Thermally driven flow provides the driving force to transport radionuclides upward to the biosphere via this pathway. The deep borehole GDS model consists of three zones, as shown in Figure 3-35:

- **Waste Disposal Zone—**The bottom 2 km of the 5-km-deep borehole where the waste is emplaced.
- **Seal Zone—**The 1-km length above the waste disposal zone, where robust sealing materials (e.g., bentonite, concrete) are placed.
- **Upper Borehole Zone—**The top 2 km of the borehole, where less robust sealing materials are placed. For modeling purposes, this zone is assumed to be connected to a surrounding aquifer. Any radionuclides that reach the top of the seal zone are assumed to enter the surrounding aquifer and are available to be pumped to the surface via a water supply well completed in the aquifer.

The FY 2012 GoldSim representation of the deep borehole GDS conceptual model is summarized in Table 3-14, with mapping to the GDSM conceptual model components (Figure 2-1). The 2012 deep borehole GDS model is unchanged from the FY 2011 deep borehole GDS model (Clayton et al. 2011, Section 3.4.2.2.1). Additional model details and input parameter values are found in Clayton et al. (2011, Section 3.4).

The thermally driven upward flow rates needed as input for the deep borehole GDS model were calculated external to GoldSim using a 3D TH flow model. The TH flow model and the resulting flow rates are described in Section 3.4.1.1.

Probabilistic sensitivity analyses, described in Section 3.4.2, were conducted using the FY 2012 deep borehole GDS model to gain insights into the important parameters contributing to total uncertainty.

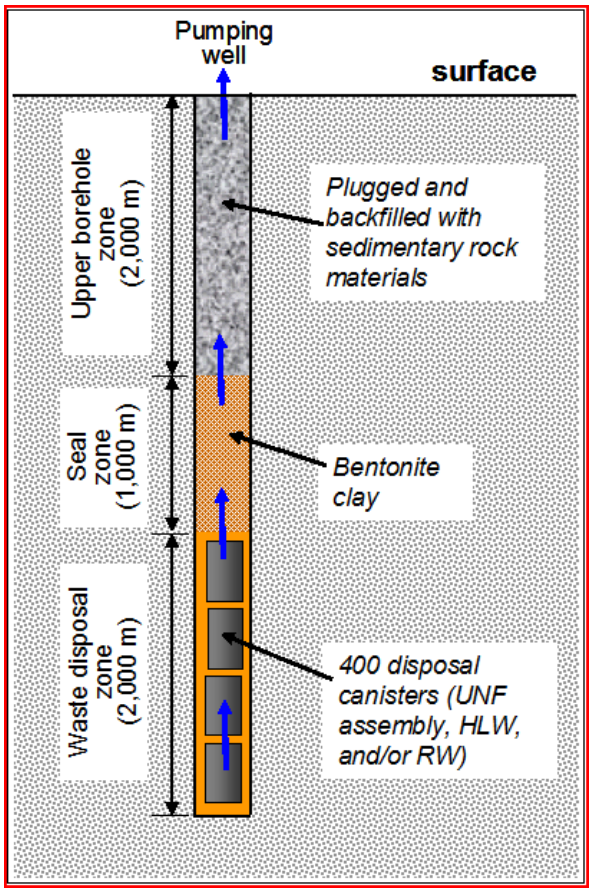

NOTE: RW = reprocessed waste

Figure 3-35. Schematic Illustration of Deep Borehole Disposal

Table 3-14. Deep Borehole GDS Model Components and Features

GDSM Component	GDSM Feature	Deep Borehole GDS Model
Source	Inventory	UNF
	Waste Form	UNF
Near Field	Waste Package	Waste Package
	Buffer / Backfill	Disposal Zone – Degraded Waste (2,000 m)
	Seals / Liner	Seal Zone - Bentonite (1,000 m)
	DRZ	included in Seals/Liner
Far Field	Host Rock	Not modeled
	Other Units	Aquifer (included in Biosphere)
Receptor	Surface / Biosphere	IAEA BIOMASS ERB1B (IAEA 2003)

3.4.1.1 Thermal Hydrology Simulation

The deep borehole GDS model uses vertical fluxes which are the output of external numerical TH simulations of the deep borehole disposal system (Hadgu et al. 2012). The geometry of the system consisted of an inner zone, representing combined borehole seal and DRZ properties with a single, equivalent permeability and a total cross sectional area of 1 m^2, surrounded by a low permeability host rock beyond the 1 m^2 cross-sectional area. The inner borehole seal and DRZ zone is termed the disturbed zone (DZ).

The TH simulations were conducted were conducted using the FEHM code (Zyvoloski et al. 1997; Zyvoloski 2007) for the disposal of a variety of UNF and HLW types. However, for this work only disposal of commercial UNF assemblies was considered. This TH model, and the parameter values used, are the same as were used to feed the FY 2011 deep borehole GDS model, documented in Clayton et al. (2011, Section 3.4.1.3.1). As shown in Table 3-15, five different DZ permeabilities were combined with each of four host rock permeabilities for a total of 20 different combinations. These 20 permeability combinations provide some additional detail beyond the combinations calculated in FY 2011; however, the bounding combinations remain the same.

Table 3-15. Host Rock and Disturbed Zone Permeability Values Used in TH Simulations

Host Rock Permeability (m^2)	**10^{-19}**	**10^{-18}**	**10^{-17}**	**10^{-16}**
Disturbed Zone Permeability (m^2)	10^{-15}	10^{-14}	10^{-13}	10^{-12}
	10^{-16}	10^{-15}	10^{-14}	10^{-13}
	10^{-17}	10^{-16}	10^{-15}	10^{-14}
	10^{-18}	10^{-17}	10^{-16}	10^{-15}
	10^{-19}	10^{-18}	10^{-17}	10^{-16}

Source: Hadgu et al. 2012.

Thermally driven flow was determined throughout a nine-borehole grid (3x3) with 200-m separation between boreholes. Figures 3-36 to 3-38 show vertical groundwater flux versus time at selected depths (3,000 m, 4,000 m, and 5,000 m) in a corner borehole of the nine-borehole grid for the 20 permeability combinations given in Table 3-15. In all cases the curve for the upper bounding case (rock permeability of 10^{-16} m^2 and DZ permeability of 10^{-12} m^2) is at the top, while the curve for the lower bounding case (rock permeability of 10^{-19} m^2 and DZ permeability of 10^{-19} m^2) is at the bottom, indicating that higher vertical fluxes are associated with higher permeability values. At 3,000-m depth, which corresponds to the top of the disposal zone, there is downward flow between about 2,000 and 10,000 years for the cases with the lower bound rock permeability of 10^{-19} m^2 (Figure 3-36). The downward groundwater flow results from cooling and the corresponding thermal contraction of groundwater. For the cases with the upper bound rock permeability, this effect is overcome by the broader pattern of upward thermal convection that occurs in the higher-permeability host rock and borehole. At 4,000-m depth, corresponding to the vertical center of the disposal zone, no downward flow is observed due to the location at the vertical center of the heat source (Figure 3-37). At 5,000-m depth (i.e., the bottom of the disposal zone) (Figure 3-38) flow patterns are similar as at 3,000-m depth, but with downward flow occurring at earlier time.

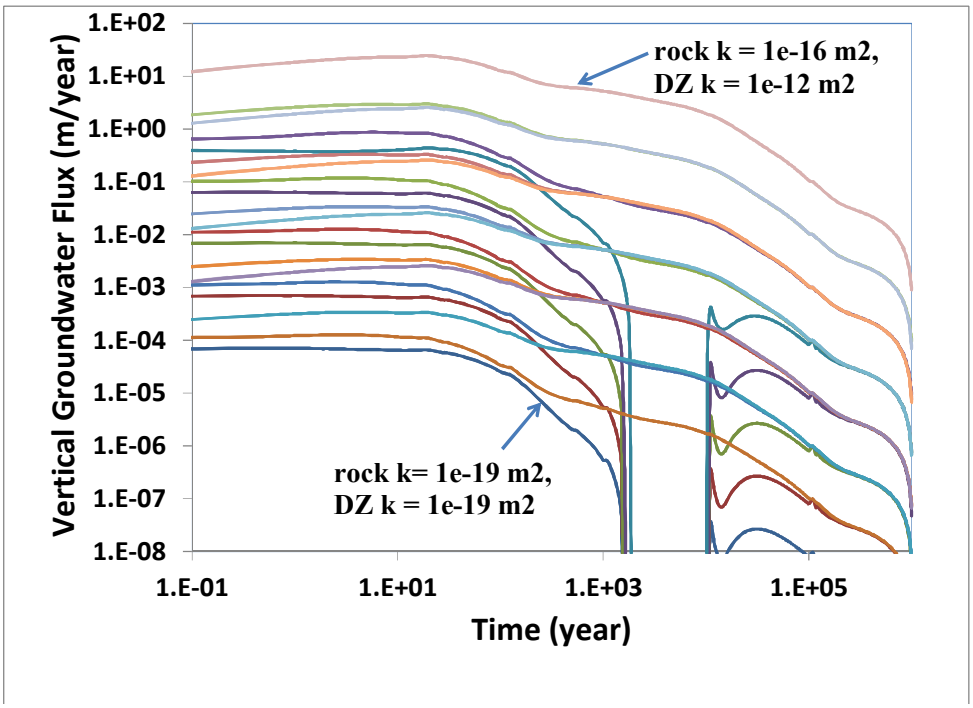

Figure 3-36. Vertical Groundwater Fluxes at Center of Corner Borehole at 3,000-m Depth as a Function of Time for all Permeability Combinations Considered

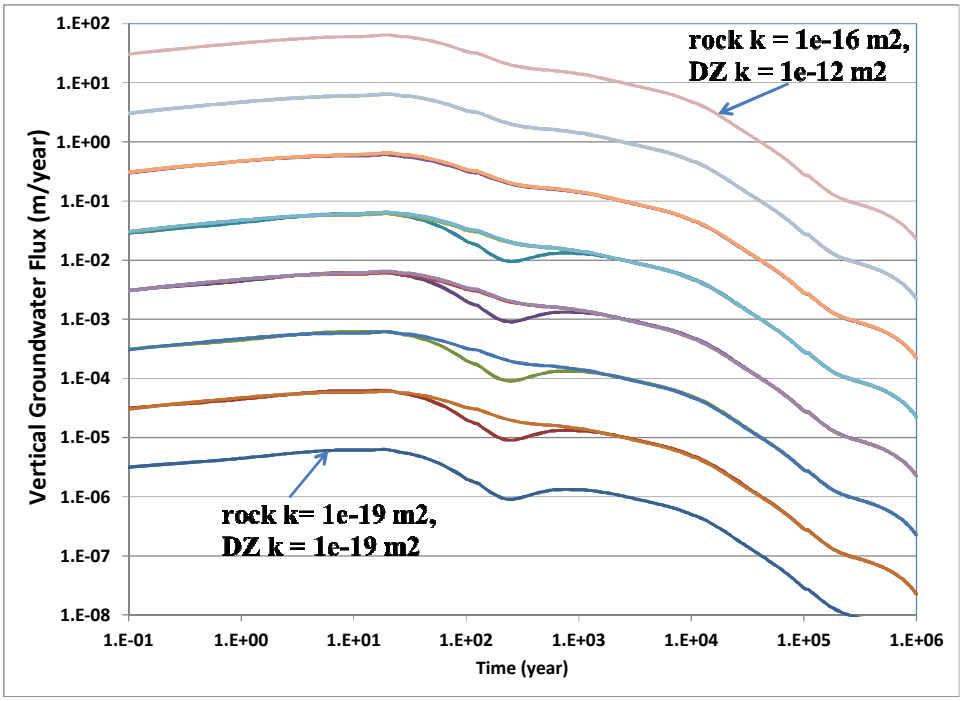

Figure 3-37. Vertical Groundwater Fluxes at Center of Corner Borehole at 4,000-m Depth as a Function of Time for all Permeability Combinations Considered

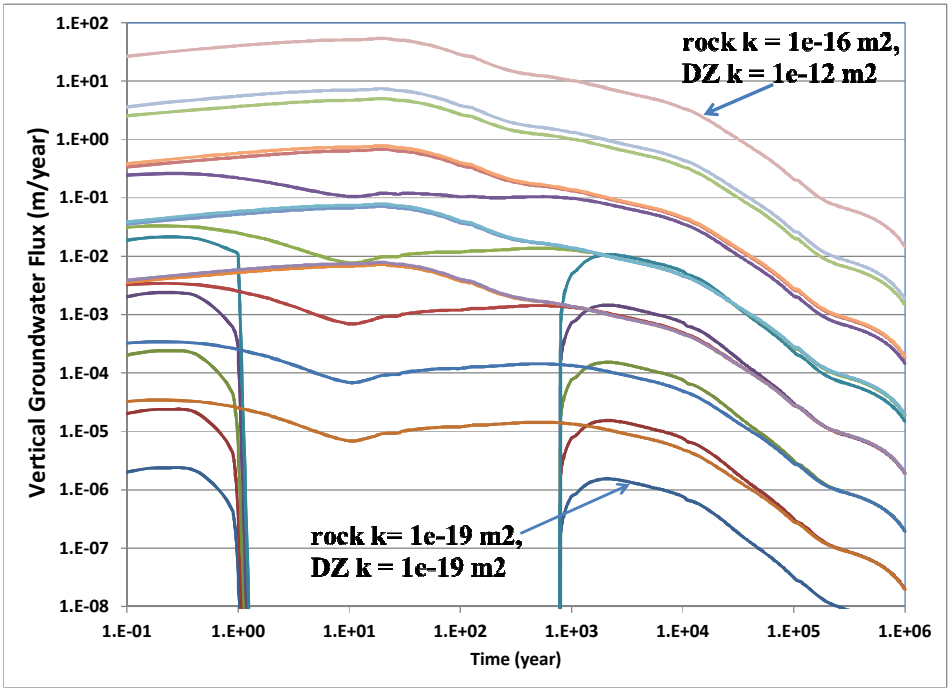

Figure 3-38. Vertical Groundwater Fluxes at Center of Corner Borehole at 5,000-m Depth as a Function of Time for all Permeability Combinations Considered

3.4.2 Probabilistic Sensitivity Analyses

3.4.2.1 Host Rock and Borehole Permeability

The deep borehole GDS model was run using a subset of the vertical groundwater flows calculated for each of the 20 combinations of host rock and borehole DZ permeabilities (Section 3.4.1.1). The other model parameter values were unchanged from those described in Clayton et al. (2011, Sections 3.4.1 and 3.4.2.2) for the model demonstration with commercial UNF inventory.

Monte Carlo simulations were carried out for a subset of the 20 permeability combinations given in Table 3-15. Latin Hypercube sampling was used for uncertain parameters with parameter distributions. The simulations were run to an assumed regulatory period of 1 million years and mean annual radiation doses were determined. Figure 3-39 shows the estimated total dose rate as a function of time for the selected permeability cases. The results provide an indication of the risk to human health associated with the range of representative values of permeability for the host rock and the disturbed zone. For the base case permeability values (rock permeability of 10^{-19} m^2 and DZ permeability of 10^{-16} m^2) radionuclide releases and dose rates at the surface are negligible. For the upper bounding permeability case (rock permeability of 10^{-16} m^2 and DZ permeability of 10^{-12} m^2) the simulated releases and dose rates correspond to a very small risk to human health. Figures 3-40 and 3-41 show mean dose rates of dominant radionuclides for the base and upper bound permeability cases. The simulations show that the non-sorbing radionuclides of iodine (^{129}I) and chlorine (^{36}Cl), and the mildly sorbing radionuclide technetium (^{99}Tc) account for most of the total dose.

An analysis was also made to evaluate the impact of sorption and retardation on dose risk from the dominant dose contributor, ^{129}I, due to its unlimited solubility, no sorption or very weak sorption, and extremely long half-life (1.57×10^7 years). One approach to mitigate the potential release of ^{129}I is to load

the seal materials with an effective sorbent for iodine. Simulations were conducted to evaluate potential impacts of iodine sorbent (getter) loaded in the seal zone on the deep borehole model performance. The simulations were performed for the upper bounding permeability case because it yields the higher peak mean doses (Figure 3-39). The impact was analyzed with the use of a linear sorption (K_d) model for Iodine with a sorbent included in the seal material. The K_d values used for Iodine sorption were based on the best estimate from an on-going research (Krumhansl et al. 2011). The dose results for the upper bound permeability case with an Iodine getter are shown in Figures 3-39 and 3-41. The results indicate that use of proper Iodine sorbents could significantly reduce the peak dose.

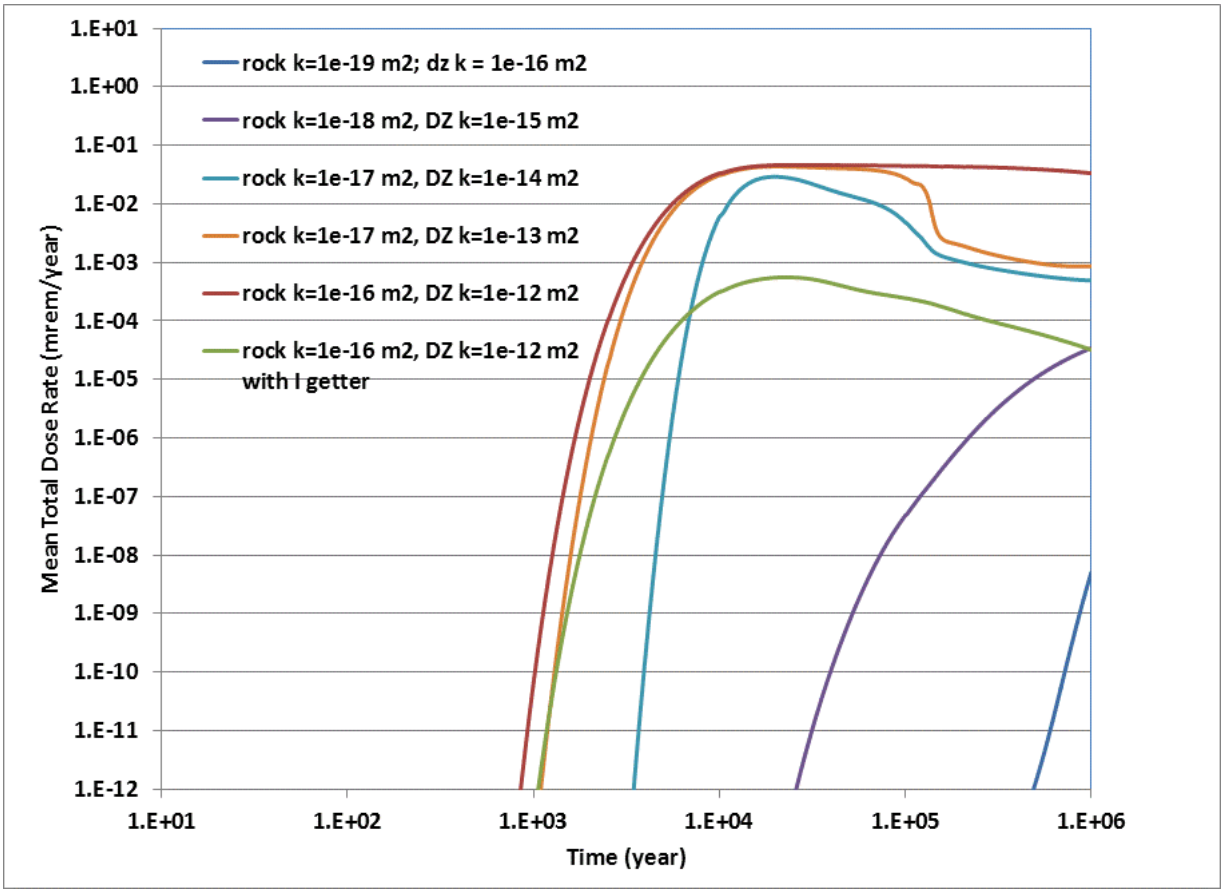

Figure 3-39. Mean Total Dose for Various Rock and Disturbed Zone Permeability Cases

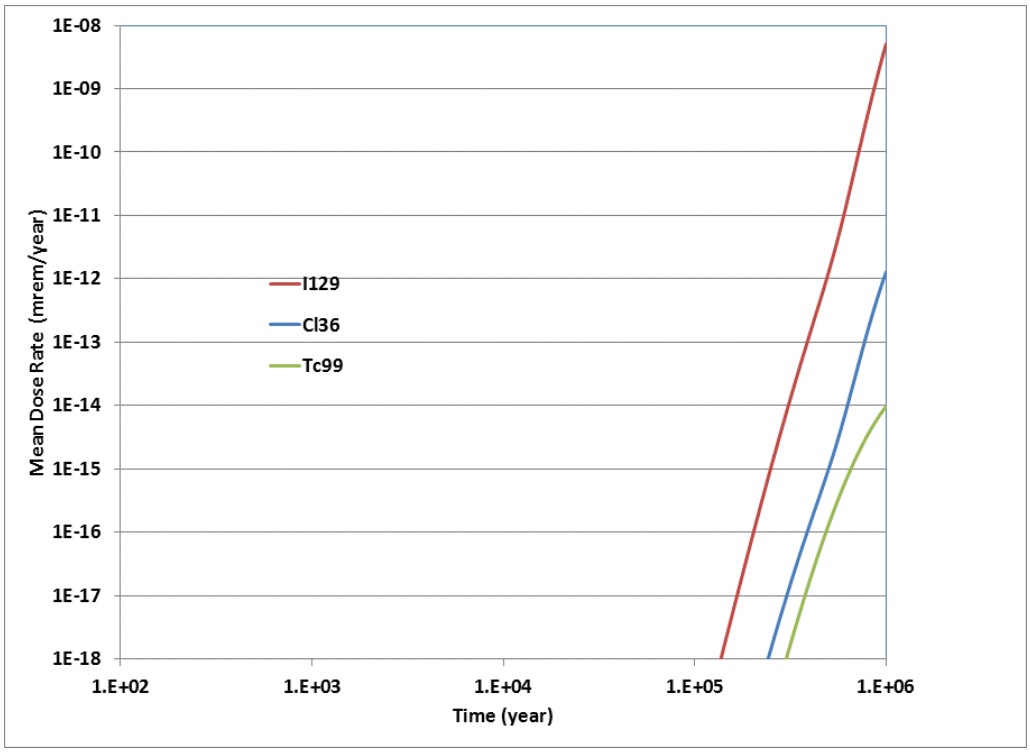

Figure 3-40. Mean Dose for Dominant Radionuclides for the Base Case Rock and Disturbed Zone Permeability Values

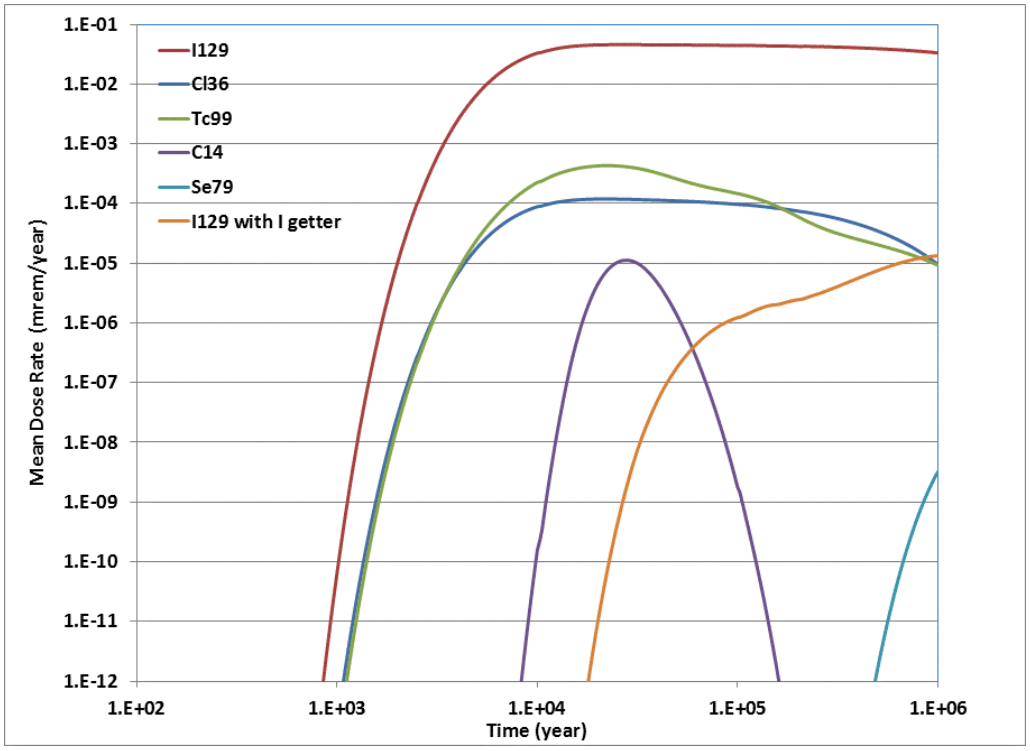

Figure 3-41. Mean Dose for Dominant Radionuclides for the Upper Bounding Case Rock and Disturbed Zone Permeability Values and the Iodine Getter Case

3.4.2.2 Sensitivity and Uncertainty Analysis

A sensitivity analysis was also conducted to determine the contributions of individual uncertain input parameters to the total uncertainty, for each DZ and host rock permeability combination used in Section 3.4.2.1. Partial rank correlation coefficients were computed for total dose as a function of time and a stepwise rank regression analysis was performed at 1 million years to confirm the results.

3.4.2.2.1 Sensitivity Analysis Including Permeability Uncertainty

Results (excluding the case with the use of iodine sorbent) have been assembled to include the effect of rock and disturbed zone permeabilities on total dose thru the use of a pointer parameter PERMEA. For the purpose of illustration, we have considered that each of the scenarios were equally likely and associated an integer to each of them: 1 represents the base case (rock permeability of 10^{-19} m^2 and DZ permeability of 10^{-16} m^2). Numbers 2 to 5 have been associated to the four variations ordered by increasing permeability. As rock and disturbed zone permeability vary together, they have been associated with one common indicator function named PERMEA. Thus PERMEA is treated as an uncertain parameter described by a uniform distribution of values between 1 and 5, inclusive. (Note: that the Latin hypercube sampling structure when incorporating the new variable (PERMEA) is preserved since all the other parameters treated with uncertainty are the same for each of the 5 possible values of PERMEA.)

Figure 3-42 displays the partial rank correlation coefficient over time for total dose. As expected, the pointer parameter to permeability (PERMEA) and the parameter for waste form degradation (WFDegRat) are the two most important parameters. Permeability plays a more important role because vertical groundwater flux is a strong function of rock and disturbed zone permeability values (Figures 3-36 to 3-38). The results for waste form degradation are also expected as iodine is the major contributor to the total dose and waste form degradation rate is the only uncertain input parameter that affects iodine (Figure 3-42). Figure 3-42 also includes other less important parameters, which are sorption (K_d) input parameters for technetium and selenium in different borehole zones (TcKdSZ, TcKdDZ, SeKdSZ, SeKdDZ, respectively).

A stepwise rank regression analysis was also performed at 1 million years. The results, shown in Table 3-16, are consistent with the findings of the partial rank correlation coefficient analysis (Figure 3-42) with permeability variation explaining about 88% of the variance, while waste form degradation rate explains 8% more.

Table 3-16. Stepwise Rank Regression Analysis over Total Dose at 1 Million Years, for Combined Results Including Uncertainties in Rock and DZ Permeability Values

Variable Name	R^2	R^2 Contribution	Stepwise Rank Regression
PERMEA	0.878	0.878	0.9656
WFDegRat	0.961	0.084	0.2905

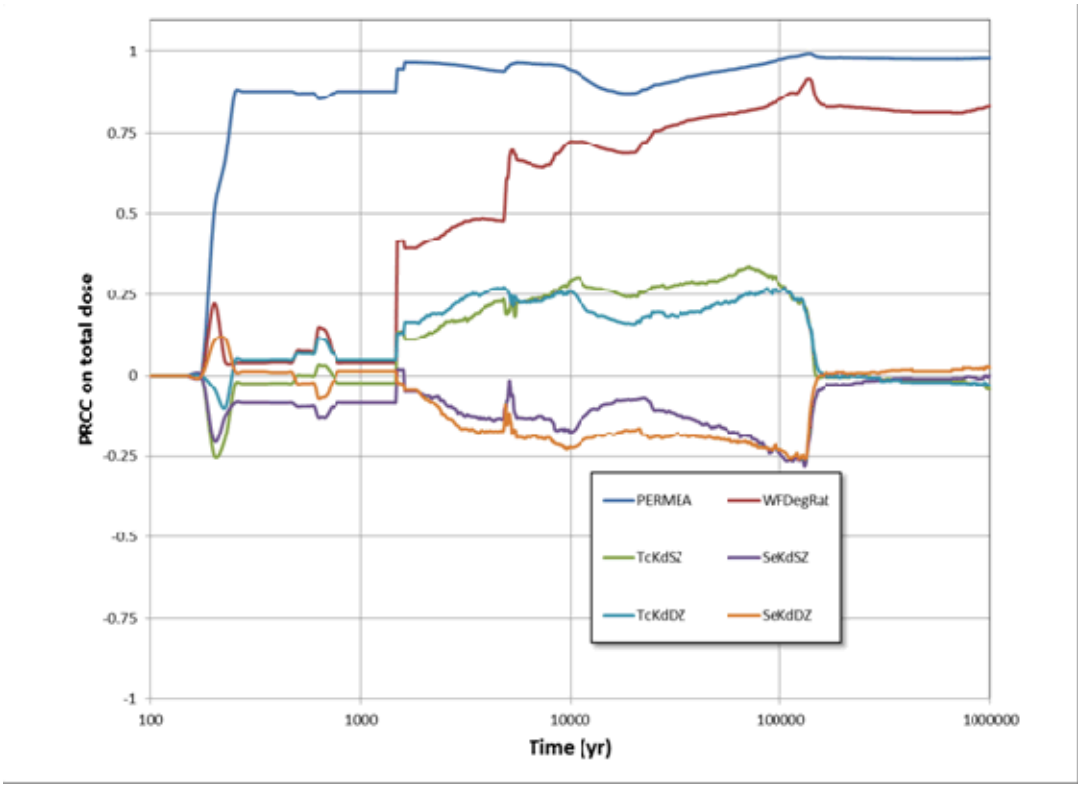

Figure 3-42. Partial Rank Correlation Coefficients on Total Dose over Time including Uncertainties in Rock and DZ Permeability Values

3.4.2.2.2 Sensitivity Analysis Excluding Permeability

The sensitivity analysis presented in Section 3.4.2.2.1 was repeated without treating permeability as uncertain in order to observe the influence of the other relevant uncertain parameters. This analysis looked at simulation cases with and without iodine sorption, shown in Figure 3-39.

For the simulation cases without iodine sorption, the waste form degradation rate parameter (WFDegRat) was the dominant parameter and thus was responsible for almost all of the variance in dose. Again, this is in line with the fact that iodine is the major contributor to the total dose, and waste form degradation rate is the only uncertain input parameter that affects iodine.

When iodine getter (sorbent) is used in the seal zone, iodine contribution to dose is reduced as shown in Figure 3-41. This leads to the increase in contribution of radionuclides such as technetium to total dose. As a result, as shown in Table 3-17, stepwise regression analysis of dose at the 1 million years shows the influence of other parameters besides waste form degradation rate (WFDegRat). These parameters are iodine getter sorption in the Seal Zone (IGETKdSZ), technetium sorption in the Upper Zone (TcKdUZ), and technetium solubility in the Disposal Zone (TcSolDZ).

Table 3-17. Stepwise Regression Analysis over Total Dose at 1 Million Years with Iodine Getter (Sorbent) and for the Upper Bounding Case Rock and DZ Permeability Values

Variable Name	R^2	R^2 Contribution	Stepwise Rank Regression
WFDegRat	0.301	0.301	0.5624
IGETKdSZ	0.457	0.155	-0.4147
TcKdUZ	0.528	0.071	-0.2695
TcSolDZ	0.582	0.054	0.2377

The corresponding variation of partial rank correlation coefficients over time is shown in Figure 3-43. The parameter waste form degradation rate (WFDegRat) is the most important parameter earlier in time but its importance is slightly reduced over time, and the importance of other parameters increases. These parameters include sorption (K_d) and solubility (Sol) input parameters for Technetium in the three borehole zones (TcKdUZ, TcKdSZ, TcSolDZ), and presence of Iodine getter in the Seal Zone (IGETKdSZ). Sorption (K_d) for Carbon is also shown in Figure 3-43 but is likely due to spurious correlation (considering that the dose contribution of Carbon in the simulation estimates is about zero).

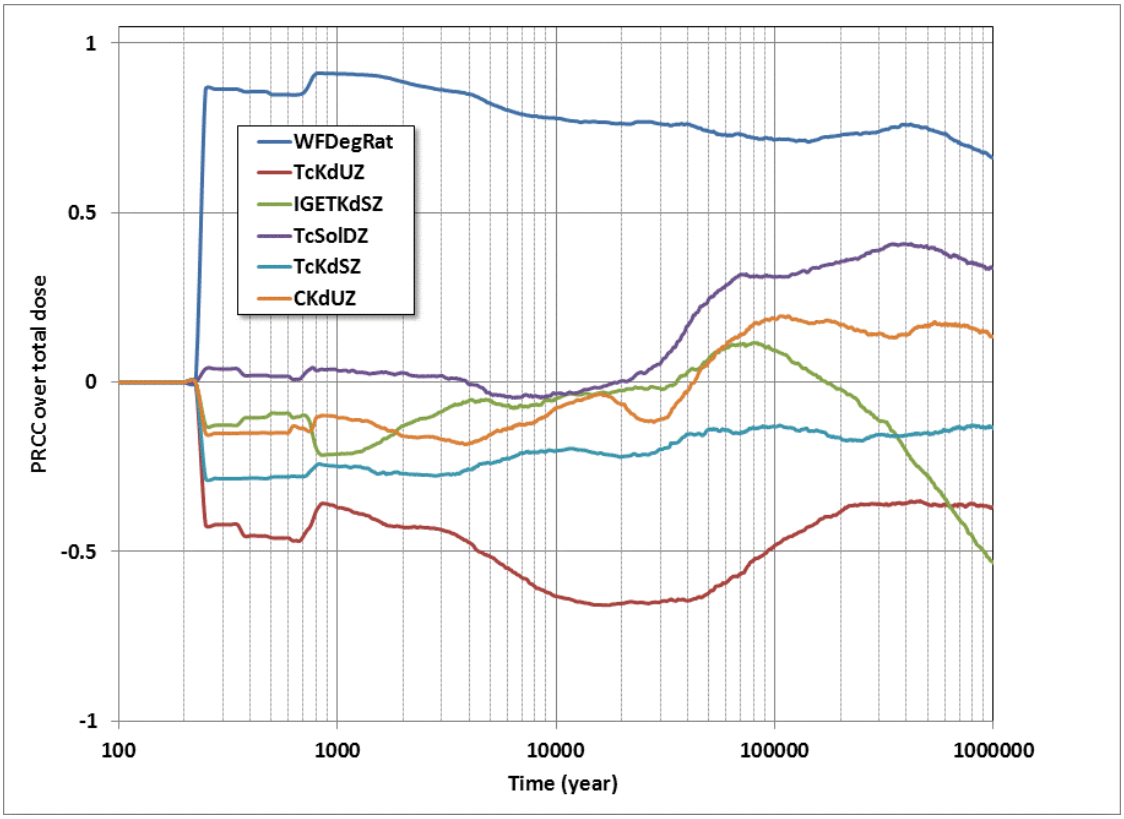

Figure 3-43. Partial Rank Correlation Coefficients on Total Dose Over Time with Iodine Getter and for the Upper Bounding Case Rock and Disturbed Zone Permeability Values.

3.5 Deterministic GDS Safety Assessments

A set of preliminary postclosure safety assessments were conducted to evaluate the behavior of the four generic deep geologic disposal options. These safety assessments support an effort within the UFDC to develop a generic deep geologic disposal safety case. Each of the four GDS safety assessments was performed within the common GDSM conceptual architecture (Figure 2-1) using modified versions of the GDS models described in Sections 3.1 through 3.4 and GoldSim as the implementing framework.

For each GDS model, deterministic simulations were performed for a generic baseline scenario. The baseline scenarios include waste form and waste package degradation, radionuclide mobilization, and advective and diffusive aqueous-phase transport through the EBS and NBS components under undisturbed conditions. The baseline scenarios also include the effects of defective waste packages, where appropriate. The effects of defective waste packages tend to enhance radionuclide transport, due to the early onset of waste from degradation and early-time radionuclide release.

For each GDS baseline scenario model, the following deterministic simulations were performed:

- **Baseline Analysis—**A single deterministic simulation of the baseline scenario. Each uncertain parameter (i.e., those parameters defined by a distribution in the probabilistic models) was represented by its mean value.
- **Sensitivity Analyses**—A set of "one-off" deterministic simulations. A single uncertain parameter value was varied from the baseline mean value in each simulation.

Some modifications were made to the GDS models for the deterministic application and to provide increased consistency across the four disposal options. These modifications are described in Section 3.5.1. The deterministic baseline analysis results are presented in Section 3.5.2. The sensitivity analysis results are presented in Section 3.5.3.

3.5.1 Model Descriptions

The bases for each of the four individual deterministic GDS models are the model descriptions in Sections 3.1 through 3.4, with further details provide in Clayton et al. (2011, Section 3). Specific details of each of the GDS baseline scenarios and deterministic models are summarized in the following subsections. The following common changes were made to all GDS models to provide for more consistency:

- The waste inventory for each of the three mined disposal options assumed a repository capacity of 70,000 MTHM. The entire 70,000 MTHM radionuclide inventory was assumed to be commercial UNF, specifically PWR fuel with a burn-up of 60 GWd/MTHM and 4.73% enrichment aged 30 years after discharge from a reactor (Carter and Luptak 2010, Table C-1). The 70,000 MTHM UNF inventory was assumed to be contained in 16,000 waste packages, with each waste package containing 10 PWR assemblies. For deep borehole disposal the repository capacity affects the total number of boreholes required (approximately 400 boreholes would be required to dispose of 70,000 MTHM), but does not affect the conceptualization of an individual borehole. A discussion of the radionuclide makeup of 70,000 MTHM model inventory is presented in Appendix C.
- The fractional waste form degradation rate for each of the four disposal options was assumed to be 2×10^{-5} yr^{-1}, which is the baseline value from the FY 2011 clay GDS model (Clayton et al. 2011, Section 3.3.3.3.2). At this fractional rate, 50% of the radionuclide mass is released from the waste form in the first 35,000 years, 95% of the mass is released by 150,000 years, and 99.9% of the mass is released by about 350,000 years. A slower fractional degradation rate of 1×10^{-7} yr^{-1}, consistent with the salt, granite and deep borehole GDS models, was examined as part of the sensitivity analyses.
- Simulations were run to 10,000,000 years and used consistent time stepping for the purpose of investigating performance out to peak dose, independent of potential regulatory time criteria.

3.5.1.1 Deterministic Salt GDS Model

The deterministic salt GDS safety assessment model derives from the FY 2011 salt GDS model (Clayton et al. 2011, Section 3.1) and is consistent with the FY 2012 salt GDS model described in Section 3.1. The salt baseline scenario includes transport through the near-field (creep consolidated backfill and salt DRZ) and far-field (anhydrite interbed) pathways. The baseline scenario does not attribute any barrier capability to the waste packages; they are assumed to fail instantaneously. The baseline scenario also does not attribute any sorptive capacity to the waste package corrosion products or backfill.

Changes from the FY 2012 salt GDS model (Section 3.1.1) include the following:

- Deterministic 10,000,000-year simulation with mean values for uncertain parameters
- Waste inventory of 70,000 MTHM UNF in 16,000 waste packages
- Fractional waste form degradation rate of 2×10^{-5} yr^{-1}
- Reduced repository length from 3,270 m to 2,146 m to be consistent with the smaller number of waste packages
- Brine flow rates through the near-field salt DRZ and far-field interbed assumed to remain constant at the 1,000,000-year value until 10,000,000 years

Additional details describing the deterministic salt GDS model input parameters are presented in Appendix C. The resulting salt baseline scenario model is summarized in Table 3-18.

It should be noted that the salt baseline scenario simulated here is representative of bedded salt. For a domal salt scenario, the far-field host salt would have properties of intact halite rather than an anhydrite interbed, but would not extend as far as the interbed.

Table 3-18. Summary of the Salt Baseline Scenario Model

GDSM Region	GDSM Feature	Salt GDS Model	Baseline Scenario Representation
Source	Inventory	UNF	70,000 MTHM
	Waste Form	UNF	2×10^{-5} yr^{-1} fractional degradation rate, no cladding credit
Near Field	Waste Package	Waste Package	Instantaneous failure
	Buffer / Backfill	Included in DRZ	Not applicable
	Seals / Liner	Not modeled	Not applicable
	DRZ	Near-Field Salt (5 m)	Diffusive transport, no sorption
Far Field	Host Rock	Salt Interbed (5,000 m)	Diffusive transport with sorption
	Other Units (Aquifer)	IAEA BIOMASS ERB1B	10,000 m^3/yr dilution rate
Receptor	Surface / Biosphere	IAEA BIOMASS ERB1B	1.2 m^3/yr water consumption rate ERB 1 Dose Coefficients

3.5.1.2 Deterministic Granite GDS Model

The deterministic granite GDS safety assessment model derives from the FY 2011 granite GDS model (Clayton et al. 2011, Section 3.2) and is similar to the FY 2012 granite GDS model described in Section

3.2. The granite baseline scenario includes transport through the near-field (bentonite buffer and granite DRZ) and far-field (fractured granite) pathways. The granite baseline scenario includes the effects of defective waste packages; 1% of the waste packages are assumed to fail instantaneously. This is a change from the FY 2012 granite GDS model described in Section 3.2.1, where all waste packages were assumed to fail instantaneously, but only between 0.1% and 1% of the radionuclides released from the failed waste packages were assumed to directly intersect fractures in the far-field granite.

Changes from the FY 2012 granite GDS model (Section 3.2.1) include the following:

- Deterministic 10,000,000-year simulation with mean values for uncertain parameters
- Waste inventory of 70,000 MTHM UNF in 16,000 waste packages
- Fractional waste form degradation rate of 2×10^{-5} yr^{-1}
- Replace the 3D representation of far-field fractured granite using the FEHM dynamically-linked library with a 1D GoldSim pipe with matrix diffusion (as for the glaciation sensitivity analysis)
- Replace the 2D representation of bentonite buffer with a set of 1D GoldSim cells
- Update distribution coefficients (K_d's) to be more representative of bentonite in the waste package and buffer, based on the waste package and bentonite K_d values used in the clay GDS model (Table C-3 and Clayton et al. 2011, Section 3.3.3.3)
- Update distribution coefficients (K_d's) to be more representative of granite in the host rock, based on Carbol and Engkvist (1997).
- Instantaneous failure of 1% (160) of the waste packages. This replaces the assumption that between 0.1% and 1% of the waste packages directly intersect a far-field fracture.

Additional details describing the deterministic salt GDS model input parameters are presented in Appendix C. The resulting granite baseline scenario is summarized in Table 3-19.

Table 3-19. Summary of the Granite Baseline Scenario Model

GDSM Region	GDSM Feature	Granite GDS Model	Baseline Scenario Representation
Source	Inventory	UNF	70,000 MTHM
	Waste Form	UNF	2×10^{-5} yr^{-1} fractional degradation rate, no cladding credit
Near Field	Waste Package	Waste Package	Instantaneous failure of 1% of waste packages
	Buffer / Backfill	Bentonite (0.36 m)	Diffusive transport with sorption
	Seals / Liner	Not modeled	Not applicable
	DRZ	Granite (0.42 m)	Advective transport in matrix with sorption
Far Field	Host Rock	Granite (5,000 m)	Advective transport in fractures, with sorption and matrix diffusion
	Other Units (Aquifer)	IAEA BIOMASS ERB1B	10,000 m^3/yr dilution rate
Receptor	Surface / Biosphere	IAEA BIOMASS ERB1B	1.2 m^3/yr water consumption rate ERB 1 Dose Coefficients

3.5.1.3 Deterministic Clay GDS Model

The deterministic clay GDS safety assessment model derives from the FY 2011 clay GDS model (Clayton et al. 2011, Section 3.3) and is consistent with the FY 2012 clay GDS model described in Section 3.3. The clay baseline scenario includes diffusive transport through near field (bentonite buffer and clay DRZ) and far field (host clay). The baseline scenario does not attribute any barrier capability to the waste packages; they are assumed to fail instantaneously.

Changes from the FY 2012 clay GDS model (Section 3.3.1) include the following:

- Deterministic 10,000,000-year simulation with mean values for uncertain parameters
- Waste inventory of 70,000 MTHM UNF in 16,000 waste packages
- Instantaneous waste package failure
- Clay thickness of 150 m overlying the emplaced waste, consistent with Hansen et al. (2010, Figure 2.1-1 and Section 4)
- Equivalent diffusive releases to the far-field clay in both the upward and downward directions

Additional details describing the deterministic clay GDS input model parameters are presented in Appendix C. The resulting clay baseline scenario is summarized in Table 3-20.

Table 3-20. Summary of the Clay Baseline Scenario Model

GDSM Region	GDSM Feature	Clay GDS Model	Baseline Scenario Representation
Source	Inventory	UNF	70,000 MTHM
	Waste Form	UNF	2×10^{-5} yr^{-1} fractional degradation rate, no cladding credit
Near Field	Waste Package	Waste Package	Instantaneous failure
	Buffer / Backfill	Bentonite (1.025 m)	Diffusive transport with sorption
	Seals / Liner	Not modeled	Not applicable
	DRZ	Fissured Clay (1.15 m)	Diffusive transport with sorption
Far Field	Host Rock	Clay (150 m)	Diffusive transport with sorption
	Other Units (Aquifer)	IAEA BIOMASS ERB1B	10,000 m^3/yr dilution rate
Receptor	Surface / Biosphere	IAEA BIOMASS ERB1B	1.2 m^3/yr water consumption rate ERB 1 Dose Coefficients

3.5.1.4 Deterministic Deep Borehole GDS Model

The deterministic deep borehole GDS safety assessment model derives from the FY 2011 deep borehole GDS model (Clayton et al. 2011, Section 3.4) and is consistent with the FY 2012 deep borehole GDS model described in Section 3.4. The deep borehole baseline scenario combines two transport pathways: up the borehole; and up the DRZ around the borehole. Transport into the surrounding rock away from the

borehole is screened out in this analysis due to the low permeability of basement crystalline rock relative to the borehole pathways and the low probability of a continuous 3,000 to 5,000-m fracture or fault from the deep basement to a hypothetical overlying aquifer. The baseline scenario does not attribute any barrier capability to the waste packages; they are assumed to fail instantaneously.

Changes from the FY 2012 deep borehole GDS model (Section 3.4.1) include the following:

- Deterministic 10,000,000-year simulation with mean values for uncertain parameters
- Waste inventory of 174 MTHM UNF per borehole in 400 waste packages
- Fractional waste form degradation rate of 2×10^{-5} yr^{-1}
- Fluid flow rates up the borehole assumed to remain constant at the 1,000,000-year values until 10,000,000 years

Additional details describing the deterministic deep borehole GDS model input parameters are presented in Appendix C. The resulting deep borehole baseline scenario is summarized in Table 3-21.

Table 3-21. Summary of the Deep Borehole Baseline Scenario Model

GDSM Region	GDSM Feature	Deep Borehole GDS Model	Baseline Scenario Representation
Source	Inventory	UNF	174 MTHM
	Waste Form	UNF	2×10^{-5} yr^{-1} fractional degradation rate, no cladding credit
Near Field	Waste Package	Waste Package	Instantaneous failure
	Buffer / Backfill	Disposal Zone Degraded Waste (2,000 m)	Advective transport with sorption
	Seals / Liner	Seal Zone Bentonite (1,000 m)	Diffusive transport with sorption
	DRZ	Included in Seals	Included in seals
Far Field	Host Rock	Not modeled	Not applicable
	Other Units (Aquifer)	Upper Borehole Rock Materials (2,000 m)	10,000 m^3/yr dilution rate
Receptor	Surface / Biosphere	IAEA BIOMASS ERB1B	1.2 m^3/yr water consumption rate ERB 1 Dose Coefficients

3.5.2 Deterministic Baseline Analyses

The baseline scenario results from the deterministic simulations provide a preliminary indication of estimated dose, given generic assumptions about source term, near field, far field, and biosphere properties.

3.5.2.1 Salt Baseline Model Results

The deterministic salt baseline scenario is summarized in Section 3.5.1.1 and Table 3-18. Under undisturbed conditions the movement of radionuclides from a salt repository is expected to be extremely slow, occurring only by diffusion. The salt baseline scenario assumes an undisturbed transport pathway, but takes only minimal credit for the EBS; 95% of waste form degradation occurs in 150,000 years, all waste packages fail instantaneously, and there is no sorption in the near-field salt DRZ between the repository and the underlying interbed. The dose receptor is located 5,000 m from the repository. The resulting annual dose over 10,000,000 years is shown in Figure 3-44.

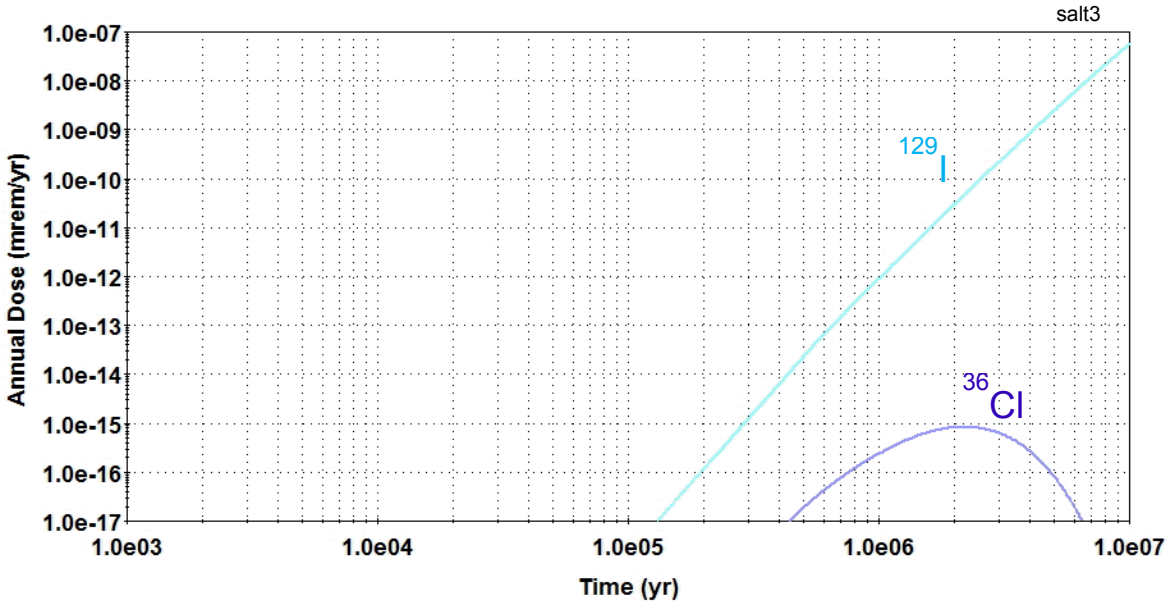

Figure 3-44. Salt Baseline Scenario Annual Dose for a Receptor 5,000 m from the Repository

In the first 10,000 years, the peak annual dose is $< 1\times10^{-23}$ mrem/yr; in the first 1,000,000 years, the peak annual dose is 9.0×10^{-13} mrem/yr (at 1,000,000 years). The peak annual dose over the entire 10,000,000-year simulation is 5.6×10^{-8} mrem/yr, occurring at 10,000,000 years.

The dose is dominated by ^{129}I, with a minor contribution from ^{36}Cl. These are the only two radionuclides with no sorption (K_d = 0 mL/g) throughout the disposal system, unlimited solubility, and long half-lives – 15,700,000 years for ^{129}I and 301,000 years for ^{36}Cl. The larger initial mass (1,363 g/WP of ^{129}I as compared to 2.2 g/WP of ^{36}Cl) and longer half-life explain why the dose contribution is much larger from ^{129}I than from ^{36}Cl.

The deterministic annual dose history in Figure 3-44 is similar to mean annual dose history estimated with the FY 2012 salt GDS probabilistic model (Figure 3-3). Both dose histories are dominated by ^{129}I, with a minor contribution from ^{36}Cl. The deterministic annual dose is generally about two orders of magnitude higher due to the faster waste form degradation rate (2×10^{-5} yr^{-1} versus a range from 1×10^{-8} to

1×10^{-6} yr^{-1}). Lesser effects result from the shortened repository length (2,146 m versus 3,270 m), which increases the dose, and the reduced inventory (~70,000 MTHM versus ~140,000 MTHM), which decreases the dose. The sensitivity analyses in Section 3.5.3.1 further examine processes affecting generic salt disposal system performance.

The relative distribution of ^{129}I mass in the natural and engineered barriers of the salt disposal system at three different times during the deterministic simulation is shown in Figure 3-45.

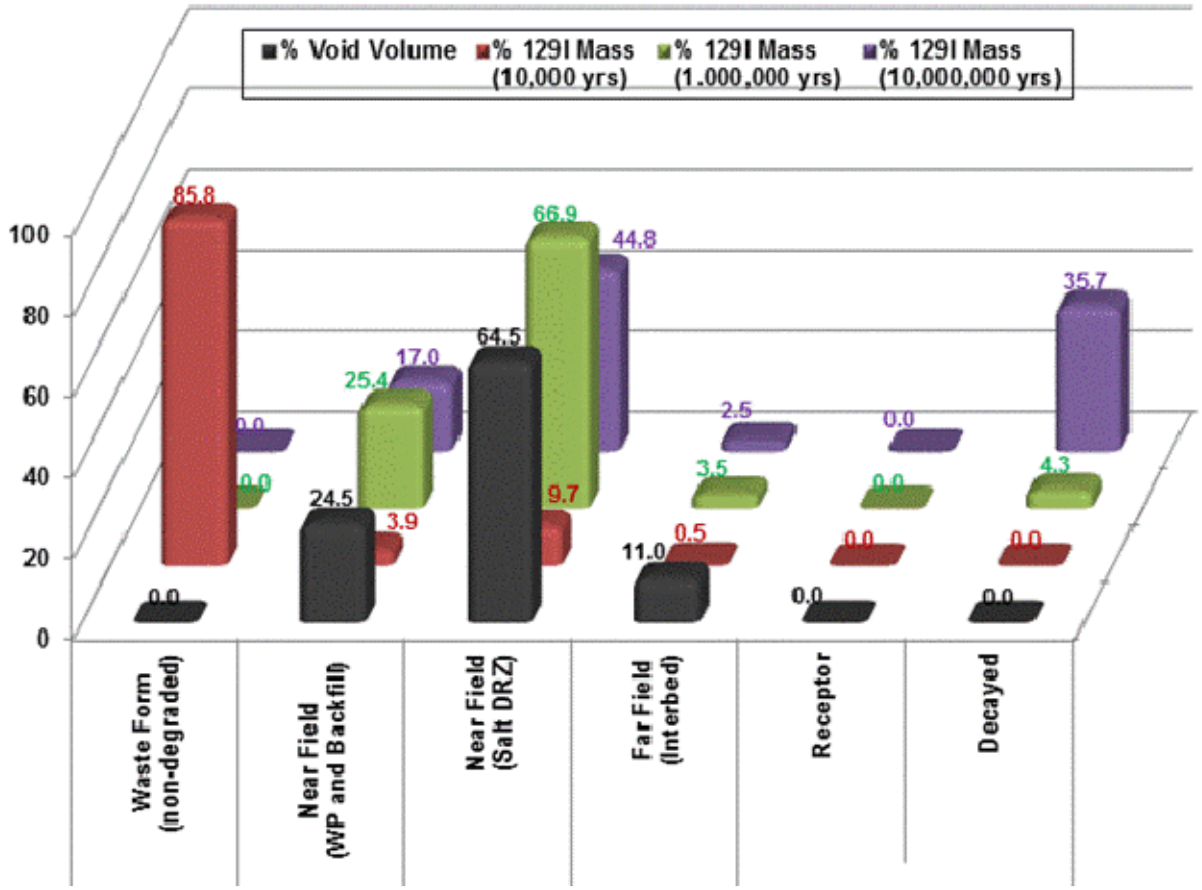

NOTE: % Void Volume provides an indication of the relative distribution of water volume across the components of the disposal system. The Waste Form, Receptor, and Decay components do not have any void volume.

Figure 3-45. Distribution of ^{129}I in the Salt GDS Model Components

At 10,000 years, 85.8% of the initial ^{129}I mass is still bound in the waste form. Less than 1% of the initial mass has been transported (by diffusion) beyond the 5-m thick near-field salt DRZ between the repository and the underlying interbed. At 1,000,000 years, the waste form has completely degraded, but only 3.5% of the initial ^{129}I mass has diffused beyond the near-field salt to the underlying interbed. The small dose at 1,000,000 years (9.0×10^{-13} mrem/yr) is due to a negligible mass of ^{129}I (2×10^{-8} g out of an initial repository ^{129}I mass of 21,830 kg) actually reaching the receptor. This negligible calculated mass at the receptor is effectively zero as it is of the same magnitude as the numerical precision of the solution. At 10,000,000 years, 35.7% of the initial ^{129}I mass has decayed. Most of the undecayed mass has still not diffused to the underlying interbed. Even at 10,000,000 years, only 0.01 g has reached the receptor.

Based on these results the following observations can be made regarding the performance of a generic salt disposal system under baseline scenario conditions:

- Radionuclide releases to the receptor location in the biosphere are minimal; for long-lived non-sorbing ^{129}I, releases are effectively zero after 10,000,000 years. The peak dose is 5.6×10^{-8} mrem/yr at 10,000,000 years.
- Radionuclide transport through the near field (the EBS and the near-field salt DRZ between the repository and the underlying interbed) is slow due to:
  - Very low brine flow rates resulting in diffusion-dominated transport
  - Salt creep closure of the repository excavation and DRZ which minimizes the potential for high-permeability fracture connections to the underlying interbed
- Radionuclide transport through the far field (anhydrite interbed) is slow due to
  - Very low brine flow rates resulting in diffusion-dominated transport
  - Radionuclide sorption
  - Absence of well-connected fractures in the interbed
  - Long migration distance (5,000 m) to the receptor location

3.5.2.2 Granite Baseline Model Results

The deterministic granite baseline scenario is summarized in Section 3.5.1.2 and Table 3-19. Under undisturbed conditions long-lived waste packages are expected to limit radionuclide releases from a granite repository. The granite baseline scenario assumes an undisturbed transport pathway, but takes only minimal credit for the EBS; 95% of waste form degradation occurs in 150,000 years (i.e., fractional degradation rate of 2×10^{-5} yr^{-1}) and 1% (160) of the waste packages fail instantaneously. The dose receptor is located 5,000 m from the repository. The resulting annual dose over 10,000,000 years is shown in Figure 3-46.

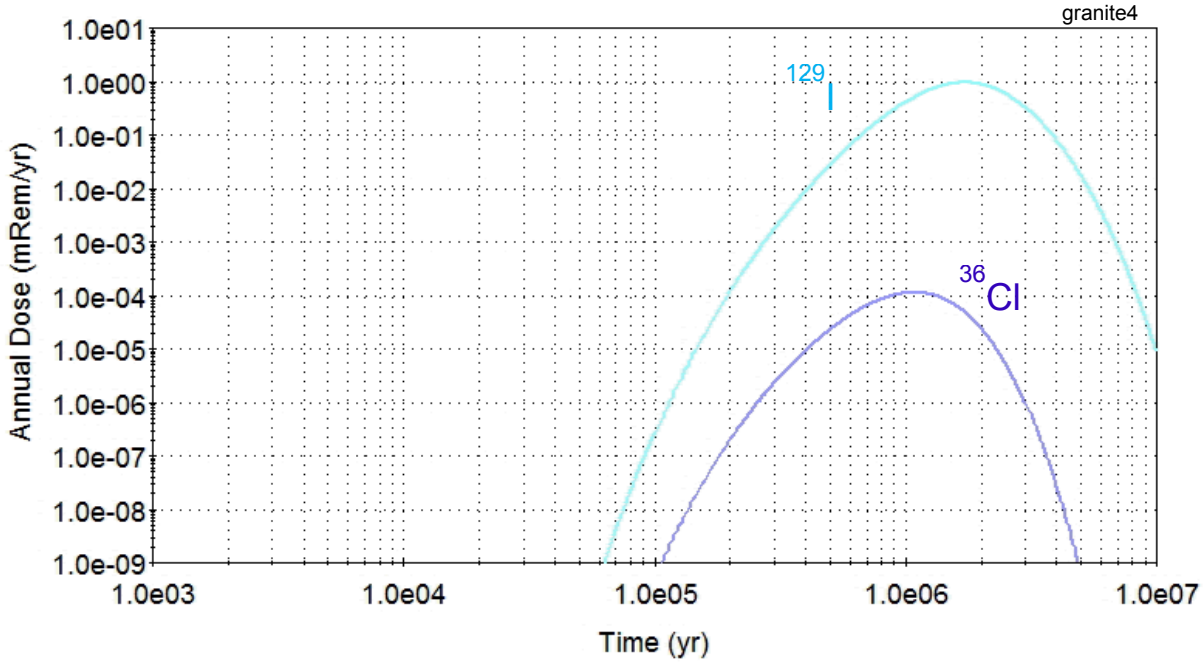

Figure 3-46. Granite Baseline Scenario Annual Dose for a Receptor 5,000 m from the Repository

In the first 10,000 years, the peak annual dose is 0 mrem/yr; in the first 1,000,000 years, the peak annual dose is 0.41 mrem/yr (at 1,000,000 years). The peak annual dose over the entire 10,000,000-year simulation is 0.95 mrem/yr, occurring at 1,730,000 years.

The dose is dominated by ^{129}I, with minor contribution from ^{36}Cl. As in the salt GDS model, ^{129}I and ^{36}Cl are the only two radionuclides with no sorption throughout the disposal system, unlimited solubility, and long half-lives. The behavior of ^{129}I and ^{36}Cl in the deterministic granite model (Figure 3-46) is similar to the behavior in the FY 2011 granite GDS probabilistic model (Clayton et al. 2011, Figure 3.2-6). The deterministic annual dose is two to three orders of magnitude higher due to (1) the faster waste form degradation rate (2×10^{-5} yr^{-1} versus a range from 1×10^{-8} to 1×10^{-6} yr^{-1}), and (2) the reduced transverse spreading (diffusion in the bentonite buffer, mechanical dispersion in the far-field granite) due to the 1D geometry used in the buffer and far-field. Lesser effects result from the reduced inventory (~70,000 MTHM versus ~90,000 MTHM), which decreases the magnitude of the dose.

In addition to ^{129}I and ^{36}Cl, several other radionuclides (e.g., ^{79}Se, ^{126}Sn) contribute to the mean annual dose in the FY 2011 granite GDS probabilistic calculations (Clayton et al. 2011, Figure 3.2-6). The presence of these radionuclides as mean annual dose contributors in the FY 2011 probabilistic calculation, but not in the deterministic calculation, is due to the probabilistic treatment of the distribution coefficient, K_d, which controls the sorption of radionuclides onto the porous medium. The effects of sorption can be quantified in terms of a retardation factor, R_f (see Equation 3-5). The retardation factor provides an indication of the travel time of a sorbed radionuclide along a travel pathway relative to the travel time of a non-sorbing radionuclide (a non-sorbing radionuclide has $K_d = 0$ and $R_f = 1$). Equation 3-5 shows that the probabilistic treatment of porosity could also affect the retardation factor, for a radionuclide with a non-zero K_d.

In the FY 2011 granite GDS probabilistic calculation, K_d values (and porosity values) for each of 100 realizations were selected from a distribution using Monte Carlo sampling. The mean annual doses for radionuclides such as^{79}Se and ^{126}Sn were dominated by realizations where low K_d values (as low as 0 for ^{126}Sn and 0.5 for ^{79}Se), corresponding to low retardation factors, were sampled. These low retardation factors, combined with long half-lives, result in the minor dose contributions from ^{79}Se and ^{126}Sn in the probabilistic model (Clayton et al. 2011, Figure 3.2-6). In addition, the dissolved concentration of ^{79}Se was not controlled by a solubility limit in the FY 2011 granite GDS model, which further enhanced its dose contribution.

In the deterministic granite model, a single K_d value was specified for each radionuclide, calculated as the mean value of the probabilistic distribution. As a result, retardation factors were large for ^{126}Sn in the bentonite buffer and for ^{79}Se in the far-field granite. These larger retardation factors were enough to prevent ^{79}Se and ^{126}Sn from being dose contributors in the deterministic granite model (Figure 3-46).

The differences in results between the FY 2011 granite GDS probabilistic model and the deterministic model provide an indication of the sensitivity of the granite model to sorption.

An additional difference between the model results is that small doses ($> 1\times10^{-9}$ mrem/yr) appear as early as 2,000 years in the FY 2011 probabilistic model but not until about 60,000 years in the deterministic model. This difference reflects differences in the characterization of far-field flow; the early doses in the FY 2011 probabilistic calculation result from realizations where a large far-field flow velocity was sampled. The sensitivity analyses in Section 3.5.3.2 further examine sorption, flow velocity, and other processes affecting generic granite disposal system performance.

The relative distribution of ^{129}I mass in the natural and engineered barriers of the granite disposal system at three different times during the deterministic simulation is shown in Figure 3-47.

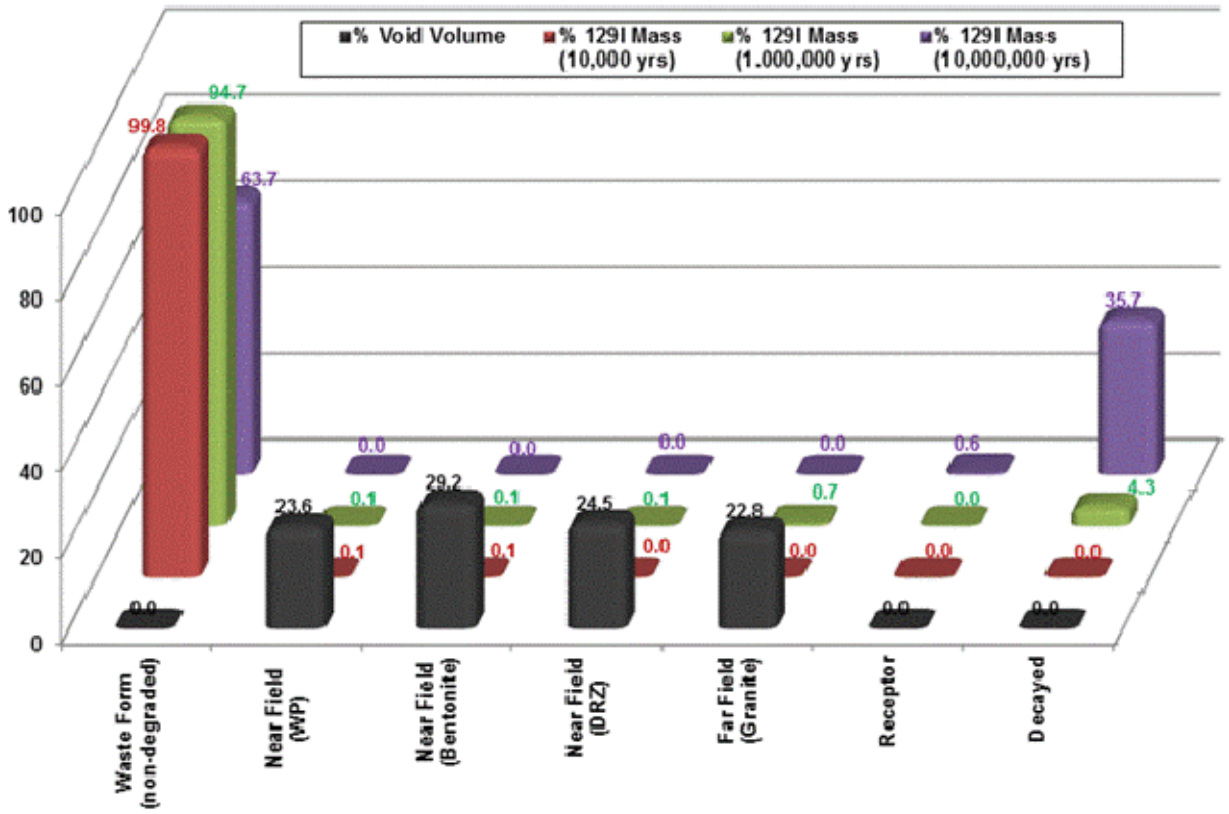

NOTE: % Void Volume provides an indication of the relative distribution of water volume across the components of the disposal system. The Waste Form, Receptor, and Decay components do not have any void volume.

Figure 3-47. Distribution of ^{129}I in the Granite GDS Model Components

The effectiveness of the waste packages (1% fail instantaneously, 99% remain intact) is demonstrated by the initial ^{129}I mass that remains bound in the waste form. At 10,000 years, 99.8% of the initial ^{129}I mass is still bound in the waste form and less than 0.1% of the initial mass has been transported (by diffusion) beyond the 0.36-m thick bentonite buffer to the granite DRZ. At 1,000,000 years, 94.7% of the initial ^{129}I mass is still bound in the waste form and 0.8% of the initial mass has diffused beyond the bentonite buffer – and is mostly present in the far-field granite. The dose at 1,000,000 years (0.41 mrem/yr) is due to the small mass of ^{129}I (10.7 kg out of an initial repository ^{129}I mass of 21,830 kg) reaching the receptor. At 10,000,000 years, 35.7% of the initial ^{129}I mass has decayed, 63.7% of the initial mass remains bound in the waste form, and 0.6% (140 kg) has reached the receptor location. The calculated peak annual dose (0.95 mrem/yr at 1,730,000 years) assumes that the entire mass from all 160 failed waste packages that is transported out of the far-field granite fracture to the overlying aquifer is captured by the pumping well at the receptor location.

Based on these results the following observations can be made regarding the performance of a generic granite disposal system under baseline scenario conditions:

- Radionuclide releases to the receptor location in the biosphere are small; for long-lived non-sorbing ^{129}I, releases are 0.05% of the initial mass after 1,000,000 years and 0.6% of the initial mass after 10,000,000 years. The peak dose is 0.95 mrem/yr at 1,730,000 years.
- Radionuclide releases from the waste form are limited by long-lived waste packages.
- Radionuclide transport through the near field (the bentonite buffer and granite DRZ) is slow due to:

  - Diffusion-dominated transport in the bentonite
  - No defects in the buffer that produce direct connection to the far-field granite fractures
  - Radionuclide sorption
- Radionuclide transport through the far field (granite fractures and matrix) is slow due to:
  - Matrix diffusion associated with fracture transport
  - Radionuclide sorption in the matrix
  - Long migration distance (5,000 m) to the receptor location

3.5.2.3 Clay Baseline Model Results

The deterministic clay baseline scenario is summarized in Section 3.5.1.3 and Table 3-20. Under undisturbed conditions radionuclide releases from a clay repository are expected to be limited by low advection, a reducing chemical environment, and sorption. The clay baseline scenario assumes an undisturbed transport pathway, but takes only limited credit for the EBS; 95% of waste form degradation occurs in 150,000 years (i.e., fractional degradation rate of 2×10^{-5} yr^{-1}) and all waste packages fail instantaneously. Additionally, the receptor is effectively assumed to be located at the edge of the clay host rock formation, only 150 m from the repository. This differs from the receptor distance of 5,000 m used for the salt and granite baseline scenarios, so direct comparisons to those disposal options cannot be made. The resulting annual dose over 10,000,000 years is shown in Figure3-48.

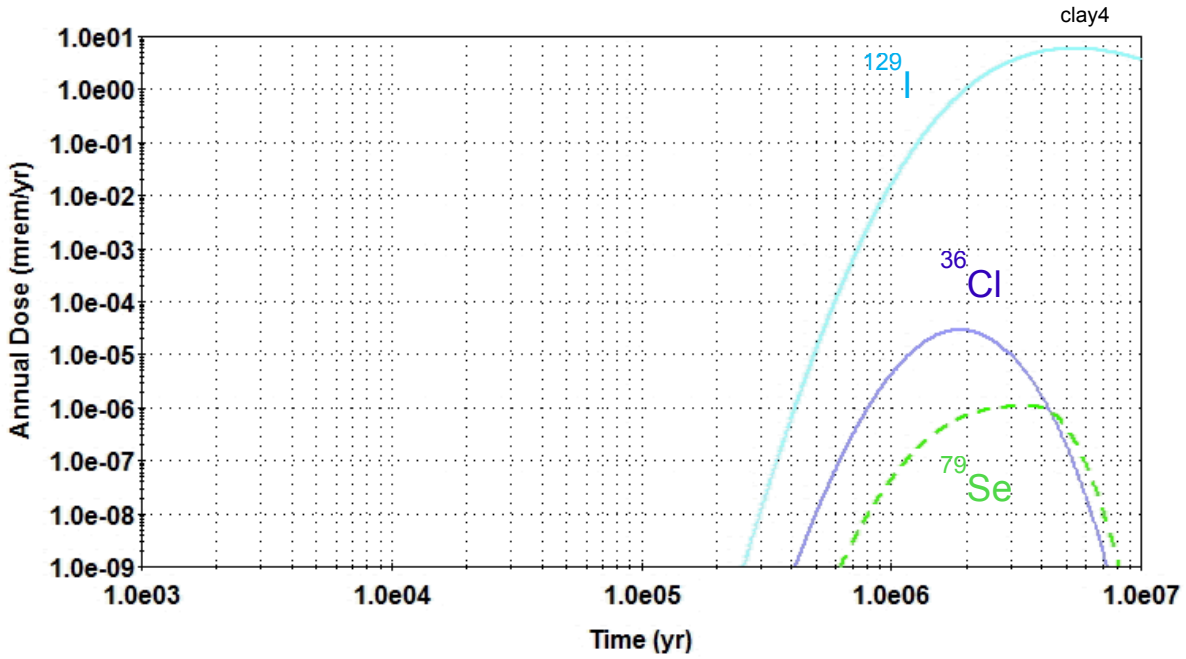

Figure 3-48. Clay Baseline Scenario Annual Dose for a Receptor 150 m from the Repository

In the first 10,000 years, the peak annual dose is 0 mrem/yr; in the first 1,000,000 years, the peak annual dose is 0.016 mrem/yr (at 1,000,000 years). The peak annual dose over the entire 10,000,000-year simulation is 5.9 mrem/yr, occurring at 5,400,000 years.

The dose is dominated by ^{129}I, with minor contributions from ^{36}Cl and ^{79}Se. As in the salt and granite GDS models, ^{129}I and ^{36}Cl are the only two radionuclides with no sorption throughout the disposal system,

unlimited solubility, and long half-lives. ^{79}Se is a minor contributor to the dose because it has no sorption along the 150-m flow pathway except for a small K_d of 4.6 mL/g in the 1-m-thick bentonite layer. The dissolved concentration of ^{79}Se is controlled by a solubility limit, which further limits its dose contribution. Even though the initial mass of ^{79}Se (45.7 g/WP) is larger than the initial mass of ^{36}Cl (2.2 g/WP) and they have similar half-lives (290,000 yrs for ^{79}Se and 301,000 yrs for ^{36}Cl), the dose contribution from ^{36}Cl is larger due to the effects of ^{79}Se sorption in the bentonite and the ^{79}Se solubility limit.

The behavior of ^{129}I, ^{36}Cl and ^{79}Se in the deterministic clay model is similar to the behavior in the FY 2011 clay GDS probabilistic model (Clayton et al. 2011, Figure 3.3-27). The deterministic annual dose is generally three to four orders of magnitude higher due to a combination of significant increases from the larger inventory (~70,000 MTHM versus 1 MTHM) and moderate decreases from the increased clay host rock thickness (150 m versus 65 m). The reduction in the waste package lifetime from 10,000 years to 0 years (i.e., instantaneous failure) has little effect on the dose because 10,000 years is short relative to the 350,000-year lifetime of the waste form.

In addition to ^{129}I, ^{36}Cl and ^{79}Se, several other radionuclides (e.g., ^{135}Cs, ^{237}Np, ^{242}Pu) contribute to the mean annual dose in the 2011 clay GDS probabilistic model (Clayton et al. 2011, Figure 3.3-27). As in the granite model, the presence of these radionuclides as mean annual dose contributors in the FY 2011 clay GDS probabilistic model, but not as annual dose contributors in deterministic clay analysis, is due to the probabilistic treatment of the distribution coefficient, K_d, which controls the sorption of radionuclides onto the porous medium. In the FY 2011 clay GDS probabilistic model, the mean annual doses for radionuclides such as ^{135}Cs, ^{237}Np, and ^{242}Pu were dominated by realizations where low K_d values were sampled, corresponding to low retardation factors. In the far-field clay host rock, retardation factors were as low as 36 for ^{135}Cs and 83 for ^{237}Np and ^{242}Pu. These low retardation factors, combined with long half-lives, result in the minor dose contributions from ^{135}Cs, ^{237}Np, and ^{242}Pu in the probabilistic calculations (Clayton et al. 2011, Figure 3.3-27). In the deterministic clay model, the single K_d values resulted in retardation factors of 16,850 for ^{135}Cs and 37,900 for ^{237}Np and ^{242}Pu in the clay host rock. These very large retardation factors explain why ^{135}Cs, ^{237}Np, and ^{242}Pu are not dose contributors in the deterministic calculation (Figure 3-48). The sensitivity analyses in Section 3.5.3.3 further examine processes affecting generic clay disposal system performance.

The relative distribution of ^{129}I mass in the natural and engineered barriers of the clay disposal system at three different times during the deterministic simulation is shown in Figure 3-49.

At 10,000 years, 81.8% of the initial ^{129}I mass is still bound in the waste form. Less than 10% of the initial mass has been transported (by diffusion) beyond the 2.175-m thick near-field (bentonite buffer and clay DRZ) to the far-field clay host rock. At 1,000,000 years, the waste form has completely degraded and 91.6% of the initial ^{129}I mass has diffused into the 150-m thick far-field clay. The dose at 1,000,000 years (0.016 mrem/yr) is due to the small mass of ^{129}I (389 g out of an initial repository ^{129}I mass of 21,830 kg) reaching the receptor. At 10,000,000 years, 35.7% of the initial ^{129}I mass has decayed, 30.3% of the initial mass remains in the far-field clay, and 33.8% (7,370 kg) has reached the receptor location. The calculated peak annual dose (5.9 mrem/yr at 5,400,000 years) assumes that the entire mass from all 16,000 waste packages that is transported out of the far-field clay host rock to the overlying aquifer is captured by the pumping well at the receptor location.

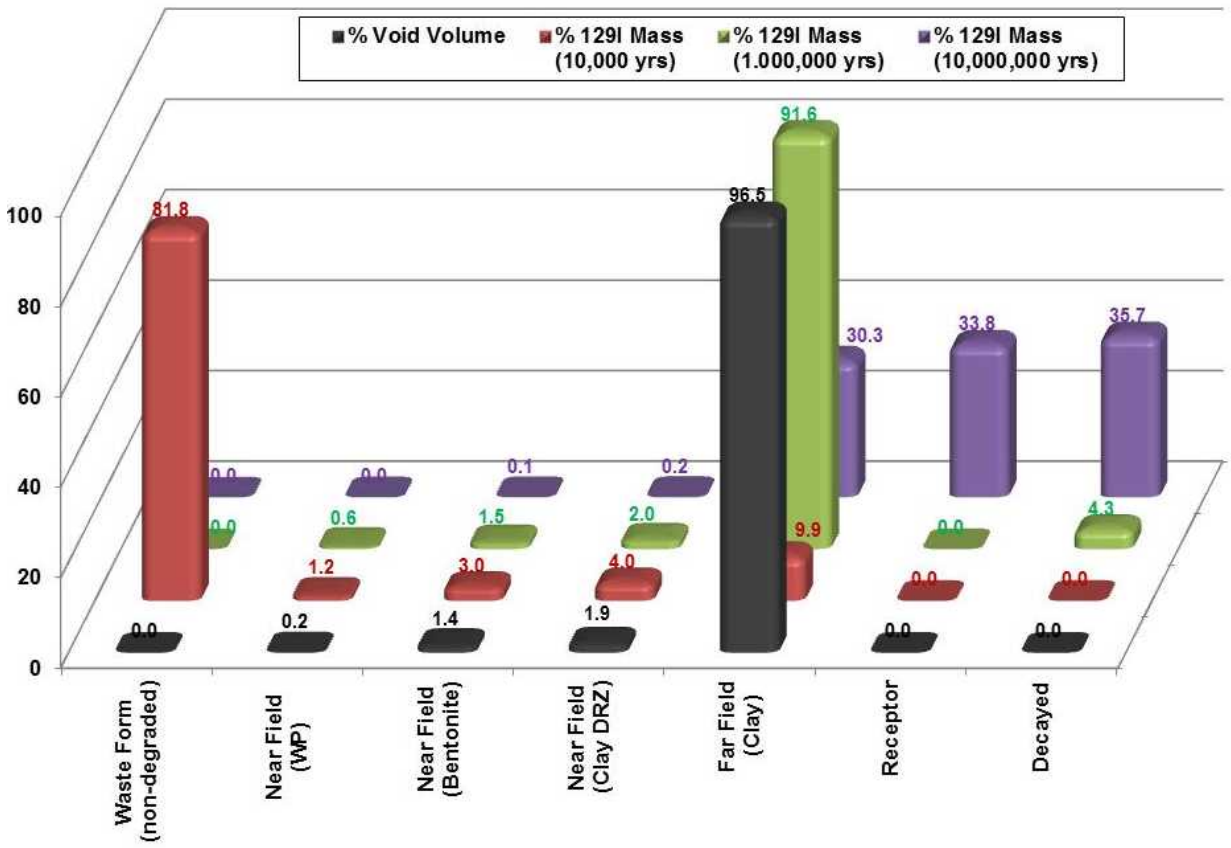

NOTE: % Void Volume provides an indication of the relative distribution of water volume across the components of the disposal system. The Waste Form, Receptor, and Decay components do not have any void volume.

Figure 3-49. Distribution of ^{129}I in the Clay GDS Model Components

Based on these results the following observations can be made regarding the performance of a generic clay disposal system under baseline scenario conditions:

- Radionuclide releases to the receptor location in the biosphere are small; for long-lived non-sorbing ^{129}I, releases are ~0.002% of the initial mass after 1,000,000 years and 33.8% of the initial mass after 10,000,000 years. The peak dose is 5.9 mrem/yr at 5,400,000 years.
- Radionuclide transport through the far field (clay host rock) is slow due to
  - Diffusion-dominated transport
  - Radionuclide sorption
  - Sufficient clay formation thickness (150 m)
- Radionuclide transport through the near field (the bentonite buffer and clay DRZ) is slow due to
  - Diffusion-dominated transport
  - Radionuclide sorption
  - Clay DRZ healing which minimizes the potential for high-permeability fissure connections to the far-field clay

3.5.2.4 Deep Borehole Baseline Model Results

The deterministic deep borehole baseline scenario is summarized in Section 3.5.1.4 and Table 3-21. In the absence of an advective pathway, diffusion cannot move radionuclides a significant distance through the borehole seal zone. The deep borehole baseline scenario assumes an initial period of thermally induced advection followed by diffusion. Only minimal credit is taken for the EBS; in the disposal zone (3,000 – 5,000-m depth) 95% of waste form degradation occurs in 150,000 years (i.e., fractional degradation rate of 2×10^{-5} yr^{-1}) and all waste packages fail instantaneously, and in the seal zone (2,000 – 3,000-m depth) an annulus of disturbed rock around the borehole is assumed to enhance the effective permeability. Additionally, no credit is taken for the upper zone (0 – 2,000-m depth) of the borehole; the pumping well that transports radionuclides to the receptor at a surface location directly above the borehole is assumed to intersect the borehole upper zone. There is no lateral distance from the borehole to the pumping well, whereas a lateral distance of 5,000 m from the repository to the pumping well is assumed in the salt and granite disposal systems. Therefore direct comparison to the other disposal options cannot be made. The resulting annual dose over 10,000,000 years is shown in Figure 3-50.

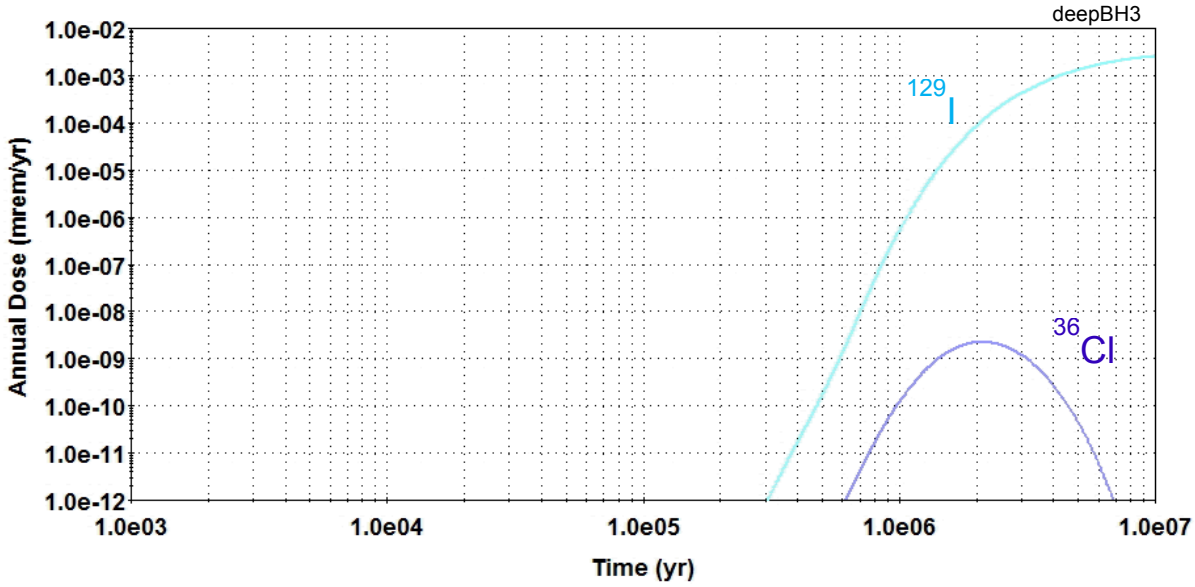

Figure 3-50. Deep Borehole Baseline Scenario Annual Dose for a Receptor Directly Above the Borehole

In the first 10,000 years, the peak annual dose is 0 mrem/yr; in the first 1,000,000 years, the peak annual dose is 5.1×10^{-7} mrem/yr (at 1,000,000 years). The peak annual dose over the entire 10,000,000-year simulation is 0.0025 mrem/yr, occurring at 10,000,000 years. The peak annual dose at 10,000,000 years assumes that the externally calculated, thermally driven flow rates up the borehole at 1,000,000 years remain constant over the next 9,000,000 years.

The dose is dominated by ^{129}I, with a minor contribution from ^{36}Cl. As for the salt, clay, and granite results, ^{129}I and ^{36}Cl are the only two radionuclides with no sorption throughout the disposal system, unlimited solubility, and long half-lives. ^{79}Se, which was a minor contributor to the clay GDS dose, does not contribute to the deep borehole GDS dose because it has a small, but non-zero, K_d in all borehole zones.

The behavior of ^{129}I and ^{36}Cl in the deterministic calculation (Figure 3-50) is similar to the behavior in the FY 2012 deep borehole probabilistic calculation (Figure 3-40). The deterministic annual dose is two to

three orders of magnitude higher due to the faster waste form degradation rate (2×10^{-5} yr^{-1} versus a range from 1×10^{-8} to 1×10^{-6} yr^{-1}) and an increased inventory (174 MTHM per borehole versus 121 MTHM per borehole). The sensitivity analyses in Section 3.5.3.4 further examine processes affecting generic deep borehole disposal system performance.

In addition to ^{129}I and ^{36}Cl, ^{99}Tc also contributed to the mean annual dose in the FY 2011 deep borehole GDS probabilistic calculations (Clayton et al. 2011, Figure 3.4-9). As in the clay and granite models, the additional dose contribution in the FY 2011 deep borehole GDS probabilistic results is due to the probabilistic treatment of the distribution coefficient, K_d, which controls the sorption of radionuclides onto the porous medium. In the FY 2011 probabilistic calculations, the mean annual dose for ^{99}Tc was dominated by realizations where low K_d values were sampled (as low as 0.00001 mL/g in the disposal zone and 0.0001 in the seal zone), corresponding to low retardation factors. In the deterministic calculation, the K_d values were 1.7 mL/g in the disposal zone and 17 in the seal zone.

The relative distribution of ^{129}I mass in the natural and engineered barriers of the deep borehole disposal system at three different times during the deterministic simulation is shown in Figure 3-51.

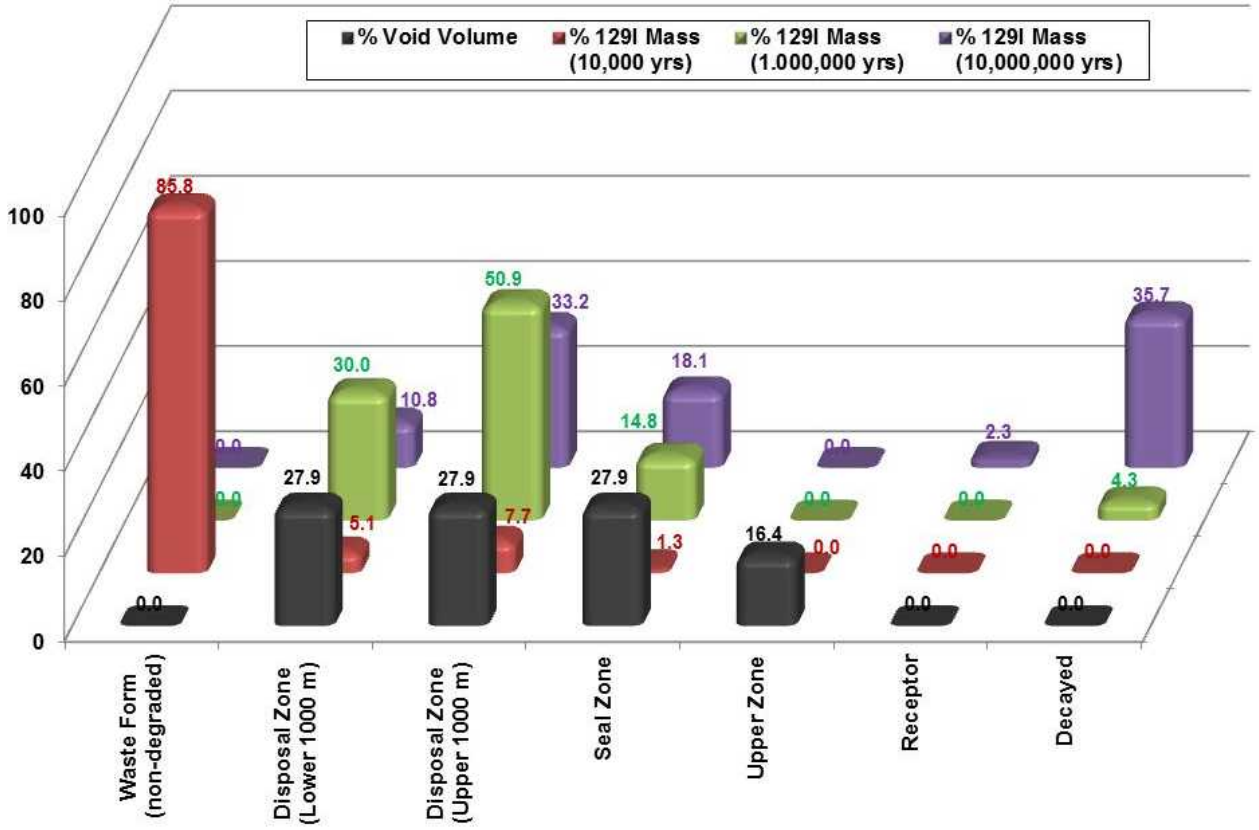

NOTE: % Void Volume provides an indication of the relative distribution of water volume across the components of the disposal system. The Waste Form, Receptor, and Decay components do not have any void volume.

Figure 3-51. Distribution of ^{129}I in the Deep Borehole GDS Model Components

At 10,000 years, 85.8% of the initial ^{129}I mass is still bound in the waste form. Only 1.3% of the initial mass has been transported (by thermally-induced advection) out of the disposal zone and into the 1,000-m

thick seal zone. At 1,000,000 years, the waste form has completely degraded, and 14.8% of the initial ^{129}I mass has been transported into the seal zone. The transport of ^{129}I out of the disposal zone is advection dominated in the first approximately 300,000 years until the thermally-induced flow rates have declined significantly. After about 700,000 years, the transport of ^{129}I out of the disposal zone is diffusion dominated. Further away from the thermal effects of the disposal zone, transport is diffusion dominated even in the first 300,000 years. The small dose at 1,000,000 years (5.1×0^{-7} mrem/yr) is due to a small mass of ^{129}I (5.1×10^{-3} g out of an initial borehole disposal zone ^{129}I mass of 54.6 kg) actually reaching the receptor. At 10,000,000 years, 35.7% of the initial ^{129}I mass has decayed, 44.0% of the initial mass remains in the disposal zone, 18.1% is in the seal zone, and 2.3% (1.3 kg) has reached the receptor location. The calculated peak annual dose (0.0025 mrem/yr at 10,000,000 years) assumes that all non-sorbing radionuclides leaving the seal zone are rapidly transported through the upper zone to the receptor.

Based on these results the following observations can be made regarding the performance of a generic deep borehole disposal system under baseline scenario conditions:

- Radionuclide releases to the receptor location in the biosphere (directly above the borehole at the surface) are small; for long-lived non-sorbing ^{129}I, releases are ~0.000001% of the initial mass after 1,000,000 years and 2.3% of the initial mass after 10,000,000 years. The peak dose is 0.0025 mrem/yr at 10,000,000 years.
- Radionuclide transport through the bentonite seal zone is slow due to:
  - Very low thermally-induced fluid flow rates resulting in diffusion-dominated transport
  - Durability of the seals with only minor DRZ bypass
  - Radionuclide sorption
  - Long migration distance (1,000 m)
- Radionuclide transport through the disposal zone is slow due to:
  - Low thermally-induced fluid flow rates that decrease over time, resulting in diffusion-dominated transport after about 700,000 years
  - Radionuclide sorption
  - Long migration distance (as much as 2,000 m) for the deepest waste packages
- Radionuclide transport through the basement deep granite is negligible due to:
  - Very low permeability and lack of significant fracture connection to overlying formations

3.5.3 Deterministic Sensitivity Analyses

The effects of uncertainties on the behavior and performance of the four disposal option baseline scenarios are investigated using sensitivity analyses in the form of one-off deterministic simulations from the baseline simulations. A one-off simulation is performed by changing the value of a single uncertain parameter from its baseline value to other values within its distribution, or to a reasonable bounding value, and examining the corresponding effect on system performance. These one-off sensitivity simulations, described in the following subsections, provide additional insights into which parameters, features, and/or barriers most significantly contribute to the overall capability of a specific disposal system to isolate waste from the biosphere under the assumed baseline scenario conditions. Sensitivities are examined with respect to impact on ^{129}I release and migration because ^{129}I is the dominant (and in some case the only) contributor to annual dose.

3.5.3.1 Salt Sensitivity Analyses

Annual dose results from the deterministic salt baseline scenario are shown in Figure 3-44. The following one-off sensitivity simulations were performed to investigate the effects on ^{129}I movement through the disposal system:

- Waste form fractional degradation rate (Figure 3-52)
- Integrity of the near-field salt DRZ between the repository and the underlying interbed (Figure 3-53)
- Brine flow rate in the EBS, DRZ, and anhydrite interbed (Figure 3-54)
- Molecular diffusion coefficient (Figure 3-55)
- Sorption (^{129}I distribution coefficient) in the anhydrite interbed (Figure 3-56)
- Distance to receptor location (Figure 3-57)

Waste Form Degradation—The effect of waste form degradation rate on ^{129}I annual dose is shown in Figure 3-52. The sensitivity analysis includes three fractional degradation rate cases:

- Fast Waste Form Degradation ($0.1\ yr^{-1}$)—100% of the radionuclide mass is released from the waste form in the first 250 years. This provides a bounding case for instantaneous release of gap and grain boundary inventory from the waste form. An estimate of the ^{129}I gap fraction from UNF is the following: 0.0204 (minimum); 0.1124 (most likely); 0.2675 (maximum) (SNL 2008d, Table 6.3.7-29).
- Baseline Waste Form Degradation ($2\times10^{-5}\ yr^{-1}$)—50% of the radionuclide mass is released from the waste form in the first 35,000 years, 95% of the mass is released by 150,000 years, and 99.9% of the mass is released by about 350,000 years.
- Slow Waste Form Degradation ($1\times10^{-7}\ yr^{-1}$)—50% of the radionuclide mass is released from the waste form after 4,800,000 years, and 76% of the mass is released by 10,000,000 years. This slow degradation rate, consistent with reducing chemical conditions, was the assumed to be the most likely rate in the FY 2011 salt, granite and deep borehole GDS models (Clayton et al. 2011).

In the fast degradation rate ($0.1\ yr^{-1}$) case, all mass is released (degraded) from the waste form in the first 250 years. This is roughly equivalent to assuming that all ^{129}I mass is instantaneously released as gap and grain boundary inventory (i.e., a ^{129}I gap fraction of 1.0 as compared to the estimated range of 0.0204–0.2675). The mass released from the waste form diffuses vertically downward through the repository and 5-m thick near-field salt, and into the 1-m thick near-field interbed underlying the repository. This vertical diffusion occurs across the repository footprint (a 2,146-m per side square with a porosity of 0.039) corresponding to a diffusion area of approximately 180,000 m^2. In the fast degradation rate case, 73% of the initial ^{129}I mass reaches the near-field salt DRZ and underlying interbed by 100,000 years, whereas in the baseline case, only 57% of the initial mass reaches the DRZ and interbed by 100,000 years, and 22% of the mass is still undegraded. Despite the greater early transport of ^{129}I mass away from the repository in the fast degradation rate case, the effect on annual dose is not significant. This is because, in a diffusion-dominated system, the effect of the early mass on annual dose is attenuated in the 5,000-m far-field interbed by (1) diffusive fluxes into the interbed that decline over time as a function of the concentration gradient, (2) the conceptual model assumptions about the system geometry, and (3) slow diffusive travel times through the interbed.

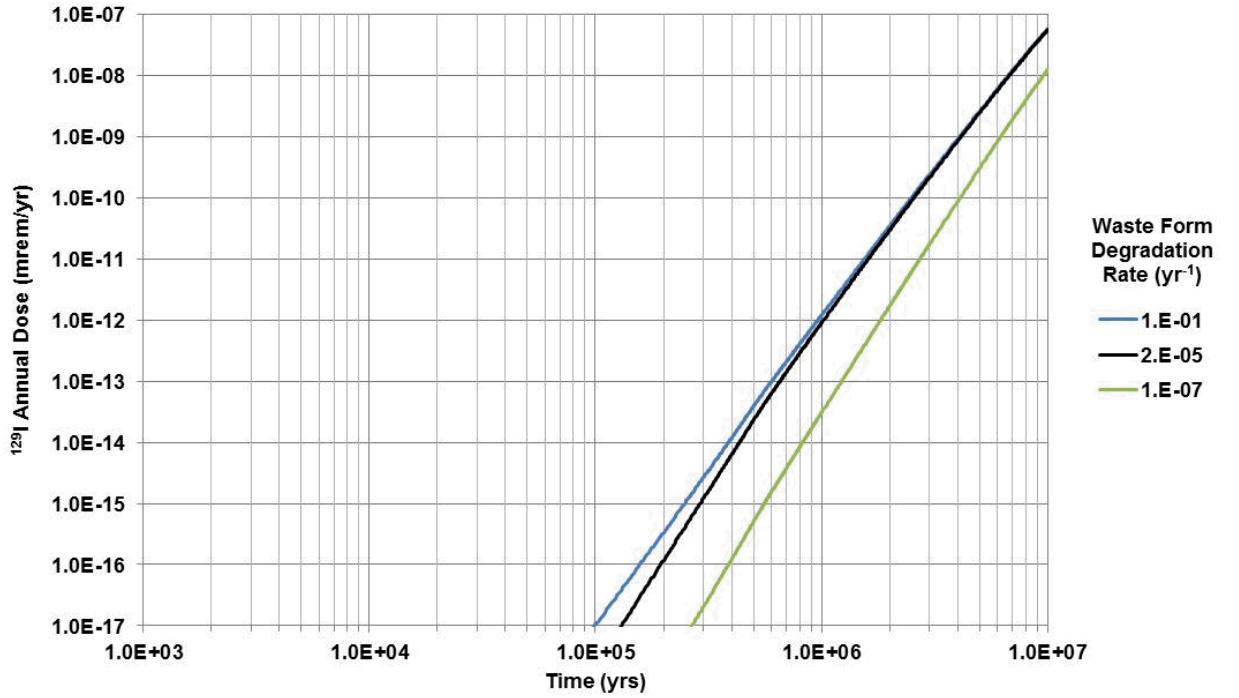

Figure 3-52. Effect of Waste Form Degradation Rate on Annual Dose from ^{129}I in the Salt GDS Model

In the fast degradation rate case, the early mass results in a larger diffusive flux into the far-field interbed at early time. However, this concentration-gradient driven flux quickly equilibrates. Conversely, in the baseline case, the early-time diffusive flux is not as large, but the concentration equilibration is slower. Over longer time scales, the cumulative flux into the interbed is similar in the two cases. The effect of the larger early-time diffusive flux in the fast degradation case is further limited by the system geometry. While the vertical diffusion from the DRZ to the interbed occurs across a 180,000-m^2 diffusion area corresponding the repository footprint void volume, the subsequent horizontal diffusion along the interbed toward the receptor location is across a 21.5-m^2 diffusion area corresponding to the interbed cross section void volume (2,146-m wide by 1-m thick with a porosity of 0.01). Therefore, the large early-time concentration gradient due to the extra early mass present in the underlying interbed in the fast degradation rate case has a limited effect on the diffusion rate along the interbed (ranging from 0.001 to 0.01 g/yr) due to the relatively small diffusion area, resulting in only about an extra 0.4 kg of ^{129}I (out of an initial mass of 21,830 kg) in the far-field interbed after 100,000 years and an extra 0.2 kg after 10,000,000 years. And finally, in both the baseline and fast waste form degradation cases, the degradation time is shorter than the travel time horizontally along the 5,000-m interbed; therefore, the horizontal travel time through the far-field interbed is the dominant process, and increases in the waste form degradation rate have little effect on annual dose.

For the slow fractional degradation rate (1×10^{-7} yr^{-1}), 50% of the radionuclide mass is not released from the waste form until 4,800,000 years, and only 76% of the mass is released by 10,000,000 years. In this case, the degradation time is slower than the travel time through the far-field interbed and the effect of the slower degradation rate is to reduce the peak dose by about a factor of 4 at 10,000,000 years.

Near-Field DRZ Integrity—The effect of the integrity of the near-field salt DRZ on ^{129}I annual dose is shown in Figure 3-53. The sensitivity analysis includes two cases:

- Baseline Intact Near-Field Salt—The near-field salt DRZ between the repository and the underlying interbed is 5-m thick and lacks any fast fracture pathways. The brine flow rate is low enough that transport through the DRZ is diffusion dominated. Specific flow values are described below in the discussion of sensitivity to flow rate.
- Damaged Near-Field Salt—The effective thickness of the near-field salt DRZ is 1 m and a multiplier of 1,000 is applied to the baseline brine flow rate history. The brine flow multiplier results in advective transport through the DRZ. These enhanced transport properties are considered to represent the effects of better-connected, non-healing fractures between the repository and the underlying interbed.

The effect of the more damaged near-field salt DRZ has a minor effect on annual dose, increasing the peak dose by about a factor of 3 at 10,000,000 years.

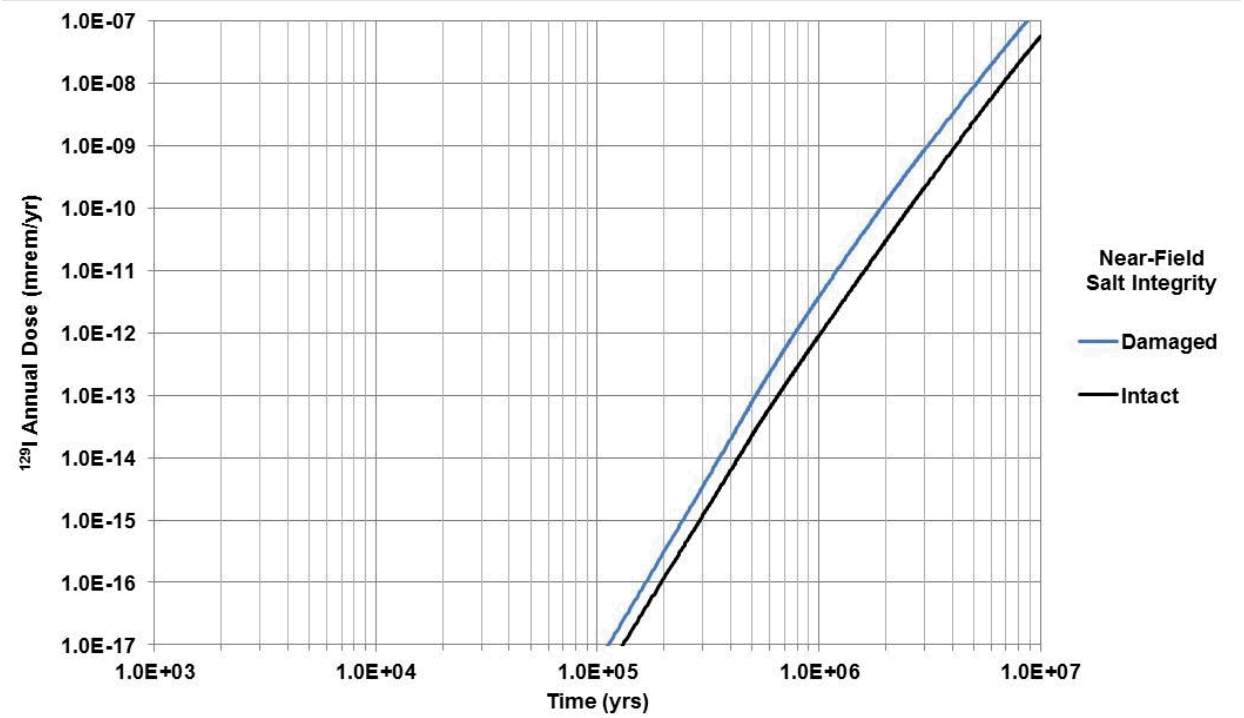

Figure 3-53. Effect of Near-Field DRZ Integrity on Annual Dose from ^{129}I in the Salt GDS Model

Brine Flow Rate—The effect of the brine flow rate on ^{129}I annual dose is shown in Figure 3-54. The sensitivity analysis includes three brine flow cases:

- Baseline Brine Flow—The brine flow rate through the EBS, near-field salt DRZ, and interbed is based on a single flow rate history realization from Clayton et al. (2011, Section 3.1.3). The baseline flow history, summarized below in Table 3-22, results in diffusion-dominated transport throughout the disposal system.
- Brine Flow Increased by a Factor of 10—A multiplier of 10 is applied to the baseline brine flow rate histories in all regions. The increased brine flow represents the potential effects of repository pressurization from creep closure and gas generation and/or higher permeability. These increased flow rates result in advective transport that is of the same order of magnitude as diffusive transport.
- Brine Flow Increased by a Factor of 100—A multiplier of 100 is applied to the baseline brine flow rate histories in all regions. These increased flow rates result in advection-dominated transport throughout the system.

Table 3-22. Summary of the Baseline Brine Flow

Time (yrs)	Darcy Velocity in EBS and Near-Field DRZ (m/yr)	Darcy Velocity in Interbed (m/yr)
0	0	0
9,000	0	0
10,000	3.36×10^{-9}	2.79×10^{-14}
100,000	2.57×10^{-6}	6.92×10^{-9}
480,000	8.89×10^{-6}	1.47×10^{-6}
1,000,000	8.56×10^{-7}	3.96×10^{-7}
10,000,000	8.56×10^{-7}	3.96×10^{-7}

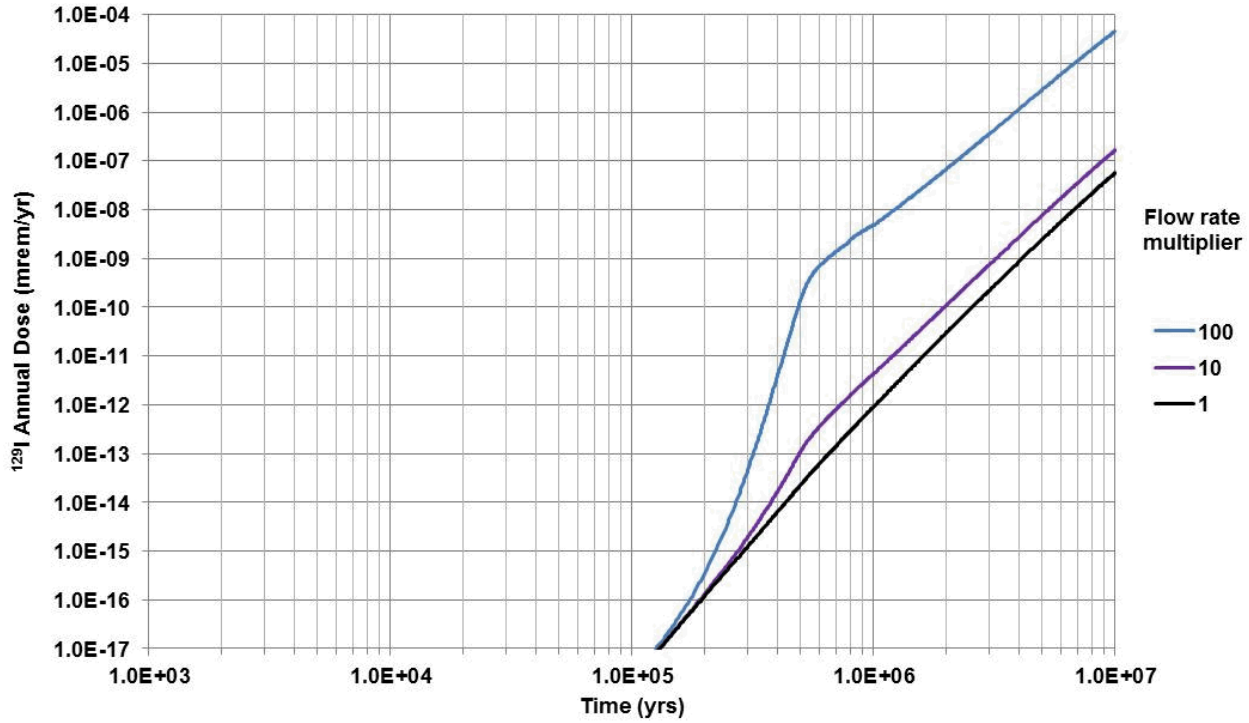

Figure 3-54. Effect of Brine Flow Rate on Annual Dose from ^{129}I in the Salt GDS Model

The case where the brine flow rates are multiplied by 100 has a much more significant effect on dose than when the flow rates are multiplied by 10. This is because the factor-of-100 multiplier changes the disposal system to advection-dominated transport. A significant flow rate increase at around 500,000 years drives the increase in annual dose for the case with the factor-of-100 multiplier. The effects of the factor-of-10 brine flow multiplier are much smaller (only about a factor of 2 increase in dose) because the increase in flow is only increasing the contribution from advective transport to a level similar to that already provided by diffusive transport.

Diffusion—The effect of the diffusion coefficient on ^{129}I annual dose is shown in Figure 3-55. The sensitivity analysis includes two cases:

- Baseline Molecular (Free Water) Diffusion Coefficient (2.30×10^{-9} m^2/s)—The corresponding effective diffusion coefficient for ^{129}I in each region is based on the local porosity and tortuosity.
- Enhanced Molecular (Free Water) Diffusion Coefficient (1.15×10^{-8} m^2/s)—This results in a corresponding effective diffusion coefficient for ^{129}I in each region that is a factor of 5 larger than the baseline value. The increased molecular diffusion coefficient reproduces potential changes in the effective diffusion coefficient for ^{129}I that might result from changes in available porosity (e.g., due to anion exclusion) or tortuosity.

The factor-of-5 increase in diffusion coefficient has a significant effect on dose. This is because of the corresponding factor-of-5 increase in diffusive flux rate in a diffusion-dominated system, which shifts the dose curve to the left by a factor of five on the time axis.

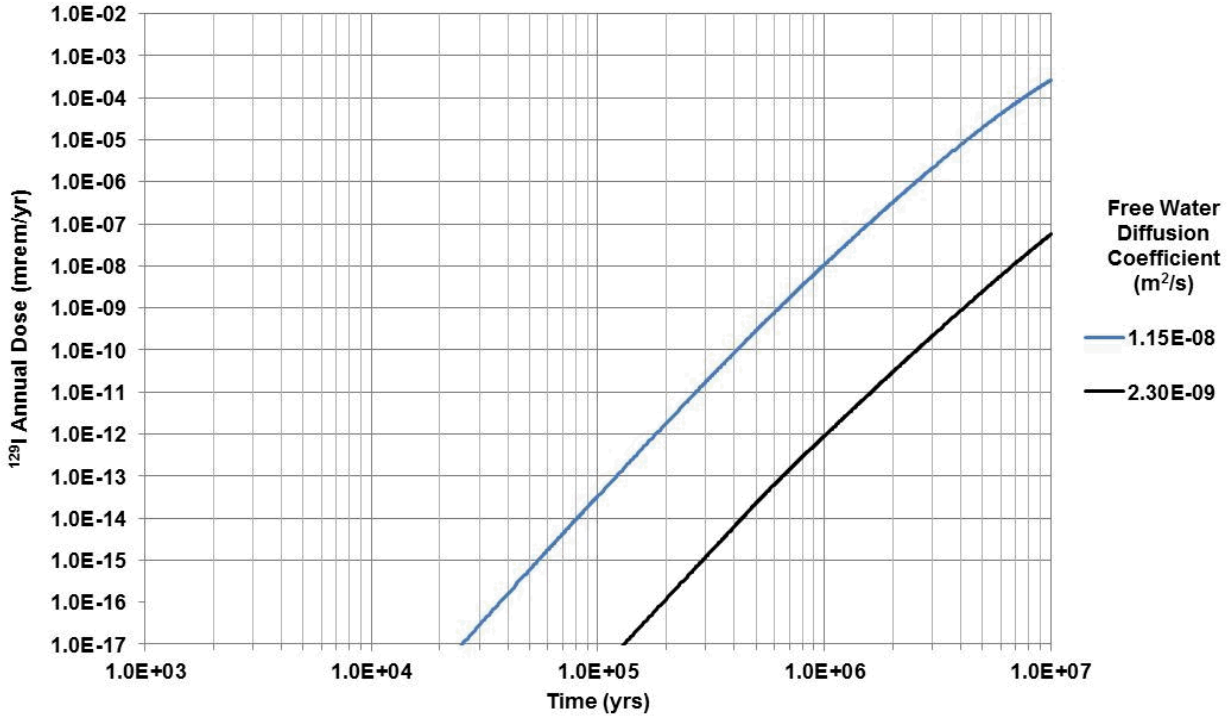

Figure 3-55. Effect of Diffusion Coefficient on Annual Dose from ^{129}I in the Salt GDS Model

Interbed Sorption—The effect of sorption in the interbed on ^{129}I annual dose is shown in Figure 3-56. The sensitivity analysis includes three cases:

- Baseline ^{129}I Sorption (K_d = 0.00 mL/g)—The corresponding retardation factor in the interbed is 1.0.
- Increased ^{129}I Sorption (K_d = 0.01 mL/g)—The corresponding retardation factor in the interbed is 3.5.
- Increased ^{129}I Sorption (K_d = 0.10 mL/g)—The corresponding retardation factor in the interbed is 26.0.

Very small changes in ^{129}I K_d have a significant effect on annual dose. This is because of the delay in transport that is represented by the associated retardation factor. For the case with K_d = 0.01 mL/g and R_f = 3.5, the dose curve shifts to the right by a factor of 3.5 on the time axis. For the case with K_d = 0.10 mL/g and R_f = 26.0, the dose curve shifts to the right by a factor of 26 on the time axis.

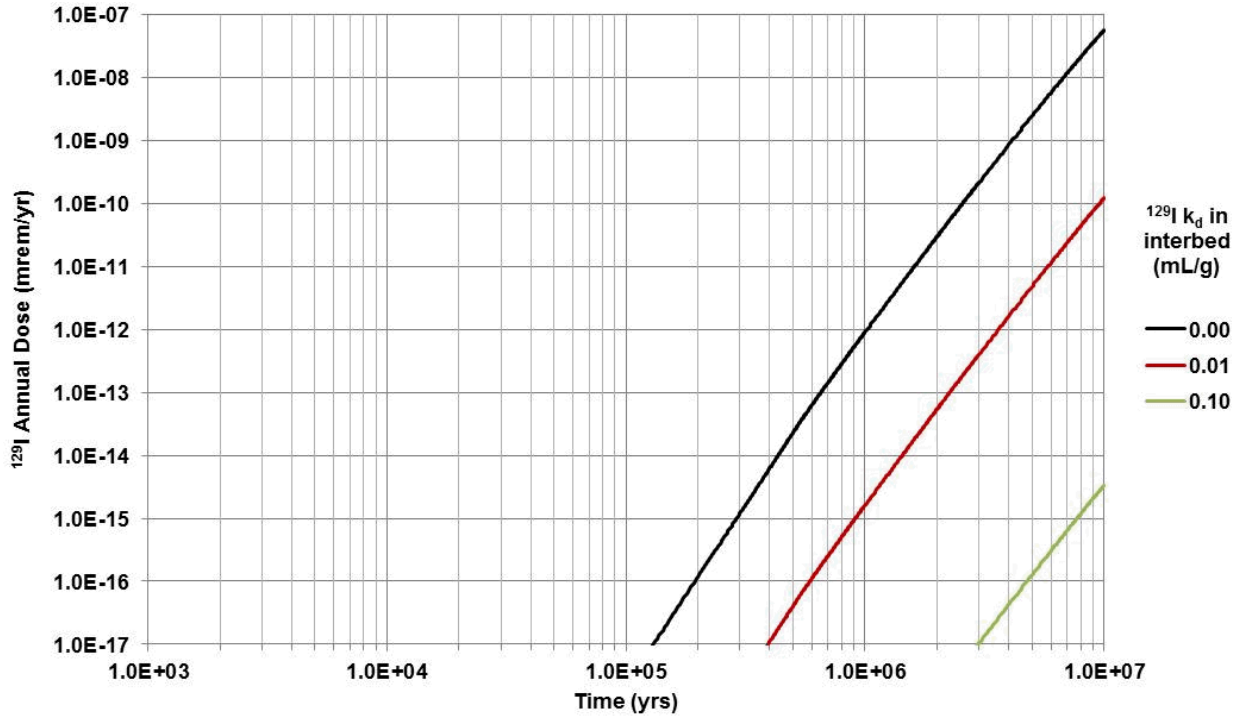

Figure 3-56. Effect of Interbed Sorption on Annual Dose from ^{129}I in the Salt GDS Model

Receptor Distance—The effect of distance to the receptor on ^{129}I annual dose is shown in Figure 3-57. The sensitivity analysis includes three cases:

- Baseline interbed length to receptor (5,000 m)
- Reduced interbed length to receptor (3,000 m)
- Reduced interbed length to receptor (1,000 m)

The annual dose is quite sensitive to the length to the receptor. The effects of reducing the length are greater than linear because, in these salt disposal system simulations, diffusion is the dominant transport mechanism in the interbed and the peak dose is controlled the leading edge of the diffusion front.

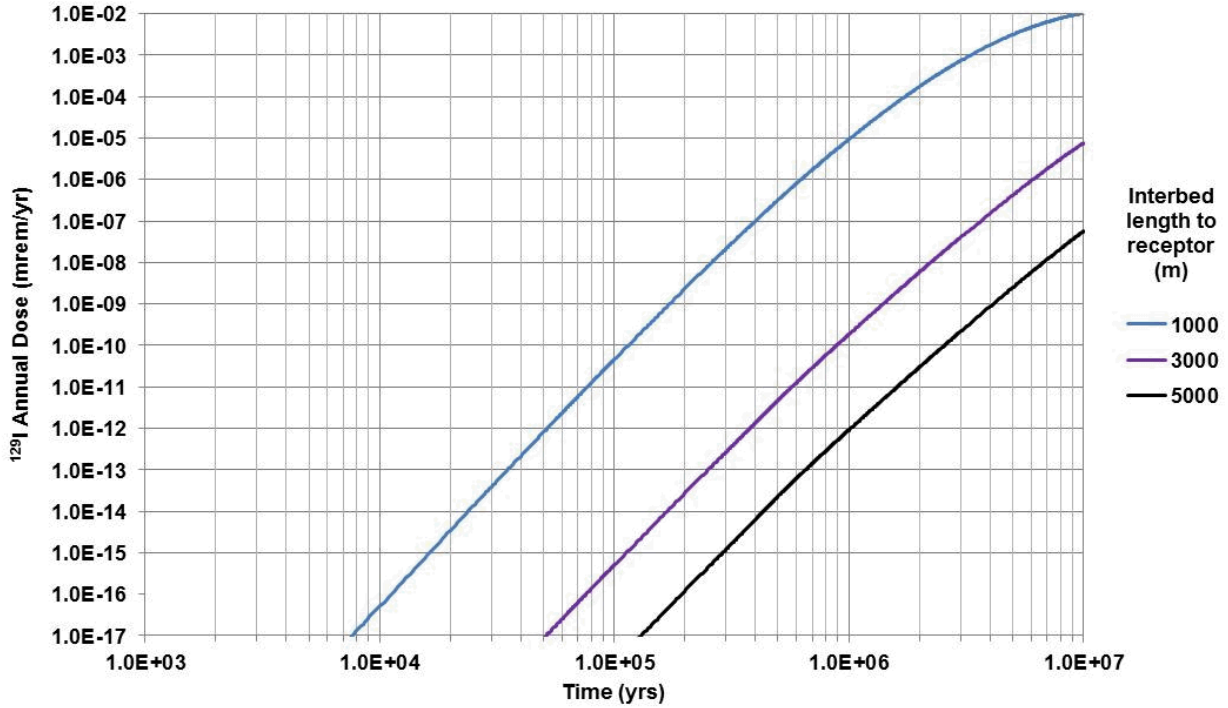

Figure 3-57. Effect of Distance to Receptor on Annual Dose from ^{129}I in the Salt GDS Model

Summary—Based on these six sensitivity analyses examining "one-off" conditions from the baseline scenario, the following observations can be made regarding the performance of a generic salt disposal system under baseline scenario conditions:

- Processes and parameters affecting radionuclide transport through the 5,000-m far-field interbed can have a significant effect on annual dose. These include sorption, K_d, and distance to receptor.
- Processes and parameters affecting radionuclide transport through the entire salt disposal system can have a significant effect on annual dose. These include brine flow rate and diffusion coefficient. These system-wide effects are most important in the far-field interbed.
- Processes and parameters affecting waste form degradation can have a moderate effect on annual dose. Increasing the degradation rate does not significantly increase the dose because the effects are mitigated by slow diffusion into and through the far-field interbed. Decreasing the degradation rate decreases the annual dose.
- Processes and parameters affecting radionuclide transport through the 5-m near-field salt DRZ have a minimal effect on dose.

3.5.3.2 Granite Sensitivity Analyses

Annual dose results from the deterministic granite baseline scenario are shown in Figure 3-46. The following one-off sensitivity simulations were performed to investigate the effects on ^{129}I movement through the disposal system:

- Waste form fractional degradation rate and gap fraction (Figure 3-58)
- Waste package lifetime (Figure 3-59)
- Sorption (^{129}I distribution coefficient) in the bentonite buffer (Figure 3-60)
- Flow rate in the near-field and far-field granite (Figure 3-61)
- Molecular diffusion coefficient (Figure 3-62)
- Sorption (^{129}I distribution coefficient) in the far-field granite (Figure 3-63)
- Fracture spacing in the far-field granite (Figure 3-64)
- Distance to receptor (Figure 3-65)

Waste Form Degradation—The effect of waste form degradation rate on ^{129}I annual dose is shown in Figure 3-58. The sensitivity analysis includes four fractional degradation rate cases:

- Fast Waste Form Degradation ($0.1\ yr^{-1}$)—100% of the radionuclide mass is released from the waste form in the first 250 years. This provides a bounding case for instantaneous release of gap and grain boundary inventory from the waste form equivalent to a gap fraction of 1.0.
- Baseline Waste Form Degradation ($2\times10^{-5}\ yr^{-1}$)—50% of the radionuclide mass is released from the waste form in the first 35,000 years, 95% of the mass is released by 150,000 years, and 99.9% of the mass is released by about 350,000 years.
- Baseline Waste Form Degradation ($2\times10^{-5}\ yr^{-1}$) with 0.2675 gap fraction—The same fractional degradation rate as the baseline case, but 26.75% of the initial ^{129}I mass is released instantaneously. This corresponds to the maximum ^{129}I gap fraction in SNL (2008d, Table 6.3.7-29).
- Slow Waste Form Degradation ($1\times10^{-7}\ yr^{-1}$)—50% of the radionuclide mass is released from the waste form after 4,800,000 years, and 76% of the mass is released by 10,000,000 years.

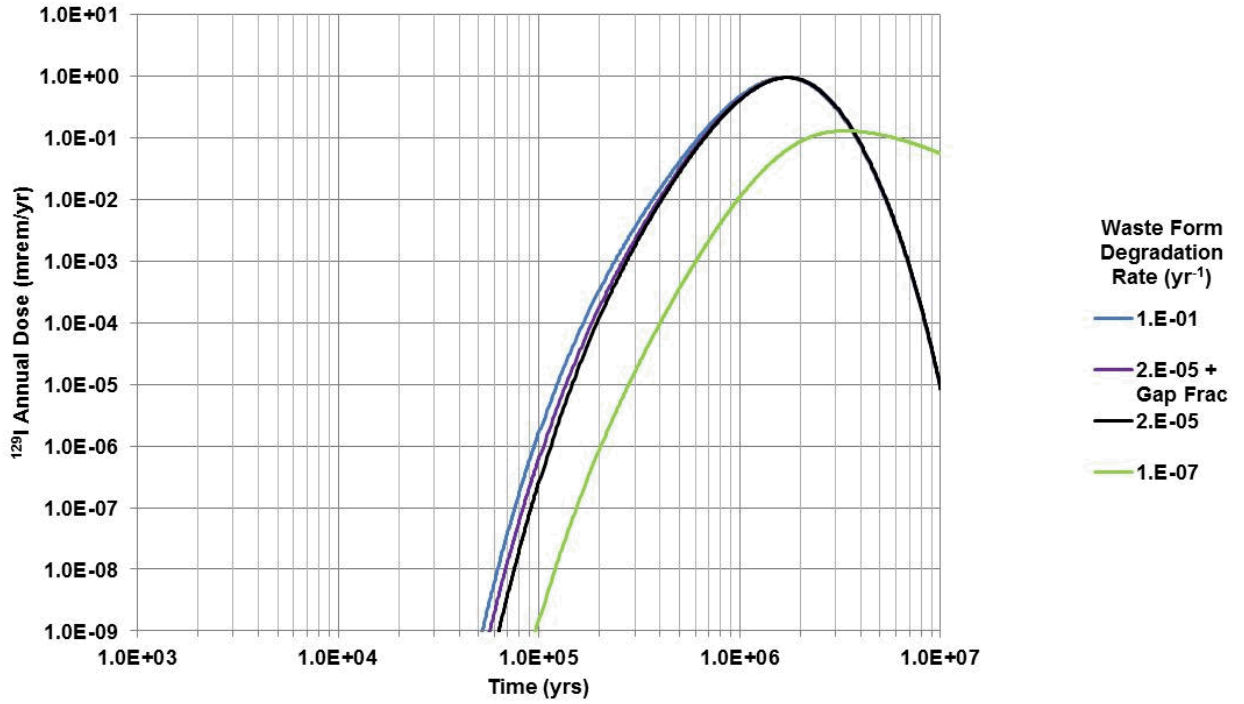

Figure 3-58. Effect of Waste Form Degradation Rate and Gap Fraction on Annual Dose from ^{129}I in the Granite GDS Model

In the fast degradation rate (0.1 yr^{-1}) case, all mass is released (degraded) from the waste form in the first 250 years. This is roughly equivalent to assuming that all ^{129}I mass is instantaneously released as gap and grain boundary inventory (i.e., a ^{129}I gap fraction of 1.0 as compared to the estimated range of 0.0204–0.2675). The mass released from the waste form diffuses vertically through the 0.36-m thick bentonite buffer, and then advects through the 0.78-m thick granite DRZ and 5,000 m of far-field fractured granite. In the fast degradation rate case, 44% of the initial ^{129}I mass reaches the granite by 100,000 years, whereas in the baseline case, only 37% of the initial mass reaches the granite by 100,000 years, and 14% of the mass is still undegraded. Despite the greater early transport of ^{129}I mass away from the repository in the fast degradation rate case, the effect on annual dose is not significant. This is because the effect of the early mass on annual dose is offset by (1) diffusion-dominated transport in the bentonite buffer which tends to attenuate the releases, and (2) long travel times through the far-field granite.

The result from the case with the baseline degradation rate and a 0.2675 gap fraction falls between the baseline result (gap fraction of 0.0) and the fast degradation rate case result (gap fraction of 1.0). This further emphasize that the gap fraction does not have a significant effect under the conceptual assumptions of this generic granite disposal system.

For the slow fractional degradation rate (1×10^{-7} yr^{-1}), 50% of the radionuclide mass is not released from the waste form until 4,800,000 years, and only 76% of the mass is released by 10,000,000 years. In this case, the degradation time is slower than the travel time through the far-field granite and the effect of the slower degradation rate is to reduce the magnitude of the peak dose by about a factor of 7 and delay the time of the peak dose by about a factor of 2.

Waste Package Degradation—The effect of waste package lifetime on ^{129}I annual dose is shown in Figure 3-59. The sensitivity analysis includes four cases:

- Baseline Waste Package Lifetime (0 years)—1% (160) of the waste packages fail instantaneously, no performance credit for the waste package.
- Moderate Waste Package Lifetime (100,000 years)—160 waste packages fail at 100,000 years.
- Long Waste Package Lifetime (500,000 years)—160 waste packages fail at 500,000 years.
- Very Long Waste Package Lifetime (1,000,000 years)—160 waste packages fail at 1,000,000 years.

The effect of waste package lifetime on system performance is to delay the onset of waste form degradation and radionuclide release from the waste form. The delay is evident in the annual dose curves; they are all shifted to the right on the time axis (100,000, 500,000, and 1,000,000 years) relative to the baseline case.

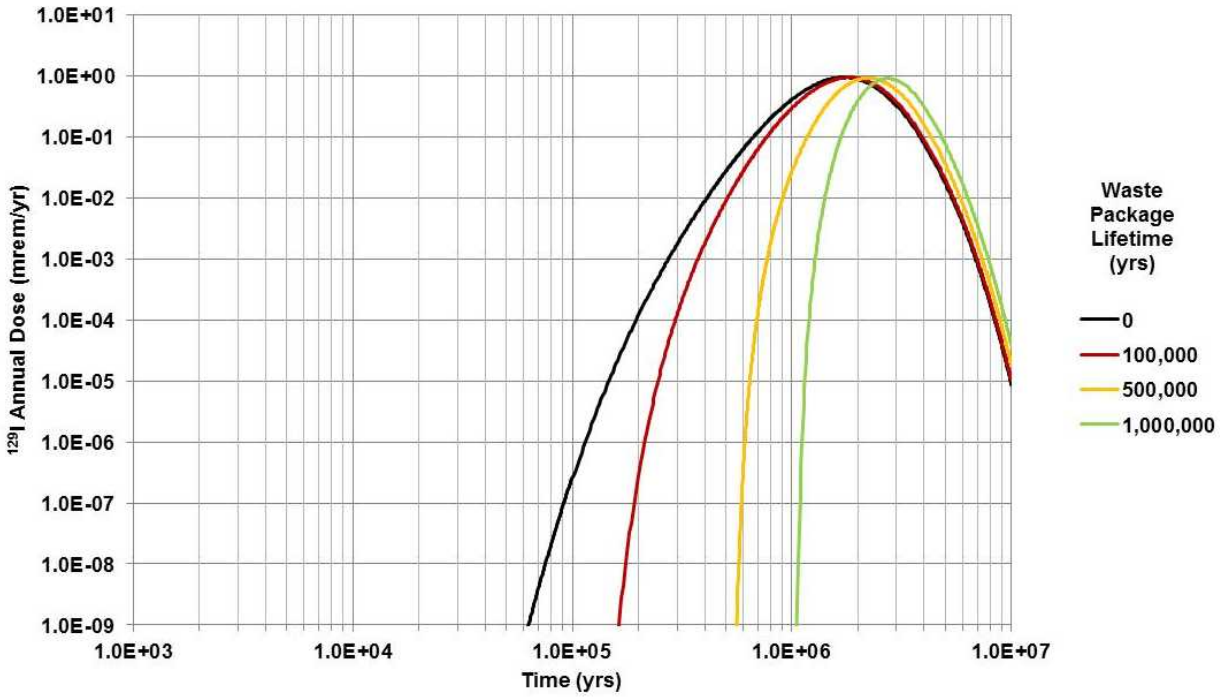

Figure 3-59. Effect of Waste Package Lifetime on Annual Dose from ^{129}I in the Granite GDS Model

Bentonite Sorption—The effect of sorption in the bentonite buffer on ^{129}I annual dose is shown in Figure 3-60. The sensitivity analysis includes three cases:

- Baseline ^{129}I Sorption (K_d = 0.0 mL/g)—The corresponding retardation factor is 1.0.
- Increased ^{129}I Sorption (K_d = 1.0 mL/g)—The corresponding retardation factor is 4.6.
- Increased ^{129}I Sorption (K_d = 5.0 mL/g)—The corresponding retardation factor is 19.0.

Very small changes in ^{129}I K_d in the bentonite buffer have a moderate effect on annual dose. This is because of the delay in transport that is represented by the associated retardation factor. However, due to the small (0.36 m) transport length of the buffer relative to the 5,000-m transport length of the far-field granite, sorption in the bentonite buffer is not as important to overall system performance as measured by annual dose. For the case with K_d = 5.0 mL/g and R_f = 19.0, the dose curve only shifts to the right by a factor of about 1.2 on the time axis relative to the baseline case.

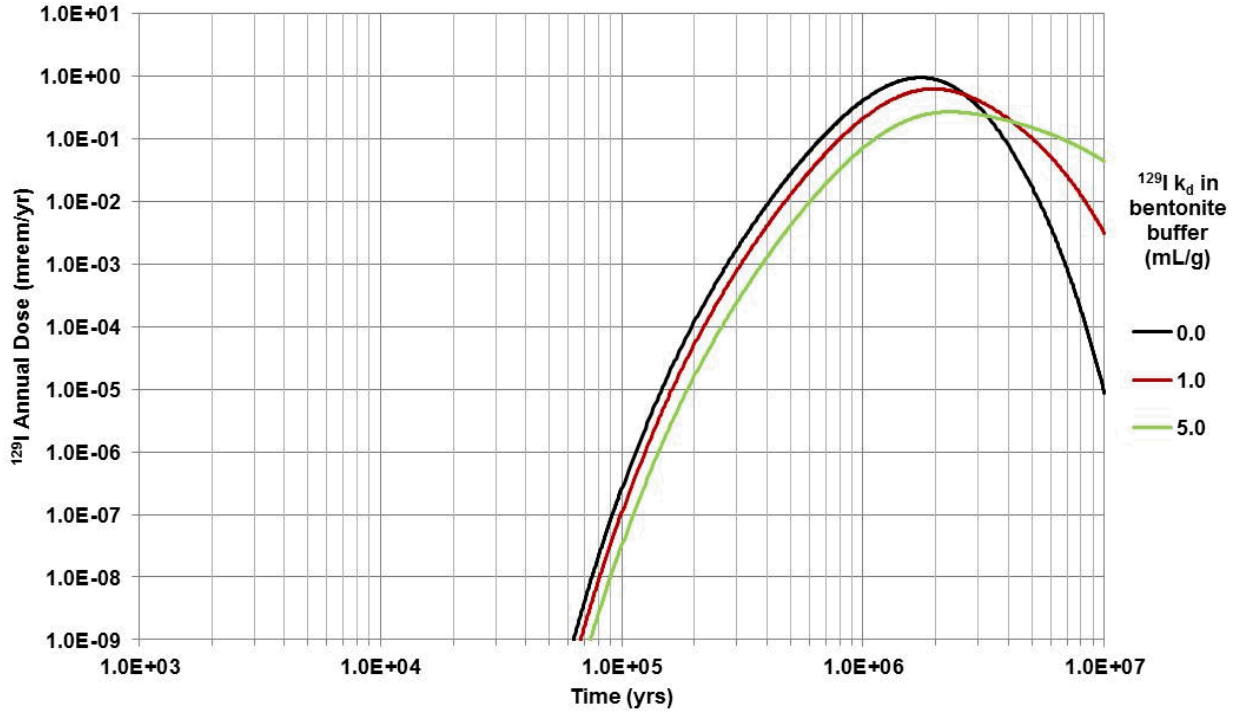

Figure 3-60. Effect of Sorption in Bentonite Buffer on Annual Dose from ^{129}I in the Granite GDS Model

Flow Rate—The effect of the flow rate on ^{129}I annual dose is shown in Figure 3-61. The sensitivity analysis includes three cases:

- Increased Volumetric Flow Rate (5.1×10^{-3} m^3/yr)—The baseline volumetric flow rate and darcy velocity through the granite is increased by a factor of 10. This increased flow velocity results in advection-dominated transport through the granite.
- Baseline Volumetric Flow Rate (5.1×10^{-4} m^3/yr)—The corresponding darcy velocity through the granite is 9.6×10^{-6} m·yr^{-1}. This flow velocity results in advection-dominated transport through the granite.
- Decreased Volumetric Flow Rate (5.1×10^{-5} m^3/yr)—The baseline volumetric flow rate and darcy velocity through the granite is reduced by a factor of 10. This reduced flow velocity still results in advection-dominated transport through the granite.

In the advection-dominated granite disposal system, the effect of changing the flow rate is to shift the time of peak dose by a corresponding factor along the time axis. The magnitude of peak is lower with lower flow rates due to greater radioactive decay and greater dispersion as the peak moves further out in time.

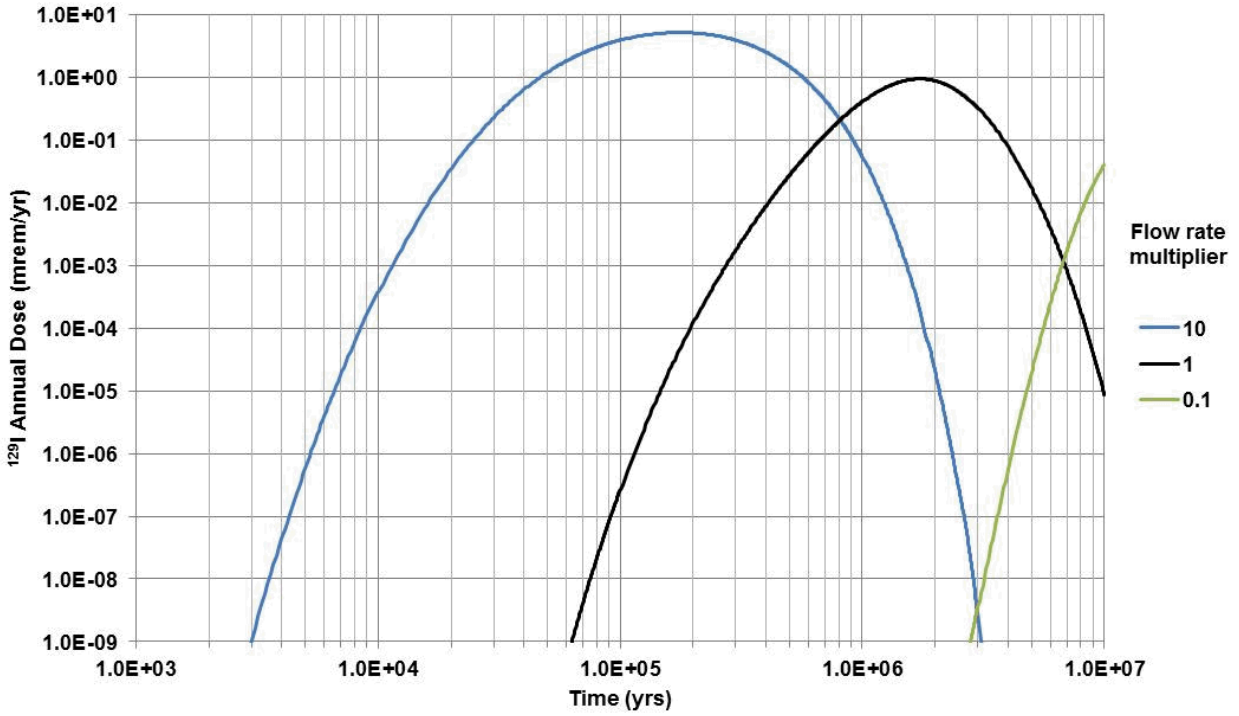

Figure 3-61. Effect of Flow Rate on Annual Dose from ^{129}I in the Granite GDS Model

Diffusion—The effect of the diffusion coefficient on ^{129}I annual dose is shown in Figure 3-62. The sensitivity analysis includes two cases:

- Baseline Molecular (Free Water) Diffusion Coefficient (2.30×10^{-9} m^2/s)—The corresponding effective diffusion coefficient for ^{129}I in each region is based on the local porosity and tortuosity.
- Enhanced Molecular (Free Water) Diffusion Coefficient (1.15×10^{-8} m^2/s)—This results in a corresponding effective diffusion coefficient for ^{129}I in each region that is a factor of 5 larger than the baseline value. The increased molecular diffusion coefficient reproduces potential changes in the effective diffusion coefficient for ^{129}I that might result from changes in available porosity (e.g., due to anion exclusion) or tortuosity.

Increasing the diffusion coefficient has no effect on the annual dose in an advection-dominated system.

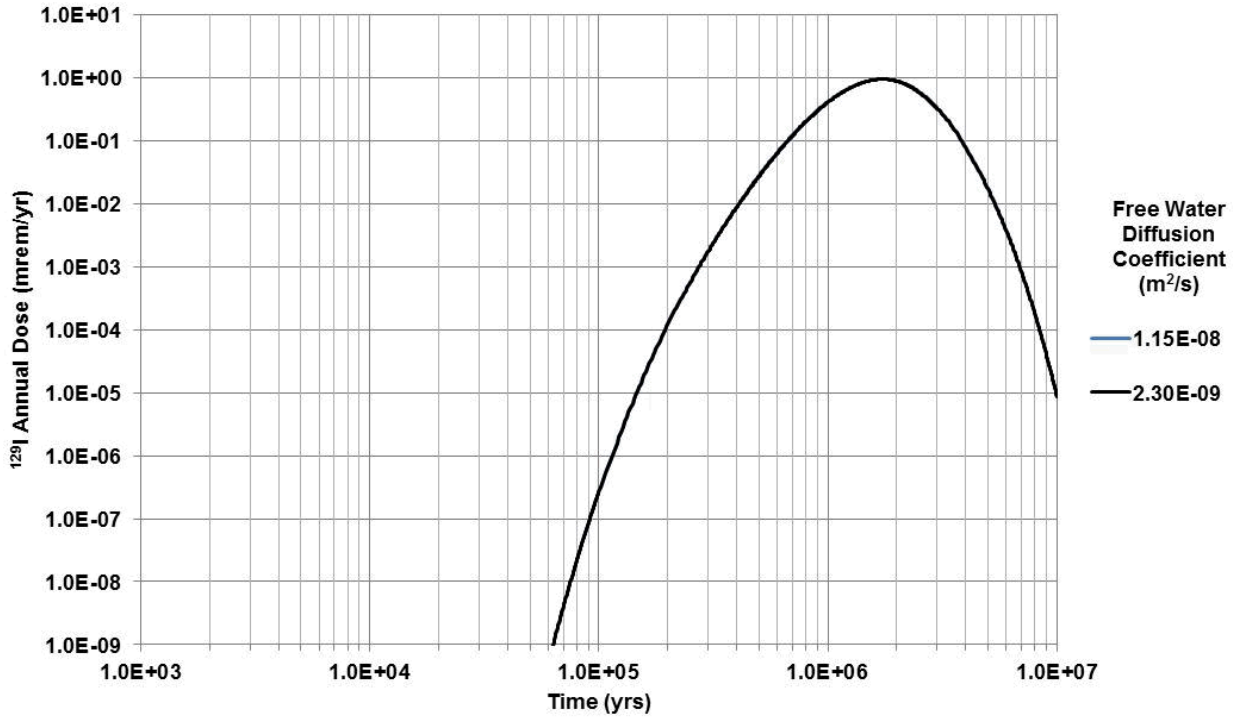

Figure 3-62. Effect of Diffusion Coefficient on Annual Dose from ^{129}I in the Granite GDS Model

Far-Field Sorption—The effect of sorption in the far-field granite on ^{129}I annual dose is shown in Figure 3-63. The sensitivity analysis includes three cases:

- Baseline ^{129}I Sorption (K_d = 0.00 mL/g)—The corresponding retardation factor is 1.0.
- Increased ^{129}I Sorption (K_d = 0.01 mL/g)—The corresponding retardation factor is 16.0.
- Increased ^{129}I Sorption (K_d = 0.10 mL/g)—The corresponding retardation factor is 151.

Very small changes in ^{129}I K_d have a significant effect on annual dose. This is because of the delay in transport that is represented by the associated retardation factor. For the case with K_d = 0.01 mL/g and R_f = 16.0, the dose curve shifts to the right by a factor of 16 on the time axis. For the case with K_d = 0.10 mL/g and R_f = 151, the dose curve shifts so far to the right on the time axis that it does not show on the plot.

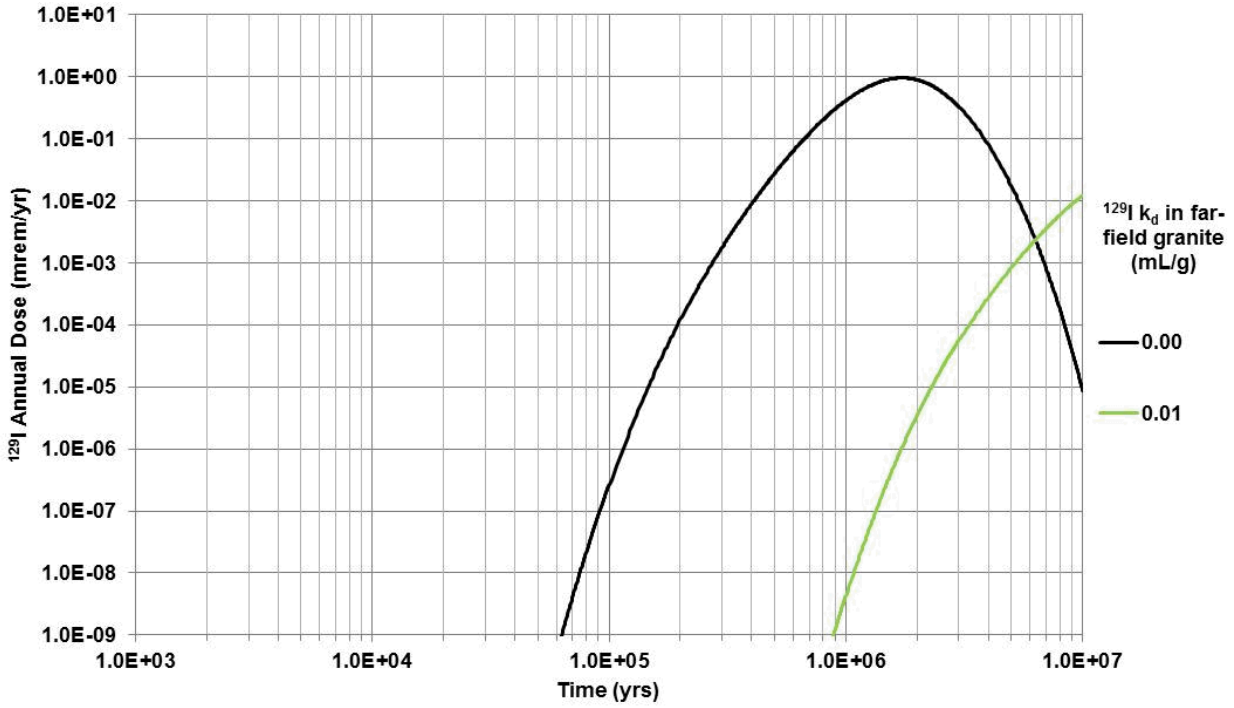

Figure 3-63. Effect of Sorption in Granite on Annual Dose from ^{129}I in the Granite GDS Model

Fracture Spacing—The effect of fracture spacing in the far-field granite on ^{129}I annual dose is shown in Figure 3-64. The sensitivity analysis includes two cases:

- Baseline fracture spacing (25 m)
- Reduced fracture spacing (10 m)

Fracture spacing in the granite affects the matrix diffusion length. The baseline case with a larger matrix diffusion length produces a more matrix diffusion and a corresponding greater delay in advective transport through the fracture.

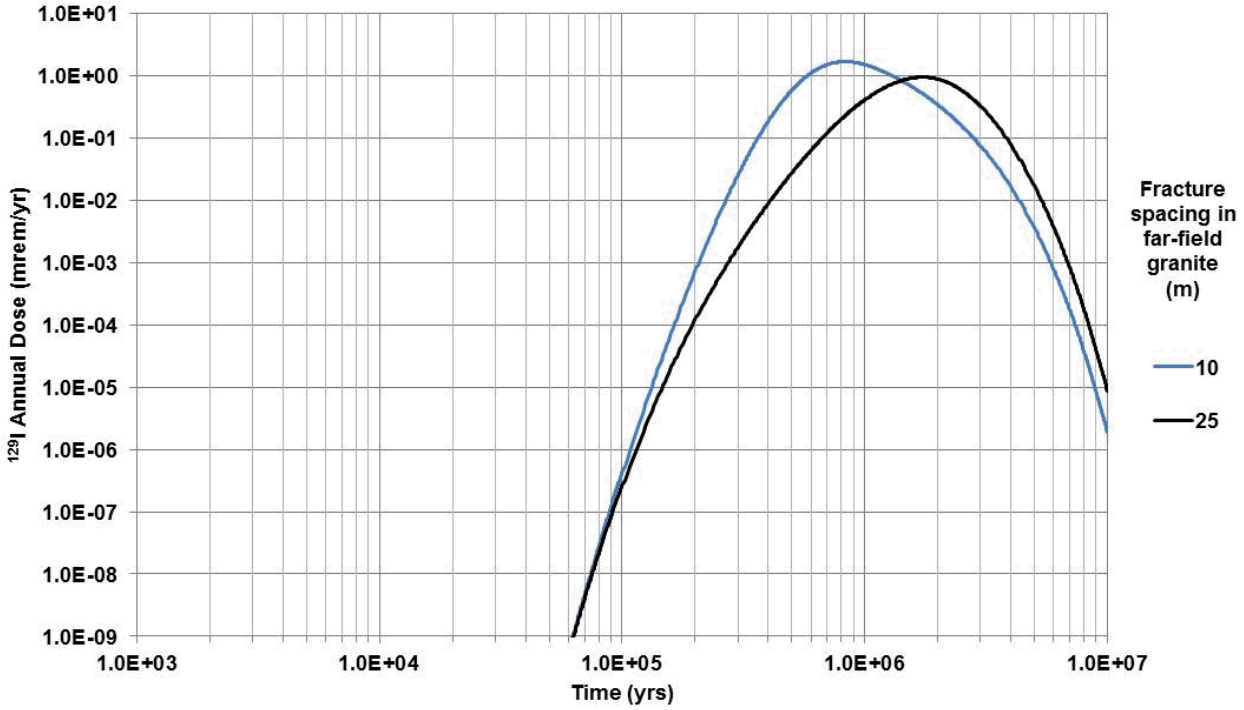

Figure 3-64. Effect of Fracture Spacing in Granite on Annual Dose from ^{129}I in the Granite GDS Model

Receptor Distance—The effect of distance to the receptor on ^{129}I annual dose is shown in Figure 3-65. The sensitivity analysis includes three cases:

- Baseline granite length to receptor (5,000 m)
- Reduced granite length to receptor (3,000 m)
- Reduced granite length to receptor (1,000 m)

The annual dose is quite sensitive to the granite length to the receptor location. In this advection dominated granite disposal system simulations, the effects of reducing the granite length are approximately linear.

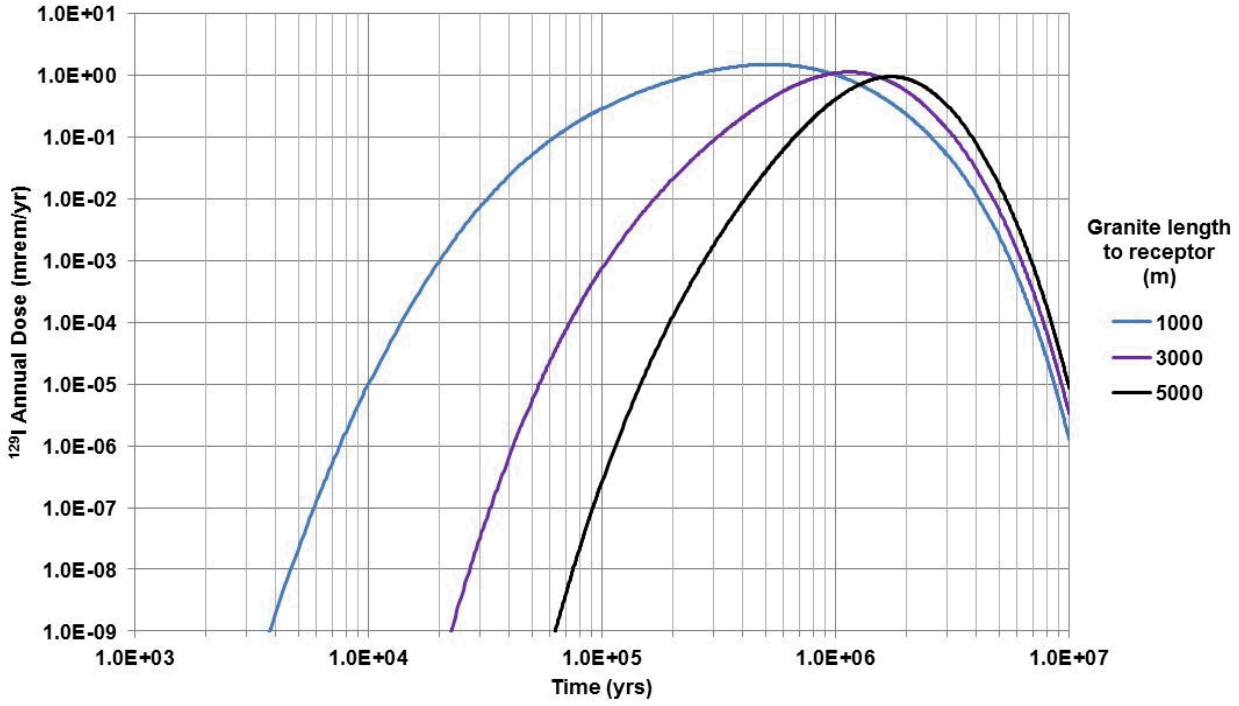

Figure 3-65. Effect of Distance to Receptor on Annual Dose from ^{129}I in the Granite GDS Model

Summary—Based on these eight sensitivity analyses examining "one-off" conditions from the baseline scenario, the following observations can be made regarding the performance of a generic granite disposal system under baseline scenario conditions:

- Processes and parameters affecting radionuclide transport through the 5,000-m far-field granite can have a significant effect on annual dose. These include sorption, K_d, distance to receptor, and fracture spacing.
- Processes and parameters affecting radionuclide transport through the entire granite disposal system can have a significant effect on annual dose. Increasing or decreasing the flow rate correspondingly affects the dose. This system-wide effect is most important in the advection-dominated far-field granite.

- Processes and parameters affecting waste form degradation can have a moderate effect on annual dose. Increasing the degradation rate does not significantly increase the dose because the effects are mitigated by slow diffusion through the bentonite buffer and a long travel time through the far-field granite. Decreasing the degradation rate decreases the annual dose.
- Processes and parameters affecting waste package lifetime can have a significant effect on annual dose. Increasing the waste package lifetime delays the onset of waste form degradation and radionuclide release from the waste form.
- Processes and parameters affecting radionuclide transport through the 0.36-m bentonite buffer can have a moderate effect on dose. These include buffer damage and sorption, K_d.

3.5.3.3 Clay Sensitivity Analyses

Annual dose results from the deterministic clay baseline scenario are shown in Figure 3-48. The following one-off sensitivity simulations were performed to investigate the effects on ^{129}I movement through the disposal system:

- Waste form fractional degradation rate (Figure 3-66)
- Waste package lifetime (Figure 3-67)
- Integrity of the bentonite buffer and DRZ clay (Figure 3-68)
- Flow rate in the EBS and far field (Figure 3-69)
- Molecular diffusion coefficient (Figure 3-70)
- Sorption (^{129}I distribution coefficient) in the far-field clay (Figure 3-71)
- Thickness of the far-field clay (Figure 3-72)

Waste Form Degradation—The effect of waste form degradation rate on ^{129}I annual dose is shown in Figure 3-66. The sensitivity analysis includes the same three fractional degradation rate cases as considered in the salt analyses:

- Fast Waste Form Degradation ($0.1\ yr^{-1}$)—100% of the radionuclide mass is released from the waste form in the first 250 years. This provides a bounding case for instantaneous release of gap and grain boundary inventory from the waste form.
- Baseline Waste Form Degradation ($2\times10^{-5}\ yr^{-1}$)—50% of the radionuclide mass is released from the waste form in the first 35,000 years, 95% of the mass is released by 150,000 years, and 99.9% of the mass is released by about 350,000 years.
- Slow Waste Form Degradation ($1\times10^{-7}\ yr^{-1}$)—50% of the radionuclide mass is released from the waste form after 4,800,000 years, and 76% of the mass is released by 10,000,000 years.

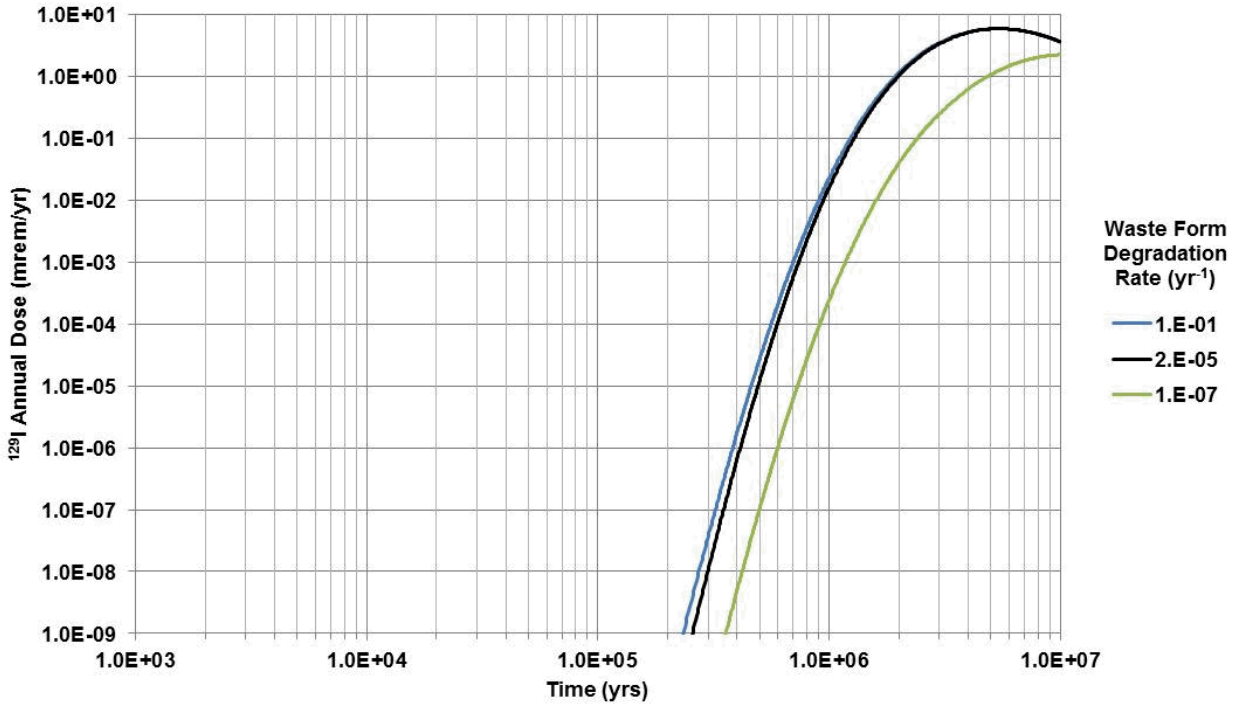

Figure 3-66. Effect of Waste Form Degradation Rate on Annual Dose from ^{129}I in the Clay GDS Model

In the fast degradation rate (0.1 yr^{-1}) case, all mass is released (degraded) from the waste form in the first 250 years. This is roughly equivalent to assuming that all ^{129}I mass is instantaneously released as gap and grain boundary inventory (i.e., a ^{129}I gap fraction of 1.0 as compared to the estimated range of 0.0204–0.2675). The mass released from the waste form diffuses vertically through the 1.025-m thick bentonite buffer and the 1.15-m thick fissured clay DRZ, and into the 150-m thick clay host rock. In the fast degradation rate case, 86% of the initial ^{129}I mass reaches the far-field clay host rock by 100,000 years, whereas in the baseline case, only 71% of the initial mass reaches the far-field clay by 100,000 years, and 14% of the mass is still undegraded. Despite the greater early transport of ^{129}I mass away from the repository in the fast degradation rate case, the effect on annual dose is not significant. This is because, in a diffusion-dominated system, the effect of the early mass on annual dose is attenuated in the 150-m far-field clay by (1) diffusive fluxes into the far-field that decline over time as a function of the concentration gradient, and (2) slow diffusive travel times through the far-field clay.

In the fast degradation rate case, the early mass results in a larger diffusive flux into the far-field clay at early time. However, this concentration-gradient driven flux quickly equilibrates. Conversely, in the baseline case, the early-time diffusive flux is not as large, but the concentration equilibration is slower. Over longer time scales, the cumulative flux into the far-field is similar in the two cases. Also, in both the baseline and fast waste form degradation cases, the degradation time is shorter than the travel time through the 150-m far-field clay; therefore, the travel time through the far-field clay is the dominant process, and increases in the waste form degradation rate have little effect on annual dose.

For the slow fractional degradation rate (1×10^{-7} yr^{-1}), 50% of the radionuclide mass is not released from the waste form until 4,800,000 years, and only 76% of the mass is released by 10,000,000 years. In this case, the degradation time is slower than the travel time through the far-field clay and the effect of the slower degradation rate is to reduce the magnitude of the peak dose by about a factor of 3 and delay the time of the peak dose by about a factor of 2.

Waste Package Degradation—The effect of waste package lifetime on ^{129}I annual dose is shown in Figure 3-67. The sensitivity analysis includes four cases:

- Baseline Waste Package Lifetime (0 years)—All 16,000 waste packages fail instantaneously, no performance credit for the waste package.
- Moderate Waste Package Lifetime (100,000 years)—All 16,000 waste packages fail at 100,000 years.
- Long Waste Package Lifetime (500,000 years)—All 16,000 waste packages fail at 500,000 years.
- Very Long Waste Package Lifetime (1,000,000 years)—All 16,000 waste packages fail at 1,000,000 years.

The effect of waste package lifetime on system performance is to delay the onset of waste form degradation and radionuclide release from the waste form. The delay is evident in the annual dose curves; they are all shifted to the right on the time axis (100,000, 500,000, and 1,000,000 years) relative to the baseline case.

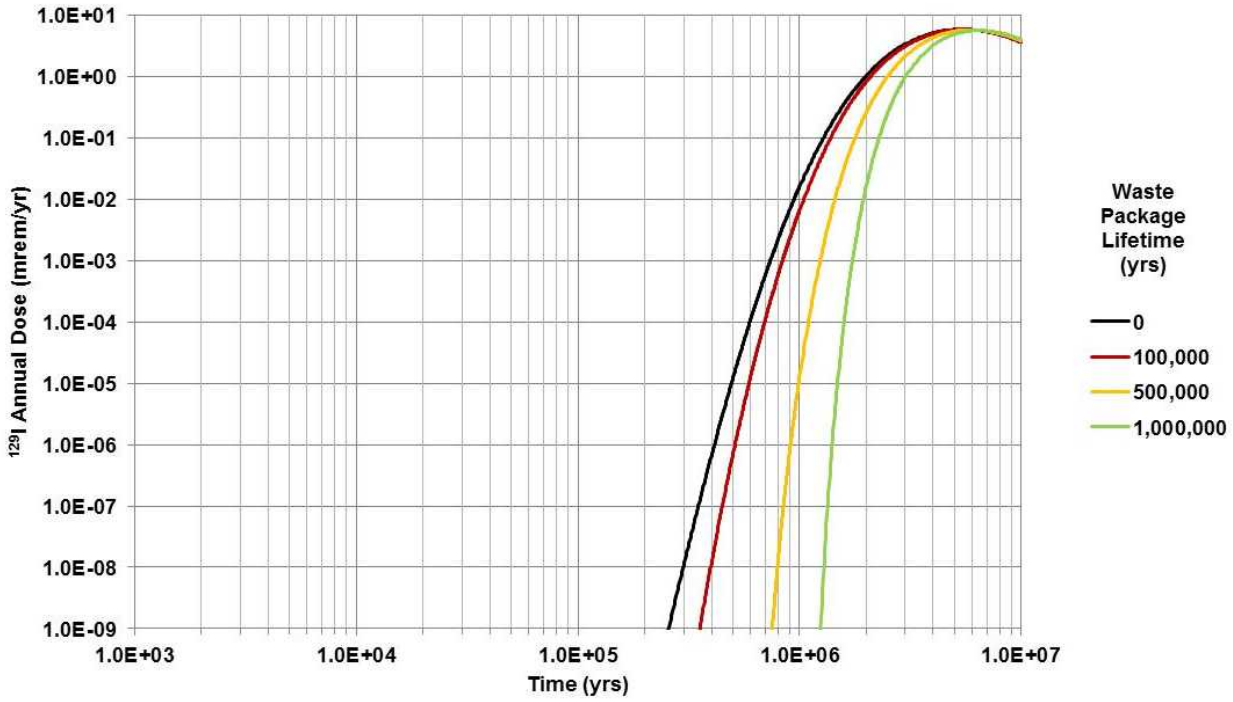

Figure 3-67. Effect of Waste Package Lifetime on Annual Dose from ^{129}I in the Clay GDS Model `

Bentonite Buffer Integrity—The effect of the integrity of the bentonite buffer and DRZ clay on ^{129}I annual dose is shown in Figure 3-68. The sensitivity analysis includes two cases:

- Baseline Intact Bentonite and DRZ—The bentonite buffer is 1.025-m thick and the fissured clay DRZ is 1.15-m thick for a total thickness of 2.175 m. There are no significant fractures through the buffer or DRZ. A constant darcy velocity through the EBS and far-field of 6.3×10^{-7} m/yr is assumed. This flow velocity is low enough that transport through the EBS and far-field is diffusion dominated.
- Damaged Bentonite and DRZ—The thickness of the bentonite buffer and the fissured clay DRZ are both reduced by a factor is 5, for a total effective thickness of 0.435 m. A multiplier of 1,000 is applied to the flow velocity in the EBS, resulting in advection-dominated transport in the EBS. These enhanced transport properties are considered to represent the effects of non-healing fractures connecting the repository and the far-field clay.

The damaged buffer has little effect on annual dose because the combined buffer and DRZ thickness of 2.175 m is much less than the overlying clay thickness of 150 m. Enhanced transport through the EBS is attenuated by slow diffusive transport in the far-field clay.

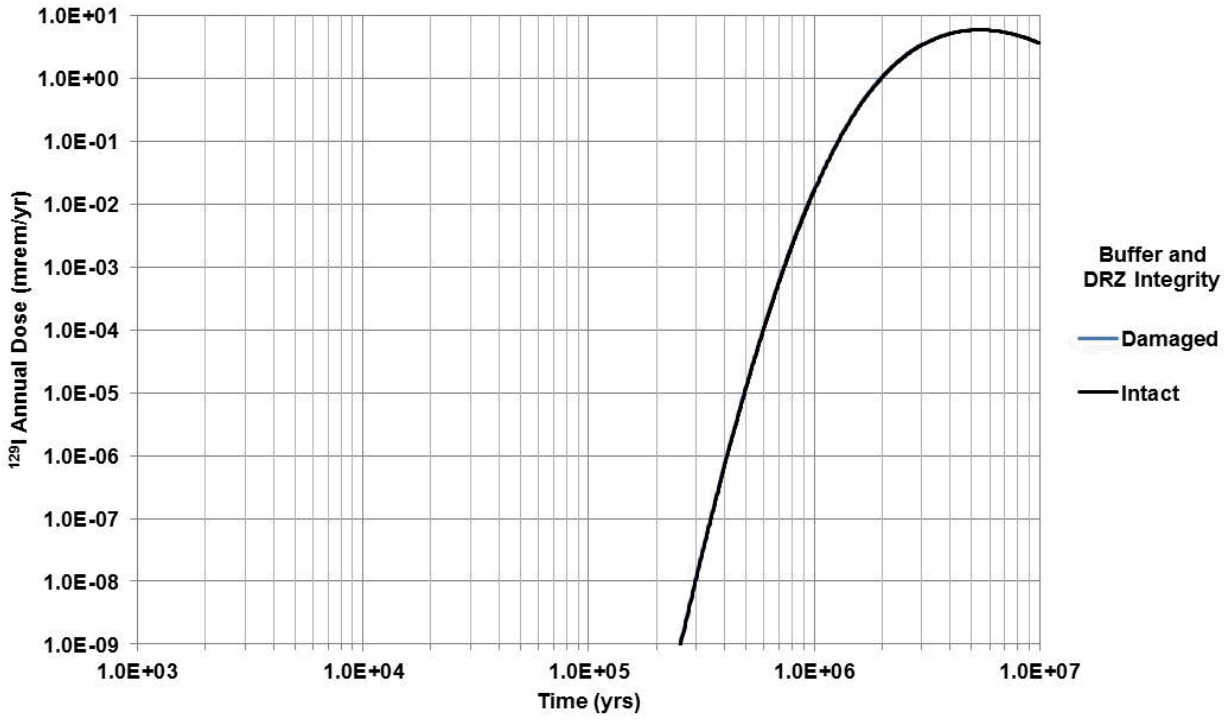

Figure 3-68. Effect of Buffer and DRZ Integrity on Annual Dose from ^{129}I in the Clay GDS Model

Flow Rate—The effect of the flow rate on ^{129}I annual dose is shown in Figure 3-69. The sensitivity analysis includes three cases:

- Increased Flow Rate (6.3×10^{-6} m/yr)—The baseline darcy velocity through the buffer, DRZ, and far-field clay is multiplied by a factor of 10. This flow velocity results in advection-dominated transport at certain times and locations within the disposal system.
- Baseline Flow Rate (6.3×10^{-7} m/yr)—The darcy velocity through the buffer, DRZ and far-field clay is 6.3×10^{-7} m/yr. This flow velocity results in diffusion-dominated transport throughout the disposal system.
- Decreased Flow Rate (6.3×10^{-8} m/yr)—The baseline darcy velocity through the buffer, DRZ, and far-field clay is reduced by a factor of 10. This flow velocity results in diffusion-dominated transport throughout the disposal system.

The case where the brine flow rates are increased has a much more significant effect on dose than when the flow rates are decreased. This is because the factor-of-10 increase results in advection-dominated transport at certain times and locations within the disposal system. The effect of the advective transport is to increase the magnitude of the peak dose by about a factor of 10 and accelerate the time of the peak dose by about a factor of 3.

The effects of the factor-of-10 brine flow decrease are much smaller (only about a factor of 2 decrease in peak dose) because the decrease in flow is only decreasing the contribution from advective transport, which is already smaller than the contribution from diffusive transport.

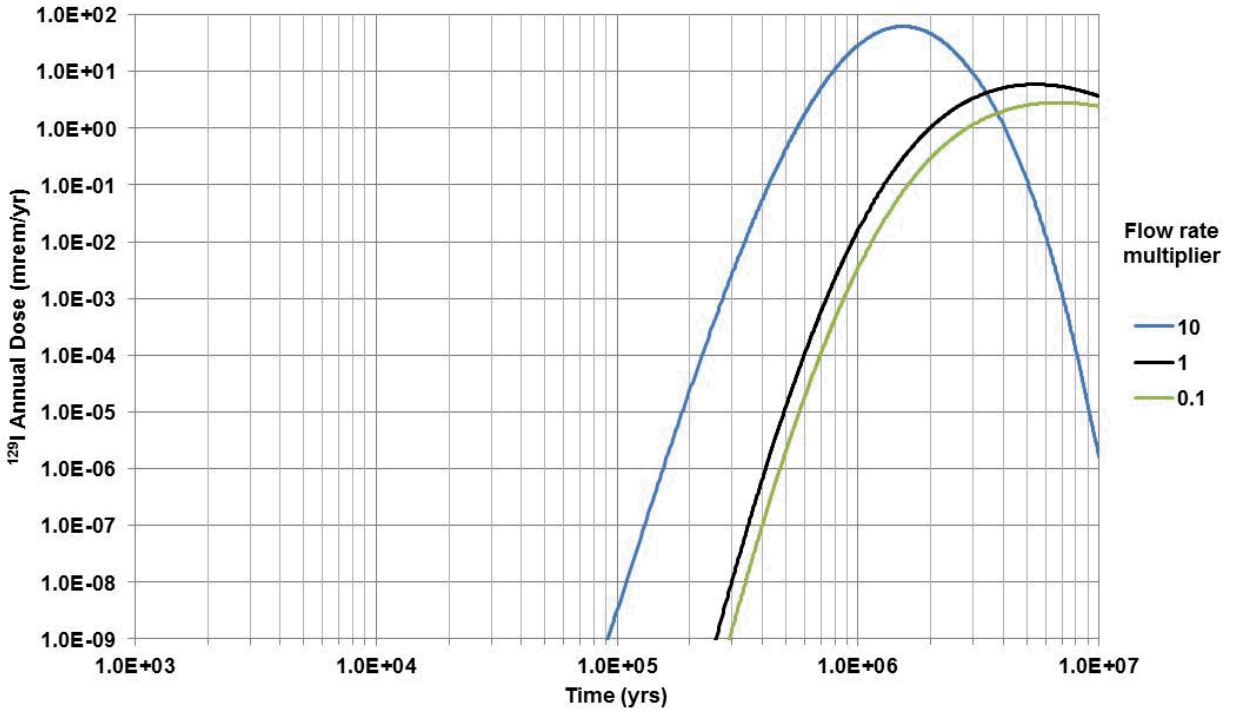

Figure 3-69. Effect of Flow Rate on Annual Dose from ^{129}I in the Clay GDS Model

Diffusion—The effect of the diffusion coefficient on ^{129}I annual dose is shown in Figure 3-70. The sensitivity analysis includes two cases:

- Baseline Molecular (Free Water) Diffusion Coefficient (2.30×10^{-9} m^2/s)—The corresponding effective diffusion coefficient for ^{129}I in each region is based on the local porosity and tortuosity.
- Enhanced Molecular (Free Water) Diffusion Coefficient (1.15×10^{-8} m^2/s)—This results in a corresponding effective diffusion coefficient for ^{129}I in each region that is a factor of 5 larger than the baseline value. The increased molecular diffusion coefficient reproduces potential changes in the effective diffusion coefficient for ^{129}I that might result from changes in available porosity (e.g., due to anion exclusion) or tortuosity.

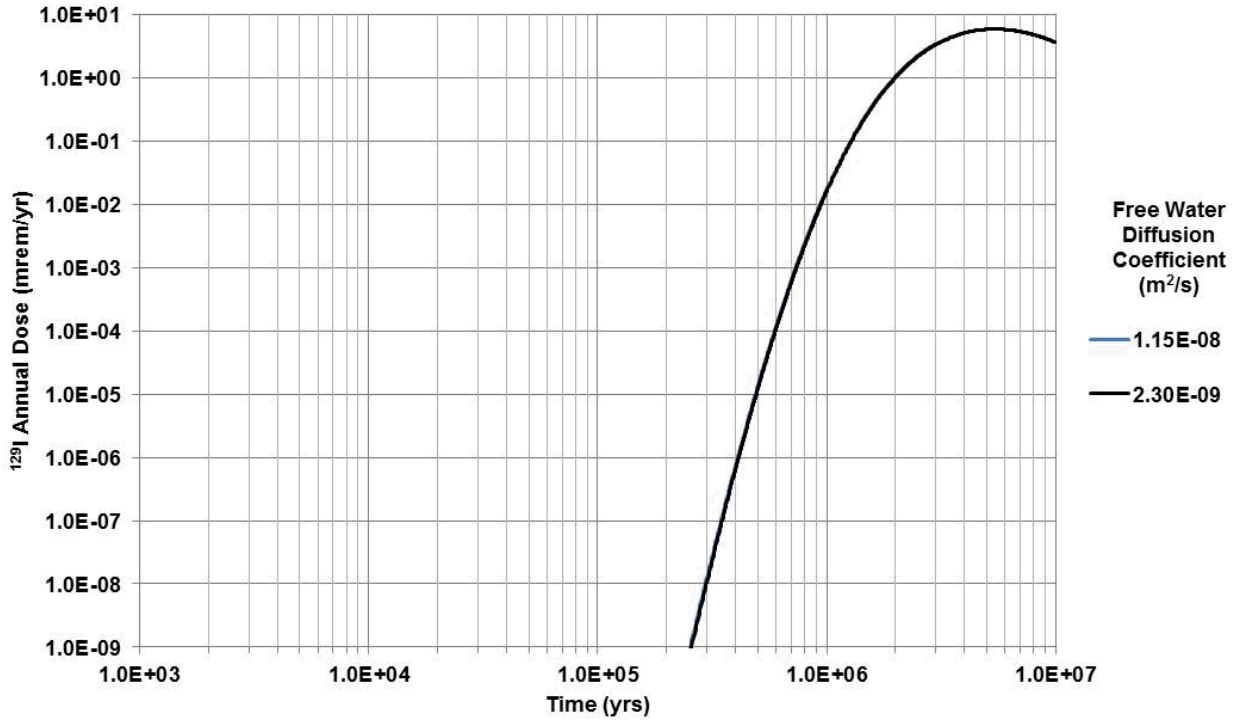

Figure 3-70. Effect of Diffusion Coefficient on Annual Dose from ^{129}I in the Clay GDS Model

In the high diffusion coefficient case, diffusive fluxes would be expected to be a factor of five higher than in the baseline case. However, the effect of the high diffusion coefficient on annual dose is not significant. This is because, in the diffusive-transport-dominated clay disposal system, the effects of a higher diffusive flux on transport through the buffer and DRZ are attenuated in the 150-m, 2D, far-field clay by (1) the conceptual model assumptions about the system geometry, and (2) lateral diffusion in the far-field clay.

At the scale of a single waste package, diffusion into the far-field clay occurs from a single DRZ cell (grid block) into a single clay inlet cell (grid block) across a 79-m^2 diffusion area, corresponding to the surface area of a cylindrical EBS (bentonite buffer and clay DRZ) around a waste package. Diffusion within the far-field clay then occurs from the single inlet cell both vertically and horizontally through a 20 × 20 2D network of cells, where the vertical diffusion area in a single cell is 1.2375 m^2 and the horizontal diffusion

area is 33.75 m^2. Diffusive transport to the receptor location is in the vertical direction, through 150 m of clay. Since diffusion into the far-field clay all enters a single cell and the diffusion area in is greater than the diffusion area out, the single clay inlet cell tends to attenuate diffusive transport. Furthermore, for the mass that does diffuse out of the clay inlet cell, horizontal (lateral) diffusion into the rest of the far-field clay tends to be much greater than vertical (longitudinal) diffusion, due to the larger diffusive area in the horizontal direction. Therefore, the higher diffusive flux associated with the high diffusion coefficient is offset by attenuation in the far-field clay inlet cell and by lateral diffusion in the far-field clay.

Far-Field Sorption—The effect of sorption in the far-field clay on ^{129}I annual dose is shown in Figure 3-71. The sensitivity analysis includes four cases:

- Baseline ^{129}I Sorption (K_d = 0.00 mL/g)—The corresponding retardation factor is 1.0.
- Increased ^{129}I Sorption (K_d = 0.01 mL/g)—The corresponding retardation factor is 1.1.
- Increased ^{129}I Sorption (K_d = 0.10 mL/g)—The corresponding retardation factor is 2.1.
- Increased ^{129}I Sorption (K_d = 1.0 mL/g)—The corresponding retardation factor is 12.1.

Very small changes in ^{129}I K_d have a significant effect on annual dose. This is because of the delay in transport that is represented by the associated retardation factor. For the case with K_d = 0.10 mL/g and R_f = 2.1, the dose curve shifts to the right by a factor of 2.1 on the time axis. For the case with K_d = 1.0 mL/g and R_f = 12.1, the dose curve shifts to the right by a factor of 12.1 on the time axis.

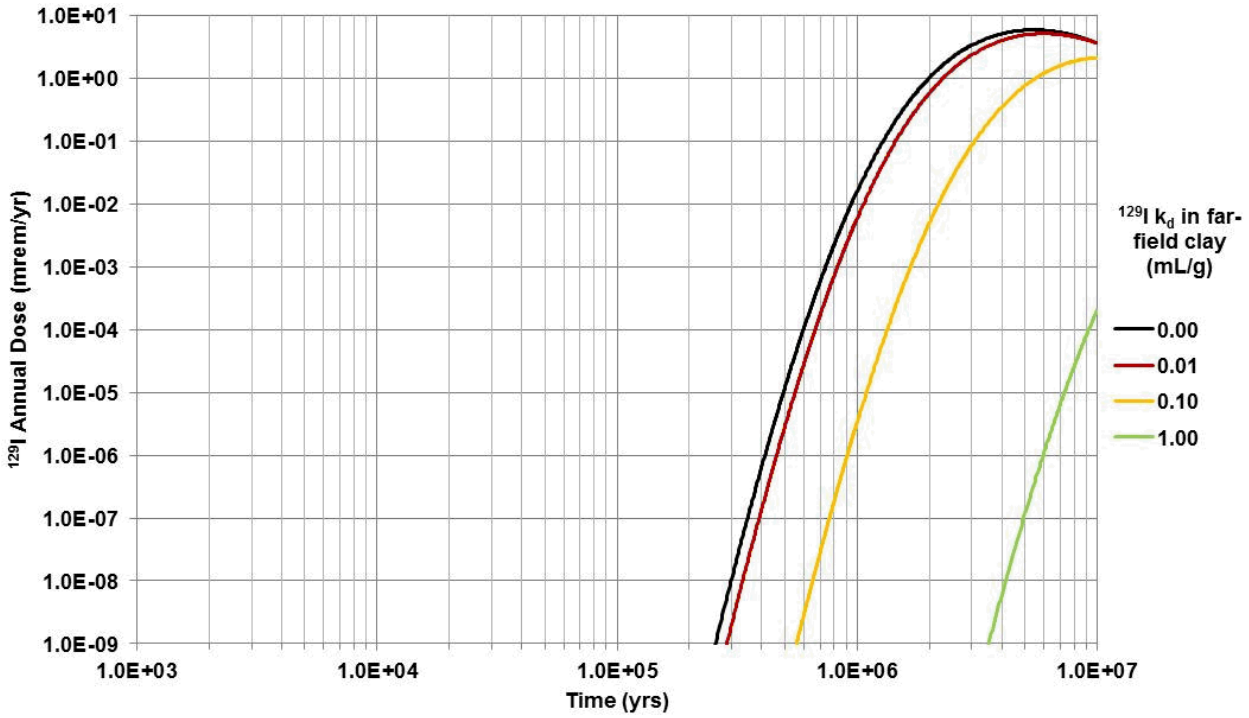

Figure 3-71. Effect of Clay Sorption on Annual Dose from ^{129}I in the Clay GDS Model

Clay Thickness—The effect of far-field clay thickness overlying the emplaced waste on ^{129}I annual dose is shown in Figure 3-72. The sensitivity analysis includes three cases:

- Reduced overlying clay thickness (75 m)
- Baseline overlying clay thickness (150 m)
- Increased overlying clay thickness (200 m)

The annual dose is quite sensitive to the thickness of the overlying far-field clay, which represents the effective distance to the receptor location. In these clay disposal system simulations, the effects of reducing the overlying clay thickness on dose are approximately linear.

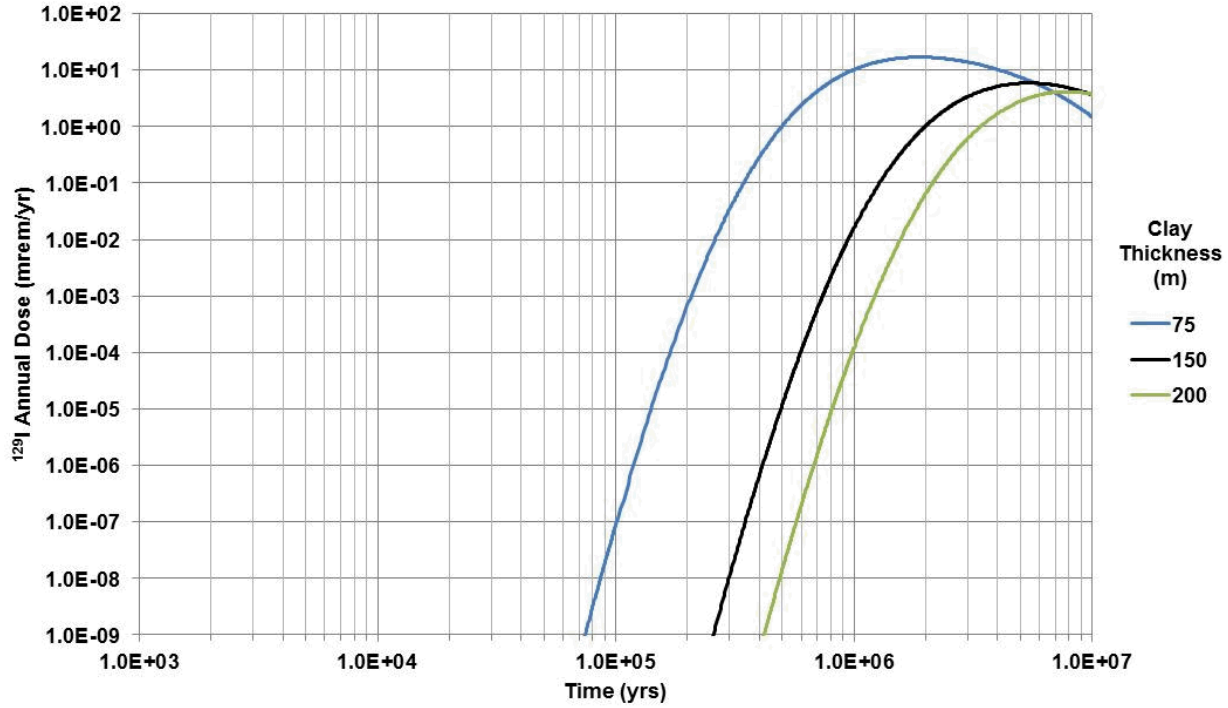

Figure 3-72. Effect of Overlying Clay Thickness on Annual Dose from ^{129}I in the Clay GDS Model

Summary—Based on these seven sensitivity analyses examining "one-off" conditions from the baseline scenario, the following observations can be made regarding the performance of a generic clay disposal system under baseline scenario conditions:

- Processes and parameters affecting radionuclide transport through the overlying 150-m far-field clay can have a significant effect on annual dose. These include sorption, K_d, and clay thickness (distance to receptor).
- Processes and parameters affecting radionuclide transport through the entire clay disposal system can have a significant effect on annual dose. Increasing the flow rate to produce advection-dominated transport increases the dose. This system-wide effect is most important in the far-field clay.

- Processes and parameters affecting waste form degradation can have a moderate effect on annual dose. Increasing the degradation rate does not significantly increase the dose because the effects are mitigated by slow diffusion through the far-field clay. Decreasing the degradation rate decreases the annual dose.
- Processes and parameters affecting waste package lifetime can have a moderate effect on annual dose. Increasing the waste package lifetime delays the onset of waste form degradation and radionuclide release from the waste form.
- Processes and parameters affecting radionuclide transport through the 2.175-m EBS (bentonite buffer and fissured clay DRZ) have a minimal effect on dose.

3.5.3.4 Deep Borehole Sensitivity Analyses

Annual dose results from the deterministic deep borehole baseline scenario are shown in Figure 3-50. The following one-off sensitivity simulations were performed to investigate the effects on ^{129}I movement through the disposal system:

- Waste form fractional degradation rate (Figure 3-73)
- Sorption (^{129}I distribution coefficient) in the disposal zone (Figure 3-74)
- Sorption (^{129}I distribution coefficient) in the seal zone (Figure 3-75)
- Molecular diffusion coefficient (Figure 3-76)

Waste Form Degradation—The effect of waste form degradation rate on ^{129}I annual dose is shown in Figure 3-73. The sensitivity analyses consider three fractional degradation rate cases:

- Fast Waste Form Degradation ($0.1\ yr^{-1}$)—100% of the radionuclide mass is released from the waste form in the first 250 years. This provides a bounding case for instantaneous release of gap and grain boundary inventory from the waste form.
- Baseline Waste Form Degradation ($2\times10^{-5}\ yr^{-1}$)—50% of the radionuclide mass is released from the waste form in the first 35,000 years, 95% of the mass is released by 150,000 years, and 99.9% of the mass is released by about 350,000 years.
- Slow Waste Form Degradation ($1\times10^{-7}\ yr^{-1}$)—50% of the radionuclide mass is released from the waste form after 4,800,000 years, and 76% of the mass is released by 10,000,000 years.

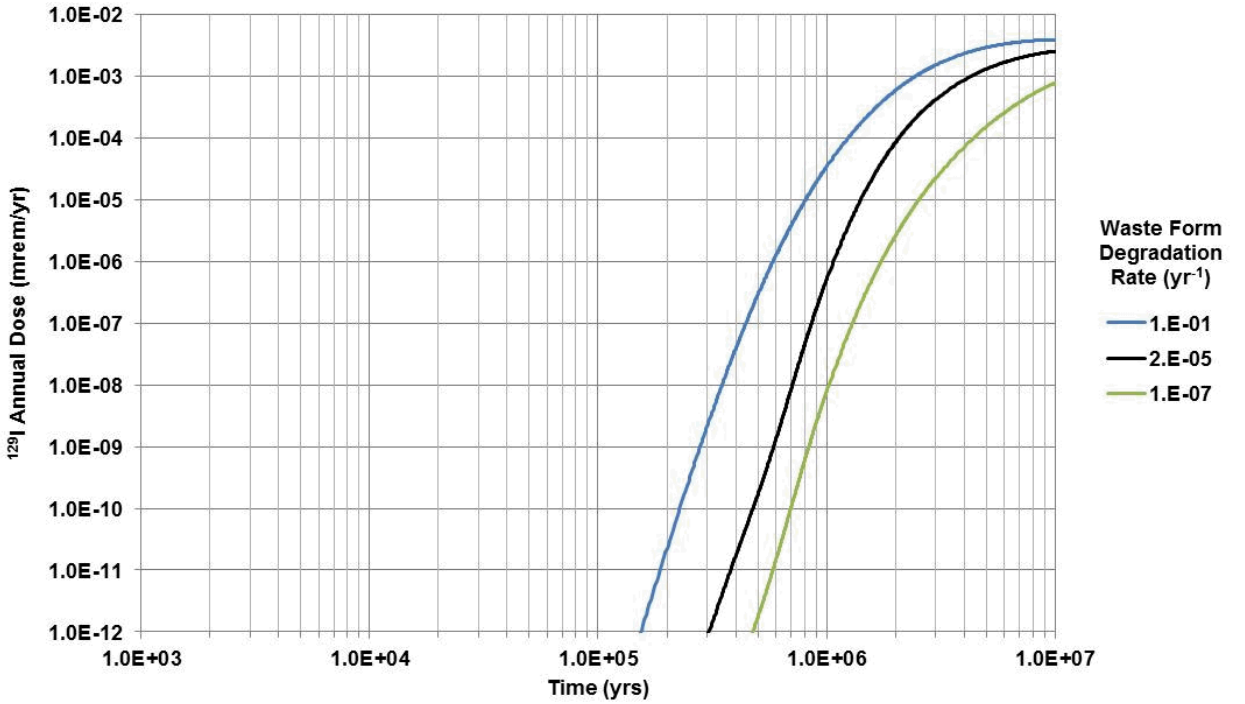

Figure 3-73. Effect of Waste Form Degradation Rate on Annual Dose from ^{129}I in the Deep Borehole Model

In the fast degradation rate (0.1 yr^{-1}) case, all mass is released (degraded) from the waste form in the first 250 years. This is roughly equivalent to assuming that all ^{129}I mass is instantaneously released as gap and grain boundary inventory (i.e., a ^{129}I gap fraction of 1.0 as compared to the estimated range of 0.0204–0.2675). The mass released from the waste forms advects upward through the 2,000-m disposal zone and then diffuses upward through the 1,000-m seal zone. However, the relative contributions of advective and diffusive transport vary with time and distance up the borehole (flow rates decrease with time and with distance up the borehole). In the fast degradation rate case, 23% of the initial ^{129}I mass reaches the seal zone by 100,000 years, whereas in the baseline case, only 11% of the initial mass reaches the seal zone by 100,000 years, and 22% of the mass is still undegraded. Despite the greater early transport of ^{129}I mass away from the repository in the fast degradation rate case, the effect on annual dose is only moderate. This is because the some of the effect of the early mass on annual dose is offset by diffusion-dominated transport in the upper part of the seal zone which tends to attenuate the releases.

For the slow fractional degradation rate (1×10^{-7} yr^{-1}), 50% of the radionuclide mass is not released from the waste form until 4,800,000 years, and only 76% of the mass is released by 10,000,000 years. In this case, the slow degradation time means that a smaller fraction of the released mass is available for transport during early time when advective transport is more predominant. As a result, the annual dose is lower than for the baseline case.

Disposal Zone Sorption—The effect of sorption in the disposal zone on ^{129}I annual dose is shown in Figure 3-74. The sensitivity analysis includes four cases:

- Baseline ^{129}I Sorption (K_d = 0.00 mL/g)—The corresponding retardation factor is 1.0.
- Increased ^{129}I Sorption (K_d = 0.01 mL/g)—The corresponding retardation factor is 1.7.
- Increased ^{129}I Sorption (K_d = 0.10 mL/g)—The corresponding retardation factor is 8.2.
- Increased ^{129}I Sorption (K_d = 1.0 mL/g)—The corresponding retardation factor is 73.2.

Very small changes in ^{129}I K_d in the disposal zone have a moderate effect on annual dose. This is because of the delay in transport that is represented by the associated retardation factor. However, sorption in the disposal zone is not as important to overall system performance as sorption in the seal zone, because transport in the disposal zone is advection-dominated over a greater length for a longer period of time. For the case with disposal zone K_d = 0.1 mL/g and R_f = 8.2, the dose curve only shifts to the right by a factor of about 1.2 on the time axis relative to the baseline case.

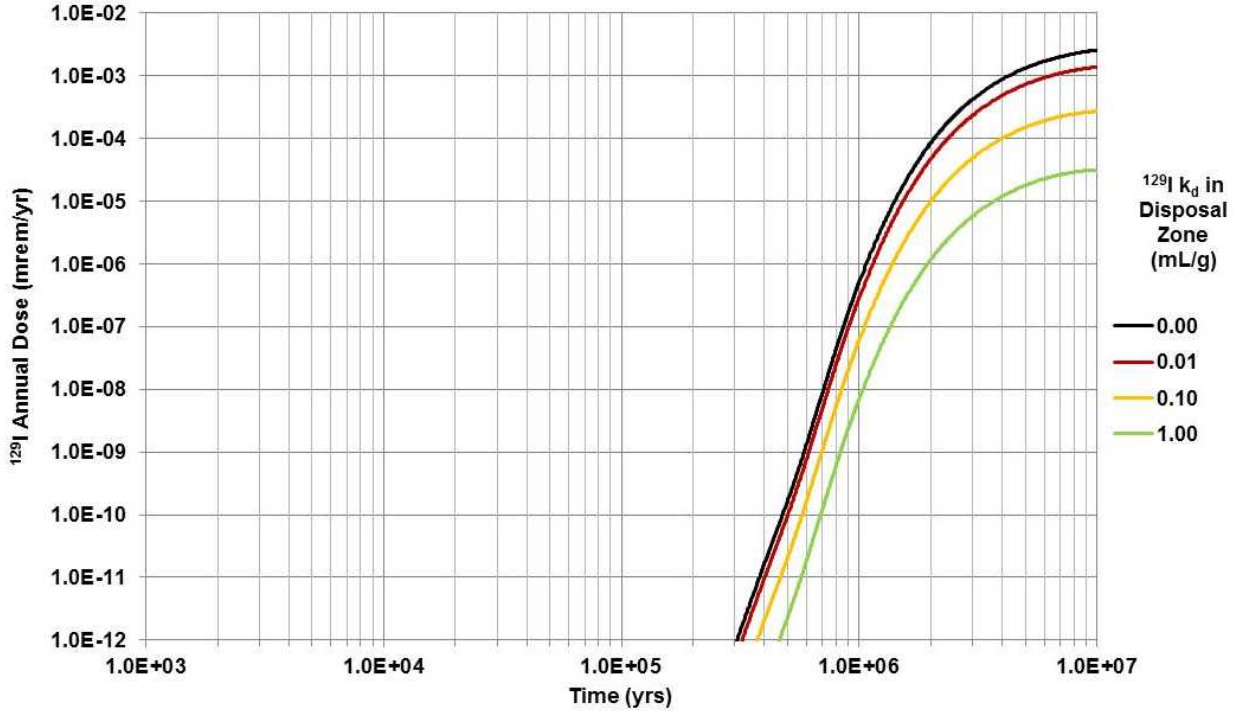

Figure 3-74. Effect of Sorption in the Disposal Zone on Annual Dose from ^{129}I in the Deep Borehole GDS Model

Seal Zone Sorption—The effect of sorption in the seal zone on ^{129}I annual dose is shown in Figure 3-75. The sensitivity analysis includes four cases:

- Baseline ^{129}I Sorption (K_d = 0.00 mL/g)—The corresponding retardation factor is 1.0.
- Increased ^{129}I Sorption (K_d = 0.01 mL/g)—The corresponding retardation factor is 1.7.
- Increased ^{129}I Sorption (K_d = 0.10 mL/g)—The corresponding retardation factor is 8.2.
- Increased ^{129}I Sorption (K_d = 1.0 mL/g)—The corresponding retardation factor is 73.2.

Very small changes in ^{129}I K_d have a significant effect on annual dose. This is because of the delay in transport that is represented by the associated retardation factor. Because transport through the seal zone is the slowest component in the deep borehole disposal system, the effect of increased seal zone K_d is to shift the dose curves to the right on the time axis by a factor that corresponds to the retardation factor.

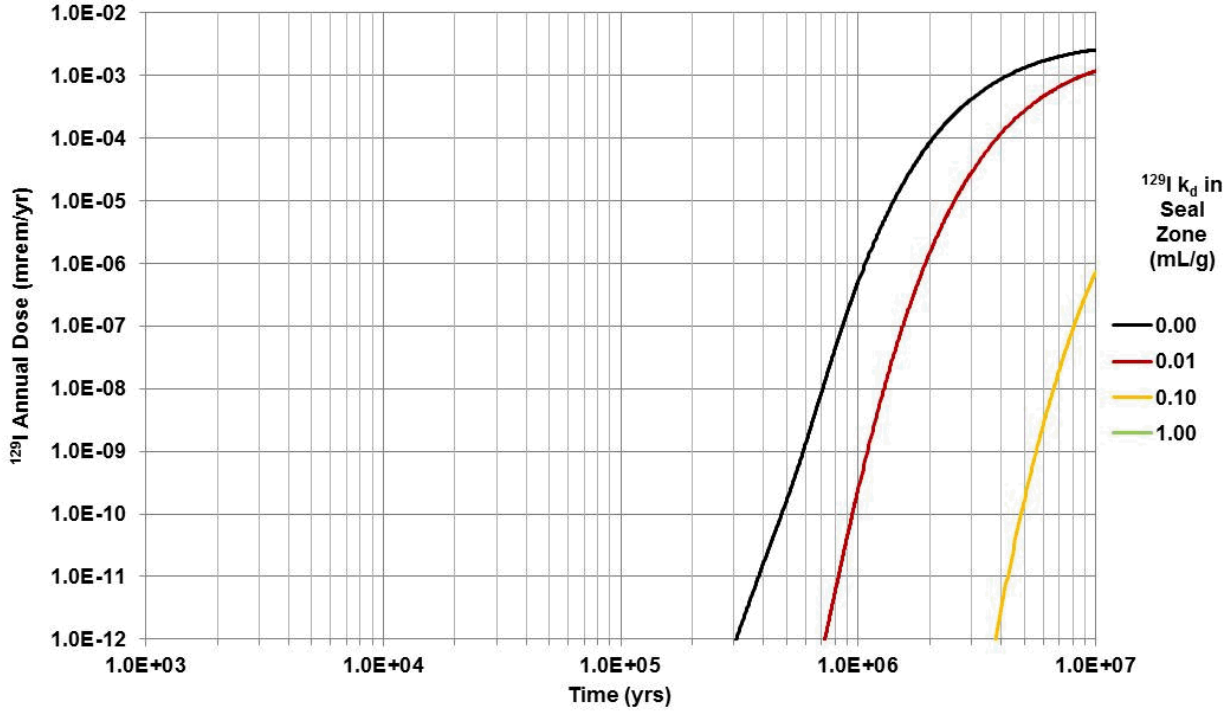

Figure 3-75. Effect of Sorption in the Seal Zone on Annual Dose from ^{129}I in the Deep Borehole GDS Model

Diffusion—The effect of the diffusion coefficient on ^{129}I annual dose is shown in Figure 3-76. The sensitivity analysis includes two cases:

- Baseline Molecular (Free Water) Diffusion Coefficient (2.30×10^{-9} m^2/s)—The corresponding effective diffusion coefficient for ^{129}I in each region is based on the local porosity and tortuosity.
- Enhanced Molecular (Free Water) Diffusion Coefficient (1.15×10^{-8} m^2/s)—This results in a corresponding effective diffusion coefficient for ^{129}I in each region that is a factor of 5 larger than the baseline value. The increased molecular diffusion coefficient reproduces potential changes in the effective diffusion coefficient for ^{129}I that might result from changes in available porosity (e.g., due to anion exclusion) or tortuosity.

The factor-of-5 increase in diffusion coefficient has a significant effect on dose. This is because the corresponding factor-of-5 increase in diffusive flux rate has a significant effect on transport in regions where diffusion is the dominant transport mechanism. Diffusion is dominant at all times in most of the seal zone, which is slowest transport component in the deep borehole disposal system. Therefore, the increase in diffusion coefficient shifts the dose curve to the left by about a factor of five on the time axis.

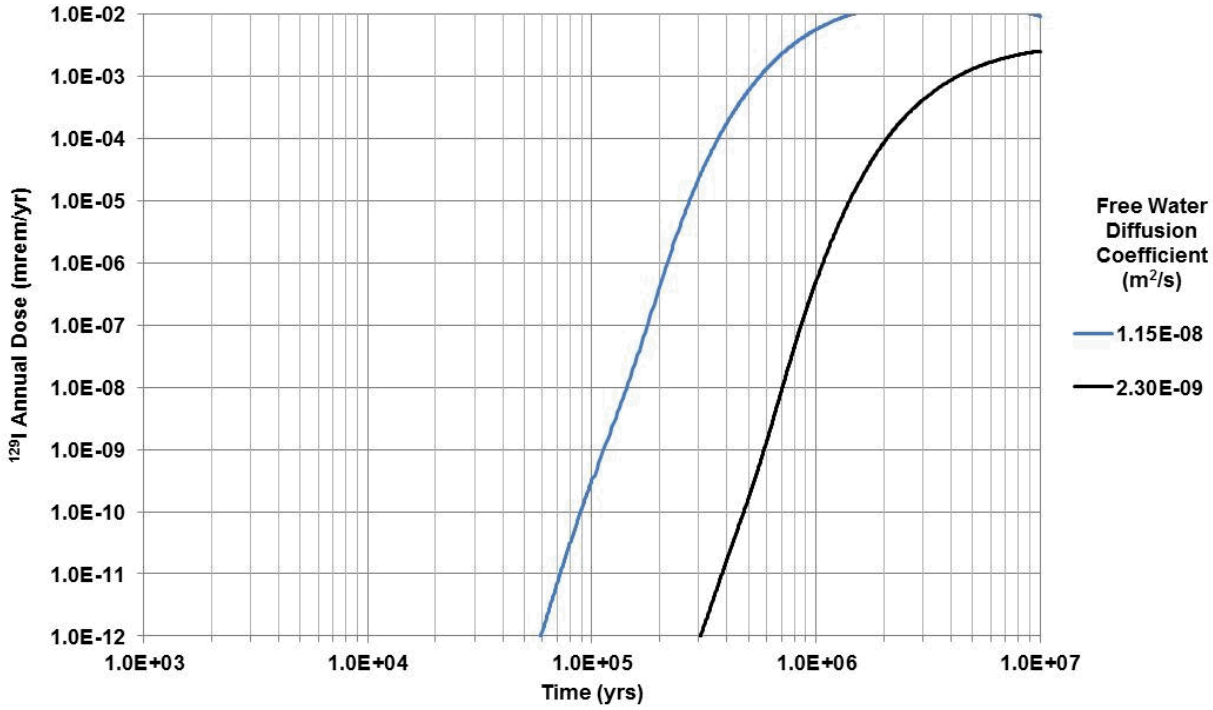

Figure 3-76. Effect of Diffusion Coefficient on Annual Dose from ^{129}I in the Deep Borehole GDS Model

Summary—Based on these four sensitivity analyses examining "one-off" conditions from the baseline scenario, the following observations can be made regarding the performance of a generic deep borehole disposal system under baseline scenario conditions:

- Processes and parameters affecting radionuclide transport through the 1,000-m seal zone can have a significant effect on annual dose. These include sorption, K_d, and seal zone integrity.

- Processes and parameters affecting radionuclide transport through the 2,000-m disposal zone can have a moderate effect on annual dose. Very small increases in sorption, K_d, can noticeably decrease the dose.
- Processes and parameters affecting radionuclide transport through the entire deep borehole disposal system can have a significant effect on annual dose. These include flow rate and diffusion coefficient. These system-wide effects are important in the both disposal zone and the seal zone.
- Processes and parameters affecting waste form degradation can have a moderate effect on annual dose.

4 CONCLUSIONS

In FY 2012, efforts to develop the capability of modeling different disposal environments and waste form options continued under the GDSM work package in support of the UFDC. Two key activities were (1) the development of a GDSM architecture capable of providing a single common structure for all UFDC disposal system models, and (2) the refinement and application of the four simplified PA models (i.e., individual GDS models representing the disposal options of salt, granite, clay, and deep borehole disposal).

As discussed in Section 2, progress on developing the GDSM architecture occurred in several areas. Advancements in the integration of the capabilities of the four individual GDS models into a single, simplified PA model framework are discussed in Section 2.2.1. However, some limitations of using GoldSim as the framework modeling tool became apparent during this effort. As a result, a decision was made to pursue an advanced generic PA modeling capability (Section 2.2.2) that provides for increased flexibility and more efficient implementation of fundamental representations of multi-physics processes and their couplings within a computational framework that is compatible with HPC technologies. The goal with this advanced modeling capability is to provide a robust total system approach by balancing the development of a conceptual model framework that can represent a range of multi-physics processes for specific subsystems with the development of a computational framework that can facilitate adequate multi-physics couplings across the entire disposal system.

Other progress with respect to the GDSM architecture includes the systematic development of conceptual models and architecture for the EBS and NBS submodel components (Sections 2.3 and 2.4, respectively). The recommended approaches take into account preliminary FEPs analyses, stress modularity and flexibility, and avoid extensive use of abstractions. In addition, work continued on an advanced approach for treating diffusion in clay or shale to account for heterogeneity and the impact of electrochemical processes (Appendix D). The GDSM Computational Parameter Database (Section 2.5) was designed in greater detail and partially implemented. Eventually, the database is intended to allow users to efficiently build disposal system model input files, archive output, and associate the input and output in a controlled environment as part of the configuration management strategy. Given that the next development stage involves interfacing to the implementing framework, further work must wait until the advanced generic PA modeling capability is sufficiently developed.

Because the GDSM architecture and the advanced modeling capability are still under development, the simplified PA models are being maintained and revised as appropriate to support (1) sensitivity analyses of various disposal system components, (2) the development of conceptual reference cases for each of the four disposal options, and (3) short-turnaround generic PA model needs. During FY 2012, probabilistic sensitivity analyses using updated parameter values were conducted with the salt GDS model (Section 3.1), granite GDS model (Section 3.2), clay GDS model (Section 3.3), and deep borehole GDS model (Section 3.4). In addition, deterministic simulations and sensitivity analyses were conducted using revised versions of the four GDS models (Section 3.5). Revisions included updating some parameter values and model components for more consistency between the four models.

The model results presented in Section 3 demonstrate current model capabilities, identify processes and parameters that could influence disposal system performance, and support a conclusion that all four of the disposal options—salt, granite, clay, and deep borehole—show promise with respect to providing acceptable containment of UNF and HLW under undisturbed conditions. Predicted doses to a human receptor are in all cases small over a 1-million-year time frame. These model insights can be used to guide the development of generic reference cases as well as identify research needs. However, it should be kept in mind that these simplified disposal system models and analyses are generic and use a number of assumptions (many of which tend to over-estimate releases) and data that require defensible justifications. Results are likely to change somewhat as site-specific information is used and disturbed

scenarios are evaluated in more detail in the future. Due to this limited pedigree, the results are not intended to screen and/or prioritize specific disposal options, designs, and sites for their suitability for a geologic disposal facility.

Moving into FY 2013, the planned activities include further development of the GDSM architecture, application and further modification of the simplified PA models to support the evolving needs of DOE and other UFDC work packages, and the development and implementation of the advanced representation of the diffusion coefficient in the clay GDS model. The FY 2013 development of the GDSM architecture will focus on two areas:

1. The evaluation and selection of an advanced framework for implementing the GDSM based on requirements summarized in Freeze and Vaughn (2012, Section 4). This will be done utilizing a demonstration problem relevant to disposal system modeling in a generic salt repository.
2. Finalization of the conceptual models for GDSM and initial implementation using the recommendation from this report and products from other UFDC work packages. This will help inform the specification of the GDSM and the demonstration problem for framework evaluation.

With respect to the first area above, Freeze and Vaughn (2012, Section 3) identified the desired requirements for an advanced PA model framework that implements the GDSM architecture. Existing codes with the potential to address the advanced multi-physics modeling and/or computational framework requirements were also identified (Freeze and Vaughn 2012, Section 4). There is no single existing code that addresses all of the requirements. However, the list of requirements is quite comprehensive; a PA modeling capability that satisfies all of the requirements would represent a significant advancement in the state of the art. Therefore, the approach to develop an advanced PA model framework capability will involve (1) an integration of multiple codes and/or code capabilities, rather than a single code, (2) a phased implementation, where requirements are prioritized and iteratively re-evaluated as UFDC program needs evolve, and (3) leveraging relevant ongoing open-source code development efforts.

Three existing code development efforts were identified as having the best combination of readily available open-source development, appropriate multi-physics capabilities, and HPC capabilities (Freeze and Vaughn 2012, Section 4). Two of these codes, ASCEM (Freeze and Vaughn 2012, Section 4.1.1) and Albany (Freeze and Vaughn 2012, Section 4.1.3), are computational framework codes that include multi-physics capabilities. The third code, PFLOTRAN (Freeze and Vaughn 2012, Section 4.2.1), is a THC multi-physics modeling code that includes some limited computational framework capabilities. Path forward decisions will be made in FY 2013.

5 REFERENCES

Andra (Agence Nationale pour la gestion des Déchets Radioactifs [French National Radioactive Waste Management Agency]). 2005a. *Dossier 2005 Argile: Evaluation of the Feasibility of a Geological Repository in an Argillaceous Formation, Meuse/Haute-Marne Site*. 2nd edition. December 2005. Paris, France: Andra. http://www.andra.fr/international/download/andra-international-en/document/editions/266va.pdf

Andra. 2005b. *Dossier 2005 Argile Tome: Safety Evaluation of a Geological Repository.* Paris, France: Andra. http://www.andra.fr/international/pages/en/menu21/waste-management/research-anddevelopment/dossier-2005-1636.html

Andra. 2005c. *Dossier 2005: Référentiel du Site Meuse/Haute-Marne*. Rapport Andra n° C RP ADS 04-0022. Châtenay-Malabry, France: Andra.

Altman, S.J., B.W. Arnold, R.W. Barnard, G.E. Barr, C.K. Ho, S.A. McKenna, and R.R. Eaton. 1996. *Flow calculations for the Yucca Mountain groundwater travel time (GWTT-95).* SAND 96-0819. Albuquerque, NM: Sandia National Laboratories.

Arnold, B.W., P.V. Brady, S.J. Bauer, C. Herrick, S. Pye, and J. Finger. 2011a. *Reference design and operations for deep borehole disposal of high-level radioactive waste*. SAND2011-6749. Albuquerque, NM: Sandia National Laboratories.

Arnold, B.W., T. Hadgu, D. Clayton, and C. Herrick. 2011b. Thermal-hydrologic-chemical-mechanical modeling of deep borehole disposal. In proceedings of *2011 International High-Level Radioactive Waste Management Conference, April 10-14, 2011, Albuquerque, NM.*

Arnold, B., E. Kalinina, and W.P. Gardner. 2012. *Generic natural system conceptual model and numerical architecture – FY2012 status report.* FCRD-UFD-2012-000179. Albuquerque, NM: Sandia National Laboratories.

Arnold, B.W., S.P. Kuzio, and B.A. Robinson. 2003. Radionuclide transport simulation and uncertainty analyses with the saturated-zone site-scale model at Yucca Mountain, Nevada. *Journal of Contaminant Hydrology* 62:401–419.

ASTM C 1174-97. 1998. *Standard practice for prediction of the long-term behavior of materials, including waste forms, used in engineered barrier systems (EBS) for geological disposal of high-level radioactive waste*. West Conshohocken, PA: American Society for Testing and Materials.

Bear, J. 1972. *Dynamics of fluids in porous materials*. New York: Elsevier. Repr. Dover Publications, 1988.

Bianchi, M., H.H. Liu, and J. Birkholzer. 2012. *Diffusion modeling in a generic clay repository: Impacts of heterogeneity and electro-chemical process.* FCRD-UFD-2012-000127. Berkeley, CA: Lawrence Berkeley National Laboratory.

Birkholzer, J.T., N. Halecky, S.W. Webb, P.F. Peterson and G.S. Bodvarsson. 2008. A modeling study evaluating the thermal-hydrological conditions in and near waste emplacement drifts at Yucca Mountain. *Nuclear Technology*. 163(1): 147–164.

Brady, P.V., B.W. Arnold, G.A. Freeze, P.N. Swift, S.J. Bauer, J.L. Kanney, R.P. Rechard, and J.S. Stein. 2009. *Deep borehole disposal of high-level radioactive waste*. SAND2009-4401. Albuquerque, NM: Sandia National Laboratories.

BSC (Bechtel SAIC Co.). 2002a. *Radionuclide screening*. ANL-WIS-MD-000006 Rev. 1. Prepared for the U.S. Department of Energy, Office of Civilian Radioactive Waste Management. Las Vegas, NV: BSC.

BSC. 2002b. *User's manual for WAPDEG 4.07*. SDN: 10000-UM-4.07-00. Prepared for the U.S. Department of Energy, Office of Civilian Radioactive Waste Management. Las Vegas, NV: BSC.

BSC. 2004a. *Aqueous corrosion rates for waste package materials*. ANL-DSD-MD-000001 Rev. 1. Prepared for the U.S. Department of Energy, Office of Civilian Radioactive Waste Management. Las Vegas, NV: BSC.

BSC. 2004b. *CSNF waste form degradation: Summary abstraction.* ANL-EBS-MD-000015 Rev. 2. Prepared for the U.S. Department of Energy, Office of Civilian Radioactive Waste Management. Las Vegas, NV: BSC.

BSC. 2005. *In-package chemistry abstraction.* ANL-EBS-MD-000037 Rev. 4. Prepared for the U.S. Department of Energy, Office of Civilian Radioactive Waste Management. Las Vegas, NV: BSC.

Carbol P. and I. Engkvist. 1997. *Compilation of Radionuclide Sorption Coefficients for Performance Assessment*. SKB R-97-13, Svensk Kärnbränslehantering AB.

Carter, J.T., F. Hansen, R. Kehrman, and T. Hayes. 2011. *A generic salt repository for disposal of waste from a spent nuclear fuel recycle facility.* SRNL-RP-2011-00149 Rev. 0. Aiken, SC: Savannah River National Laboratory.

Carter, J.T. and A.J. Luptak. 2010. *Fuel cycle potential waste inventory for disposition*. FCR&D-USED-2010-000031 Rev 2. Washington, DC: U.S. Department of Energy, Office of Used Fuel Disposition.

Chu, S. 2012. *Status report on generic granite system model improvements.* FCRD-UFD-2012-000254. Los Alamos, NM: Los Alamos National Laboratory.

Chu, S., E. Morris, W. Nutt, B. A. Robinson and Y. Wang. 2008. *Generic repository concept analyses to support the establishment of waste form performance requirements – Fiscal year 2008 status.* GNEP-WAST-PMO-MI-DV-2008-000146.

Clayton, D., G. Freeze, T. Hadgu, E. Hardin, J. Lee, J. Prouty, R. Rogers, W.M. Nutt, J. Birkholzer, H.H. Liu, L. Zheng, S. Chu. 2011. *Generic disposal system modeling—Fiscal year 2011 progress report.* FCRD-USED-2011-000184; SAND2011-5828P. Albuquerque, NM: Sandia National Laboratories.

Code of Federal Regulations. 2008. *Public health and environmental radiation protection standards for Yucca Mountain, Nevada*. Title 40 Part 197. U.S. Environmental Protection Agency. FR Vol. 73, No. 200.

CRWMS M&O (Civilian Radioactive Waste Management System Management & Operating Contractor). 1999. *License application design selection report*. B00000000-01717-4600-00123 Rev. 01 ICN 01. Prepared for the U.S. Department of Energy, Office of Civilian Radioactive Waste Management. Las Vegas, NV: CRWMS M&O.

Cundall, P.A. and O.D.L. Strack. 1979. A discrete numerical model for granular assemblies. *Geotechnique* 29(1): 47–65.

De Windt, L., D. Pellegrini and J. van der Leel. 2004. Reactive transport modelling of a spent fuel repository in a stiff clay formation considering excavation damage zones. *Radiochimica Acta.*92:841–848.

De Wit, A. 1995. Correlation structure dependence of the effective permeability of heterogeneous porous-media. *Physics of Fluids* 7(11): 2553–2562.

DOE (U.S. Department of Energy). 1996. *Title 40 CFR Part 191 Compliance Certification Application for the Waste Isolation Pilot Plant.* DOE/CAO-1996-2184. Carlsbad, NM: DOE.

DOE. 2004. *Title 40 CFR Part 191 Compliance Recertification Application for the Waste Isolation Pilot Plant.* DOE/WIPP 2004-3231. Carlsbad, NM: DOE.

DOE. 2008. *Yucca Mountain Repository License Application Safety Analysis Report*. DOE/RW-0573, Rev. 1. http://www.nrc.gov/waste/hlw-disposal/yucca-lic-app/yucca-lic-app-safety-report.html#1

DOE. 2009. *Title 40 CFR Part 191 Subparts B and C Compliance Recertification Application for the Waste Isolation Pilot Plant.* DOE/WIPP-09-3424. Carlsbad, NM: DOE.

DOE. 2010. *Research objective 3 implementation plan, developing sustainable fuel cycle options*. FCRD-TIO-2011-000025. Washington, D.C.: DOE.

DOE. 2011. *Used fuel disposition campaign disposal research and development roadmap.* FCR&D-USED-2011-000065 Rev. 0. Washington, D.C.: DOE.

Dole, L. et al. 2004. *Cost-effective cementitious material compatible with Yucca Mountain repository geochemistry*. ORNL/TM-2004/296. Oak Ridge, TN: Oak Ridge National Laboratory.

Freeze, G., P. Mariner, J.A. Blink, F.A. Caporuscio, J.E. Houseworth, and J.C. Cunnane. 2011. *Disposal system features, events, and processes: FY11 progress report.* FCRD-USED-2011-000254; SAND2011-6059P. Albuquerque, NM: Sandia National Laboratories.

Freeze, G., P. Mariner, J.E. Houseworth, J.C. Cunnane, and F.A. Caporuscio. 2010. *Used fuel disposition campaign features, events, and processes (FEPs): FY10 progress report.* FCRD-USED-2011-000034; SAND2010-5902. Albuquerque, NM: Sandia National Laboratories.

Freeze, G., and P. Vaughn. 2012. *Performance assessment framework requirements for advanced disposal system modeling.* FCRD-UFD-2012-000227. Albuquerque, NM: Sandia National Laboratories.

Freeze, R.A. and J.A. Cherry. 1979. *Groundwater*. Englewood Cliffs, NJ: Prentice-Hall.

GoldSim Technology Group. 2010a. *GoldSim probabilistic simulation environment user's guide,* ver. 10.5, vol. 1 and 2. GoldSim Technology Group LLC, Issaquah, Washington.

GoldSim Technology Group. 2010b. *Users guide: GoldSim contaminant transport module*, ver. 6.0. Issaquah, Washington: GoldSim Technology Group LLC.

Gunnarsson, D.L. Moren, P. Sellin and P. Keto. 2006. *Deep repository – engineered barrier systems*. SKB-R-06-71. Stockholm, Sweden: Swedish Nuclear Fuel and Waste Management Co.

Hadgu, T., and B.W. Arnold. 2010. Thermal hydrology modeling of deep borehole disposal of high-level radioactive waste. In proceedings of *American Geophysical Union Fall Conference*, December 10-14, 2011, San Francisco, CA.

Hadgu, T., B.W. Arnold, J.H. Lee, G. Freeze, P. Vaughn, P.N. Swift, and C. Sallaberry. 2012. Sensitivity analysis of seals permeability and performance assessment of deep borehole disposal of radioactive waste. In proceedings of *PSAM11 ESREL2012 Conference, June 25 –29, 2012, Helsinki, Finland.*

Hansen, F.D., E.L. Hardin, R.P. Rechard, G.A. Freeze, D.C. Sassani, P.V. Brady, C.M. Stone, M.J. Martinez, J.F. Holland, T. Dewers, K.N. Gaither, S.R. Sobolik, and R.T. Cygan. 2010. *Shale disposal of U.S. high-level radioactive waste.* SAND2010-2843. Albuquerque, NM: Sandia National Laboratories.

Hansen, F.D. and M.K. Knowles. 2000. Design and analysis of a shaft seal system for the Waste Isolation Pilot Plant. *Reliability Engineering and System Safety* 69 (2000): 87–98.

Hardin, E. 2012. *Generic engineered barrier system model and system architecture*. FCRD-UFD-2012-000180. U.S. Department of Energy, Office of Nuclear Energy, Used Fuel Disposition Campaign, Washington, D.C.

Hardin, E., J. Blink, H. Greenberg, M. Sutton, M. Fratoni, J. Carter, M. Dupont and R. Howard. 2011. *Generic repository design concepts and thermal analysis (FY11)*. FCRD-USED-2011-000143 Rev. 2. Prepared for the U.S. Department of Energy, Used Fuel Disposition R&D Campaign.

Huff, K.D. and W.M. Nutt. 2012. *FY12 Sensitivity studies using the UFD clay generic disposal system model.* FCRD-USED-2012-000141. Argonne, IL: Argonne National Laboratory.

IAEA (International Atomic Energy Agency). 1996. *International basis safety standards for protection against ionizing radiation and the safety of radiation sources*. Tech. Rep. 115. Vienna, Austria: International Atomic Energy Agency.

IAEA. 2003. *Reference biospheres for solid radioactive waste disposal*. IAEA-BIOMASS-6. Vienna, Austria: International Atomic Energy Agency.

Jovancicevic, V. and Bockris, J.O'M. 1986. The mechanism of oxygen reduction on iron in neutral solutions. *Journal of the Electrochemical Society*. 133(9): 1797–1807. Manchester, New Hampshire: Electrochemical Society.

Jove-Colon, C. et al. 2012. *Evaluation of generic EBS design concepts and process models: Implications to EBS design optimization*. FCRD-USED-2012-000140. Prepared for U.S. Department of Energy, Office of Used Nuclear Fuel Disposition.

Krumhansl, J.L., P.V. Brady, and H.L. Anderson. 2011. Deep borehole radionuclide sequestration. In proceedings of *International High-Level Radioactive Waste Management Conference, Albuquerque, NM*.

Lasaga, A.C. J.M. Soler, J. Ganor, T.E. Burch and K.L. Nagy. 1994. Chemical weathering rate laws and global geochemical cycles. *Geochimica et Cosmochimica Acta*. 58(10): 2361–2386.

Lee, J.H., Arnold, B. W., Swift P. N., Hadgu, T., Brady P. V., Freeze G., and Wang Y. 2012. A prototype performance assessment model for generic deep borehole repository for high-level nuclear waste. In proceedings of *Waste Management Conference, February 26 – March 1, 2012, Phoenix, AZ.*

Lee, J.H., Siegel, M., Jove-Colon, C., and Wang, Y. 2011. A performance assessment model for generic repository in salt formation. In proceedings of *13th International High-Level Radioactive Waste Management Conference (IHLRWMC), April 10-14, 2011, Albuquerque, NM*.

Lemos, J. and B. Damjanac. 2002. *New Developments in 3DEC version 2.01*. Minneapolis, Minnesota: Itasca Consulting Group.

Mariner, P.E., J.H. Lee, E.L. Hardin, F.D. Hansen, G.A. Freeze, A.S. Lord, B. Goldstein, and R.H. Price. 2011. *Granite Disposal of U.S. high-level radioactive waste*. SAND2011-6203. Albuquerque, NM: Sandia National Laboratories.

McKinley, I.G., F.B. Neall, H. Kawamura, and H. Umeki. 2006. Geochemical optimization of a disposal system for high-level radioactive waste. *Journal of Geochem. Explor*. 90:1–8.

Meacham, P.G., D.R. Anderson, E.J. Bonano, and M.G. Marietta. 2011. *Sandia National Laboratories performance assessment methodology for long-term environmental programs: The history of nuclear waste management*. SAND2011-8270. Albuquerque, NM: Sandia National Laboratories.

Mousseau, V.A., K. N. Belcourt, G. A. Freeze, G. A. Hansen, P. Mariner, and D. Vigil. 2012. *Modeling and simulation for UFD.* SAND2012-8236. Albuquerque, NM: Sandia National Laboratories.

Nagra (Nationale Genossenschaft für die Lagerung Radioaktiver Abfälle [Swiss National Cooperative for the Disposal of Radioactive Waste]). 2002. *Project Opalinus Clay Safety Report: Demonstration of Disposal Feasibility for Spent Fuel, Vitrified High-Level Waste and Long-Lived Intermediate-Level Waste (Entsorgungsnachweis).* Technical Report 02-05.

NRC (U.S. Nuclear Regulatory Commission). 1999. *Regulatory perspectives on model validation in high-level radioactive waste management programs: A joint NRC/SKI white paper*. NUREG-1636. Washington, DC: U.S. Nuclear Regulatory Commission.

NRC. 2003. *Yucca Mountain review plan*. NUREG-1804 Rev. 2. Washington, DC: NRC, Office of Nuclear Material and Safeguards.

Nutt, W.M., E. Morris, Y. Wang, L. Joon, C. Jove-Colon, and S. Chu. 2009. *Generic repository concept analyses to support the establishment of waste form performance reuqirements*. Tech. Rep. GNEP–WAST–PMO–MI–DV–2008-000146. Prepared for US–DOE–NE Separations and Waste Form Campaign.

Painter, S. 2011. Development of discrete fracture network modeling capability. In proceedings of *Nuclear Waste Technical Review Board, Fall 2011 Meeting, Salt Lake City, UT, September 13, 2011*. www.nwtrb.gov

Painter, S., and V. Cvetkovic. 2005. Upscaling discrete fracture network simulations: An alternative to continuum transport modeling. *Water Resour. Res.* 41:W02002. doi:10.1029/2004WR003682.

Painter, S., V. Cvetkovic, J. Mancillas and O. Pensado. 2008. Time domain particle tracking methods for simulating transport with retention and first-order transformation. *Water Resour. Res.* 44:W01406. doi:10.1029/2007WR005944.

Phipps, P.B.P. and D.W. Rice. 1979. The role of water in atmospheric corrosion. Chapter 8 of *Corrosion chemistry*. Brubaker, G.R. and P.B.P. Phipps, eds. ACS Symposium Series 89. Washington, D.C.: American Chemical Society.

Pratt, H.R., D.E. Stephenson, G. Zandt, M. Bouchon and W.A. Hustrulid. 1979. Earthquake damage to underground facilities. In proceedings of *1979 RETC* Vol. 1. Littleton, CO: American Institute of Mining Engineers.

Robinson, B.A., Z.V. Dash and G. Srinivasan. 2010. A particle tracking transport method for the simulation of resident and flux-averaged concentrations of solute plumes in groundwater models. *Compt. Geosci.* 14:779–792.

Robinson, B.A., C. Li and C.K. Ho. 2003. Performance assessment model development and analysis of radionuclide transport in the unsaturated zone, Yucca Mountain, Nevada. *Journal of Contaminant Hydrology* 62:249–268.

Rutqvist, J., C. Steefel, J. Davis, I. Bourg, R. Tinnacher, J. Galindez, M. Holmboe, J. Birkholzer, and H.H. Liu. 2012. *Investigation of reactive transport and coupled THM processes in EBS: FY12 report.* FCRD-UFD-2012-000125. Prepared for U.S. Department of Energy.

Rutqvist, J., Y.F. Yu, C.-F. Tsang and G.S. Bodvarsson. 2002. A modeling approach for analysis of coupled multi-phase fluid flow, heat transfer, and deformation in fractured porous rock. *Intl. Journal of Rock Mech. & Min. Sci.* 39:429–442.

Sassani, D.C. 2011. *Waste form degradation and radionuclide mobilization: FY11 summary report*. FCRD-USED-2011-000403. Albuquerque, NM: Sandia National Laboratories.

Schwartz, F. W. and H. Zhang. 2004. Fundamentals of ground water. *Environmental Geology* 45:1037–1038.

Sharma, S. and W.R. Judd. 1991. Underground opening damage from earthquakes. *Engineering Geology* 30(3-4): 263–276.

SKB (Svensk Kämbränslehantering AB [Swedish Nuclear Fuel and Waste Management Co.]). 2010a. *Fuel and canister process report for the safety assessment SR-Site*. SKB-TR-10-46.

SKB. 2010b. *Radionuclide transport report for the safety assessment SR-Site*, Technical Report TR-10-50 (December 2010).

SKB. 2011. *Long-term safety for the final repository for spent nuclear fuel at Forsmark: Main report of the SR-Site project*. SKB-TR-11-01 (3 volumes).

SNL (Sandia National Laboratories). 2004. *Drift degradation analysis*. ANL-EBS-MD-000027 Rev. 03. Prepared for the U.S. Dept. of Energy, Office of Civilian Radioactive Waste Management. Las Vegas, NV: Sandia National Laboratories.

SNL. 2007a. *Drift-scale THC seepage model*. MDL-NBS-HS-000001 Rev. 5. Prepared for the U.S. Dept. of Energy, Office of Civilian Radioactive Waste Management. Las Vegas, NV: Sandia National Laboratories.

SNL. 2007b. *EBS radionuclide transport abstraction*. ANL-WIS-PA-000001 Rev. 3. Prepared for the U.S. Dept. of Energy, Office of Civilian Radioactive Waste Management. Las Vegas, NV: Sandia National Laboratories.

SNL. 2007c. *Engineered barrier system: Physical and chemical environment*. ANL-EBS-MD-000033 Rev. 6. Prepared for the U.S. Dept. of Energy, Office of Civilian Radioactive Waste Management. Las Vegas, NV: Sandia National Laboratories.

SNL. 2007d. *General corrosion and localized corrosion of waste package outer barrier*. ANL-EBS-MD-000003 Rev. 3. Prepared for the U.S. Dept. of Energy, Office of Civilian Radioactive Waste Management. Las Vegas, NV: Sandia National Laboratories.

SNL. 2007e. *Mechanical assessment of degraded waste packages and drip shields subject to vibratory ground motion*. MDL-WIS-AC-000001 Rev. 0. Prepared for the U.S. Dept. of Energy, Office of Civilian Radioactive Waste Management. Las Vegas, NV: Sandia National Laboratories.

SNL. 2008a. *Features, events, and processes for the total system performance assessment: Analyses*. ANL-WIS-MD-000027 Rev. 0. Prepared for the U.S. Dept. of Energy, Office of Civilian Radioactive Waste Management. Las Vegas, NV: Sandia National Laboratories.

SNL. 2008b. *Multiscale thermohydrologic model*. ANL-EBS-MD-000049 Rev. 3 Addendum 2. Prepared for the U.S. Dept. of Energy, Office of Civilian Radioactive Waste Management. Las Vegas, NV: Sandia National Laboratories.

SNL. 2008c. *Postclosure analysis of the range of design thermal loadings*. ANL-NBS-HS-000057 Rev. 0. Prepared for the U.S. Dept. of Energy, Office of Civilian Radioactive Waste Management. Las Vegas, NV: Sandia National Laboratories.

SNL. 2008d. *Total system performance assessment model/analysis for the license application*. MDL-WIS-PA-000005 Rev. 0 Addendum 1. Prepared for the U.S. Dept. of Energy, Office of Civilian Radioactive Waste Management. Las Vegas, NV: Sandia National Laboratories.

Stout, R.B. and H.R. Leider. 1998. *Waste form characteristics report.* CD-ROM Version. UCRL-ID-132375. Livermore, CA: Lawrence Livermore National Laboratory.

Swift, P.N., B.W. Arnold, P.V. Brady, G. Freeze, T. Hadgu, J. Lee, and Y. Wang. 2011. Thermal-hydrologic-chemical-mechanical modeling of deep borehole disposal. In proceedings of *2011 International High-Level Radioactive Waste Management Conference, April 10-14, 2011, Albuquerque, NM*.

Swift, P., C.W. Hansen, E. Hardin, R.J. MacKinnon, D. Sassani and S.D. Sevougian. 2010. Potential impacts of alternative waste forms on long-term performance of geological repositories for radioactive waste. In proceedings of *International Association for Probabilistic Safety Assessment and Management, 10th Conference, June 7-11, 2010, Seattle, WA.*

Walkow, W. 2012. *GDSM architecture: Major revisions to architecture diagram and descriptions of components.* version 7.0. Albuquerque, NM: Sandia National Laboratories.

Wang, Y. 2011. *Integration plan for Used Fuel Disposition (UFD) data management*. FCRD-USED-2011-000386. Albuquerque, NM: Sandia National Laboratories.

Wang, Y., J.G. Arguello, G.A. Freeze, H.C. Edwards, T.A. Dewers, T.J. Fuller, C.F. Jove-Colon, J.H. Lee, P.E. Mariner, M.D. Siegel, and S.W. Webb. 2011. *Nuclear Energy Advanced Modeling and Simulation (NEAMS) waste integrated performance and safety codes (IPSC): Gap analysis for high fidelity and performance assessment code development.* SAND 2011-1831, Albuquerque, NM: Sandia National Laboratories.

Weetjens, E., J. Perko and L. Yu. 2009. *Final report on gas production and transport*. Performance Assessment Methodologies in Application to Guide the Development of the Safety Case (PAMINA). Milestone No. M 3.2.16. Euratom Research and Training Programme on Nuclear Energy, Sixth Framework Programme (2002-2006).

Zheng, C. 1990. *MT3D: A modular three-dimensional transport model*. Rockville, MD: S.S. Papadopulos & Associates.

Zheng, L., H.H. Liu, J. Birkholzer and W.M. Nutt. 2011. *Diffusion modeling in a generic clay repository.* FCRD-LBNL-2011-SLM: 25.

Zyvoloski, G.A. 2007. *FEHM: A control volume finite element code for simulating subsurface multi-phase multi-fluid heat and mass transfer*. Los Alamos Unclassified Report LA-UR-07-3359. Los Alamos, NM: Los Alamos National Laboratory.

Zyvoloski, G.A., B.A. Robinson, Z.V. Dash, and L.L. Trease. 1997. *Summary of the models and methods for the FEHM application A Finite-Element Heat- and Mass-Transfer Code*. LA-13307-MS. Los Alamos, NM: Los Alamos National Laboratory.

Appendix A

Summary of the Preliminary Generic FEP Evaluation for the EBS

APPENDIX A—SUMMARY OF THE PRELIMINARY GENERIC FEP EVALUATION FOR THE EBS

As discussed in Section 2.3.2, a preliminary FEP screening was performed to identify important EBS processes that should be included in EBS conceptual models (Hardin 2012, Section 3 and Appendices A and B). A draft model architecture (Figure 2-3) was assembled and mapped to the generic UFDC FEP list (Freeze et al. 2011) following the approach taken by Clayton et al. (2011, Appendix B). While the mapping in Clayton et al. (2011) was for simple generic PA models, the objective in Hardin (2012) was to provide a general mapping for a more widely applicable set of PA models.

The tables below summarize the mapping of included EBS FEPs to four components of the generic PA model architecture:

- Outer EBS Components (Upstream and Downstream) (Table A-1)
- Interior EBS Components (Upstream and Downstream) (Table A-2)
- Waste Package Components (Diversion and Containment) (Table A-3)
- Waste Form and Waste Package Internals Components (Table A-4)

Within each of the tables, the FEPs are organized according to whether they are part of the base case or included to address the following key issues:

A. Thermal Management

B. Waste Package Containment Lifetime

C. Waste Form Degradation Rates

D. Alteration of Host Rock by the Repository

E. Alternative EBS Closure Concepts

F. Gas Generation

G. Interaction with Liner/Reinforcement and Cementitious Materials

H. Disruptive Events

These key issues are described in Section 2.3.2. The capability to address these issues in the EBS part of the system model should be included in addition to flow and transport, i.e., in addition to porous medium flow within and around the EBS as well as radionuclide attenuation and transport processes (diffusion, advection, sorption). Mapping the generic UFDC FEPs to these key issues helps to identify which FEPs need to be included in the generic system model.

The screening decisions provided in these tables are largely based on the judgment of subject matter experts (Hardin 2012) and on previous prioritization analyses in the UFDC Research and Development Roadmap (DOE 2011).

Table A-1. Included FEPs for Outer EBS Components (Upstream and Downstream)

UFDC FEP No.	FEP Description
Base Case (Upstream and Downstream)	
2.1.05.01	Degradation of Seals*
2.1.08.04	Flow Through Seals*
2.1.08.09	Influx/Seepage Into the EBS*
2.1.11.01	Heat Generation in EBS
2.1.11.10	Thermal Effects on Flow in EBS
2.1.11.11	Thermally-Driven Flow (Convection) in EBS
Base Case (Downstream Transport)	
2.1.01.02	Radioactive Decay and Ingrowth
2.1.09.05	Chemical Interaction of Water with Corrosion Products
2.1.09.13	Radionuclide Speciation and Solubility in EBS
2.1.09.51	Advection of Dissolved Radionuclides in EBS
2.1.09.52	Diffusion of Dissolved Radionuclides in EBS
2.1.09.53	Sorption of Dissolved Radionuclides in EBS
Issue A: Thermal Management	
(no additional outer EBS FEPs)	
Issue B: Waste Package Containment Lifetime	
(no additional outer EBS FEPs)	
Issue C: Waste Form Degradation Rates	
(no additional outer EBS FEPs)	
Issue D: Alteration of Host Rock by the Repository	
2.1.08.06	Alteration and Evolution of EBS Flow Pathways
Issue E: Alternative EBS Closure Concepts	
2.1.08.06	Alteration and Evolution of EBS Flow Pathways
2.1.08.07	Condensation Forms in Repository*
2.1.08.08	Capillary Effects in EBS*
Issue F: Gas Generation	
(no additional outer EBS FEPs)	
Issue G: Liner/Reinforcement and Cementitious Materials	
2.1.09.07	Chemical Interaction of Water with Liner/Rock Reinforcement and Cementitious Materials in EBS*
Issue H: Disruptive Events (Seismic)	
1.2.03.01	Seismic Activity Impacts EBS and/or EBS Components

NOTE: * Potentially significant in the outer EBS, for only some disposal concepts

Table A-2. Included FEPs for Interior EBS Components (Upstream and Downstream)

UFDC FEP No.	FEP Description
Base Case (Upstream and Downstream)	
2.1.04.01	Evolution and Degradation of Backfill
2.1.08.01	Flow Through the EBS
2.1.08.06	Alteration and Evolution of EBS Flow Pathways
2.1.08.09	Influx/Seepage Into the EBS*
2.1.09.01	Chemistry of Water Flowing into the Repository
2.1.09.03	Chemical Characteristics of Water in Backfill*
2.1.09.06	Chemical Interaction of Water with Backfill*
2.1.11.01	Heat Generation in EBS
2.1.11.03	Effects of Backfill on EBS Thermal Environment*
2.1.11.10	Thermal Effects on Flow in EBS
2.1.11.11	Thermally-Driven Flow (Convection) in EBS
2.1.11.12	Thermally-Driven Buoyant Flow / Heat Pipes in EBS*
2.1.11.13	Thermal Effects on Chemistry and Microbial Activity in EBS
Base Case (Downstream Transport)	
2.1.01.02	Radioactive Decay and Ingrowth
2.1.09.05	Chemical Interaction of Water with Corrosion Products
2.1.09.13	Radionuclide Speciation and Solubility in EBS
2.1.09.51	Advection of Dissolved Radionuclides in EBS
2.1.09.52	Diffusion of Dissolved Radionuclides in EBS
2.1.09.53	Sorption of Dissolved Radionuclides in EBS
Issue A: Thermal Management	
(no additional interior EBS FEPs)	
Issue B: Waste Package Containment Lifetime	
(no additional interior EBS FEPs)	
Issue C: Waste Form Degradation Rates	
(no additional interior EBS FEPs)	
Issue D: Alteration of Host Rock by the Repository	
2.1.08.03	Flow in Backfill*
2.1.08.05	Flow Through Liner/Rock Reinforcement Materials in EBS*
Issue E: Alternative EBS Closure Concepts	
2.1.07.01	Rockfall*
2.1.07.02	Drift Collapse*
2.1.07.08	Mechanical Impact on Other EBS Components
2.1.07.10	Mechanical Degradation of EBS
2.1.08.07	Condensation Forms in Repository*
2.1.08.08	Capillary Effects in EBS*
2.1.09.12	Chemical Effects of Drift Collapse*
2.1.11.04	Effects of Drift Collapse on EBS Thermal Environment*

Table A-2. Included FEPs for Interior EBS Components (Upstream and Downstream) (continued)

UFDC FEP No.	FEP Description
Issue F: Gas Generation	
2.1.12.02	Effects of Gas on Flow Through the EBS
Issue G: Liner/Reinforcement and Cementitious Materials	
2.1.09.07	Chemical Interaction of Water w/ Liner/Rock Reinforcement and Cementitious Materials in EBS*
2.1.09.08	Chemical Interaction of Water with Other EBS Components
Issue H: Disruptive Events (Seismic)	
1.2.03.01	Seismic Activity Impacts EBS and/or EBS Components
2.1.07.10	Mechanical Degradation of EBS

NOTE: * Potentially significant in the interior EBS for only some disposal concepts

Table A-3. Included FEPs for Waste Package Components (Diversion and Containment)

UFDC FEP No.	FEP Description
Base Case	
2.1.03.01	Early Failure of Waste Packages
2.1.03.02	General Corrosion of Waste Packages
2.1.03.08	Evolution of Flow Pathways in Waste Packages
2.1.08.01	Flow Through the EBS
2.1.08.02	Flow In and Through Waste Packages
2.1.08.06	Alteration and Evolution of EBS Flow Pathways
2.1.09.02	Chemical Characteristics of Water in Waste Packages
2.1.09.05	Chemical Interaction of Water with Corrosion Products
2.1.09.08	Chemical Interaction of Water with Other EBS Components
2.1.09.13	Radionuclide Speciation and Solubility in EBS
2.1.09.51	Advection of Dissolved Radionuclides in EBS
2.1.09.52	Diffusion of Dissolved Radionuclides in EBS
2.1.09.53	Sorption of Dissolved Radionuclides in EBS
2.1.11.01	Heat Generation in EBS
2.1.11.13	Thermal Effects on Chemistry and Microbial Activity in EBS
Issue A: Thermal Management	
(no additional waste package FEPs)	
Issue B: Waste Package Containment Lifetime	
2.1.03.03	Stress Corrosion Cracking (SCC) of Waste Packages*
2.1.03.04	Localized Corrosion of Waste Packages*
2.1.03.06	Microbially Influenced Corrosion (MIC) of Waste Packages*
Issue C: Waste Form Degradation Rates	
(no additional waste package FEPs)	
Issue D: Alteration of Host Rock by the Repository	
(no additional waste package FEPs)	
Issue E: Alternative EBS Closure Concepts	
2.1.07.01	Rockfall*
2.1.07.02	Drift Collapse*
2.1.07.05	Mechanical Impact on Waste Packages
2.1.07.10	Mechanical Degradation of EBS
Issue F: Gas Generation	
2.1.12.01	Gas Generation in EBS
2.1.12.02	Effects of Gas on Flow Through the EBS
Issue G: Liner/Reinforcement and Cementitious Materials	
2.1.09.07	Chemical Interaction of Water with Liner/Rock Reinforcement and Cementitious Materials in EBS*
2.1.09.08	Chemical Interaction of Water with Other EBS Components

Table A-3. Included FEPs for Waste Package Components (Diversion and Containment) (continued)

UFDC FEP No.	FEP Description
Issue H: Disruptive Events (Seismic)	
1.2.03.01	Seismic Activity Impacts EBS and/or EBS Components
2.1.07.10	Mechanical Degradation of EBS

NOTE: * Potentially significant for the waste package, for only some disposal concepts

Table A-4. Included FEPs for Waste Form and Waste Package Internals Components

UFDC FEP No.	FEP Description
Base Case	
2.1.01.01	Waste Inventory
2.1.01.02	Radioactive Decay and Ingrowth
2.1.02.01	SNF (Commercial, DOE) Degradation
2.1.02.02	HLW (Glass, Ceramic, Metal) Degradation
2.1.02.06	SNF Cladding Degradation and Failure
2.1.03.08	Evolution of Flow Pathways in Waste Packages
2.1.08.02	Flow In and Through Waste Packages
2.1.08.06	Alteration and Evolution of EBS Flow Pathways
2.1.09.02	Chemical Characteristics of Water in Waste Packages
2.1.09.05	Chemical Interaction of Water with Corrosion Products
2.1.09.13	Radionuclide Speciation and Solubility in EBS
2.1.09.51	Advection of Dissolved Radionuclides in EBS
2.1.09.52	Diffusion of Dissolved Radionuclides in EBS
2.1.09.53	Sorption of Dissolved Radionuclides in EBS
2.1.11.01	Heat Generation in EBS
2.1.11.13	Thermal Effects on Chemistry and Microbial Activity in EBS
Issue A: Thermal Management	
(no additional waste form FEPs)	
Issue B: Waste Package Containment Lifetime	
(no additional waste form FEPs)	
Issue C: Waste Form Degradation Rates	
2.1.02.02	HLW (Glass, Ceramic, Metal) Degradation
2.1.11.06	Thermal-Mechanical Effects on Waste Form and In-Package EBS Components
2.1.13.01	Radiolysis
2.1.13.02	Radiation Damage to EBS Components
Issue D: Alteration of Host Rock by the Repository	
(no additional waste form FEPs)	
Issue E: Alternative EBS Closure Concepts	
2.1.07.06	Mechanical Impact on SNF Waste Form
2.1.07.07	Mechanical Impact on HLW Waste Form
Issue F: Gas Generation	
2.1.12.01	Gas Generation in EBS
2.1.12.02	Effects of Gas on Flow Through the EBS

Table A-4. Included FEPs for Waste Form and Waste Package Internals Components (continued)

UFDC FEP No.	FEP Description
Issue G: Liner/Reinforcement and Cementitious Materials	
2.1.09.07	Chemical Interaction of Water with Liner/Rock Reinforcement and Cementitious Materials in EBS*
2.1.09.08	Chemical Interaction of Water with Other EBS Components
Issue H: Disruptive Events (Seismic)	
1.2.03.01	Seismic Activity Impacts EBS and/or EBS Components
2.1.07.10	Mechanical Degradation of EBS

NOTE: * Potentially significant for the waste form, for only some disposal concepts

Appendix B

Summary of the Preliminary Generic FEP Evaluation for the NBS

APPENDIX B—SUMMARY OF THE PRELIMINARY GENERIC FEP EVALUATION FOR THE NBS

The UFDC FEP list in Freeze et al. (2011a) identifies 51 FEPs applicable to the NBS or "geosphere". Unlike the EBS FEPs, the geosphere FEPs are not waste-type specific. The same geosphere processes are applicable to the different types of wastes.

As documented in Arnold et al. (2012, Appendix A), the NBS-related FEPs were mapped to different geosphere components and sub-components. The evaluation also considered the FEPs in terms of other characteristics such as their applicability, relative importance, and priority level. Of the 51 NBS FEPs, 35 have been included and 16 excluded. Table B-1 lists the included NBS FEPs.

Table B-1. Included FEPs for the Natural Barrier System

UFDC FEP No.	FEP Description
2.2.01.01	Evolution of EDZ
2.2.02.01	Stratigraphy and Properties of Host Rock
2.2.03.01	Stratigraphy and Properties of Other Geologic Units
2.2.05.01	Fractures
2.2.05.02	Faults
2.2.07.01	Mechanical Effects on Host Rock
2.2.08.01	Flow through the Host Rock
2.2.08.02	Flow through the Other Geologic Units
2.2.08.03	Effects of Recharge on Geosphere Flow
2.2.08.04	Effects of Repository Excavation on Flow through the Host Rock
2.2.08.05	Condensation Forms in Host Rock
2.2.08.06	Flow through EDZ
2.2.08.08	Groundwater Discharge to Biosphere Boundary
2.2.08.09	Groundwater Discharge to Well
2.2.09.01	Chemical Characteristics of Groundwater in Host Rock
2.2.09.02	Chemical Characteristics of Groundwater in Other Geologic Units
2.2.09.03	Chemical Interactions and Evolution of Groundwater in Host Rock

Table B-1. Included FEPs for the Natural Barrier System (continued)

UFDC FEP No.	FEP Description
2.2.09.51	Advection of Dissolved Radionuclides in Host Rock
2.2.09.52	Advection of Dissolved Radionuclides in Other Geologic Units
2.2.09.53	Diffusion of Dissolved Radionuclides in Host Rock
2.2.09.54	Diffusion of Dissolved Radionuclides in Other Geologic Units
2.2.09.55	Sorption of Dissolved Radionuclides in Host Rock
2.2.09.56	Sorption of Dissolved Radionuclides in Other Geologic Units
2.2.09.57	Complexation in Host Rock
2.2.09.58	Complexation in Other Geologic Units
2.2.09.59	Colloidal Transport in Host Rock
2.2.09.60	Colloidal Transport in Other Geologic Units
2.2.09.61	Radionuclide Transport Through EDZ
2.2.09.62	Dilution of Radionuclides in Groundwater
2.2.09.64	Radionuclide Release from Host Rock
2.2.09.65	Radionuclide Release from Other Geologic Units
2.2.11.01	Thermal Effects on Flow in Geosphere
2.2.11.02	Thermally-Driven Flow (Convection) in Geosphere
2.2.11.06	Thermal-Mechanical Effects on Geosphere
2.2.12.03	Gas Transport in Geosphere

Appendix C

Documentation of Deterministic GoldSim Parameter Inputs

APPENDIX C—DOCUMENTATION OF DETERMINISTIC GOLDSIM PARAMETER INPUTS

As discussed in Section 3.5, safety assessments were conducted for each of the four disposal options using deterministic implementations of the GoldSim–based GDS models. The deterministic GoldSim parameter inputs for those analyses are documented in this appendix.

C-1. INVENTORY

The potential future UNF and HLW inventory requiring disposal is estimated by Carter and Luptak (2010). It is assumed that the entire future UNF and HLW inventory will be disposed of in more than one repository. For the three mined disposal options considered in this report, a 70,000 MTHM capacity is assumed. This single-repository capacity is consistent with 40 CFR 197 (Preamble Sec II, p. 32081), which states "Section 114(d) of the Nuclear Waste Policy Act limits the capacity of the repository to 70,000 metric tons of SNF and HLW." Note that for deep borehole disposal the repository capacity affects the total number of boreholes required, but does not affect the conceptualization of an individual borehole.

The potential UNF inventory under four future nuclear power generation scenarios is estimated by Carter and Luptak (2010, Section 3.2). The lowest estimate, 140,000 metric tons uranium (MTU) of UNF in 2055, derives from the scenario that assumes all existing nuclear reactors will be decommissioned after 60 years of operation and will not be replaced with new reactor capacity. Under this future scenario a single PWR assembly is assumed to contain 0.435 MTU (91,000 MTU/209,000 PWR assemblies) (Carter and Luptak (2010, Table 3-5). The same 36 radionuclides (listed in Clayton et al. (2011, Table 3.1-8)) are assumed to represent the UNF inventory for each of the four disposal options. The initial mass of each radionuclide in a single PWR assembly (reported as g/MTHM), assumes fuel with a burn-up of 60 GWd/MTHM and 4.73% enrichment aged 30 years after discharge from a reactor (Carter and Luptak 2010, Table C-1).

For the single-repository safety assessments of the three mined disposal options, the UNF inventory was assumed to be contained in 16,000 waste packages, with each waste package containing 10 PWR assemblies. This results in a single-repository inventory of 69,665 MTHM. For the deep borehole disposal simulations the UNF inventory in a single borehole was assumed to be contained in 400 waste packages, with each waste package containing 1 PWR assembly. This results in a single-borehole inventory of 174 MTHM. Under these assumptions, approximately 400 boreholes would be required to dispose of 70,000 MTHM.

A few of the radionuclide half-lives were revised from the values used in the FY 2011 GDS models (Clayton et al. 2011, Table 3.1-3). The only significant change is for ^{129}I, which changed from 1.7×10^{7} yr to 1.57×10^{7} yr.

C-2. SALT GDS MODEL

Values for input parameters for the deterministic salt GDS model derive from the FY 2011 salt GDS model (Clayton et al. 2011, Section 3.1) [*GDSE Salt FY11 Baseline v2 (Ref Scenario May09-2011).gsm*]. Key changes include:

- Deterministic simulation with mean values for uncertain parameters (see Table C-1 for further details)
- Waste inventory of 70,000 MTHM UNF in 16,000 waste packages
- Fractional waste form degradation rate of 2×10^{-5} yr^{-1}

- Reduced repository length from 3,270 m to 2,146 m to be consistent with the smaller number of waste packages
- Brine flow rates through the near-field salt DRZ and far-field interbed assumed to remain constant at the 1,000,000-year value until 10,000,000 years.

Deterministic values for uncertain parameters were calculated based on mean values of each uncertainty distribution. These deterministic values are summarized in Table C-1. Constant parameter values that are unchanged from their deterministic treatment in the FY 2011 salt GDS model are not listed in Table C-1.

Table C-1. Summary of the Deterministic Approximations for the Salt GDS Model

Parameter	Distribution Type	FY 2011 GDSM Probabilistic Values	Deterministic Value
Waste Form			
UNF fractional degradation rate (yr^{-1})	Log Triangular	1×10^{-8} (min); 1×10^{-7} (mode); 1×10^{-6} (max)	1.53×10^{-5}
Near Field Salt DRZ			
Am solubility (mol/L)	Triangular	1.85×10^{-7} (min); 5.85×10^{-7} (mode); 1.85×10^{-6} (max)	8.73×10^{-7}
Np solubility (mol/L)	Triangular	4.79×10^{-10} (min); 1.51×10^{-9} (mode); 4.79×10^{-9} (max)	2.26×10^{-9}
Pu solubility (mol/L)	Triangular	1.40×10^{-6} (min); 4.62×10^{-6} (mode); 1.53×10^{-5} (max)	7.11×10^{-6}
Tc solubility (mol/L)	Log Triangular	4.56×10^{-10} (min); 1.33×10^{-8} (mode); 3.91×10^{-7} (max)	3.17×10^{-8}
Th solubility (mol/L)	Triangular	2.00×10^{-3} (min); 4.00×10^{-3} (mode); 7.97×10^{-3} (max)	4.66×10^{-3}
Sn solubility (mol/L)	Triangular	9.87×10^{-9} (min); 2.66×10^{-8} (mode); 7.15×10^{-8} (max)	3.60×10^{-8}
U solubility (mol/L)	Triangular	4.89×10^{-8} (min); 1.12×10^{-7} (mode); 2.57×10^{-7} (max)	1.39×10^{-7}
Waste Package (degraded) porosity	Uniform	0.30 (min); 0.50 (max)	0.40
Salt porosity	Log-uniform	0.010 (min); 0.100 (max)	0.039
Brine Flow Rate to Underlying Interbed (m/yr)	N/A	Sampled from 100 brine flow rate histories (Clayton et al. (2011, Section 3.1.3))	8.56×10^{-7}
Far Field Interbed			
Am solubility (mol/L)	Triangular	3.34×10^{-7} (min); 1.06×10^{-6} (mode); 3.34×10^{-6} (max)	1.58×10^{-6}
Np solubility (mol/L)	Log Triangular	1.11×10^{-6} (min); 1.11×10^{-5} (mode); 1.11×10^{-4} (max)	1.70×10^{-5}
Pu solubility (mol/L)	Triangular	7.80×10^{-7} (min); 2.58×10^{-6} (mode); 8.55×10^{-6} (max)	3.97×10^{-6}
Th solubility (mol/L)	Triangular	8.84×10^{-6} (min); 1.76×10^{-5} (mode); 3.52×10^{-5} (max)	2.05×10^{-5}
Sn solubility (mol/L)	Triangular	1.78×10^{-8} (min); 4.80×10^{-8} (mode); 1.29×10^{-7} (max)	6.49×10^{-8}
U solubility (mol/L)	Triangular	9.16×10^{-5} (min); 2.64×10^{-4} (mode); 7.62×10^{-4} (max)	3.73×10^{-4}
Brine Flow Rate in Interbed (m/yr)	N/A	Sampled from 100 brine flow rate histories Clayton et al. (2011, Section 3.1.3))	3.96×10^{-7}

Table C-1. Summary of the Deterministic Approximations for the Salt GDS Model (continued)

Parameter	Distribution Type	FY 2011 GDSM Probabilistic Values	Deterministic Value
Ac K_d (mL/g)	Log-uniform	5 (min); 500 (max)	107.5
Am K_d (mL/g)	Uniform	25 (min); 100 (max)	62.5
C K_d (mL/g)	Uniform	0 (min); 0.6 (max)	0.3
Cm K_d (mL/g)	Log-uniform	5 (min); 500 (max)	107.5
Cs K_d (mL/g)	Uniform	1 (min); 20 (max)	10.5
Np K_d (mL/g)	Uniform	1 (min); 10 (max)	5.5
Pu K_d (mL/g)	Uniform	70 (min); 100 (max)	85
Pa K_d (mL/g)	Log-uniform	1 (min); 500 (max)	80.3
Ra K_d (mL/g)	Uniform	1 (min); 80 (max)	40.5
Se K_d (mL/g)	Uniform	0.2 (min); 0.5 (max)	0.35
Sn K_d (mL/g)	Uniform	2 (min); 10 (max)	6
Sr K_d (mL/g)	Uniform	1 (min); 80 (max)	40.5
Tc K_d (mL/g)	Uniform	0 (min); 2 (max)	1
Th K_d (mL/g)	Uniform	100 (min); 1000 (max)	550
U K_d (mL/g)	Uniform	0.2 (min); 1 (max)	0.6
Zr K_d (mL/g)	Log-uniform	3 (min); 500 (max)	97.1

NOTE: UNF fractional degradation rate (yr^{-1}) of 1.53×10^{-5} is larger than the maximum of the distribution of values for the purpose of examining performance with a very conservative EBS.

C-3. GRANITE GDS MODEL

Values for input parameters for the deterministic granite GDS model derive from the FY 2011 granite GDS model (Clayton et al. 2011, Section 3.2) [*generic_granite_undisturbed_36species+Dummy_FY11report.gsm*] and from a subsequent generic granite model [*Generic_PA_Model_R01_001v_Map_simplifiedGraniteGDS1.gsm*]. Key changes from the FY 2011 granite model include:

- Deterministic simulation with mean values for uncertain parameters (see Table C-2 for further details)
- Waste inventory of 70,000 MTHM UNF in 16,000 waste packages
- Fractional waste form degradation rate of 2×10^{-5} yr^{-1}
- Replace the 3D representation of far-field fractured granite using the FEHM dynamically-linked library with a 1D GoldSim pipe with matrix diffusion
- Replace the 2D representation of bentonite buffer with a set of 1D GoldSim cells.
- Update solubility values to be more representative of granite pore waters (based on Mariner et al. 2011, Table 2-5)
- Update distribution coefficients (K_d's) to be more representative of bentonite in the waste package and buffer, based on the waste package and bentonite K_d values used in the clay GDS model (Table E-2 and Clayton et al. 2011, Section 3.3.3.3)

- Update distribution coefficients (K_d's) to be more representative of granite in the host rock (based on Carbol and Engkvist 1997).
- Instantaneous failure of 1% (160) of the waste packages. This replaces the FY 2011 GDS model assumption that between 0.1% and 1% of the waste packages directly intersect a far-field fracture.

Deterministic values for uncertain parameters were calculated based on mean values of each uncertainty distribution. Table C-2 summarizes these deterministic values and also lists constant parameter values that changed. Constant parameter values that are unchanged from their deterministic treatment in the FY 2011 granite GDS model are not listed in Table C-2.

Table C-2. Summary of the Deterministic Approximations for the Granite GDS Model

Parameter	Distribution Type	FY 2011 GDSM Probabilistic Values	Deterministic Value
Waste Form			
UNF fractional degradation rate (yr^{-1})	Log Triangular	1×10^{-8} (min); 1×10^{-7} (mode); 1×10^{-6} (max)	2×10^{-5}
Waste Package			
Ac solubility (mol/L)	Constant	Unlimited	6×10^{-6}
Am solubility (mol/L)	Triangular	1.85×10^{-7} (min); 5.85×10^{-7} (mode); 1.85×10^{-6} (max)	6×10^{-6}
Cm solubility (mol/L)	Constant	Unlimited	6×10^{-6}
Nb solubility (mol/L)	Constant	Unlimited	4×10^{-5}
Np solubility (mol/L)	Triangular	4.79×10^{-10} (min); 1.51×10^{-9} (mode); 4.79×10^{-9} (max)	1×10^{-9}
Pa solubility (mol/L)	Constant	Unlimited	1×10^{-9}
Pd solubility (mol/L)	Constant	Unlimited	3×10^{-6}
Pu solubility (mol/L)	Triangular	1.40×10^{-6} (min); 4.62×10^{-6} (mode); 1.53×10^{-5} (max)	2×10^{-7}
Ra solubility (mol/L)	Constant	Unlimited	1×10^{-6}
Sb solubility (mol/L)	Constant	Unlimited	1×10^{-7}
Se solubility (mol/L)	Constant	Unlimited	4×10^{-8}
Sn solubility (mol/L)	Triangular	9.87×10^{-9} (min); 2.66×10^{-8} (mode); 7.15×10^{-8} (max)	3×10^{-8}
Tc solubility (mol/L)	Log Triangular	4.56×10^{-10} (min); 1.33×10^{-8} (mode); 3.91×10^{-7} (max)	3×10^{-8}
Th solubility (mol/L)	Triangular	2.00×10^{-3} (min); 4.00×10^{-3} (mode); 7.97×10^{-3} (max)	4×10^{-7}
U solubility (mol/L)	Triangular	4.89×10^{-8} (min); 1.12×10^{-7} (mode); 2.57×10^{-7} (max)	4×10^{-10}
Zr solubility (mol/L)	Constant	Unlimited	2×10^{-8}
Waste Package (degraded) porosity	Uniform	0.30 (min); 0.50 (max)	0.40
Ac K_d (mL/g)	Uniform	300 (min); 29,400 (max)	3125
Am K_d (mL/g)	Uniform	300 (min); 29,400 (max)	3125
C K_d (mL/g)	Constant	5	52.9
Cm K_d (mL/g)	Uniform	300 (min); 29,400 (max)	0
Cs K_d (mL/g)	Uniform	120 (min); 1,000 (max)	4.9
I K_d (mL/g)	Uniform	0 (min); 13 (max)	0
Np K_d (mL/g)	Uniform	30 (min); 1,000 (max)	804
Pa K_d (mL/g)	Uniform	30 (min); 1,000 (max)	804

Table C-2. Summary of the Deterministic Approximations for the Granite GDS Model (continued)

Parameter	Distribution Type	FY 2011 GDSM Probabilistic Values	Deterministic Value
Pu K_d (mL/g)	Uniform	150 (min); 16,800 (max)	3125
Ra K_d (mL/g)	Uniform	50 (min); 3,000 (max)	8.2
Se K_d (mL/g)	Uniform	4 (min); 30 (max)	0
Sr K_d (mL/g)	Uniform	50 (min); 3,000 (max)	0.34
Tc K_d (mL/g)	Uniform	50,000 (min); 60,000 (max)	0
Th K_d (mL/g)	Uniform	63 (min); 23,500 (max)	3125
U K_d (mL/g)	Uniform	90 (min); 1,000 (max)	529
Near-Field Bentonite Buffer			
Bulk density (kg/m^3)	Constant	2780	1562
Porosity	Constant	0.18	0.435
Fraction connected to far-field fractures	Uniform	0.001 (min); 0.01 (max)	0.01
Ac K_d (mL/g)	Uniform	300 (min); 29,400 (max)	0
Am K_d (mL/g)	Uniform	300 (min); 29,400 (max)	55,458
C K_d (mL/g)	Constant	5	0
Cm K_d (mL/g)	Uniform	300 (min); 29,400 (max)	0
Cs K_d (mL/g)	Uniform	120 (min); 1,000 (max)	202
I K_d (mL/g)	Uniform	0 (min); 13 (max)	0
Nb K_d (mL/g)	Constant	0	145,576
Np K_d (mL/g)	Uniform	30 (min); 1,000 (max)	4622
Pa K_d (mL/g)	Uniform	30 (min); 1,000 (max)	0
Pd K_d (mL/g)	Constant	0	1821
Pu K_d (mL/g)	Uniform	150 (min); 16,800 (max)	4622
Ra K_d (mL/g)	Uniform	50 (min); 3,000 (max)	0
Se K_d (mL/g)	Uniform	4 (min); 30 (max)	4.6
Sn K_d (mL/g)	Constant	0	22,252
Sr K_d (mL/g)	Uniform	50 (min); 3,000 (max)	0
Tc K_d (mL/g)	Uniform	50,000 (min); 60,000 (max)	60,726
Th K_d (mL/g)	Uniform	63 (min); 23,500 (max)	13,864
U K_d (mL/g)	Uniform	90 (min); 1,000 (max)	462,146
Zr K_d (mL/g)	Constant	0	202,142
Near-Field Granite DRZ			
Ac solubility (mol/L)	Constant	Unlimited	6×10^{-6}
Am solubility (mol/L)	Triangular	3.34×10^{-7} (min); 1.06×10^{-6} (mode); 3.34×10^{-6} (max)	6×10^{-6}
Cm solubility (mol/L)	Constant	Unlimited	6×10^{-6}
Nb solubility (mol/L)	Constant	Unlimited	4×10^{-5}

Table C-2. Summary of the Deterministic Approximations for the Granite GDS Model (continued)

Parameter	Distribution Type	FY 2011 GDSM Probabilistic Values	Deterministic Value
Np solubility (mol/L)	Log Triangular	1.11×10^{-6} (min); 1.11×10^{-5} (mode); 1.11×10^{-4} (max)	1×10^{-9}
Pa solubility (mol/L)	Constant	Unlimited	1×10^{-9}
Pd solubility (mol/L)	Constant	Unlimited	3×10^{-6}
Pu solubility (mol/L)	Triangular	7.80×10^{-7} (min); 2.58×10^{-6} (mode); 8.55×10^{-6} (max)	2×10^{-7}
Ra solubility (mol/L)	Constant	Unlimited	1×10^{-6}
Sb solubility (mol/L)	Constant	Unlimited	1×10^{-7}
Se solubility (mol/L)	Constant	Unlimited	4×10^{-8}
Sn solubility (mol/L)	Triangular	1.78×10^{-8} (min); 4.80×10^{-8} (mode); 1.29×10^{-7} (max)	3×10^{-8}
Tc solubility (mol/L)	Constant	Unlimited	3×10^{-8}
Th solubility (mol/L)	Triangular	8.84×10^{-6} (min); 1.76×10^{-5} (mode); 3.52×10^{-5} (max)	4×10^{-7}
U solubility (mol/L)	Triangular	9.16×10^{-5} (min); 2.64×10^{-4} (mode); 7.62×10^{-4} (max)	4×10^{-10}
Zr solubility (mol/L)	Constant	Unlimited	2×10^{-8}
Porosity	Uniform	0.0005 (min); 0.01 (max)	0.0018
Tortuosity	Normal	0.0144 (mean); 4.176×10^{-3} (sdev)	0.011
Volumetric flow rate (m^3/yr)	Constant	4.5×10^{-4}	5.1×10^{-4}
Ac K_d (mL/g)	Uniform	300 (min); 29,400 (max)	2,485
Am K_d (mL/g)	Uniform	300 (min); 29,400 (max)	2,485
C K_d (mL/g)	Constant	5	1.1
Cm K_d (mL/g)	Uniform	300 (min); 29,400 (max)	2,485
Cs K_d (mL/g)	Uniform	120 (min); 1,000 (max)	39.1
I K_d (mL/g)	Uniform	0 (min); 13 (max)	0
Nb K_d (mL/g)	Constant	0	1,395
Np K_d (mL/g)	Uniform	30 (min); 1,000 (max)	3,909
Pa K_d (mL/g)	Uniform	30 (min); 1,000 (max)	1,954
Pd K_d (mL/g)	Constant	0	12.5
Pu K_d (mL/g)	Uniform	150 (min); 16,800 (max)	3,909
Ra K_d (mL/g)	Uniform	50 (min); 3,000 (max)	39.1
Se K_d (mL/g)	Uniform	4 (min); 30 (max)	2.0
Sn K_d (mL/g)	Constant	0	0.16
Sr K_d (mL/g)	Uniform	50 (min); 3,000 (max)	0.39
Tc K_d (mL/g)	Uniform	50,000 (min); 60,000 (max)	1,173
Th K_d (mL/g)	Uniform	63 (min); 23,500 (max)	3,909
U K_d (mL/g)	Uniform	90 (min); 1,000 (max)	3,909
Zr K_d (mL/g)	Constant	0	1,395
Far-Field Fractured Granite Host Rock			
Porosity	Uniform	0.0005 (min); 0.01 (max)	0.0018

Table C-2. Summary of the Deterministic Approximations for the Granite GDS Model (continued)

Parameter	Distribution Type	FY 2011 GDSM Probabilistic Values	Deterministic Value
Tortuosity	Normal	0.0144 (mean); 4.176×10^{-3} (sdev)	0.011
Fracture aperture (m)	Uniform	0.00001 (min); 0.00050 (max)	0.0002
Fracture spacing (m)	Constant	25	25
Fracture height (m)	Constant	1.00	3.12
Ac K_d (mL/g)	Cumulative	1,000 (min); 3,000 (mode); 5,000 (max)	2,485
Am K_d (mL/g)	Cumulative	1,000 (min); 3,000 (mode); 5,000 (max)	2,485
C K_d (mL/g)	Cumulative	0.5 (min); 1.0 (mode); 2.0 (max)	1.1
Cm K_d (mL/g)	Cumulative	1,000 (min); 3,000 (mode); 5,000 (max)	2,485
Cs K_d (mL/g)	Cumulative	100 (min); 500 (mode); 1000 (max)	39.1
Nb K_d (mL/g)	Cumulative	500 (min); 1,000 (mode); 3,000 (max)	1,395
Np K_d (mL/g)	Cumulative	1,000 (min); 5,000 (mode); 10,000 (max)	3,909
Pa K_d (mL/g)	Cumulative	500 (min); 1,000 (mode); 5,000 (max)	1,954
Pd K_d (mL/g)	Cumulative	10 (min); 100 (mode); 500 (max)	12.5
Pu K_d (mL/g)	Cumulative	1,000 (min); 5,000 (mode); 10,000 (max)	3,909
Ra K_d (mL/g)	Cumulative	50 (min); 100 (mode); 500 (max)	39.1
Se K_d (mL/g)	Cumulative	0.5 (min); 1.0 (mode); 5.0 (max)	2.0
Sn K_d (mL/g)	Cumulative	0 (min); 1.0 (mode); 10 (max)	0.16
Sr K_d (mL/g)	Cumulative	5 (min); 10 (mode); 50 (max)	0.39
Tc K_d (mL/g)	Cumulative	300 (min); 1,000 (mode); 3,000 (max)	1,173
Th K_d (mL/g)	Cumulative	1,000 (min); 5,000 (mode); 10,000 (max)	3,909
U K_d (mL/g)	Cumulative	1,000 (min); 5,000 (mode); 10,000 (max)	3,909
Zr K_d (mL/g)	Cumulative	500 (min); 1,000 (mode); 3,000 (max)	1,395

NOTE: UNF fractional degradation rate (yr^{-1}) of 2×10^{-5} is larger than the maximum of the distribution of values for the purpose of examining performance with a very conservative EBS. Some other deterministic values are outside the range of the probabilistic distribution of values due to updated property values considered more representative of a granite repository system.

C-4. CLAY GDS MODEL

Values for input parameters for the deterministic clay GDS model derive from the FY 2011 clay GDS model (Clayton et al. 2011, Section 3.3) [*FY11_Clay_GDSE_Model_0105.gsm*]. Key changes include:

- Deterministic simulation with mean values for uncertain parameters (see Table C-3 for further details)
- Waste inventory of 70,000 MTHM UNF in 16,000 waste packages
- Instantaneous waste package failure
- Clay thickness of 150 m overlying the emplaced waste, consistent with Hansen et al. (2010, Figure 2.1-1 and Section 4)
- Equivalent diffusive releases to the far-field clay in both the upward and downward directions

Deterministic values for uncertain parameters were calculated based on mean values of each uncertainty distribution. These deterministic values are summarized in Table C-3. Constant parameter values that are unchanged from their deterministic treatment in the FY 2011 clay GDS model are not listed in Table C-3.

Table C-3. Summary of the Deterministic Approximations for the Clay GDS Model

Parameter	Distribution Type	FY 2011 GDSM Probabilistic Values	Deterministic Value
Waste Package			
Ac K_d (mL/g)	Log Triangular	1000 (min); 5000 (mode); 5000 (max)	3125
Am K_d (mL/g)	Log Triangular	1000 (min); 5000 (mode); 5000 (max)	3125
C K_d (mL/g)	Log Triangular	10 (min); 100 (mode); 100 (max)	52.9
Cs K_d (mL/g)	Log Triangular	0 (min); 300 (mode); 300 (max)	5.1
Np K_d (mL/g)	Log Triangular	500 (min); 1000 (mode); 1000 (max)	804
Pu K_d (mL/g)	Log Triangular	1000 (min); 5000 (mode); 5000 (max)	3125
Pa K_d (mL/g)	Log Triangular	500 (min); 1000 (mode); 1000 (max)	804
Ra K_d (mL/g)	Log Triangular	0 (min); 500 (mode); 500 (max)	8.5
Sr K_d (mL/g)	Log Triangular	0 (min); 20 (mode); 20 (max)	0.35
Th K_d (mL/g)	Log Triangular	1000 (min); 5000 (mode); 5000 (max)	3125
U K_d (mL/g)	Log Triangular	100 (min); 1000 (mode); 1000 (max)	529
Near-Field Bentonite Buffer			
Am solubility (mol/L)	Log Triangular	1.0×10^{-12} (min); 1.0×10^{-10} (mode); 1.0×10^{-8} (max)	4.6×10^{-10}
C solubility (mol/L)	Log Triangular	2.3×10^{-5} (min); 2.3×10^{-3} (mode); 2.3×10^{-1} (max)	1.1×10^{-2}
Np solubility (mol/L)	Log Triangular	4.0×10^{-11} (min); 4.0×10^{-9} (mode); 4.0×10^{-7} (max)	1.8×10^{-8}
Nb solubility (mol/L)	Log Triangular	2.0×10^{-9} (min); 2.0×10^{-7} (mode); 2.0×10^{-5} (max)	9.2×10^{-7}
Pd solubility (mol/L)	Log Triangular	4.0×10^{-9} (min); 4.0×10^{-7} (mode); 4.0×10^{-5} (max)	1.8×10^{-6}
Pu solubility (mol/L)	Log Triangular	1.99×10^{-9} (min); 1.99×10^{-7} (mode); 1.99×10^{-5} (max)	9.2×10^{-7}
Se solubility (mol/L)	Log Triangular	5.0×10^{-12} (min); 5.0×10^{-10} (mode); 5.0×10^{-8} (max)	2.3×10^{-9}
Tc solubility (mol/L)	Log Triangular	4.0×10^{-11} (min); 4.0×10^{-9} (mode); 4.0×10^{-7} (max)	1.8×10^{-8}
Th solubility (mol/L)	Log Triangular	1.0×10^{-11} (min); 1.0×10^{-9} (mode); 1.0×10^{-7} (max)	4.6×10^{-9}
Sn solubility (mol/L)	Log Triangular	1.0×10^{-10} (min); 1.0×10^{-8} (mode); 1.0×10^{-6} (max)	4.6×10^{-8}
U solubility (mol/L)	Log Triangular	5.0×10^{-10} (min); 5.0×10^{-8} (mode); 5.0×10^{-6} (max)	2.3×10^{-7}
Zr solubility (mol/L)	Log Triangular	2.0×10^{-10} (min); 2.0×10^{-8} (mode); 2.0×10^{-6} (max)	9.2×10^{-8}
Bulk density (kg/m^3)	Triangular	2,070 (min); 2,300 (mode); 2,530 (max)	2,300
Tortuosity	Triangular	0.072 (min); 0.725 (mode); 1.0 (max)	0.599
Available porosity – anions (C, Cl, I, Nb, Se)	Triangular	0.001 (min); 0.01 (mode); 1.0 (max)	0.337
Available porosity – cations	Triangular	0.10 (min); 1.0 (mode); 1.0 (max)	0.700

Table C-3. Summary of the Deterministic Approximations for the Clay GDS Model (continued)

Parameter	Distribution Type	FY 2011 GDSM Probabilistic Values	Deterministic Value
Am K_d (mL/g)	Log Triangular	120 (min); 12,000 (mode); 1.2×10^{6} (max)	55,457
Cs K_d (mL/g)	Log Triangular	0.437 (min); 43.7 (mode); 4370 (max)	202
Nb K_d (mL/g)	Log Triangular	315 (min); 31,500 (mode); 3.15×10^{6} (max)	145,580
Np K_d (mL/g)	Log Triangular	10 (min); 1,000 (mode); 100,000 (max)	4622
Pd K_d (mL/g)	Log Triangular	3.94 (min); 394 (mode); 39,400 (max)	1821
Pu K_d (mL/g)	Log Triangular	10 (min); 1,000 (mode); 100,000 (max)	4622
Se K_d (mL/g)	Log Triangular	0.01 (min); 1 (mode); 100 (max)	4.6
Sn K_d (mL/g)	Log Triangular	48.1 (min); 4,810 (mode); 481,000 (max)	42,854
Tc K_d (mL/g)	Log Triangular	131 (min); 13,100 (mode); 1.31×10^{6} (max)	60,726
Th K_d (mL/g)	Log Triangular	30 (min); 3,000 (mode); 300,000 (max)	13,864
U K_d (mL/g)	Log Triangular	1000 (min); 100,000 (mode); 1×10^{7} (max)	462,150
Zr K_d (mL/g)	Log Triangular	437 (min); 43,700 (mode); 4.37×10^{6} (max)	389,300
Near-Field Clay DRZ			
Ac solubility (mol/L)	Log Triangular	4.0×10^{-9} (min); 4.0×10^{-7} (mode); 4.0×10^{-5} (max)	1.8×10^{-6}
Am solubility (mol/L)	Log Triangular	4.0×10^{-9} (min); 4.0×10^{-7} (mode); 4.0×10^{-5} (max)	1.8×10^{-6}
C solubility (mol/L)	Log Triangular	2.3×10^{-5} (min); 2.3×10^{-3} (mode); 2.3×10^{-1} (max)	1.1×10^{-2}
Cm solubility (mol/L)	Log Triangular	4.0×10^{-9} (min); 4.0×10^{-7} (mode); 4.0×10^{-5} (max)	1.8×10^{-6}
Np solubility (mol/L)	Log Triangular	4.0×10^{-11} (min); 4.0×10^{-9} (mode); 4.0×10^{-7} (max)	1.8×10^{-8}
Nb solubility (mol/L)	Log Triangular	2.0×10^{-9} (min); 2.0×10^{-7} (mode); 2.0×10^{-5} (max)	9.2×10^{-7}
Pa solubility (mol/L)	Log Triangular	1.0×10^{-8} (min); 1.0×10^{-6} (mode); 1.0×10^{-4} (max)	4.6×10^{-6}
Pb solubility (mol/L)	Log Triangular	4.0×10^{-8} (min); 4.0×10^{-6} (mode); 4.0×10^{-4} (max)	1.8×10^{-5}
Pd solubility (mol/L)	Log Triangular	4.0×10^{-9} (min); 4.0×10^{-7} (mode); 4.0×10^{-5} (max)	1.8×10^{-6}
Pu solubility (mol/L)	Log Triangular	2.0×10^{-9} (min); 2.0×10^{-7} (mode); 2.0×10^{-5} (max)	9.2×10^{-7}
Ra solubility (mol/L)	Log Triangular	1.0×10^{-9} (min); 1.0×10^{-7} (mode); 1.0×10^{-5} (max)	4.6×10^{-7}
Se solubility (mol/L)	Log Triangular	5.0×10^{-12} (min); 5.0×10^{-10} (mode); 5.0×10^{-8} (max)	2.3×10^{-9}
Tc solubility (mol/L)	Log Triangular	4.0×10^{-11} (min); 4.0×10^{-9} (mode); 4.0×10^{-7} (max)	1.8×10^{-8}
Th solubility (mol/L)	Log Triangular	6.0×10^{-9} (min); 6.0×10^{-7} (mode); 6.0×10^{-5} (max)	2.8×10^{-6}
Sn solubility (mol/L)	Log Triangular	1.0×10^{-10} (min); 1.0×10^{-8} (mode); 1.0×10^{-6} (max)	4.6×10^{-8}
U solubility (mol/L)	Log Triangular	7.0×10^{-9} (min); 7.0×10^{-7} (mode); 7.0×10^{-5} (max)	3.2×10^{-6}
Zr solubility (mol/L)	Log Triangular	2.0×10^{-10} (min); 2.0×10^{-8} (mode); 2.0×10^{-6} (max)	9.2×10^{-8}
Tortuosity	Triangular	0.060 (min); 0.60 (mode); 0.61 (max)	0.423
Available porosity – anions (C, Cl, I, Nb, Se)	Triangular	0.002 (min); 0.02 (mode); 1.0 (max)	0.341
Available porosity – cations	Triangular	0.10 (min); 1.0 (mode); 1.0 (max)	0.700
Fracture spacing (m)	Triangular	0.25 (min); 0.50 (mode); 1.00 (max)	0.58
Fracture aperture (m)	Triangular	0.0005 (min); 0.0010 (mode); 0.0050 (max)	0.0022

Table C-3. Summary of the Deterministic Approximations for the Clay GDS Model (continued)

Parameter	Distribution Type	FY 2011 GDSM Probabilistic Values	Deterministic Value
Ac K_d (mL/g)	Log Triangular	500 (min); 50,000 (mode); 5.0×10^6 (max)	231,070
Am K_d (mL/g)	Log Triangular	500 (min); 50,000 (mode); 5.0×10^6 (max)	231,070
C K_d (mL/g)	Log Triangular	0.00414 (min); 0.414 (mode); 41.4 (max)	1.9
Cm K_d (mL/g)	Log Triangular	500 (min); 50,000 (mode); 5.0×10^6 (max)	231,070
Cs K_d (mL/g)	Log Triangular	3.88 (min); 388 (mode); 38,800 (max)	1,849
Nb K_d (mL/g)	Log Triangular	48.1 (min); 4,810 (mode); 481,500 (max)	22,210
Np K_d (mL/g)	Log Triangular	9 (min); 900 (mode); 90,000 (max)	4,159
Pa K_d (mL/g)	Log Triangular	10 (min); 1,000 (mode); 100,000 (max)	4,622
Pb K_d (mL/g)	Log Triangular	1.6 (min); 160 (mode); 16,000 (max)	739
Pd K_d (mL/g)	Log Triangular	8.05 (min); 805 (mode); 80,500 (max)	3,722
Pu K_d (mL/g)	Log Triangular	9 (min); 900 (mode); 90,000 (max)	4,159
Ra K_d (mL/g)	Log Triangular	10 (min); 1,000 (mode); 100,000 (max)	4,622
Sn K_d (mL/g)	Log Triangular	161 (min); 16,100 (mode); 1.61×10^6 (max)	74,451
Tc K_d (mL/g)	Log Triangular	11.5 (min); 1,150 (mode); 115,000 (max)	5,324
Th K_d (mL/g)	Log Triangular	80 (min); 8,000 (mode); 800,000 (max)	36,972
U K_d (mL/g)	Log Triangular	80 (min); 8,000 (mode); 800,000 (max)	36,972
Zr K_d (mL/g)	Log Triangular	11.5 (min); 1,150 (mode); 115,000 (max)	5,324
Far-Field Clay Host Rock			
Solubility (mol/L)		same as Near-Field DRZ Clay	
Tortuosity		same as Near-Field DRZ Clay	
Available porosity		same as Near-Field DRZ Clay	
K_d (mL/g)		same as Near-Field DRZ Clay	

C-5. DEEP BOREHOLE GDS MODEL

Values for input parameters for the deterministic deep borehole GDS model derive from the FY 2011 deep borehole GDS model (Clayton et al. 2011, Section 3.4) [*(UNF Base Perm_May26) DBH FY11 (Baseline v3_May23-2011).gsm*]. Key changes include:

- Deterministic simulation with mean values for uncertain parameters (see Table C-4 for further details)
- Waste inventory of 174 MTHM UNF per borehole in 400 waste packages
- Fractional waste form degradation rate of 2×10^{-5} yr^{-1}
- Fluid flow rates up the borehole assumed to remain constant at the 1,000,000-year values until 10,000,000 years

Deterministic values for uncertain parameters were calculated based on mean values of each uncertainty distribution. These deterministic values are summarized in Table C-4. Constant parameter values that are unchanged from their deterministic treatment in the FY 2011 deep borehole GDS model are not listed in Table C-4.

Table C-4. Summary of the Deterministic Approximations for the Deep Borehole GDS Model

Parameter	Distribution Type	FY 2011 GDSM Probabilistic Values	Deterministic Value
Waste Form			
UNF fractional degradation (yr^{-1})	Log Triangular	1×10^{-8} (min); 1×10^{-7} (mode); 1×10^{-6} (max)	1.53×10^{-5}
Waste Disposal Zone			
Am solubility (mol/L)	Triangular	7.8×10^{-10} (min); 6.5×10^{-9} (mode); 4.4×10^{-8} (max)	1.7×10^{-8}
Np solubility (mol/L)	Triangular	6.0×10^{-7} (min); 1.9×10^{-6} (mode); 6.0×10^{-6} (max)	2.8×10^{-6}
Pu solubility (mol/L)	Triangular	3.40×10^{-14} (min); 3.56×10^{-14} (mode); 3.73×10^{-13} (max)	1.48×10^{-13}
Tc solubility (mol/L)	Log Triangular	4.56×10^{-10} (min); 1.33×10^{-8} (mode); 3.91×10^{-7} (max)	3.17×10^{-8}
Th solubility (mol/L)	Triangular	1.7×10^{-8} (min); 3.4×10^{-8} (mode); 6.8×10^{-8} (max)	3.9×10^{-8}
Sn solubility (mol/L)	Triangular	9.87×10^{-9} (min); 2.66×10^{-8} (mode); 7.15×10^{-8} (max)	3.60×10^{-8}
U solubility (mol/L)	Triangular	4.17×10^{-13} (min); 9.46×10^{-13} (mode); 2.19×10^{-12} (max)	1.18×10^{-12}
Fluid Flow Rate (m/yr)	N/A	Sampled from 100 flow rate histories (Clayton et al. (2011, Section 3.4.1.3))	1 flow rate history
Ac K_d (mL/g)	Log-uniform	5 (min); 500 (max)	107.5
Am K_d (mL/g)	Log-uniform	5 (min); 500 (max)	107.5
C K_d (mL/g)	Uniform	0 (min); 0.6 (max)	0.3
Cm K_d (mL/g)	Log-uniform	5 (min); 500 (max)	107.5
Cs K_d (mL/g)	Uniform	5 (min); 40 (max)	22.5
Np K_d (mL/g)	Log-uniform	1 (min); 500 (max)	80.3
Pu K_d (mL/g)	Log-uniform	1 (min); 500 (max)	80.3
Pa K_d (mL/g)	Log-uniform	1 (min); 500 (max)	80.3
Ra K_d (mL/g)	Uniform	0.4 (min); 3 (max)	1.7
Se K_d (mL/g)	Uniform	0.2 (min); 0.5 (max)	0.35
Sn K_d (mL/g)	Uniform	2 (min); 10 (max)	6
Sr K_d (mL/g)	Uniform	0.4 (min); 3 (max)	1.7
Tc K_d (mL/g)	Log-uniform	0.00001 (min); 25 (max)	1.7
Th K_d (mL/g)	Log-uniform	3 (min); 500 (max)	97.1
U K_d (mL/g)	Log-uniform	0.4 (min); 500 (max)	70.1
Zr K_d (mL/g)	Log-uniform	3 (min); 500 (max)	97.15
Seal Zone			
Fluid Flow Rate (m/yr)	N/A	Sampled from 100 flow rate histories (Clayton et al. 2011, Section 3.4.1.3)	1 flow rate history

Table C-4. Summary of the Deterministic Approximations for the Deep Borehole GDS Model (continued)

Parameter	Distribution Type	FY 2011 GDSM Probabilistic Values	Deterministic Value
Ac K_d (mL/g)	Log-uniform	300 (min); 29,400 (max)	6,347
Am K_d (mL/g)	Log-uniform	300 (min); 29,400 (max)	6,347
Cm K_d (mL/g)	Log-uniform	300 (min); 29,400 (max)	6,347
Cs K_d (mL/g)	Log-uniform	120 (min); 1,000 (max)	415
Np K_d (mL/g)	Log-uniform	30 (min); 1,000 (max)	277
Pa K_d (mL/g)	Log-uniform	30 (min); 1,000 (max)	277
Pd K_d (mL/g)	Uniform	5 (min); 12 (max)	8.5
Pu K_d (mL/g)	Log-uniform	150 (min); 16,800 (max)	3,529
Ra K_d (mL/g)	Log-uniform	50 (min); 3,000 (max)	721
Se K_d (mL/g)	Uniform	4 (min); 20 (max)	12
Sn K_d (mL/g)	Uniform	17 (min); 50 (max)	33.5
Sr K_d (mL/g)	Log-uniform	50 (min); 3,000 (max)	721
Tc K_d (mL/g)	Log-uniform	0.0001 (min); 250 (max)	17
Th K_d (mL/g)	Log-uniform	63 (min); 23,500 (max)	3,958
U K_d (mL/g)	Log-uniform	90 (min); 1,000 (max)	378
Zr K_d (mL/g)	Log-uniform	100 (min); 5,000 (max)	1,253
Upper Borehole Zone			
Volumetric Fluid Flow Rate (m^3/yr)	Constant	0.00235	0.00235
Ac K_d (mL/g)	Log-uniform	100 (min); 100,000 (max)	14,462
Am K_d (mL/g)	Log-uniform	100 (min); 100,000 (max)	14,462
C K_d (mL/g)	Log-uniform	0.0001 (min); 2,000 (max)	119
Cm K_d (mL/g)	Log-uniform	100 (min); 100,000 (max)	14,462
Cs K_d (mL/g)	Log-uniform	10 (min); 10,000 (max)	1,446
Np K_d (mL/g)	Log-uniform	10 (min); 1,000 (max)	215
Pa K_d (mL/g)	Log-uniform	10 (min); 1,000 (max)	215
Pd K_d (mL/g)	Uniform	4 (min); 100 (max)	52
Pu K_d (mL/g)	Log-uniform	300 (min); 100,000 (max)	17,163
Ra K_d (mL/g)	Log-uniform	5 (min); 3,000 (max)	468
Se K_d (mL/g)	Uniform	1 (min); 8 (max)	4.5
Sn K_d (mL/g)	Log-uniform	50 (min); 700 (max)	246
Sr K_d (mL/g)	Log-uniform	5 (min); 3,000 (max)	468
Tc K_d (mL/g)	Log-uniform	0.0001 (min); 1,000 (max)	62
Th K_d (mL/g)	Log-uniform	800 (min); 60,000 (max)	13,711
U K_d (mL/g)	Log-uniform	20 (min); 1,700 (max)	378
Zr K_d (mL/g)	Log-uniform	10 (min); 8,300 (max)	1,233

NOTE: UNF fractional degradation rate (yr^{-1}) of 1.53×10^{-5} is larger than the maximum of the distribution of values for the purpose of examining performance with a very conservative EBS.

Appendix D

Diffusion Modeling in a Generic Clay Repository

APPENDIX D—DIFFUSION MODELING IN A GENERIC CLAY REPOSITORY

One of the activities in GDSM is to identify and develop improved descriptions of scientific submodels and processes for inclusion into the GDSM capability. In FY 2011 the treatment of diffusion in clay was identified as an area for improvement and initial work was conducted to identify the nature of the improvements. The dominant transport mechanism of chemical species at locations away from the DRZ in clay-rich geological formations is diffusion, which is influenced by factors such as the heterogeneity of the diffusive parameters and electrochemical processes. The latter are the results of interactions between chemical species in solutions and charged surfaces of clay minerals. Numerical models for conducting PA analyses of clay repositories need to consider these factors in order to correctly simulate the long-term transport behavior.

The FY 2012 work extended and focused the clay diffusion efforts by developing an improved approach to dealing with impacts of heterogeneity and electrochemical processes and associated uncertainties and presenting a rigorous and practical framework to account for heterogeneity of the diffusive parameters suitable for disposal system modeling. The work is documented in Bianchi et al. (2012) and briefly summarized in this appendix.

The work addresses FEP 2.2.09, Chemical Process—Transport (shale), which has been ranked *medium* in importance (DOE 2011, Table 7). The work reports results of upscaling D in anisotropic and heterogeneous clay-rock formations. Expressions for upscaling the diffusion coefficient are developed based on the analogy between diffusion and water flow in saturated heterogeneous porous media. Comparisons between numerical and analytical values of the equivalent upscaled diffusion coefficient show that conventional stochastic and power-averaging upscaling methods can be effectively applied to upscale laboratory-scale D measurements for large scale numerical models.

A new model to handle the impacts of electrochemical processes on diffusion, which was initially developed and reported in the FY 2011 report (Zheng et al. 2011), is developed to be practical for routine disposal system calculations. The model is evaluated and results indicate a good match between analytical predictions from this model and experimental data for different chemical species from the Opalinus Clay and Callovo-Oxfordian argillites. By fitting the model to the experimental data, the electrical potential in the Opalinus Clay and in the Callovo-Oxfordian formations is equal to about -11 mV and 23 mV, respectively. Analogously, for both geological formations, the optimal values for the macropore water fraction were found to be equal zero. This result suggests that the entire pore space is subject to electrochemical processes.

The model conceptualizes pore water as divided into two parts: (1) mobile water in macropores that is not subject to electrochemical processes, and (2) pore water in the double-diffusion layer that is strongly impacted by electrochemical processes. Based on the assumption that tortuosity and constrictivity and chemical potentials are the same for both macropore water and the double-diffusion layer, Zheng et al. (2011) derived the following expression:

$$\frac{D_i}{D_M} = f + (1-f)exp\left[-\frac{z_i\varphi}{RT}\right] \quad \text{Eq. D-1}$$

where:

D_i = Diffusion coefficient of the species i

D_M = Diffusion coefficient in the macropore space

f = Volumetric fraction of macropore water relative to the pore porosity

z_i = Charge number

R = Gas constant

T = Absolute temperature

φ = Electrical potential

The other assumption used in deriving Equation D-1 is that φ is constant for a given formation. This assumption allows for significant simplification of the procedure to estimate the impacts of electrochemical processes, which is necessary for disposal system modeling while more accurate consideration of electrochemistry may be needed in subprocess models (Rutqvist et al. 2012). This treatment will be evaluated as part of the evaluation of Equation D-1.

The diffusion coefficient in the macropore space D_M can be calculated with the following expression:

$$D_M = \frac{D_{HTO}D_{w,i}}{D_{w,HTO}} \quad \text{Eq. D-2}$$

where D_{HTO} is the diffusion coefficient of for tritiated water (HTO) that is not subject to electrochemical interactions and subscript w refers to the diffusion coefficient in free water.

In previous work (Zheng et al. 2011), Equation D-1 was evaluated by comparing analytical predictions with few experimental data from the Opalinus Clay formation. In this work, we completed our previous evaluation by including all the data available in the literature for the Opalinus Clay. We also expanded evaluation by including also data collected in the Callovo-Oxfordian argillites.

The model represented by Equation D-1 is evaluated by comparing analytical estimates with experimental diffusion coefficient values for different chemical species all of which available in the literature. In particular we focused on the Opalinus Clay and Callovo-Oxfordian argillites since the majority of the data on diffusive parameters that is available in the literature were collected for these two geological formations. With respect to the Opalinus Clay data the model represented in Equation D-1 provides a very good match between measured and estimated values. The optimal values for the fitting parameters f and φ are equal to 0.0 and about −11 mV. When compared to the Callovo-Oxfordian argillite data, Equation D-1 is a less accurate predictor of the experimental data. Further refinement of Equation D-1 and associated evaluation based on the data sets is on-going.